Mechanisms underlying the endogenous neuroprotection of hamartin in ischaemic stroke

Gina Louise Hadley

Harris Manchester College
University of Oxford

A thesis submitted for the degree of Doctor of Philosophy
Radcliffe Department of Medicine

Hilary Term 2016

“Discovery consists of seeing what everybody has seen and thinking what nobody has thought.”

Albert Szent-Gyorgyi, *in Irving Good, The Scientist Speculates (1962)*

US (Hungarian-born) biochemist (1893 - 1986)

Abstract

Introduction: Hamartin has been shown to mediate the endogenous resistance of Cornu Ammonis 3 (CA3) neurons to ischaemia. Proposed mechanisms concern the inhibition of mammalian target of rapamycin (mTOR) which could promote productive autophagy and prevent endoplasmic reticulum (ER) stress. A small molecule targeted at these pathways could protect neurons and buy valuable time for recanalization therapy for stroke.

Methods: *In vivo*, the modified four vessel occlusion model of global cerebral ischaemia was used in male Wistar rats. A temporal and spatial profile for hamartin and mTOR proteins and their downstream mechanisms of autophagy and ER stress was characterised using Western blotting. *In* vitro, small molecules were assessed in E18 neuronal cultures exposed to oxygen and glucose deprivation (OGD) in an attempt to replicate hamartin's protective effect.

Results: Time course experiments revealed that global ischaemia selectively induced hamartin expression in the membrane fraction of the hippocampal CA3 region, peaking at 12 hours of reperfusion. Autophagy-associated proteins were differentially expressed in CA1 and CA3 after global ischaemia. Decreased levels of ER stress proteins were observed in CA3 neurons while increased ER stress was found in CA1 neurons after global ischaemia. *In vitro*, hamartin's neuroprotective effect appeared to be due to the induction of productive autophagy. The mTOR inhibitor rapamycin did not replicate hamartin's protective effect. Induction of autophagy with metformin and attenuation of the ER stress response with salubrinal also failed to afford neuroprotection. A novel mTORC1/2 inhibitor, AZD2014, currently in clinical trials for cancer, caused increased neurotoxicity following OGD which was associated with increased ER stress.

Conclusions: The selective dynamic response of hamartin is involved in the endogenous resistance of CA3 neurons to global ischaemia. The temporal association between increased hamartin expression, induction of productive autophagy and decreased ER stress levels in CA3 neurons may contribute to the mechanism of hamartin's endogenous protective effect. None of the pharmacological agents that targeted downstream mechanisms of hamartin replicated these neuroprotective effects. Further research is needed to fully understand the neuroprotection elicited by hamartin and discover a small molecule that can mimic these effects.

Executive Summary

Manipulating the mechanism by which hamartin 'fine-tunes' the brain's endogenous neuroprotective response could ultimately lead to the identification of a small molecular target. This compound could offer the pharmacological modulation endogenously provided by hamartin and prove to be the neuroprotectant yet to be discovered and extrapolated to the clinic. 'Time is brain' (Saver, 2006) and any small molecule that could be given in the ambulance with the aim of targeting the ischaemic cascade at source without increasing the risk in haemorrhagic stroke patients could increase the amount of time available to image, treat, and restore blood flow to the brain, improving functional outcome. Harnessing endogenous protective mechanisms could indeed bring a cure from within that could not only benefit stroke patients, but extend to a multitude of neurodegenerative diseases.

The early increase in hamartin expression in the resistant hippocampal CA3 region following global cerebral ischaemia (Chapter 3) corroborates recent findings that hamartin has a neuroprotective effect (Papadakis *et al.,* 2013). The key function of hamartin is the inhibition of mTOR which implicates this mechanism in neuroprotection. However, there are a number of downstream effector pathways of mTOR that hamartin could also influence such as the promotion of productive autophagy (Chapter 4) and the inhibition of the ER stress pathway (Chapter 5). Indeed, the expression of autophagy proteins was differentially altered in both CA1 and CA3 regions of the hippocampus following global ischaemia, and hamartin inhibition prevented productive autophagy. Furthermore, decreased levels of ER stress proteins were observed in CA3 while increased protein expression was found in CA1 after global ischaemia. There is a complex interplay between autophagy and ER stress and pharmacological manipulation with mTOR, autophagy or ER stress modulators did not manage to replicate hamartin's endogenous neuroprotective effect. Interestingly, a novel mTORC1/2 inhibitor and promising candidate currently in cancer trials AZD2014 significantly increased neuronal cell death in the context of neuronal ischaemia. A dose response experiment with AZD2014 demonstrated that increased ER stress proteins may play a role in this detrimental effect. Figure 6.1 summarises the findings in this thesis (Chapter 6). Overall, hamartin represents a novel endogenous neuroprotectant and understanding its mechanism and harnessing this potential by identifying a small molecule that could replicate its effects could open a novel therapeutic avenue for the treatment of ischaemic stroke.

Acknowledgements

It has been a privilege to be part of such an amazing lab over the past few years. 'Thank you' doesn't seem sufficient to Professor Alastair Buchan for believing in me through various attempts at funding applications and for providing unwavering support at all times, no matter how busy he was. Also for his words of encouragement at every stage and being utterly un-phased by the news that I was pregnant. Twice.

The project was begun under the supervision of Dr Michalis Papadakis whose original observation this work is based upon. His endless patience in showing me methods that have been pivotal to the data generated for this thesis is in itself worthy of a medal. For always teaching me the reasons behind everything he showed me, striving for scientific excellence to the extent that I can still hear his voice every time I do an experiment – especially if I have any doubt in my mind that it might fall short of his exacting standards. To my shame his command of the English language when it came to reworking drafts of papers and condensing applications to meet word limits proved far superior to mine.

Upon Michalis' departure to run a start-up company aimed at improving treatment for stroke patients, the Senior Post Doc in the lab, Dr Brad Sutherland had the pleasure of inheriting me and my lack of grasp of Prism. He too demonstrated amazing patience reviewing various attempts at presentations and documents often at very short notice and furnished me with the ability to do cell culture. *In vitro* facilities were originally introduced to the lab by Professor Zoran Redzic who worked with us 2011-2012. He became a great friend and was never short of incredibly sensible advice and helped me to keep things in perspective. A recent (welcome) addition to the group, Dr Yvonne Couch has doubled the female presence in the group and taken up where Michalis left off in constantly questioning why we do what we do and most importantly is always 'making science happen'. Dr Gabriele De Luca has been a constant presence and collaborator and encouraged the Clinician Scientist and Teacher within, me providing me with many opportunities to contribute to the Graduate Entry Course and provided moral support during on calls. I have known Professor Christopher Pugh throughout my 10 years in Oxford and he has provided guidance and sound advice throughout and I hope that I have lived up to the aims of OUCAGS. I am incredibly grateful for the funding provided by OUCAGS and over the past few years, Dr Denise Best has been incredibly tolerant in accommodating my constant deviations from the conventional Academic Clinical Fellow route, fighting my corner when she really wasn't obliged to and for being a real advocate for women in Academic Medicine.

Ain Neuhaus is so much more than ‘the other DPhil student in the lab’. He has become a great friend and tremendous support over the past 3 years. Not only does he have a wealth of knowledge of the literature, a natural aptitude for science and a better command of the English language than me, but he is a genuinely altruistic person who will do anything to help. This includes, but is by no means not restricted to helping me with various IT calamities including the (at least) monthly ‘I have lost EVERYTHING’, ‘putting my experiment on’ overnight on a Sunday so I can get an extra day’s worth of work in and finishing experiments that had to be handed over due to the impending deadline of nursery pick-up. He is half of the dynamic duo of ‘Team 4-VO’ and has contributed to method development in this thesis. He is also constantly buying cake to make unnecessary amends for things that Yvonne and I have convinced him are his fault. On the subject of contemporaries, Dr Zita-Rose Manjaly, who has caused just as much trouble as I have by taking a slightly alternative yet identical approach to the ACF programme but is always one step ahead on multiple occasions pointing out the necessary paperwork to be completed and pitfalls to avoid.

Professor Buchan’s PA, Pramodi Majithia has always sought to make me feel part of the team, helped me with various official paperwork conundrums and looked after the whole group, without exception and far exceeded the remit of her job. She also has a stash of chocolate that she maintains as a barometer of whether or not I have another baby on the way……

Rachel Teal is not only an excellent research nurse, but an amazing proof-reader, spotting typos that no one else managed!

My family, latterly for the wrap around childcare that a basic science DPhil necessitates and for always being supportive of my next academic endeavour.

Publications and Presentations Relevant to this Thesis

Publications

Sutherland, B.A., Neuhaus, A.A., Couch, Y., Balami, J.S., DeLuca, G.C., **Hadley. G.**, Harris, S.L., Grey, A.N. and Buchan AM. (2016). The transient intraluminal filament middle cerebral artery occlusion model as a model of endovascular thrombectomy in stroke. *J Cereb Blood Flow Metab.* **36**(2):363-9.

Balami, J.S., Sutherland, B.A., Edmunds, L.D., Grunwald, I.Q., Neuhaus, A.A., **Hadley, G**., Karbalai, H., Metcalf, K.A., DeLuca, G.C. and Buchan, A.M. (2015). A systematic review and meta-analysis of randomized controlled trials of endovascular thrombectomy compared with best medical treatment for acute ischemic stroke. *Int J Stroke* **10**(8):1168-78.

Balami, J.S., Hadley, G.**,** Sutherland, B.A., Karbalai, H., Buchan, A.M. (2015). Reply: Intravenous thrombolysis for ischaemic strokes: a call for reappraisal. *Brain* **138**(Pt 4):e342.

Balami, J.S., **Hadley, G.**, Sutherland, B.A., Karbalai, H. and Buchan, A.M. (2014). Reply: Thrombolysis in acute ischaemic stroke. *Brain* **137**(Pt 6):e282.

Neuhaus, A.A., Rabie, T., Sutherland, B.A., Papadakis, M., **Hadley, G.**, Cai, R. and Buchan, A.M. (2014). Importance of preclinical research in the development of neuroprotective strategies for ischemic stroke. *JAMA Neurol.* May;71(5):634-9.

Balami JS, **Hadley G**, Sutherland BA, Karbalai H, Buchan AM. (2013). The exact science of stroke thrombolysis and the quiet art of patient selection. *Brain* **136**(Pt 12):3528-53.

Hadley, G., De Luca, G.C., Papadakis, M. and Buchan, A.M. (2013). Endogenous neuroprotection: Hamartin modulates an austere approach to staying alive in a recession. *Int J Stroke* **8**(6):449-50.

Papadakis, M., **Hadley, G.**, Xilouri, M., Hoyte, L.C., Nagel, S., McMenamin, M.M., Tsaknakis, G., Watt, S.M., Drakesmith, C.W., Chen, R., Wood, M.J., Zhao, Z., Kessler, B., Vekrellis, K. and Buchan, A.M. (2013). Tsc1 (hamartin) confers neuroprotection against ischemia by inducing autophagy. *Nat Med.* **19**(3):351-7.

Presentations

Hadley G., Papadakis M., Buchan A. (2014). The Potential Role of the Endoplasmic Reticulum Stress Response in Neuroprotection Conferred By Hamartin 8th International Symposium on Neuroprotection and Neurorepair. The Magdeburg Meeting Series. April 9th-12th 2014. Magdeburg, Germany.

Hadley G., Papadakis M., Zhao Z., Buchan A. (2012). Neuroprotective pathways in cerebral ischaemia: could hamartin hold the key to a novel stroke treatment? 7th International Symposium on Neuroprotection and Neurorepair. The Magdeburg Meeting Series. May 2nd-5th 2012. Potsdam, Germany. Also at Oxford Neuroscience Symposium (March 2013) and Academic Medical Forum Trinity Term 30th April 2013: Poster Session, Oxford University Clinical Academic Graduate Scheme (OUCAGS)

Book Chapters

Hadley G, Neuhaus AA, Buchan AM. Lessons from clinical trials-Stroke, in Studies on Atherosclerosis, edited by Rodriguez-Porcel M and Miller JD, Springer (in submission)

Hadley, G., Papadakis, M. and Buchan A.M. (2014). A method of inducing global cerebral ischemia. *Methods Mol Biol.***1135**:111-20.

Table of Contents

List of Figures and Tables

Figures

Tables

Abbreviations

2-VO: two-vessel occlusion

4-VO: four-vessel occlusion

10-NCP: 4'-(N-diethylamino)butyl]-2-chlorophenoxazine

AD: Alzheimer's disease

Akt: Serine/threonine kinase

ALS: amyotrophic lateral sclerosis

AMPA: 2-amino-3-3-hydroxy-5-methyl-isoxazol-4-yl propanoic acid

AMPK: 5' adenosine monophosphate-activated protein kinase

ASPECTS: Alberta Stroke Programme Early CT Score

ATF-4: activating transcription factor-4

ATP: Adenosine-5'-triphosphate

BAD: Bcl-2-associated death promoter

BAX: bcl-2-like protein 4

Bcl-2: B-cell lymphoma-2

BCL-X_L:close homolog of Bcl-2

CA: Cornu Ammonis

CaM: Calmodulin

CBF: cerebral blood flow

Cdk1: Cyclin-dependent kinase 1

CHAPS: 3-[(3-cholamidopropyl)dimethylammonio]-1-propanesulfonate.

CHOP: C/EBP-homologous protein

CT: Computed tomograpy

DAPI: 4',6-diamidino-2-phenylindole

DAPK: death-associated protein kinase

DC: Detergent compatile

DTT: dithiothreitol

ECL: enhanced chemilumininescence

EDTA: ethylenediaminetetraacetic acid

eIF2 alpha: eukaryotic initiation factor 2 alpha

ER: Endoplasmic reticulum

ERAD: ER-associated protein degradation

ERK: extracellular regulated kinase

ERM: ezrin-radixin-moesin

ESCAPE: Endovascular Treatment for Small Core and Anterior Circulation Proximal Occlusion with Emphasis on Minimizing CT to Recanalization Times

EUROHYP-1: European, multicentre, randomised, phase III, clinical trial of hypothermia plus medical treatment versus best medical treatment alone for acute ischaemic stroke

EXTEND-IA: Extending the Time for Thrombolysis in Emergency Neurological Deficits — Intra-Arterial

FoxO1: Forkhead box-containing protein O1

GABA: (γ-aminobutyric acid)

GAP: GTPase-activating protein

GFAP: Glial fibrillary acidic protein

GI: Global ischemia

GSK3: glycogen synthesis kinase 3

HEPES: 2-[4-(2-hydroxyethyl)piperazin-1-yl]ethanesulfonic acid

HERC1: HECT And RLD Domain Containing E3 Ubiquitin Protein Ligase Family Member 1

H_2O_2: Hydrogen peroxide

HBSS: Hank's balanced salt solution

H&E: Haematoxylin and Eosin

Hsp70: heat shock protein 70

ICAM-1: Intercellular Adhesion Molecule 1

i.m: intramuscular

IMPase: inositol monophosphatase

IMS III: Interventional Management of Stroke III

IPC: ischemic preconditioning

IV: intravenous

LAM: lymphangioleiomyomatosis

LDF: Laser Doppler flowmetry

LDH: lactate dehydrogenase

MCA: middle cerebral artery

MCAO: middle cerebral artery occlusion

Merlin: Moesin/ezrin/radixin like protein

MPTP: 1-methyl-4-phenyl-1,2,3,6-tetrahydropyridine

MR CLEAN: Multicenter Randomized Clinical Trial of Endovascular Treatment for Acute Ischemic Stroke in the Netherlands

MR RESCUE: Mechanical Retrieval and Recanalization of Stroke Clots Using Embolectomy

MRC: Medical Research Council

mRS: modified Rankin Scale

mTOR: mammalian target of rapamycin

mTORC1: mammalian target of rapamycin complex 1

mTORC2: mammalian target of rapamycin complex 2

NAD: Nicotinamide adenine dinucleotide

NADE: p75NTR-associated cell death executor

NADPH: Nicotinamide adenine dinucleotide phosphate

NBM: Neurobasal Medium

NIC: Non-ischaemic controls

NF-L: Neurofilament light polypeptide 68 kDa

NINDS: National Institute of Neurological Disorders and Stroke

NMDA: N-methyl-D-aspartate

NO: Nitric Oxide

NVU: Neurovascular unit

OGD: Oxygen Glucose Deprivation

PE: phosphatidylethanolamine

PERK: RNA-dependent protein kinase-like ER eIF2 alpha kinase

PI3K/AKT: Phosphatidylinositol 3-kinase/protein kinase B

Plk1: polo-like kinase 1

PMSF: Phenylmethylsulfonyl fluoride

PRKA: protein kinase, AMP-activated

PTEN: Phosphatase and tensin homolog nutrient

PVDF: Polyvinylidene difluoride

Rheb: RAS-homologue expressed in brain

REVASCAT: Randomized Trial of Revascularization with Solitaire FR Device versus Best Medical Therapy in the Treatment of Acute Stroke Due to Anterior Circulation Large Vessel Occlusion Presenting within Eight Hours of Symptom Onset

rt-PA: recombinant tissue plasminogen activator

ROS: Reactive Oxygen Species

SAD: Synapses of the Amphid Defective

SDS: sodium dodecyl sulfate

SEM: Standard Error of the Mean

Ser: Serine

STAIR: Stroke Therapy Academic Industry Roundtable

SWIFT PRIME: Solitaire with the Intention for Thrombectomy as Primary Endovascular Treatment

SYNTHESIS: Systemic Thrombolysis for Acute Ischemic Stroke

TBC1D7: Tre2-Bub2-Cdc16 (TBC) 1 domain family, member 7

Thr: Theronine

TS: Tuberous sclerosis

TSC: Tuberous sclerosis complex

TSC1: Tuberous sclerosis complex gene 1 (hamartin)

TSC2: Tuberous sclerosis complex gene 2 (tuberin)

TUNEL: Terminal deoxynucleotidyl transferase dUTP nick end labelling

Ulk1: mammalian autophagy-initiating kinase, a homologue of yeast ATG1.

UPR: unfolded protein response

UPLC- QTOF MS: Ultra-performance liquid chromatography tandem quadrupole time-of-flight mass spectrometry

VEGF: vascular endothelial growth factor

XBP: 1: X-box binding protein 1

Chapter 1: General Introduction

1.1 Executive Summary

The holy grail in ischaemic stroke is neuroprotection - the defence of neurons from injury and degeneration. Thrombolysis (NINDS, 1995) and thrombectomy (Balami *et al.,* 2015) are the only current treatments in the UK for acute ischaemic stroke, restoring blood flow to the ischaemic area. There has, to date, been a failure to achieve neuroprotection via pharmacological means (O'Collins *et al.,* 2006). The importance of standardising preclinical research in the development of neuroprotective strategies for ischemic stroke is vital (Neuhaus *et al.,* 2014). Effective neuroprotective treatments would increase the time window for reperfusion and minimise the adverse effects of this phenomenon. Animal models include focal models of ischaemia mimicking human ischaemic stroke. The global model of ischaemia provides mechanistic insight to potential neuroprotective strategies. Strictly a model of cardiac arrest, the global ischaemia model provides a robust finding that the two areas of the hippocampus respond very differently to ischaemia: CA1 neurons exhibit delayed cell death whereas CA3 neurons survive. In addition, CA1 neurons have demonstrated resilience to cell death under certain conditions, namely ischaemic preconditioning, hypothermia and hypoglycaemia. This differential response was instrumental in discovering the endogenous neuroprotective effect of hamartin (Papadakis *et al.,* 2013).

Hamartin (TSC1) is part of the tuberous sclerosis complex, a tumour suppressor which inhibits mTOR. Inhibiting mTOR stimulates productive autophagy and energy conservation and also includes alleviation of the deleterious effects of ER stress via decreased protein synthesis. The post-ischaemic brain is an austere environment which is oxygen, glucose and nutrient deprived. It is therefore not surprising that there are links to the effects of caloric and more specifically dietary restriction. The tuberous sclerosis complex itself has been linked with longevity (Kapahi *et al.,* 2004), where overexpression of TSC1 and TSC2 in *Drosophila* extends lifespan via decreased mTORC1 signalling. Oxygen glucose deprivation is an *in vitro* model of stroke that allows pharmacological screening of compounds and will be used to assess neuroprotection with targeted small molecules in rodent neurons.

The unifying hypothesis is that hamartin modulates an adaptive mechanism that enables survival in times of austerity, such as what occurs in the CA3 region of the hippocampus following global ischaemia. Do caloric restriction and endogenous neuroprotection 'happen to' increase longevity (Blagosklonny *et al.,* 2009) via mTOR or is there an independent evolutionary advantage that we are unaware of? Afterall, the 'older old' reveal that longevity is not necessarily linked to late-life disability and disease (Fontana and Partridge, 2015) and that harnessing the mechanisms driving endogenous neuroprotection could open up a therapeutic avenue leading to protection of the brain in stroke and other neurological diseases.

1.2 Introduction to Stroke

Stroke is the fourth single largest cause of death in the UK and second largest cause of death globally. Significantly, half of all stroke survivors are living with a disability (State of the Nation Stroke Statistics, Jan 2016).

The majority of strokes are ischaemic in nature (85%) and the remainder (15%) are haemorrhagic. Stroke is a medical emergency and should be viewed as a 'brain attack'. Haemorrhagic strokes are caused by rupture of weakened blood vessels. From this point on, the use of the word 'stroke' will refer to ischaemic stroke. Ischaemic stroke is caused by occlusion of blood vessels in the brain by blood clots. Immediately adjacent tissue, the core of the infarct, suffers extensive tissue damage, whereas surrounding the core has reduced cerebral blood flow and metabolism, but may be salvageable following reperfusion; this area has been coined the penumbra (Astrup *et al.,* 1981).

In the macaque model an ischaemic penumbra has been identified for up to 3 hours after the onset of the event. In selected human patients the penumbra may exist for up to 48 hours (demonstrated by DWI (diffusion weighted imaging), PI (perfusion imaging) and PET (positron emission tomography) (Phan *et al*., 2002). The '3 compartment model' for the ischaemic penumbra was suggested by Astrup, Siesjo and Symons in 1977 (Astrup *et al*., 1977), based on a baboon model of focal ischaemia. The first compartment, being of critically hypoperfused tissue cerebral blood flow (CBF) less than 6-10mL/100g/min) which was irreversibly damaged, the second, a compartment of moderately hypoperfused penumbral tissue (CBF <20 mL/100g/min) that was

salvageable and third, a peripheral compartment that was moderately hypoperfused (oligaemia) (Astrup *et al*., 1977). This penumbral tissue is described as being 'dynamic', that is the ischaemic core increases whilst the penumbral tissue decreases with time (Phan *et al*., 2002). The time window upon which thrombolytic trials were originally based is in part due to the finding that in animal models, tissues with a CBF of 15mL/100g/min may remain viable for 3 hours, compared to a CBF of 5mL/100g/min that would only support viable tissue for a maximum of 2 hours (Jones *et al*., 1981).

It has been suggested that the ischaemic core lies predominately within the subcortical white matter and the penumbra in the cortical grey matter (Phan *et al*., 2002). The existence of a penumbra in lacunar strokes is controversial. Lacunar strokes are caused by the occlusion of penetrating arteries that supply deep brain structures. It can be postulated that the absence of collateral vessels in these perforator arteries do not provide the graduated hypoperfusion needed for the creation of a penumbra (Serena *et al.,* 2001). Alternatively, others have used the presence of penumbral tissue to explain the haemodynamic instability observed in some patients (Del Bene *et al*., 2012). Imaging is difficult and acute post mortem tissue is not readily available owing to the good prognosis of these patients, meaning that the exact pathological processes are ultimately poorly understood (Wardlaw *et al*., 2013).

With the noteworthy exception of recombinant tissue plasminogen activator (NINDS, 1995), there have been no treatments translated effectively for stroke patients (O'Collins *et al.,* 2006). One of the major scientific goals in the neurosciences has been to develop so-called neuroprotectants which, if they worked in man, would increase the amount of time we had to image, treat, and restore blood flow to the brain and, if possible, would protect the brain against ischaemia, resulting in less damage. Studies have so far concentrated on suppressing the "ischaemic cascade" which at best amounts to 'damage limitation'. Is it time to approach the problem from a different angle? Could discovering and amplifying endogenous protective mechanisms produce a tangible clinical effect at protecting the brain after stroke (see Section 1.6)?

1.3 Models of Stroke

Pre-clinical research is important to determine pathophysiological mechanisms of stroke as well as assessing novel treatments using both *in vivo* and *in vitro* models. *In vitro* models are more suitable for mechanistic studies—to elucidate the roles of individual cell types (neuronal, glial, vascular, or immune) or for target validation at the molecular level—owing to our ability to control the conditions, intervene more extensively, and use a greater variety of tools than would be possible *in vivo*. However, *in vitro* conditions are no replacement for the complicated *in vivo* setting of the brain.

In *in vivo* models of ischaemic stroke, blood supply to the brain is interrupted, leading to either global or focal ischaemia. Most *in vivo* models are carried out in rats or mice. Global ischaemia provides a mechanistic insight by comparing regions that are vulnerable to ischaemia with those that are resistant (see Section 1.3.3). The main caveat of global ischaemia is that its extent, severity, and duration do not match clinical ischemic stroke; instead, it replicates cardiac arrest (Traystman, 2003). Focal ischaemia models typically involve the occlusion of one of the major cerebral arteries, typically the middle cerebral artery, using mechanical means, vasoconstrictors, or thrombi (Macrae, 2011) and are more representative of clinical ischaemic stroke but they remain imperfect (Sutherland *et al.,* 2012; Neuhaus *et al.,* 2014).

Seventeen years ago, the Stroke Therapy Academic Industry Roundtable (STAIR) emphasized the importance of targeting multiple mechanisms and multiple cell types in the treatment of stroke (STAIR, 1999). These criteria addressed numerous shortcomings in categories such as blinding, randomization, exclusion criteria, sample size calculations, and transparent reporting, proposing ways in which these categories could be improved on. It was hoped that if a neuroprotectant fulfilled these criteria preclinically then it would improve the chances of clinical success.

However, notable compounds such as NXY-059, a nitrone with free radical scavenging ability, had extensive preclinical data, fulfilling the STAIR criteria and yet still failed to translate efficacy to the clinic (Diener *et al.,* 2008), questioning the models and methodologies used.

1.3.1 Focal models of ischaemia

Focal ischaemia involves the occlusion of a single artery in the brain, resulting in an infarct with a core and penumbra. The core has the lowest level of cerebral perfusion and the tissue undergoes necrosis and is deemed unsalvageable. The degree of cerebral perfusion depending upon the distance from the infarct was described in the 1970s (Symon *et al.,* 1977) and the area surrounding the core was described as the 'ischaemia penumbra' (Astrup *et al.,* 1981). The core infarct contains cells that are structurally and metabolically compromised, whereas the cells in the penumbra are metabolically paralysed, but structurally intact.

Models of focal ischaemia are typically induced by surgical occlusion of an artery or placement of a clot. Other variants include activating thrombosis and injecting vasoconstrictors (see Table 1.1). The most popular variant is the reversible intraluminal filament model (Longa *et al.,* 1989) in which middle cerebral artery occlusion is achieved using a remotely inserted filament into the internal carotid artery that can be retracted to reperfuse the tissue. Unfortunately, these models do not precisely reproduce the underlying pathophysiology of ischaemic stroke.

Model	Brief Description	Advantages	Disadvantages
Intraluminal filament middle cerebral artery occlusion (MCAO)	Filament inserted into internal carotid artery to block origin of middle cerebral artery (MCA).	Reproducible, permanent or transient, no craniectomy	No visual occlusion confirmation, haemorrhage risk
Direct MCA ligation or cauterization	Transient ligation of MCA with clip or suture, or permanent cauterisation of MCA through craniectomy	Reproducible, control infarct size and location, low mortality	Requires craniectomy, technically challenging
Photothrombosis	Rose Bengal dye injected intravenous (iv) and laser or cold white light shone over cortex to induce photothrombosis	Reproducible, control infarct location, low mortality	Limited deficit due to small infarct, early vasogenic oedema
Endothelin-1 injection	Topical or intraparenchymal injection of endothelin-1 to cause localised transient vasoconstriction	Reproducible, control infarct size and location, low mortality	Requires craniectomy, dependent on consistency of endothelin-1 potency from batch to batch
Thromboembolism	Injection of autologous blood clots into the internal carotid artery to occlude the MCA origin	Closest to clinical stroke, suitable for thrombolysis studies	Less reproducible, less control over infarct size and location, variability, secondary clot formation

Table 1.1: Table of most commonly used focal stroke animal models Adapted from Macrae (2011).

1.3.2 Global ischaemia

Analogous to the effect on the brain of the human clinical condition of cardiac arrest rather than stroke, global models of ischaemia provide mechanistic insight into ischaemia of the entire cerebrum. There are two main models of global ischaemia, the two vessel occlusion (2-VO) bilateral common carotid artery occlusion model with hypotension (Eklöf and Siesjö, 1972) and the 4-VO (Pulsinelli and Brierley, 1979). Both models display the phenomenon of delayed selective hippocampal vulnerability (see 1.3.3). In the 2-VO model, in addition to bilateral carotid artery occlusion, hypotension is generally produced by bleeding alone, although in a few cases this has been accompanied by addition of agents (Traystman, 2003).

The 4-VO model involves bilateral occlusion of the vertebral and carotid arteries resulting in lack of blood flow to the striatum, hippocampus and cortex (See Figure 1.1). It is two-step procedure with permanent cauterization of the vertebral arteries and identification and preparation of the carotid arteries occurring on day 1 with the ischaemic insult on day 2 (see Chapter 2). Although the 4-VO model is surgically more demanding and time consuming, the 2-VO model could produce data confounded by the drugs used to achieve hypotension which could, in turn confound data interpretation (Traystman, 2003). In addition exsanguination and reperfusion are technically difficult. The 4-VO model was selected for the studies contained in this thesis and will be discussed in more detail in Chapter 2.

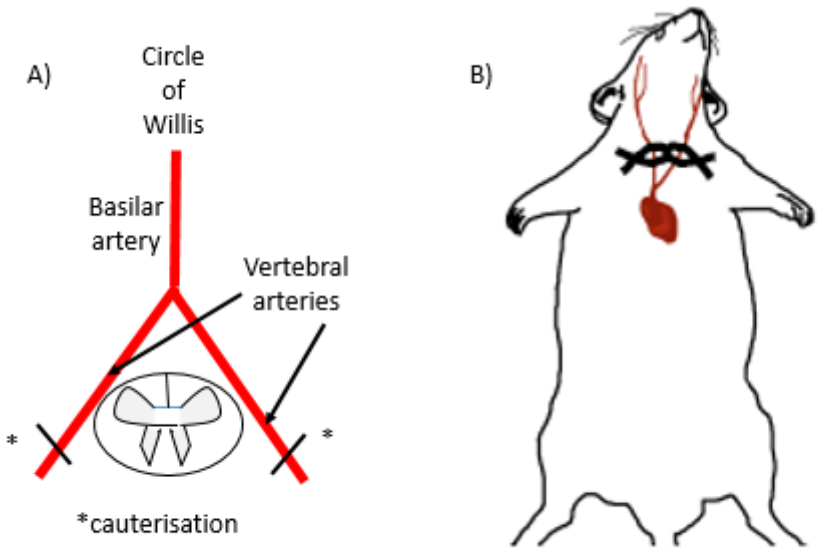

Figure 1.1: Four Vessel Occlusion Model A) Cauterisation of the two vertebral arteries 24 hours prior to 4-VO during preparatory surgery. B) Occlusion of the two common carotid arteries by aneurysm clips during 4-VO. This results in near complete cessation of blood flow to the cerebrum. Adapted from Papadakis, Hadley *et al.,* 2013.

1.3.3 Selective hippocampal vulnerability

The evaluation of differential susceptibility to neuronal injury in the face of ischaemia requires the study of brain regions with anatomically proximate yet physiologically distinct neuronal populations that may respond uniquely to ischemic stress. The hippocampus, a structure important for anterograde memory, fits these criteria. It has four main areas called Cornu Ammonis (CA) 1-4 which lie in close proximity to one another, share a common vascular supply and yet demonstrate selective vulnerability to a variety of insults (see Figure 1.2). The differential response in the hippocampus to ischaemia within CA3 cells (tolerant) and CA1 (susceptible) is well documented (Kirino, 1982).

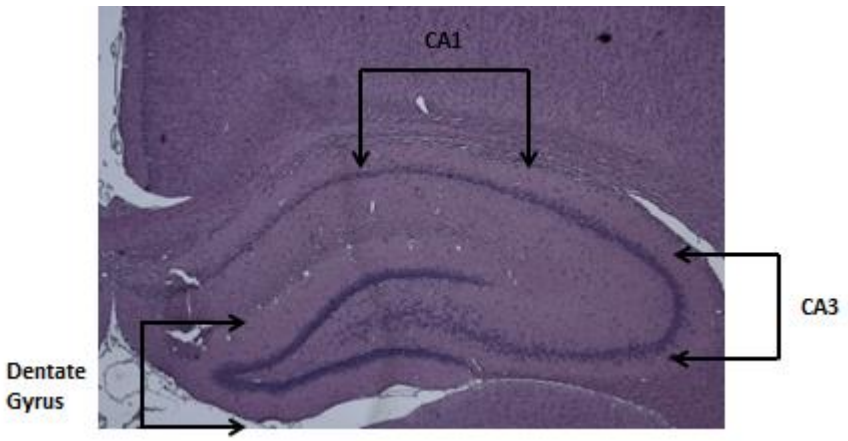

Figure 1.2 The rodent hippocampus The hippocampus contains a distinct neuronal layer that is composed of a number of CA regions. The locations of CA1, CA3 and the dentate gyrus are indicated.

CA1 undergoes selective neuronal injury/loss in epilepsies, degenerative dementias, and stroke compared to CA3 which remains relatively intact (Mattson *et al.,* 1989). An early clinical manifestation of Alzheimer's disease is the loss of 'sense of place' and indeed, examination of the hippocampus demonstrated a propensity for neurofibrillary tangles in the CA1 region of the hippocampus and layer II of the entorhinal cortex. The CA3 region of the hippocampus was largely spared and involvement of layer IV of the entorhinal cortex varied (Hyman *et al.,* 1984). In 2014, the Nobel Prize in Physiology or Medicine was awarded to John O'Keefe who identified 'place cells' by recording CA1 neurons in the hippocampus that were activated when a rat assumed a certain position in its environment providing an inner map (O'Keefe and Dostrovsky, 1971) and May-Britt Moser and Edvard Moser who identified 'grid cells', neurons in the entorhinal cortex that were activated when

the rat passed specific locations **(**Hafting *et al.,* 2005)**.** Networks between hippocampal 'place' cells and entorhinal 'grid cells' are said to be a physiological global positioning system.

The peculiar distinction amongst neuronal groups has led to these regions being labelled 'Sommer's vulnerable sector' (CA1) and 'Spielmeyer's resistant sector' (CA3) (Duvernoy *et al.,* 2005). The mechanism by which these hippocampal neuronal regions differ in their susceptibility to homeostatic challenges remains poorly understood despite extensive study. The aetiology of selective hippocampal degeneration in the face of anoxia has been of particular interest. Studies dating back to the early 1920s focused on differential arrangements of penetrating arteries into the different CA regions. Uchimura described that the vulnerable sector, CA1 was supplied by long arteries, compared to the shorter arteries of CA3 (Uchimura, 1928). The hypothesis put forward was that longer arteries predisposed to increased sensitivity to blood pressure variation and hence selective injury. The vascular theory was further propagated by Spielmeyer who proposed that epileptic seizures induce vascular spasm leading to some injury (Spielmeyer, 1927; Spielmeyer, 1930). Interestingly, the vascular arrangement in the hippocampus is similar to that which supplies the cerebellar Purkinje layer, which is also particularly vulnerable to anoxic insult (Cervós-Navarro and Diemer, 1991). The vascular theory remained en vogue until later investigators demonstrated intrinsic neuronal differences in metabolism, synapses and/or receptors (Duvernoy *et al.,* 2005) which are further discussed below.

An authoritative addition to the literature on selective hippocampal degeneration was put forward by Friede who demonstrated histochemical differences between CA sections (Friede, 1966). It was noted that CA1 differed from CA2 and CA3 in terms of altered levels of zinc, lactate dehydrogenase, Nicotinamide adenine dinucleotide (NAD)-diaphorase acetyl cholinesterase and acid phosphatase, fuelling support to the physical chemical hypothesis originally proposed by Vogt in the 1930s (Duvernoy *et al.,* 2005).

The seminal work by Friede shifted the focus of hippocampal research into exploring other metabolic, synaptic and receptor candidates, but the results have been conflicting (Duvernoy *et al.,* 2005). Such theories include the over secretion of glutamate from CA3 acting on CA1 via Schaffer's collaterals, over-activity of N-methyl-D-aspartate (NMDA) glutamate receptors leading to differential excitotoxic degeneration of CA1 neurons, dysregulation of γ-Aminobutyric acid (GABA)-ergic interneuronal connections, intracellular calcium induced

cellular toxicity, free radical mediated neuronal injury and apoptosis. More recent explanations include differences in response to superoxide and dealing with iron (Wilde *et al.,* 1997) the varying levels of caspase activity between the two regions (Chen *et al.,* 1998), and the differential downregulation of glutamate transporters in astrocytes (Ouyang *et al.,* 2007). A recent paper has suggested that bone-marrow mononuclear cells reduce neurodegeneration in hippocampal CA1 layer via modulation of the microglial response following transient global ischaemia in rats (Ramos *et al.,* 2013). Despite these important contributions, the origin of selective vulnerability of hippocampal neurons to anoxia has continued to evade understanding.

The evolutionary advantage for the resistance of CA3 neurons to an hypoxic insult is not well understood and indeed, there remains the distinct possibility that it could in fact be a maladaptive response that has persisted.

Memory in the animal kingdom could promote survival by allowing escape from predators and dangerous situations. However, memories of traumatic events could equally lead to detrimental psychopathology (Maren, 2011). In humans, this correlates with the inability to extinguish conditioned fear observed in anxiety disorders such as posttraumatic stress disorder (Wolpe *et al.,* 1988).

The functions of CA1 and CA3 in memory encoding and retrieval have been summarised. CA3 is responsible for the rapid encoding of new information and interacts with CA1 to recode and stabilise the information in the neocortex permitting recall from long term memory (Ji and Maren, 2008). These authors used a paired auditory conditional stimulus with an aversive footshock. It was found that whereas both CA1 and CA3 were involved in the acquisition of context-dependent extinction, only lesions in CA1 impaired it. Therefore only CA1 is necessary for contextual memory retrieval (Ji and Maren, 2008).

For 30 years of neuroprotection research, the research community has been exploring the mechanism of neuronal cell death particularly in the CA1 hippocampal cells and trying to discern mechanisms which account for the exquisite susceptibility of these cells following ischaemia. Instead of asking the age old question of why CA1 cells die, why not look at what it is responsible for CA3 cell survival despite the same ischaemic insult? Otherwise vulnerable CA1 cells have demonstrated resilience to cell death under certain conditions, namely ischaemic preconditioning, hypothermia and hypoglycaemia. The differential response allows us to investigate

the molecular determinants of either resistance or vulnerability in a given region, thus potentially uncovering endogenous neuroprotective strategies (Papadakis *et al.,* 2013).

1.3.4 Ischaemic Preconditioning

Brief periods of ischaemia, sufficient to induce cellular stress but not long enough to cause cell death, confer tolerance on the CA1 neurons to subsequent ischaemic insults. This phenomenon is called ischaemic preconditioning (IPC) (Dirnagl *et al.,* 2009) and was first observed in a canine model of coronary ischaemia (Murry *et al.,* 1986) and noted in the brain a few years later (Kitagawa *et al.,* 1990). Early phase preconditioning occurs within minutes of the preconditioning insult whereas late phase is observed at 48-72 hours and the effect decreases with time.

There are multiple mechanisms through which IPC can provide neuroprotective effects. Changing permeability of ion channels is thought to underlie the early phase whereas protein synthesis is required for the late phase (Gidday, 2006). Other mechanisms include the activation of protein kinases, the induction of transcription factors and induction of intermediate-early genes. In addition, nitric oxide (NO) could exert protective effects via activation of the Ras/extracellular regulated kinase (ERK) 1/2 pathway. Furthermore, free radicals produced during preconditioning could induce tolerance to subsequent insults via the production of neuroprotective heat shock proteins, antioxidant enzymes and antiapoptotic proteins (Pignataro *et al.,* 2009). Maturation of injury is slowed and delayed by briefer durations of ischaemia but once ischaemic thresholds are exceeded, cells will die (Colbourne *et al.,* 1999), with temperature (van der Worp *et al.,* 2007) and glucose (van der Worp and van Gijn, 2007) importantly modulating the rate of cell death.

1.3.5 *In vitro* Models of Stroke

In these models, either cell cultures (primary cortical or hippocampal) or organotypic slice preparations are deprived of oxygen and glucose, or exposed to excitotoxic agents (e.g. glutamatergic agonists) to mimic ischaemic conditions. *In vitro* OGD induces oxidative and metabolic stress, excitotoxity, autoinflammatory responses and apoptosis. It can also be used to model reperfusion post-stroke via the addition of complete media to the cells following the defined period of OGD. The reductionist nature of these models comes at the

cost of similarity to actual strokes: although simple to perform, the influence of different physiological and homeostatic factors on cell death cannot be evaluated (Neuhaus *et al.,* 2014).

In vitro models are excellent for mechanistic investigations as they are more amenable to knockdown/overexpression methods enable study of cell-specific responses more conveniently than selective knockout animals (Papadakis *et al.,* 2013). These models are also useful to screen pharmacological compounds before moving to *in vivo* models (Tsvetkov *et al.,* 2010).

1.4 The Neurovascular Unit

Increasingly, the emphasis in stroke research is on the neurovascular unit (NVU), a conceptual approach that addresses interactions between the vasculature, glia and neurons instead of targeting a single cell type (Arai *et al.,* 2011). This is particularly relevant for oxidative stress research, as stroke causes superoxide- and peroxynitrite-mediated vascular damage and blood-brain barrier breakdown (Gürsoy-Ozdemir *et al.,* 2004). Indeed, the promising candidate neuroprotectant edaravone not only exhibits protective effects on neurons, but also reduces oxidative stress damage in astrocyte and endothelial cultures (Lee *et al.,* 2010a). It is not currently possible to distinguish between direct neuronal and broader neurovascular effects in the context of clinical trials, but the preclinical evidence suggests that the putative beneficial effects of antioxidants could be at least partly due to protection of the NVU. One mechanism by which antioxidants might exert protective effects is through restoration of microvascular patency. Recanalisation does not always result in reperfusion of the affected tissue, which diminishes the potential benefit of thrombolysis (Soares *et al.,* 2010). Similarly, no-reflow and post-ischemic hypoperfusion are a well-established concept in preclinical studies, where opening the experimentally occluded arteries does not fully restore flow to the developing infarct (Ames *et al.,* 1968; Del Zoppo, 2013). There are multiple explanations for these phenomena, including adhesion of leukocytes and platelets in the affected region leading to obstruction of capillaries and venules, altered vascular tone and swelling of astrocytic endfeet surrounding the microvessels (Hossmann, 1997). More recently, the constriction of pericytes – vascular mural cells closely surrounding the endothelium – have been implicated in no-reflow. Notably, preventing oxidative and nitrative stress through scavenger compounds restores capillary patency in mice following stroke (Yemisci *et al.,* 2009). In cerebellar slices, ischaemia resulted in pericyte constriction and death in rigour, which

could be reduced by nitric oxide synthase blockers but not by reactive oxygen species (ROS) scavengers (Hall *et al.,* 2014). Nonetheless, these recent publications highlight the importance of neurovascular function following stroke, and indicate potential roles for antioxidants in achieving reperfusion.

However, the picture is further complicated by reperfusion injury. Although the clinical benefit of reperfusion is clearly supported by a great deal of evidence (see Section 1.5), we also know that the NVU is susceptible to further damage when flow is restored, and in some animal models of late reperfusion there is a marked increase in blood-brain barrier damage, oedema and infarct size (Aronowski *et al.,* 1997; Yang and Betz, 1994). This is again a multifactorial complication, featuring multiple forms of cell death and inflammatory damage. Inflammation in particular is potentially amenable to antioxidant therapies, given the propensity of inflammatory cells to produce various free radical species (Eltzschig and Eckle, 2011). The exact radical species involved are uncertain, with both reactive oxygen and nitrogen species being implicated. Some studies have reported beneficial effects from NO donors through ROS scavenging following ischaemia/reperfusion (Pluta *et al*., 2001).

1.5 Stroke Therapy

No effective treatment has been translated from animal studies to stroke patients with the exception of recombinant tissue plasminogen activator (NINDS, 1995) for achieving reperfusion, and antiplatelet agents for preventing further coagulation. Edaravone was approved in 2001 in Japan for use in ischemic stroke within 24 hours (Lapchak, 2010; Amaro and Chamorro, 2011). It is a low molecular weight, lipophilic compound that readily crosses the blood-brain barrier and is a scavenger of hydroxyl, peroxyl, and superoxide radicals. The neuroprotective effects of edaravone are not thought to be solely due to its scavenging ability, but also to inhibition of lipoxygenase and the oxidation of low density lipoprotein in addition to combating microglia-induced neurotoxicity, suppressing delayed neuronal death and reducing inflammation (Lapchak, 2010). The mixed results from clinical trials suggest why it is not more widely used.

In the past few months, evidence for acute endovascular intervention has become compelling, despite the fact that other trials (Interventional Management of Stroke (IMS) III, Systemic Thrombolysis for Acute Ischemic Stroke (SYNTHESIS Expansion) and Mechanical Retrieval and Recanalization of Stroke Clots Using

Embolectomy (MR RESCUE)), had failed to demonstrate benefit (Broderick *et al.,* 2013; Ciccone *et al.,* 2013; Kidwell *et al.,* 2013). Reasons for the lack of positive findings in these trials have been suggested such as lack of pretreatment imaging to confirm proximal intracranial arterial occlusion, a long time interval before intra-arterial treatment was commenced, and limited use of 'third generation' mechanical thrombectomy devices such as retrievable stents (Berkhemer *et al.,* 2015).

In the Multicenter Randomized Clinical Trial of Endovascular Treatment for Acute Ischemic Stroke in the Netherlands (MR CLEAN) trial, a multicentre study with 500 patients (n=233 intra-arterial treatment and n= 267 to usual care) in patients with acute ischemic stroke caused by a proximal intracranial occlusion of the anterior circulation, intra-arterial treatment administered within 6 hours after stroke onset produced a significant increase in functional independence in daily life (0-2 score on the modified Rankin Scale (mRS) at 90 days) without an increase in mortality (Berkhemer *et al.,* 2015).

The Endovascular Treatment for Small Core and Anterior Circulation Proximal Occlusion with Emphasis on Minimizing computed tomography (CT) to Recanalization Times (ESCAPE) Trial, a large multicentre trial was recently terminated early due to highly statistically significant efficacy (Goyal *et al.,* 2015), following findings from MR CLEAN study (Berkhemer *et al.,* 2015). In patients with acute ischemic stroke with a proximal vessel occlusion, a small infarct core, and moderate-to-good collateral circulation, rapid endovascular treatment improved functional outcomes (using modified Rankin Scale) and reduced mortality.

Randomized Trial of Revascularization with Solitaire FR Device versus Best Medical Therapy in the Treatment of Acute Stroke Due to Anterior Circulation Large Vessel Occlusion Presenting within Eight Hours of Symptom Onset (REVASCAT) demonstrated reduced disability and increased functional independence using the modified Rankin Scale (Jovin *et al.,* 2015).

The Solitaire with the Intention for Thrombectomy as Primary Endovascular Treatment (SWIFT PRIME) trial also demonstrated that treatment within 6 hours after symptom onset resulted in improved functional outcomes at 90 days again measured using the modified Rankin Scale (Saver *et al.,* 2015).

Another trial that was stopped early due to clear signs of efficacy was the Extending the Time for Thrombolysis in Emergency Neurological Deficits — Intra-Arterial (EXTEND-IA) trial, that demonstrated treatment within 4.5 hours of symptom onset improved reperfusion, early neurologic recovery, and functional outcome, again measured by the modified Rankin scale (Campbell *et al.,* 2015).

The overwhelming efficacy of the latter endovascular trials demonstrate that the 'art of patient selection' (Balami *et al.,* 2013) is pivotal in identifying patients who stand to gain the most from intervention, with imaging key in arriving at the most appropriate therapeutic decision. In a recent meta-analysis of 2,531 patients, there was a clear evidence for improvement in functional independence with endovascular thrombectomy compared to standard medical care suggesting that endovascular thrombectomy should be considered the standard effective treatment alongside IV thrombolysis in eligible patients (Balami *et al.,* 2015).

Nicotinamide adenine dinucleotide phosphate (NADPH) oxidase inhibitors have shown promise, but are yet to be validated in clinical trials. They target an enzymatic source of reactive oxygen species, rather than the downstream ischaemic cascade, therefore offering the potential of damage limitation (Sutherland *et al.,* 2012). There however remains a dearth of prospective candidates in stroke therapy, meaning that further research in this area is vital.

Immunotherapy is also a current approach under consideration. GSK249320 is a monoclonal antibody that inhibits myelin-associated glycoprotein (MAG). Levels of MAG have been shown to increase after stroke (Li and Carmichael, 2006) and removing its inhibitory effect could allow neurite sprouting and growth, permitting new neural connections to be formed (Irving *et al*., 2005).

Studies in rodents have shown counteraction of MAG-mediated inhibition led to behavioural recovery which was associated with neurite outgrowth following cortical injury (Irving et al., 2005; Thompson et al., 2006). In a small study of nine squirrel monkeys receiving GSK249320, started 24 hours after a focal cortical ischemic infarct at one week intervals over 6 weeks (Barbay *et al.,* 2015) , functional recovery was observed . Recent safety (Abila et al., 2013) and tolerability studies have been conducted in humans (Cramer et al., 2013).

1.6 Endogenous Neuroprotection

In the rodent model of global transient ischaemia (Section 1.3.2), the hippocampus provides an excellent natural experiment. The CA1 neurons are vulnerable to the insult whereas the CA3 cells are resistant. Researchers have until now tried to understand what makes CA1 neurons die. Instead, we decided to ask why CA3 neurons survive, a phenomenon known as endogenous neuroprotection. Recently a protein implicated in tuberous sclerosis has been linked to neuroprotection following ischaemic stroke (Papadakis *et al.,* 2013). Proteomic analysis revealed that the protein encoded by tuberous sclerosis complex *Tsc1*, called 'hamartin', was associated with the resistive properties of CA3. Hamartin was selectively and significantly induced in the CA3 region of the hippocampus following global ischaemia (Papadakis *et al.,* 2013). Hamartin expression was also associated with neuroprotective preconditioning of the otherwise vulnerable CA1 cells. Hamartin is part of the phosphatidylinositol 3-kinase (PI3K)/protein kinase B pathway. *In vivo*, hamartin is the protein product of the gene *Tsc1* and tuberin is the protein product of the gene *Tsc2*. Hamartin and tuberin bind to form the tuberous sclerosis complex (TSC), a tumour suppressor (Jozwiak, 2006) which inhibits the mammalian target of rapamycin complex 1 (mTORC1). The mechanism of TSC-induced mTOR inhibition is via its GTPase activating protein activity toward Ras homolog enriched in brain (Rheb). Inhibiting mTORC1 reduces energy consumption by preventing protein synthesis and by promoting recycling of existing proteins, a cellular austerity mechanism called productive autophagy (see Figure 1.3).

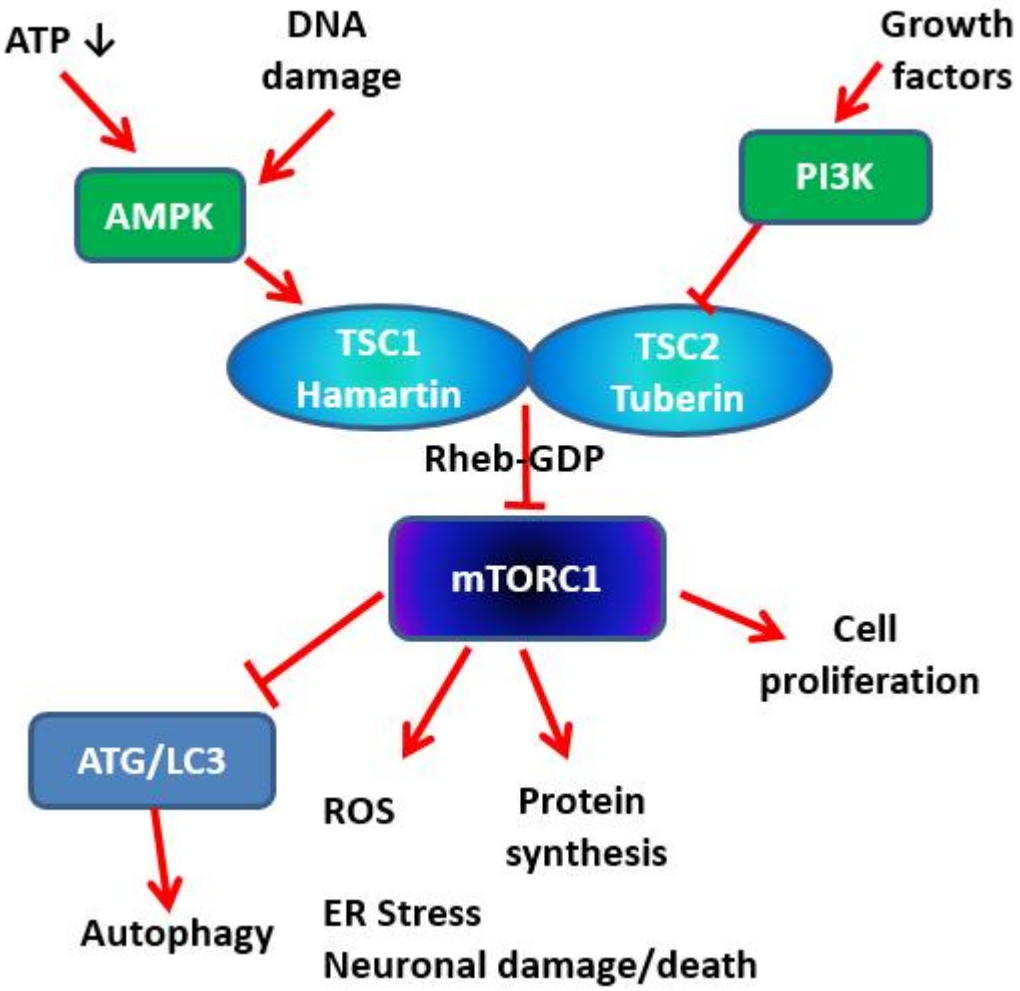

Figure 1.3 Hamartin's role in the mTOR pathway Hamartin together with its binding partner, tuberin mediate three inputs to regulate mTOR activity: growth factor signals, amino acids and ATP availability, therefore regulating cell growth. mTOR is implicated in transcription, ubiquitin-dependent proteolysis, autophagy, membrane trafficking and microtubule and actin cytoskeleton dynamics. mTOR is activated by the active GTP-bound form of the GTPase rheb. The TSC complex forms a GTPase activating protein (GAP) complex which catalyses the switch from the active GTP-bound rheb to the inactive form (GDP-bound rheb), thus inhibiting mTOR. When the inhibitory effect of the TSC complex is removed, mTOR is unregulated which results in uncontrolled protein synthesis and inhibition of autophagy.

1.6.1 Tuberous sclerosis

Prior to the implication of hamartin in endogenous neuroprotection, TSC's only medical association was with the developmental disease, tuberous sclerosis (TS). TS belongs to a family of phakomatoses (including neurofibromatosis) which are ectodermal in origin and have benign cutaneous lesions associated with neurological disorders. Désiré-Magloire Bourneville, a French neurologist, first described the potato-like consistency of gyri with hypertrophic sclerosis in 1880 (Bourneville, 1880). The frequency of TS has been reported at 1 in 12,000 to 1 in 14,000 in those less than 10 years of age (O'Callaghan *et al.,* 1998). Hamartin and tuberin are expressed in a plethora of tissues (Johnson *et al.,* 2001) and accordingly, TS is a multisystem disease with variable penetrance. Mutations in TS genes lead to disrupted cell division, abnormal cell differentiation, dysregulated cell size control and abnormal cellular migration (Crino *et al.,* 2004), resulting in cortical lesions, such as tubers, subependymal nodules and subependymal giant-cell tumours (Curatolo *et al.,* 2008) . The clinical manifestations of brain lesions in TS tend to be epilepsy, cognitive impairment and autism. Large dysplastic neurons (the most prominent abnormal tuber cell type), have disrupted radial orientation in the cortex and abnormal dendritic arborisation with a GABA transport defect and low GABAergic inhibition (Calcagnotto *et al.,* 2005). Epileptogenesis is a result of diminished neuronal inhibition, secondary to molecular changes of GABA receptors in giant cells and dysplastic neurons and enhanced excitation which are secondary to molecular changes of glutamate receptors in dysplastic neurons. Glutamatergic synapses are also altered as a result of loss of TSC genes (Tavazoie *et al.,* 2005).

1.6.2 The Tuberous Sclerosis Complex

The gene *Tsc1* encodes for hamartin (chromosome 9q34) (van Slegtenhorst *et al.,* 1997) and the gene *Tsc2* encodes for tuberin (chromosome 16p13.3) (European Chromosome 16 Tuberous sclerosis Consortium, 1993). *Tsc1* interacts with *Tsc2* with high affinity via its coiled-coiled domain (Inoki and Guan, 2009) to form heterodimers (Plank *et al.,* 1998, van Slegtenhorst *et al.,* 1998). Hamartin stabilises tuberin by inhibiting its interaction with HERC1 ubiquitin ligase (Chong-Kopera *et al.,* 2006). Tuberin interferes with homomeric dimerization of hamartin via the coiled-coiled domain and keeps hamartin in a soluble form in the cytosol (Nellist *et al.,* 1999). *Tsc1* can augment the expression of the *Tsc2* product tuberin by inhibiting its ubiquitination

(Benvenuto *et al.,* 2000). Missense mutations in TSC2 tend to cluster in the GTPase activating protein (GAP) binding domain (exons 35 through 39) (Maheshwar *et al.,* 1997). A more recent discovery is that Tre2-Bub2-Cdc16 (TBC) 1 domain family, member 7 (TBC1D7) is a core component of the TSC-TBC complex and regulates Rheb and mTORC1 signalling in response to alterations in specific cellular growth conditions to control downstream cellular processes (Dibble *et al.,* 2012). TBC1D7 knockdown decreases the association of TSC1 and TSC2 leading to decreased Rheb-GAP activity, without effects on the localization of TSC2 to the lysosome. It results in increased mTORC1 signalling, delayed induction of autophagy, and enhanced cell growth under poor growth conditions (Dibble *et al.,* 2012). Therefore, normal function of TSC is vital for controlling mTOR and subsequent downstream effects.

1.6.3 Hamartin

Hamartin, the protein product of TSC1, is a 160kDa protein (in the brain) containing 1164 amino acids (Figure 1.4). Residues 1-418 of hamartin interact with residues 302-430 of tuberin. While hamartin and tuberin binding is critical to maintain an effect on mTOR function, *Tsc1* overexpression is sufficient to suppress cell proliferation even in the absence of TSC2 (Miloloza *et al.,* 2002). Hamartin and tuberin form heterodimers *in vivo* with high affinity, however, Hamartin can also form homomeric protein complexes (Rosner et al., 2008). The TBC1D7-binding site of TSC1 was localised to the C-terminal region of the coiled-coil domain (residues 939-977) (Santiago *et al.,* 2014). A recent crystal structure of the TSC1-TBC1D7 demonstrates a predominantly hydrophobic interface involving the α4 helix of TBC1D7 at residues 939-992 (Qin *et al.,* 2016). Every TBC1D7 protein interacts with two parallel TSC1 helices from two TSC1 molecules. This indicates that TBC1D7 could stabilise TSC complexes potentially by tethering the C-terminal portions of two TSC1 coiled-coils (Qin *et al.,* 2016).

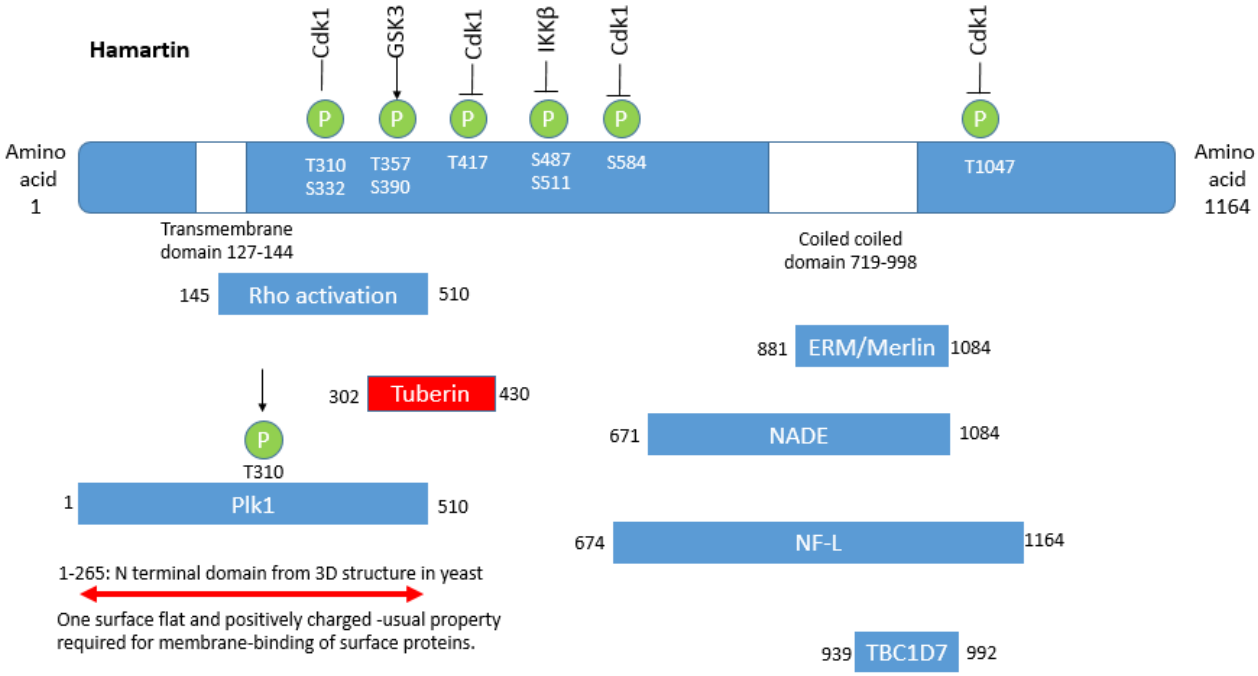

Figure 1.4: Hamartin's amino acid sequence, binding and phosphorylation sites. The 3D structure of TSC1 in yeast spans the N-terminal region (Sun *et al.,* 2013). Key binding and phosphorylation sites are demonstrated Cdk1: Cyclin-dependent kinase 1, GSK3: glycogen synthesis kinase 3, IKKβ: IkappaB kinase beta, ERM: ezrin-radixin-moesin, Merlin: Moesin/ezrin/radixin like protein, NADE: p75NTR-associated cell death executor , NF-L Neurofilament light polypeptide 68 kDa, Plk1: polo-like kinase 1, TBC7 TBC [Tre-2/Bub2/Cdc16] 1 domain family member 7. (Rosner *et al.,* 2008; Qin *et al.,* 2016).Schematic: not to scale.

The first 3D structure of TSC1 (Figure 1.5) has recently been published in yeast (Sun *et al*., 2013). Human TSC1 demonstrates sequence homology with the yeast TSC1 (Matsumoto *et al*., 2002), with the most conserved region being the hTSC1 region which spans the N-terminal (approximately 265 residues) which contains the bulk of disease-associated TSC1 mutations (Sun *et al*., 2013).

TSC1 and TSC2 have no obvious sequence homology with other proteins, with the exception of the TSC2 GAP domain which has sequence homology with the Rap family of small G-proteins (Sun *et al.,* 2013). This coupled with challenging biochemical properties mean that crystal and NMR structures have not been forthcoming (Sun *et al*., 2013).

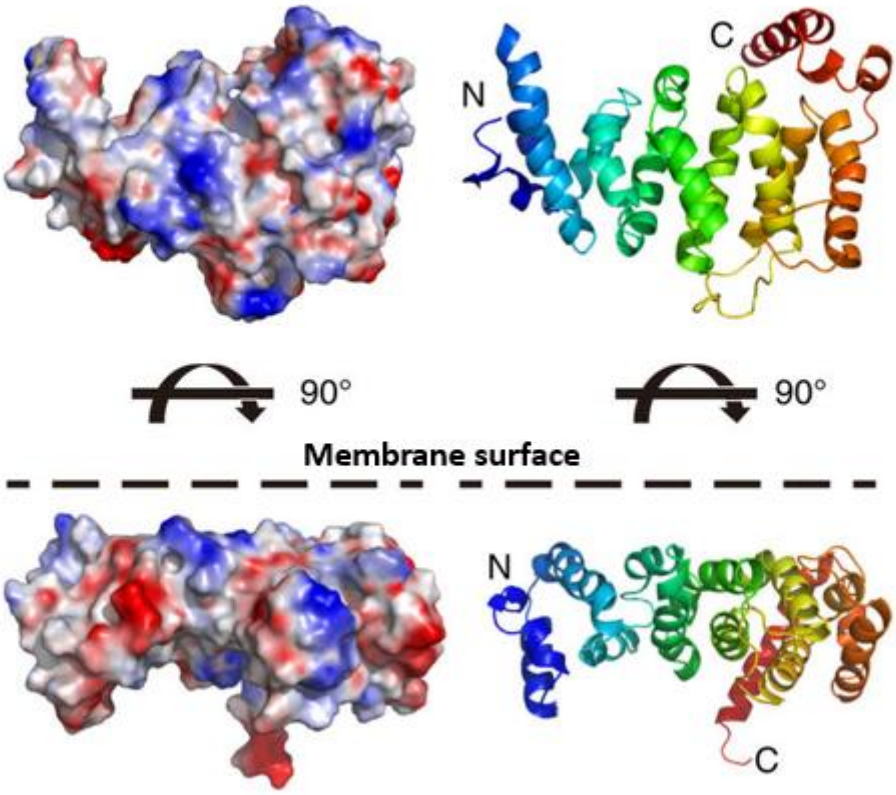

Figure 1.5 Proposed membrane-binding surface of human TSC1-NTD Reproduced from Sun *et al.,* 2013. Two orthogonal views of hTSC1-NTD are shown in top and bottom panels. Electrostatic surfaces (left) and cartoon views (right). The flat and positively charged top surface of the upper orientation is predicted to have a role in membrane binding.

Explanations for the function of TSC1-NTD in TSC1 stability (Sun *et al*., 2013) include facilitation of the localisation of tuberin to the membrane, when acting as a tumour suppressor (Cai *et al*., 2006). One of the surfaces of the expected human TSC1-NTD structure is flat and positively charged which is a usual property required for membrane-binding of surface proteins (Figure 1.5) (Sun *et al*., 2013). In addition, TSC1-NTD may protect the TSC1 structure components required by the protein degradation system. Indeed, TSC1-NTD is essential for TSC1 oligomerization and aggregation (Hoogeveen-Westerveld *et al.,* 2010)

1.6.3.1 Cell morphology

TSC1 has been shown to regulate cell morphology by influencing the actin-based cytoskeleton and cell adhesion (Lamb *et al.,* 2000; Tavazoie *et al.,* 2005). Indeed, following ischaemia reperfusion, CA3 cells actively

preserved their cytoskeletal integrity (Papadakis *et al.,* 2013). It is postulated that TSC1 could be required for the proper subcellular localisation of tuberin and acts as a tuberin-localising scaffolding protein through interactions with the ezrin-radixin-moesin (ERM) family and neurofilament-L (Astrinidis and Henske, 2005). It has been suggested that hamartin inhibits tumour formation by regulating cellular adhesion through the actin-binding proteins of the ERM family and Rho (Jozwiak *et al.,* 2005; Lamb *et al.,* 2000). Due to its subcellular localisation, it has been postulated that hamartin might convey information regarding cell adhesion to the nucleus (Lugnier *et al.,* 2009). Therefore, hamartin is heavily involved in the regulation of cell morphology.

1.6.3.2 Cell cycle

Hamartin has been shown to negatively regulate cell proliferation (Miloloza *et al.,* 2000) and this can occur independently of tuberin (Miloloza *et al.,* 2002).

Hamartin is phosphorylated by CDC2/cyclin B1 during the G2/M phase of the cell, at several sites (Threonine) Thr^{417}, (Serine) Ser^{584}, Thr^{1047}, (Astrinidis *et al.,* 2006). In dividing and non-dividing cells, hamartin localises to the centrosome (Astrinidis *et al.,* 2006). This coupled with the finding that the mitotic kinase Plk1 (polo-like kinase 1) interacts with the hamartin/tuberin complex suggests that hamartin and the mTOR pathway might play a functional role in the regulation of centrosome maturation and/or mitotic progression (Astrinidis *et al.,* 2006).

1.6.3.3 Cell death

Hamartin has been implicated in the cellular stress response due to interactions with NADE (p75NTR-associated cell death executor) and heat shock protein 70 (Hsp70) (Inoue *et al.,* 2009; Yasui *et al.,* 2007). Hamartin interacts with NADE via its coiled-coiled domain; this association could explain why hamartomas, hence aberrant cells are not eliminated via apoptosis in TS (Yasui *et al.,* 2007). NADE is known to mediate nerve growth factor-induced apoptosis, contribute to ischaemic neurodegeneration in rat hippocampal CA1 neurons and p75NTR-induced cortical neuronal death (Yasui *et al*., 2007).

Hamartin binds directly to Hsp70, even in the absence of tuberin, and is indeed stabilised during heat shock (Inoue *et al.,* 2009). Hamartin acts as a scaffolding protein that transfers the Akt signal to tuberin. Tuberin

undergoes degradation (probably via the proteosome) in an Akt-dependent manner through phosphorylation at Thr^{1462} (Inoue *et al.,* 2009). Phosphorylated hamartin-Hsp70 complex regulates apoptosis via mitochondrial localization (Inoue *et al.,* 2010).

1.6.3.4 Other interactions

In addition, glycogen synthesis kinase 3 (GSK3)β phosphorylates hamartin at residues Thr^{357} and Thr^{390}, increasing the stability of TSC1/TSC2 and causing attenuation of β-catenin (implicated in a number of malignancies) signalling (Mak *et al.,* 2005; Astrinidis & Henske, 2005). IKKβ, a major downstream kinase in the TNFα signaling pathway, physically interacts with and phosphorylates hamartin at Ser^{487} and Ser^{511} and may provide a link to inflammatory processes (Lee *et al.,* 2007). Hamartin has an array of other interactions reviewed by Rosner *et al.,* (2008b).

1.6.4 Tuberin

Tuberin, the protein product of TSC2, is a 200kDa protein, comprised of 1807 amino acids (Figure 1.6). Physiologically, there is a GTPase-activating protein (GAP) domain within tuberin that accelerates the conversion of Rheb-GTP (active form) to Rheb-GDP (inactive form). The function of tuberin is to inhibit Rheb which in turn suppresses mTOR and activates B-Raf, leading to decreased cell growth and differentiation (Astrinidis and Henske, 2005). The Rheb-GAP domain of tuberin is phosphorylated by several kinases that signal in response to growth factor stimulation or low cellular energy levels (Jozwiak, 2006). The regulation of tuberin is considered below (Section 1.6.7).

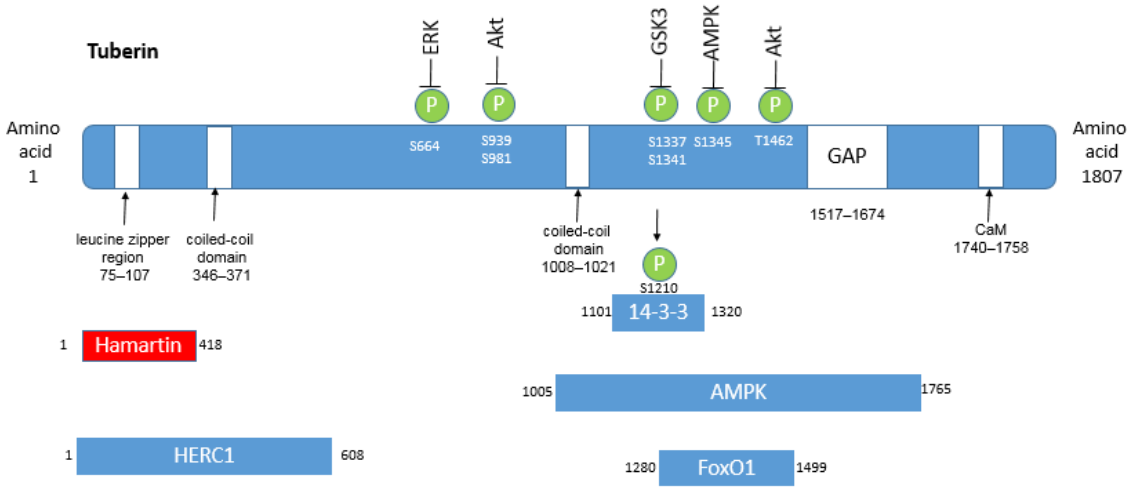

Figure 1.6: Tuberin's amino acid sequence, binding and phosphorylation sites. Key binding and phosphorylation sites are demonstrated AMPK: AMP-activated protein kinase, CaM: Calmodulin, Erk: Extracellular signal-regulated kinase, FoxO1 Forkhead box-containing protein O1, GAP: GTPase-Activating Protein, GSK3: Glycogen synthase kinase 3, HERC1 hect [Homologous to the E6-AP [UBE3A] carboxyl terminus] domain and RCC1 [CHC1]-like domain [RLD] 1. (Rosner *et al.,* 2008).Schematic: not to scale.

1.6.4.1 Cell morphology

Tuberin has been implicated in controlling cell morphology. Loss of tuberin leads to increased phosphorylation at a conserved LIM-kinase phosphorylation site, Ser 3 (S3) of the actin-depolymerization factor, cofilin, resulting in morphological changes (Tavazoie *et al.,* 2005). Tuberin also interacts with the 14-3-3 proteins whose cellular functions include trafficking of ion channels from the endoplasmic reticulum and regulation of the actin cytoskeleton (Tavazoie *et al*., 2005).

1.6.4.2. Cell cycle

Binding to hamartin is not essential for tuberin to affect proliferation (Miloloza *et al*., 2002). Overexpression of hamartin or tuberin negatively regulates cell cycle progression (as reviewed by Rosner *et al.,* 2008b). Tuberin negatively regulates cdk2 which when complexed with cyclin E, promotes the growth 1(G1) to synthesis (S) phase of the cell cycle (Rosner *et al.,* 2004).

1.6.4.3 Cell death

Tuberin can be an effector of cell death. A putative mechanism for the proapoptotic potential of tuberin is due to its negative effects on S6K, a downstream effector of mTOR. Tuberin leads to downregulation of the phosphorylation of the proapoptotic molecule BAD on Ser^{136}. These effects cause an upregulation of the interaction of Bcl-2-associated death promoter (BAD)/Bcl-2 B-cell lymphoma 2 (Bcl-2) and BAD/BCL-X_L (close homolog of Bcl-2) which leads to induction of apoptosis (Freilinger *et al.,* 2006). BCL-2, the first member of the BCL-2 family and BCL-X_L are antiapoptotic, whereas other members of the family for example BAD or BAX (bcl-2-like protein 4), are proapoptotic (Freilinger *et al.,* 2006). TSC2 has also been shown to bind to the death associated protein kinase DAPK (death-associated protein kinase) which has a multitude of roles including growth factor activation, apoptosis, and autophagy. DAPK can phosphorylate and inactivate tuberin leading to the stimulation of mTOR in response to growth factor signalling (Stevens *et al.,* 2009). In addition tuberin binding to DAPK can promote the degradation of DAPK through a lysosome-dependent degradation pathway under steady state conditions (Lin *et al.,* 2011).

1.6.4.4 Other interactions

Like hamartin, tuberin is also implicated in the wnt β-catenin pathway. Wnt stimulation down-regulates the association between tuberin and GSK3 and the scaffold protein, Axin. The ability of GSK3 activation of tuberin to block mTOR is inhibited (Rosner *et al.,* 2008b). There is much evidence for a role for tuberin in regulating transcription of a number of genes. Tuberin is thought to regulate the expression of vascular endothelial growth factor (VEGF). Loss of tuberin leads to accumulation of hypoxia-inducible factor (HIF) (Rosner *et al.,* 2008b). The carboxyl terminus of tuberin associates with the forkhead transcription factor FOXO1 which inhibits tuberin's GAP activity towards Rheb and degrades the TSC (Cao *et al.,* 2006). Tuberin has also been shown to modulate transcription controlled by members of the steroid/nuclear receptor family (Rosner *et al.,* 2008b). Tuberin has an array of other interactions reviewed by Rosner *et al.,* (2008b).

1.6.5 mTOR (Mammalian Target of Rapamycin)

A serine/threonine kinase, mTOR regulates growth and protein synthesis for mammalian cells. TOR genes were initially discovered in 1991 in yeast (Heitman *et al.,* 1991) and mTOR was discovered in 1994 (Brown *et al.,* 1994; Chiu *et al.,* 1994; Sabatini *et al.,* 1994). mTOR is implicated in transcription, ubiquitin-dependent proteolysis, autophagy, membrane trafficking and microtubule and actin cytoskeleton dynamics. TSC1/TSC2 complex mediates three inputs to mTOR activation: growth factor signals, amino acids and ATP availability, therefore regulating cell growth (Inoki *et al.,* 2005). The first experiments on hamartin and tuberin and their function in cell growth, signalling and the TOR pathway were performed in *Drosophila* and were in the context of insulin receptor signalling pathways (Gao and Pan, 2001). This study demonstrated that TSC1 and TSC2 formed a tumour suppressor complex acting as negative regulators downstream of Akt (Gao and Pan, 2001) and therefore negatively regulating the mTOR pathway, preventing protein synthesis and cell growth.

The TSC inhibits mTOR activity by stimulating the conversion of active Rheb-GTP to the inactive form. TSC2 protein acts as a GTPase activating protein towards Ras homolog enriched in brain (Rheb), a Ras family GTPase (as reviewed by Wong, 2010). GTP-bound Rheb activates mTOR by preventing the association on mTOR with its endogenous inhibitor FKBP38. The constitutive activation of mTOR increases protein synthesis by phosphorylating the substrate p70S6 which then activates the ribosomal protein S6 kinase (S6K) and also 4E-BP1. pS70S6K phosphorylates the ribosomal protein S6 at S240/244 leading to increased ribosome biogenesis. S6K selectively increases mRNAs encoding ribosomal proteins and other translation regulators. The specific mRNAs generated frequently encode ribosomal proteins and translation regulators which increases translational ability of the cells. 4E-BP1 releases the eukaryotic initiation factor eIF-4E and stimulates protein translation. Overexpressing eIF4E enhances cell growth and transforms cells by increasing the translation of growth promoting proteins, e.g. cyclin D-1, c-Myc and VEGF(as reviewed by Inoki *et al.,* 2005). The TSC acting through TORC1 has been shown to modulate SAD (Synapses of the Amphid Defective), regulating axon formation (Choi *et al.,* 2008). Loss of TSC (Tsc1 or Tsc2) function was associated with an increase in SAD kinase protein levels in rodent neuronal cultures and in cortical tubers from a TSC patient. Multiple axon formation is seen *in vivo* and in the mouse brain (Choi *et al.,* 2008). Therefore TSC is one of the central

controllers of cell growth and protein synthesis. TSC activity through inhibition of mTOR promotes autophagy, a cellular recycling mechanism which is discussed in Section 1.8.

There are two known mTOR complexes, namely mTOR complex 1 (mTORC1) and complex 2 (mTORC2). mTORC1 is composed of the proteins mTOR, raptor (regulatory associated protein of mTOR), mLST8 (mammalian lethal with sec-13 protein 8, also known as G-protein β subunit-like protein or GβL) (DeYoung *et al.,* 2008) and PRAS40 (proline–rich AKT substrate 40kDA) (Siroky *et al.,* 2009). mTORC2 also contains mTOR and mLST8, as well as rictor (rapamycin-insensitive companion of mTOR) and sin (stress-activated protein kinase-interacting protein) proteins (see Figure 1.7). mTORC1 is acutely sensitive to the macrolide, rapamycin. Rapamycin has been very useful in studying mTORC1, binding to FKBP12 (FK506-binding protein 12) and inhibiting mTOR. Rapamycin can affect mTORC2, but only after prolonged treatment can it affect assembly and function in some cells (Huang and Manning, 2008).

mTORC2 has a role in cytoskeletal integrity. TSC promotes mTORC2 activity in a Rheb independent manner thought to involve the direct binding of the TSC with components of mTORC2. Activated mTORC2 phosphorylates and activates Akt which in turn can activate TSC2. In addition to the PDK-1 phosphorylation of Akt at Thr^{308}, mTORC2 facilitates another activating phosphorylation site on Akt (Ser^{473}). One of the consequences of this activation of Akt is to promote mTORC1 activity (as reviewed by Fletcher *et al.,* 2013). mTORC1 communicates with mTORC2 via the inhibition of rictor by S6K1 (as reviewed by Han and Sahin, 2011). As Han and Sahin point out, most of these studies were performed in non-neuronal cells so should be extrapolated with caution (Han and Sahin, 2011).

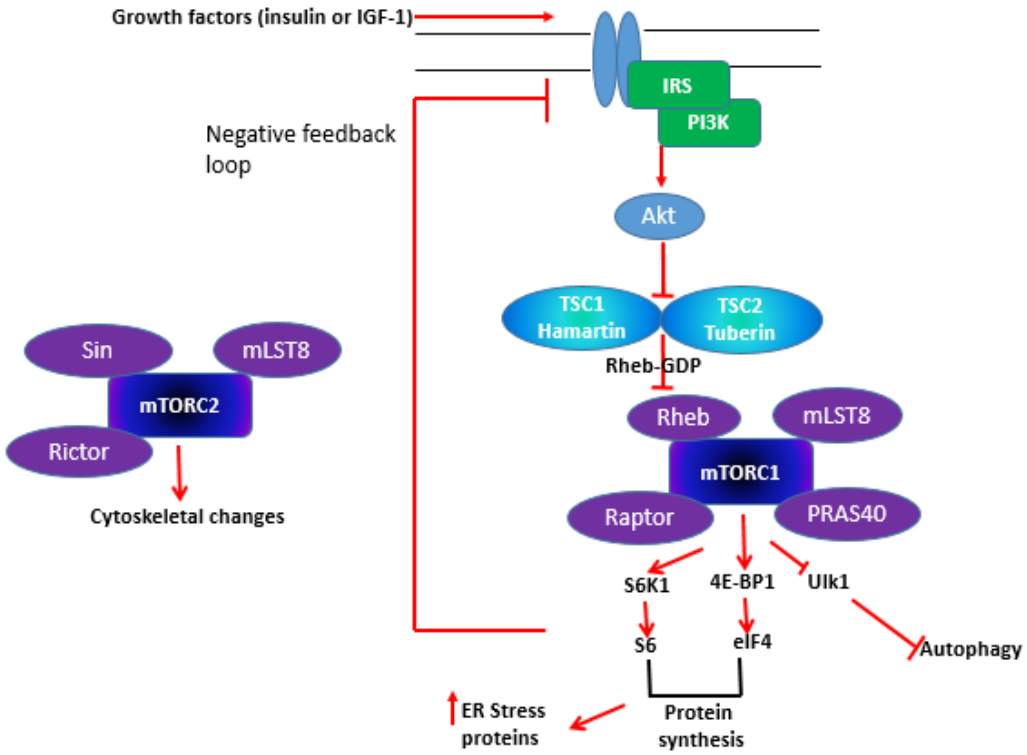

Figure 1.7 mTORC1 and mTORC2 pathways There are two known mTOR complexes, mTOR complex 1 (mTORC1) and complex 2 (mTORC2). mTORC1 is composed of the proteins mTOR, raptor (regulatory associated protein of mTOR), mLST8 (mammalian lethal with sec-13 protein 8, also known as G-protein β subunit-like protein or GβL) and PRAS40 (proline–rich AKT substrate 40kDa). mTORC2 also contains mTOR and mLST8, as well as rictor (rapamycin-insensitive companion of mTOR) and sin (stress-activated protein kinase-interacting protein) proteins. Downstream effectors of mTORC1 include S6K1, 4E-BP1 leading to increased protein synthesis. mTORC1 also has an inhibitory effect on autophagy as well as a negative feedback loop preventing upstream Akt phosphorylation. Activation of mTORC2 leads to PKC phosphorylation and cytoskeletal changes.

There exist non-canonical pathways that have TSC-dependent but mTORC1 independent mechanisms. These include the formation of the primary cilium (TSC1 is found at the base of the primary cilium in cultured human retinal pigmented and kidney epithelial cells) and the aggresome two centrosome-dependent cellular structures (Neuman and Henske, 2011). The cilia convey signals concerning extracellular flow and are central for signal transduction pathways such as Hedgehog. Aggresomes are perinuclear inclusion bodies that contain aggregated, misfolded proteins that have surpassed the capacity of proteosome and autophagy-mediated degradation. Also, Notch and B-Raf are two pathways involved in cell fate and differentiation are said to be mTORC1 independent yet Rheb dependent (Neuman and Henske, 2011).

1.6.6 Subcellular Localisation of Hamartin, Tuberin and mTOR

The TSC complex appears to be localised to the cytoplasm *in vivo* (Plank *et al.,* 1998; van Slegtenhorst *et al.,* 1998; Astrinidis *et al.,* 2006; Lugnier *et al.,* 2009). Hamartin, however has been localised to the membrane/particulate fraction of cultured cells (van Slegtenhorst *et al*., 1998; Yamamoto *et al*., 2002) and also to the nucleus (Fukuda *et al*., 2000). In dividing and non-dividing cells, it was also found that hamartin localised to the centrosome (Astrinidis *et al.,* 2006).

Tuberin has been reported to be present in the Golgi apparatus (Wienecke *et al.,* 1996) and nucleus (Lou *et al.,* 2001) but also the cytosol and membrane fraction within the cytoplasm and the nucleus (Rosner *et al*., 2008b). In response to Akt-mediated phosphorylation at Ser^{939} and Ser^{981}, tuberin translocates to the cytosol where it is then bound by 14-3-3 (Cai *et al.,* 2006). In neuronal cultures, hamartin and tuberin were found to be mainly cytoplasmic, colocalising homogenously through the soma and processes (Gutmann *et al.,* 2000)

Concerning the subcellular localisation of mTOR, in neuronal cultures from E17 Sprague-Dawley rats, immunofluorescence in normoxic conditions showed that mTORC1 (phosphorylated at Ser^{2448}) was predominantly in the cytoplasm, whereas mTORC2 (phosphorylated at Ser^{2481}) was found in the cytoplasm, nucleus and cell extensions, corroborating a study in human cell lines where mTORC1 was cytoplasmic and mTORC2 in the cytoplasm, nucleus and cell extensions (as reviewed by Rosner and Hengstschläger, 2008; Fletcher *et al.,* 2013).

mTORC1 is activated primarily on the lysosome of cells. Menon *et al.,* (2014) and Demetriades *et al.,* (2014) show that mTORC1 deactivation on the lysosome is determined by recruitment of its negative regulator, the tumour suppressor complex TSC1-TSC2. These reports highlight the importance of subcellular localization in the regulation of mTORC1. In order to be activated, mTORC1 needs to bind a molecule of Rheb in the GTP-bound (active) state (Inoki *et al.,* 2003). When amino acids are plentiful, mTORC1 is active owing to its lysosomal localisation, via the Rag GTPases. When amino acids are removed, Rag GTPases release mTORC1 causing it to become cytoplasmic and inactive (Demetriades *et al.,* 2014) and recruit TSC2 to the lysosome where it can act on Rheb. Spatial localisation is also important in response to insulin. Insulin activates mTORC1

via the PI3K-Akt pathway. It has recently been shown that insulin stimulates acute dissociation of the TSC from the lysosomal surface following Akt-mediated TSC2 phosphorylation (Menon *et al.,* 2014). TSC has also been found to localise to the peroxisome and control mTOR and autophagy in response to ROS (Zhang *et al.,* 2013b). Understanding the subcellular localisation of TSC is important as it may provide more insight into the physiological mechanisms it controls.

1.6.7 Regulation of TSC

TSC acts to integrate the energy status of the cell with the availability of nutrients and growth factor signalling (Orlova and Crino, 2010) and has many regulators that control expression, subcellular localisation and ultimately mTOR activity.

Insulin or insulin-like growth factors inhibit TSC primarily through Akt-mediated phosphorylation and inactivation of TSC2 which results in mTOR activation via phosphorylation on residues Ser^{939} and Thr^{1462}. A major form of negative feedback inhibition of PI3K results from activated growth signalling via mTOR and downstream p70 S6 kinase (S6K) (Harrington *et al.,* 2005). This negative feedback loop involves direct phosphorylation of insulin receptor substrate 1 (IRS-1) inhibiting PI3K and therefore Akt and results in a decrease in mTOR (Tremblay and Marette, 2001; Harrington *et al.,* 2004) (Figure 1.7). The tumour suppressor, phosphatase and tensin homolog (PTEN) also inhibits insulin signalling and preventing Akt from deactivating TSC leading to mTOR inhibition. Loss of PTEN therefore increases Akt activity which down regulates tuberin's function (Rosner *et al*., 2008a).

1.6.7.1 TSC, mTOR and austerity

Under conditions that are adverse for proliferation (for example in the absence of nutrients or certain growth factors), TSC1/TSC2 is activated and inhibits mTOR. Cells deficient for TSC1 or TSC2 fail to down-regulate mTOR function in response to growth factor deprivation (Brugarolas and Kaelin, 2004). However, activating phosphorylations of TSC can occur through the LKB1/AMPK (AMP-dependent protein kinase) pathway under conditions of energy deprivation and long term hypoxic stress (DeYoung *et al*., 2008).

1.6.7.1.1 Nutrient deprivation

Availability of amino acids has been shown to regulate the mTOR pathway. Amino acid depletion can suppress mTORC1 independently of TSC, but may also regulate the spatial interaction between mTORC1 and active Rheb. Some amino acids, especially leucine, regulate mTORC1 by controlling the ability of Rheb-GTP to activate mTORC1 (Avruch *et al*., 2009). Direct application of L-leucine (but not L-valine) in the vicinity of the arcuate nucleus region in the rat hypothalamus stimulates hypothalamic mTOR signalling and results in anorexia and weight loss (Avruch *et al*., 2009) whereas the withdrawal of amino acids (or just leucine and arginine) diminishes the ability of recombinant Rheb to bind to endogenous or co-expressed recombinant mTOR (Avruch *et al*., 2009) decreasing mTOR activity.

The interaction between mTORC1 and amino acids and growth factors and subsequent activation has been localised to the lysosome (Zoncu *et al.,* 2011). A recent study has demonstrated that upon growth factor withdrawal, the TSC translocates to the lysosomal surface where it inhibits mTORC1 by promoting guanosine 5'-triphosphate (GTP) hydrolysis and inactivation by Rheb (Menon *et al.,* 2014). A member of the solute carrier (SLC) family of proteins SLC38A9 is a candidate to link luminal lysosomal amino acids with mTORC1-activating machinery (Abraham, 2015; Rebsamen *et al.,* 2015; Wang *et al.,* 2015). Therefore, the availability of amino acids is critical for mTOR function.

1.6.7.1.2 Energy depletion

Any stress that depletes cellular ATP, such as oxidative stress, hypoxia, nutrient deprivation and metabolic poisoning, results in the activation of AMPK through LKB (Hardie, 2004). LKB1 activation by energy deprivation activates AMPK, which in turn phosphorylates and activates TSC2. The LKB1 pathway appears to be responsible for limiting protein synthesis and cell growth and protecting against apoptosis (Hardie, 2004). As TSC2 activation results in the inactivation of mTOR, this allows cells to preserve energy by preventing the translation of proteins and other energy dependent processes that make up the translational machinery itself.

In conditions of glucose starvation AMPK and GSK3 cooperatively phosphorylate TSC2 on Ser^{1337} and Ser^{1341} following a priming phosphorylation on Ser^{1345} by AMPK (Inoki *et al.,* 2006), enhancing its activity and inhibiting

mTOR (Inoki and Guan, 2009). TSC2 has been shown to integrate Wnt and energy signals via a co-ordinated phosphorylation by AMPK and GSK3 to regulate cell growth (Inoki *et al*., 2006).

Overall, these are key energy and glucose sensing pathways that can alter the activity of TSC and mTOR.

1.6.7.1.3 Hypoxia

Hypoxia can affect mTOR signalling through more than one mechanism. The decrease in ATP production resulting in the activation of AMPK (Huang and Manning, 2008) has been considered above. Conditions of less severe hypoxia do not result in a decrease in cellular ATP and increase in AMPK, suggesting that oxygen is able to regulate the mTOR pathway independently of cellular energy homeostasis (Arsham *et al*., 2003). Indeed, hypoxia was shown to rapidly and reversibly trigger hypophosphorylation of mTOR leading to reduced downstream effects. Signalling pathways shown to be implicated were those related to insulin, amino acids and phorbol esters. Down-regulation of mTOR activity by hypoxia requires de novo mRNA synthesis and correlates with increased expression of the hypoxia-inducible REDD1 gene. Disruption of REDD1 abrogates the hypoxia-induced inhibition of mTOR, and REDD1 overexpression is sufficient to down-regulate S6K phosphorylation in a TSC1/TSC2-dependent manner (Brugarolas *et al.,* 2004).

In summary, the austere environment inhabited by neurons in the post-ischaemic brain is hypoxic, energy-depleted and nutrient-deprived. TSC and therefore mTOR have been implicated in all of these three stresses upon the ischaemic cell. Nutrient deprivation results in decreased availability of amino acids which has been shown to negatively regulate the mTOR pathway (Huang and Manning, 2008). Any stress that depletes cellular ATP (the cell's energy source), such as oxidative stress, hypoxia, nutrient deprivation and metabolic poisoning, results in the activation of AMPK which directly phosphorylates and activates part of the TSC leading to inhibition of mTOR (Hardie, 2004). Hypoxia has been shown to reduce mTOR signalling through more than one mechanism (Arsham *et al.,* 2003; DeYoung *et al.,* 2008; Huang and Manning, 2008). Therefore, TSC and mTOR are central processes involved in controlling metabolism under stressful conditions.

1.7 Neuroprotection by hamartin

Given the poor understanding of the differential susceptibility between CA1 and CA3 neurons following global ischaemia, a proteomic study was carried out to determine molecular proteins and pathways responsible for the survival of CA3 cells. Tissue was obtained from rats subjected to either sham ischaemia or 10 min ischaemia. Following 24 h of reperfusion, the CA1 and CA3 regions were microdissected. The proteomes were determined by UPLC-QTOF MS (Figure 1.8 A). Proteins in each region were identified, in addition to the biological pathways and networks of interactions, using Ingenuity Pathway Analysis (IPA), in a non-biased manner (Figure 1.8 B). Pathways significantly altered by ischemia within CA1 and CA3 regions were compared and proteins selectively induced within CA3 were identified. In CA3 neurons, the PI3K-Akt intracellular signalling pathway was most significantly associated with the protein expression changes induced by ischemia when compared to sham CA3 ($p = 0.00032$). Hamartin was part of a network of proteins most significantly associated with expression changes induced by ischemia in the CA3 region compared to sham CA3 ($p < 0.05$) (Papadakis *et al.,* 2013).

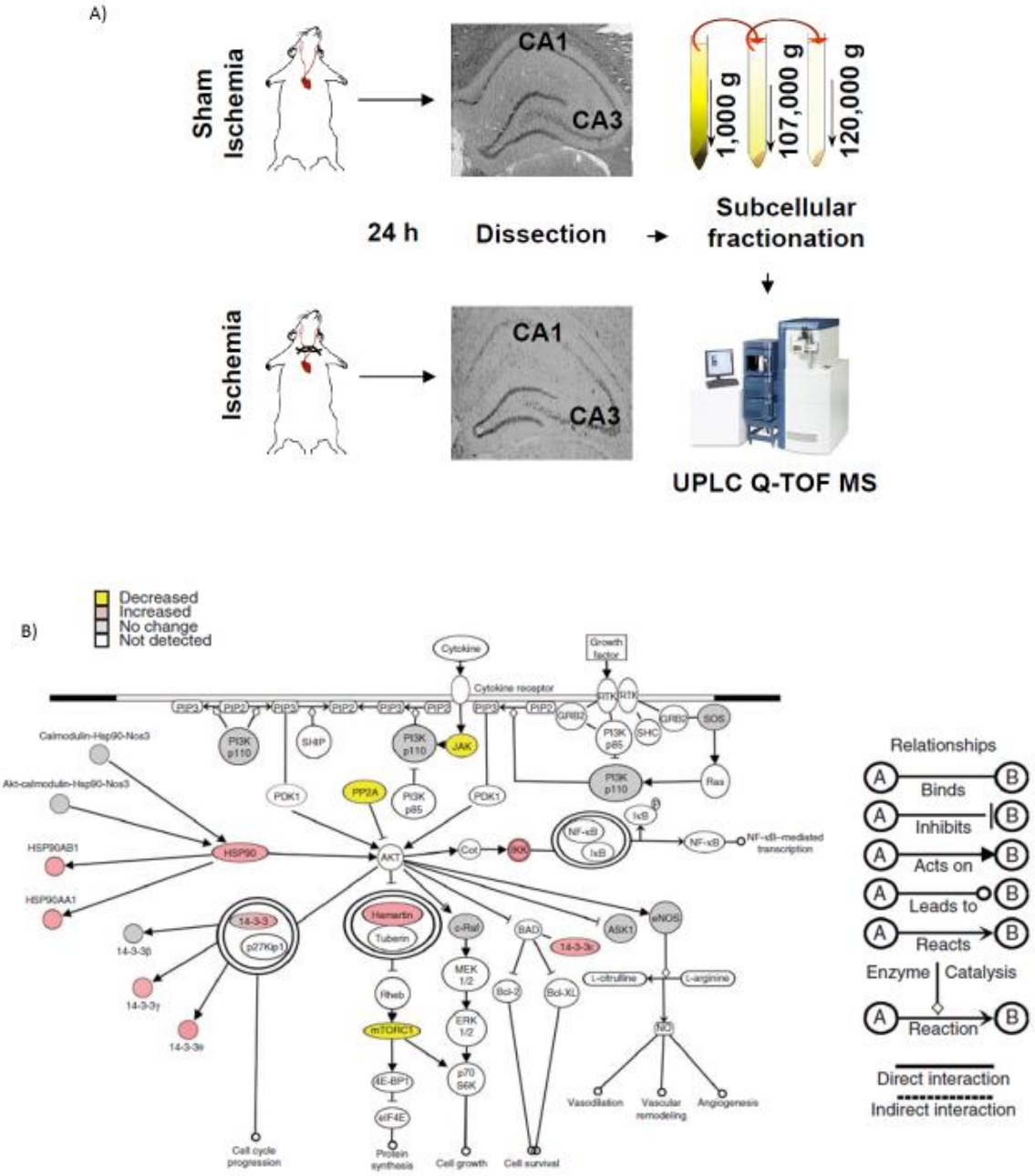

Figure 1.8 Proteomics Experiments A) Experimental design Rats were subjected to either sham ischaemia or 10 min ischaemia. Following 24 h of reperfusion, the CA1 and CA3 regions were microdissected and each region was subcellularly fractionated by differential centrifugation to generate a cytoplasmic and a membrane fraction. Each fraction was quantitatively analysed to define its proteome using UPLC-QTOF MS. **B) Illustration of the PI3K-Akt pathway** This pathway was significantly associated with and selectively induced in the CA3 region following ischaemia. Proteins in pink and yellow were upregulated and downregulated, respectively, by ischaemia. Proteins in grey were detected by the proteomic analysis, but their expression was unaffected. Proteins in white participate in the pathway or network but were not detected in the proteomic study. Images were created using IPA software. The relationships between the displayed proteins are indicated. (From Figure 1 a, b Papadakis, Hadley *et al.,* 2013).

Additional ischaemic preconditioning studies indicated that hamartin expression was associated with protecting otherwise vulnerable CA1 cells. After ischaemia, hamartin protein expression was significantly higher ($p < 0.01$) in the CA1 region of rats subjected to 2 min IPC compared to sham IPC (Papadakis *et al.,* 2013).

In addition to *in vivo* experiments, *in vitro* experiments were conducted that demonstrated that hamartin regulates neuronal susceptibility to OGD-induced cell death. Primary hippocampal neurons where hamartin expression is attenuated with TSC1 shRNA lentiviral vectors exhibit increased vulnerability to *in vitro* OGD. Following 3 hours OGD and 24 h reperfusion, cell viability assays demonstrated that TSC1 shRNA–transduced cultures showed a 34 ± 6.7% higher cell death compared with control shRNA–transduced cultures ($p < 0.0001$) (Papadakis *et al.,* 2013).

Subsequently *in vivo* experiments were conducted also showed that the same TSC1 shRNA lentiviral vector introduced to the CA3 area of the rat hippocampus made the normally resistant CA3 neurons more vulnerable to global ischaemia (Papadakis *et al.,* 2013). This was corroborated by an increase in locomotor activity in the open field test (Papadakis *et al.,* 2013), a sign of inability to habituate and loss of hippocampal function (Andersen *et al.,* 1997; Kesner, 2007).

As silencing hamartin made neurons more vulnerable to ischaemia, an experiment was carried out to test whether hamartin overexpression was sufficient to protect neurons from ischaemic insults. Hippocampal neurons were transduced with a lentiviral vector expressing rat *Tsc1*-eGFP (rat TSC1) that caused overexpression of hamartin or a control vector expressing eGFP alone (GFP). The number of cells surviving OGD versus normoxia was 31 ± 8.6% higher in rat TSC1– compared to GFP-transduced cells, ($p = 0.0066$) (Papadakis *et al.,* 2013). These results provide direct evidence that hamartin is neuroprotective.

The mechanisms by which hamartin promotes this neuroprotection are mainly centred around the mTOR pathway and its effects on productive autophagy (see Section 1.8) and energy conservation, but may also include alleviation of the deleterious effects of ER stress (see Section 1.9).

1.8 Autophagy

Cell death can be divided into three categories, apoptosis (I), autophagy (II) and necrosis (III). Autophagy is the process by which a cell clears or recycles cellular components/debris as a method of protecting itself or leading to cell death without harming neighbouring cells. Autophagy was first described in the 1960s by Christian de Duve and has been described as a cell survival mechanism that acts alongside cell death, but that does not necessarily lead to it (Tsujimoto and Shimizu, 2005). 'Macroautophagy' is non-selective, whereas microautophagy, mitophagy, and chaperone-assisted autophagy are more selective (Rouschop *et al.,* 2010). 'Autophagy' will refer to 'macroautopagy' for the purposes of this thesis. Autophagy is vital in postmitotic cells such as neurons as they do not have the ability to dilute detrimental accumulating proteins and organelles by cell division (Damme *et al.,* 2015). Autophagy is thought to be controlled mainly by mTOR and to happen predominantly in response to nutrient starvation or signals prompting cellular remodelling (Meijer and Codogno, 2006). Activation of mTOR by increased amino acid availability (class III PI3K-Rheb pathway) or by trophic factors (TSC-Rheb pathway) results in the inhibition of autophagy. Inhibiting mTOR by decreased amino acid availability, energetic stress resulting in AMPK activation, or rapamycin can lead to an increase in autophagy. Autophagy is not only triggered by nutrient starvation but also by reduced growth factor signalling (mainly insulin/insulin-like growth factor (IGF-1)-PI3K). Autophagosomes develop and engulf organelles and other cellular components before fusing with lysosomes, therefore resulting in mass proteolysis (Lockshin and Zakeri, 2004). Basal levels of autophagy are necessary for neuron health (neurodegeneration and ubiquitinated protein aggregates occur in animal models that lack this process) (Cherra and Chu, 2008). The relevance of autophagy to stroke is that it removes misfolded or long-lived proteins and organelles that are damaged or surplus to requirements and is an adaptive response to provide nutrients and energy following cellular stress.

1.8.1 The process of autophagy

In summary, the steps involved in autophagy are induction, cargo recognition/packaging, maturation, fusion and breakdown (Figure 1.9).

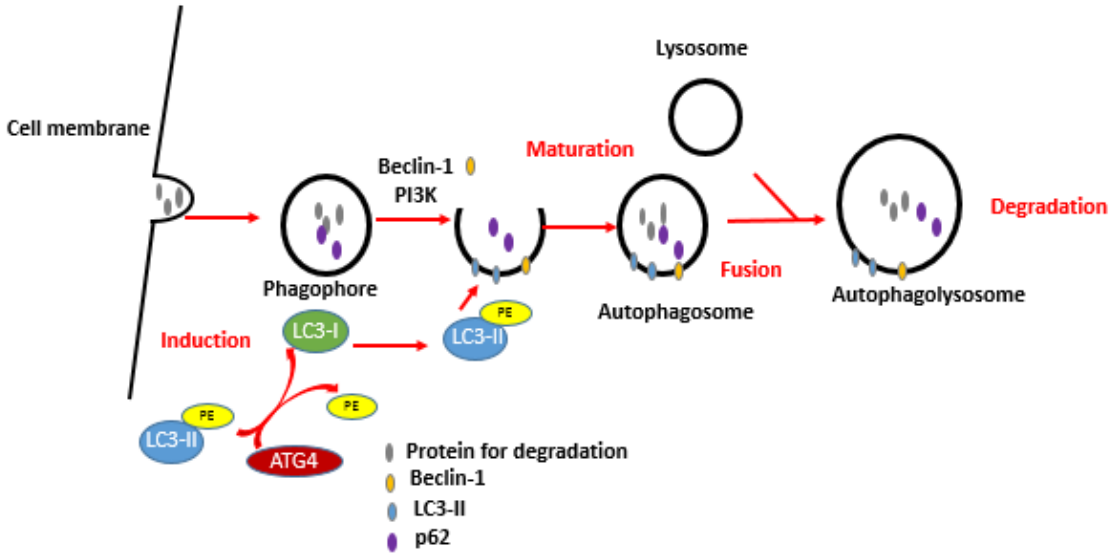

Figure 1.9 The autophagic process The steps in autophagy involve: induction, cargo recognition/packaging, vesicle formation, retrieval, fusion/breakdown, efflux. The three key proteins used to assess autophagy are beclin-1, LC3 and p62 (see Chapter 4). After triggers from a number sources, autophagy is induced leading to the formation of cisternae that engulf cytoplasmic organelles leading to the development of phagophores (isolation membranes). Phagophores then form autophagosomes which are vacuoles containing the engulfed organelles. After maturation, autophagosomes fuse with the lytic compartments lysosomes and endosomes to form autophagolysosomes. Autophagolysosomes degrade the cellular proteins and organelles leading to either the recycling of cellular components or cell death. PE: phosphatidylethanolamine

Induction involves the formation of double-membraned cisternae that subsequently engulf cytoplasmic organelles to form double-membrane vacuoles, known as APs. APs are formed by phagophores (also called isolation membranes). It has been suggested that regions of the ER known as 'omegasomes' might provide important components for AP formation (Axe *et al.,* 2008). Atg (autophagy-related proteins) are required for the formation of the isolation membrane, namely, Atg5-Atg12-Atg16 complex, the LC3- phosphatidylethanolamine protein-to-lipid conjugation complex and conjugating enzymes (reviewed by Wong and Cuervo, 2010). The rate-limiting step appears to be the class III phosphatidylinositol-3-kinase complex (PI3K) responsible for the nucleation of the phagophore. The required proteins for this complex are beclin-1, Vps15 and Vps34 (reviewed by Wong and Cuervo, 2010).

During cargo sequestration, p62 binds to a surface ubiquitin linkage (Lys63) on protein aggregates conveying autophagosome formation to them via its interaction with LC3 (Tan *et al.,* 2007). P62 also recognises organelles and pathogens. Other cargo recognition molecules are NBR1 (protein-only recognition) and NDP52 (recognises

ubiquitin-coated bacteria) (reviewed by Wong and Cuervo, 2010). In order for clearance to occur fusion with lysosomes or endosomes (with lytic capabilities) is necessary.

After maturation, APs merge with lysosomes for bulk degradation of the cargo contents (Yorimitsu and Klionsky, 2005). Hence, the appearance of APs under transmission electron microscopy (EM) is a morphological hallmark unique to autophagy.

Degradation of the sequestered cargo only occurs when autophagosomes fuse to lytic compartments (that is, lysosomes or late endosomes). Rab7 GTPase and the SNARE Vtilb are required for mammalian autophagic fusion in conjunction with cellular cytoskeleton and cytosolic modulators (reviewed by Wong and Cuervo, 2010. The fusing together of autophagosomes and lysosomes facilitates the delivery of the autophagic cargo into the lysosomal lumen. Accordingly, autophagosomes that are formed but not cleared could interfere with intracellular trafficking (Yu *et al.,* 2005) or become 'leaky' over time resulting in the release of degradative enzymes into the cytosol leading to cell death (Kaasik *et al.,* 2005).

The degradation of cellular proteins can replenish amino acid stocks, coupled with degradation of lipids and glycogen granules and restoration of ATP levels in the austere ischaemic environment (Jiang *et al.,* 2014).

There is a link between the ubiquitin proteasome system (UPS) and autophagy. If the UPS is blocked, autophagy is upregulated. If the blockage persists autophagy is constitutively upregulated but seemingly has no capacity to respond to stress. If autophagy is blocked the function of UPS is compromised (reviewed by Wong and Cuervo, 2010).

1.8.2 Region and sex-specific differences

Autophagy may be influenced by brain region and sex differences. In stroke-prone spontaneously hypertensive rats (SHRSP) that underwent MCAO, autophagy was implicated in secondary thalamic damage after focal cerebral infarction (Xing *et al.,* 2012). A recent paper that used rodent neonatal hypoxia–ischemia has demonstrated that there was impaired autophagy in the cortex compared to the hippocampus (Weis *et al.,* 2014). Decreased lysosomes were observed in the cortex compared to the hippocampus which was thought to

be a fault in the fusion process between autophagosomes and lysosomes or a deficit in lysosomes degradative functions (Weis *et al.,* 2014). It should however be noted that, unlike the author's interpretation the presence of fewer lysosomes may not be compatible with a fusion defect as this would actually lead to more storage.

In the cortex, females appear to have a partial failure of lysosomal protease function compared to males. Females have higher cleavage and activation of caspase-3 in both the cortex and the hippocampus. There are clearly region and sex-specific differences that may contribute to the precise dissection of the mechanism of autophagy following ischaemia (Weis *et al.,* 2014).

1.8.3 Regulation of autophagy

mTOR regulates autophagy via amino acid sensing when resources are plentiful, it phosphorylates and inhibits ATG13 and Unc-51-like-kinase1/2 ULK1/ULK2 subunits via phosphorylation. Under starvation conditions, autophagy is initiated by reduced phosphorylation of ULK1/ULK2 at Ser^{757} which then becomes activated via phosphorylation on two additional serine residues by AMPK (Damme *et al.,* 2015). In Tsc1/2 deficient cells, loss of Tsc2 results in autophagic activity via AMPK-dependent activation of ULK1 on Ser^{555} resulting in autophagic flux and accumulation of autolysosomes (Di Nardo *et al.,* 2014).

mTOR is also involved in a transcription-dependent regulation of autophagy. In nutrient-rich times, mTORC1 phosphorylates TFEB at Ser^{211}, which keeps it in the cytoplasm. In the absence of mTORC1, TFEB can translocate to the nucleus where it is responsible for lysosomal and autophagic gene expression (Sardiello *et al.,* 2009). Autophagy is not necessarily governed by mTOR. Lithium induces mTOR-independent autophagy via the inhibition of inositol monophosphatase (IMPase) and reduction of inositol and IP3 levels (Sarkar *et al.,* 2008). The insulin signalling pathway can also result in autophagy despite activation of Akt, mTOR, and S6 kinase (Yamamoto *et al.,* 2006). Rheb affects both autophagy via mTORC1 and aggresome independent of mTORC1 to counteract the toxicity of misfolded protein via inhibiting dynein-dependent transportation of misfolded proteins (Zhou *et al.,* 2009).

Human post mortem samples of hypoxic-ischaemic encephalopathy and a rodent model of severe perinatal asphyxia display enhanced autophagy promoting cell death in the thalamus (Ginet *et al.,* 2014). The promotion

of cell death can involve apoptosis (Xue *et al.,* 1999; Zhang *et al.,* 2009), necrosis (Samara *et al.,* 2008; Wang *et al.,* 2011a) or can be independent of both (Clarke, 1990; Denton *et al.,* 2009).

Using a cell-penetrating autophagy-inducing peptide, Tat-Beclin 1, high levels of autophagy were achieved (Liu *et al.,* 2013). The resulting mechanism of cell death was termed 'autosis' attenuated by inhibitors of autophagy but not apoptosis and necroptosis. Autosis has distinct morphological characteristics and it was also seen in nutrient-starved cells *in vitro* and *in vivo* in rodent hippocampal following cerebral hypoxia-ischemia and was inhibited by cardiac glycosides (antagonists of Na(+),K(+)-ATPase) (Liu *et al.,* 2013).

1.8.4 Is autophagy neuroprotective or neurotoxic?

The effects of autophagy are contentious in the context of cerebral ischaemia. There are studies that suggest it is detrimental (Wen *et al.,* 2008; Zheng *et al.,* 2009) and equally studies that suggest a neuroprotective role (Carloni *et al.,* 2008, Wang *et al.,* 2012). The difference between autophagy's protective effect during ischaemia and detrimental effect during reperfusion could be explained due to the differing pathological processes underpinning these two processes (Jiang *et al.,* 2014). It has also been suggested that in the mouse heart the mechanism of autophagy is different in ischaemia and reperfusion (Takagi *et al.,* 2007). Autophagy is stimulated through an AMP-activated protein kinase (AMPK)-dependent mechanism during ischaemia where it is thought to be protective. During reperfusion, autophagy is thought to be detrimental and the mechanism is Beclin 1-dependent, but AMPK-independent (Takagi *et al.,* 2007).

A selection of the evidence for the detrimental and beneficial effects of autophagy that have been observed is presented below. In experimental systems, reducing the magnitude of autophagy induction in response to oxidative, hypoxic-ischaemic and ion-channel excitotoxic injuries confers neuroprotection, implicating overactivation of autophagy in neuronal injury (Cherra and Chu, 2008). Using rat MCAO, autophagy suppression by exercise pretreatment and MAPK (p38) inhibition was shown to be neuroprotective in cerebral ischemia (Zhang *et al.,* 2014a). A multitude of other studies suggest that autophagy has a detrimental effect in neuronal ischaemia (Adhami *et al.,* 2006; Koike *et al.,* 2008; Uchiyama *et al.,* 2008; Qin *et al.,* 2010a; Wang *et al.,* 2011a).

Evidence for a beneficial effect includes loss of Atg7 which is essential for autophagy leads to neurodegeneration (Komatsu *et al.,* 2006). In rodent hippocampal neurons, excitotoxic glutamate insults were demonstrated to block autophagic flux. Furthermore, an autophagy inhibitor chloroquine had no effect on neuronal survival. Significant neuroprotection was seen with rapamycin (mTOR-dependent) and trehalose (mTOR-independent), two inducers of autophagy that act via different mechanisms (Kulbe *et al.,* 2014). In rat cortical neurons HIF-1α overexpression resulted in mitochondrial autophagy, thereby increasing neuronal survival (Gong *et al.,* 2014). In a focal MCAO model in rats, remote preconditioning of femoral arteries was protective through autophagy activation (Su *et al.,* 2014). An increase in Beclin-1 post ischaemia is indicative of a protective role for autophagy in neonatal hypoxia-ischaemia (Carloni *et al.,* 2008).

In an attempt to address these differing findings, Buckley *et al.,* (2014) sought to compare an inducer of autophagy (rapamycin) with an inhibitor (chloroquine). They found that both compounds decreased infarct size and improved neurological scores but it was the rapamycin treated mice who had an improved outcome and survival (Buckley *et al.,* 2014). On balance, induction of autophagy was protective, however, some inhibitors of autophagy have 'off target effects' such as those that chloroquine has on apoptosis (Buckley *et al.,* 2014).

Global ischaemia has been shown to increase autophagosome number in CA1 indicative of ineffective autophagy (Liu *et al.,* 2010). It has previously been suggested that autophagy might be the mechanism by which IPC confers neuroprotection to CA1 (Sheng *et al.,* 2010). Autophagy can repair cells undergoing ischemic stress. The upregulation of hamartin following ischaemia could result in the induction of autophagy as a protective mechanism (Papadakis *et al.,* 2013) and further work presented in this thesis will probe this mechanism.

1.9 ER Stress

Physiologically, the endoplasmic reticulum (ER) is involved in the synthesis and processing of intracellular proteins, co-ordinating protein folding, lipid biosynthesis and calcium storage, and release. ER stress is caused by depletion of ATP and glucose and nutrient deficiencies, lowering of intraluminal calcium levels and inhibition of protein glycosylation and the disruption of disulfide bond formation which result in the build-up of unfolded

proteins within the ER lumen (Gao *et al.,* 2013). The ER stress response is evolutionarily conserved. The unfolded protein response (UPR) temporarily slows accumulation of new proteins in the ER lumen, at the same time upregulating transcription of genes for ER resident chaperones and enzymes that ablate the effects of ER stress (Kumar *et al.,* 2003).

There are three transmembrane effector proteins in the UPR. These three specialized stress sensors constituting the UPR located at the ER membrane are: Inositol-requiring enzyme 1 (IRE1), Activating transcription factor 6 (ATF6) and Protein kinase RNA-like ER kinase (PERK) (Korennykh and Walter, 2012) (see Figure 1.10). IRE1 is a serine/threonine protein kinase and endoribonuclease which is responsible for the transcription of X-box binding protein 1 (XBP1) via the unconventional splicing of mRNA. XBP1 translocates to the nucleus and controls genes involved in protein folding, ER-associated protein degradation (ERAD), protein translocation into the ER, lipid synthesis and other processes (Hetz and Mollereau, 2014). ATF6 activation results in translocation to the Golgi apparatus for proteolytic processing then translocates to the nucleus activating the transcription of ERAD genes and *XBP1* (Hetz and Mollereau, 2014). The suppression of most protein translation occurs via the phosphorylation of eukaryotic translation initiation factor 2 subunit a (eIf2a) by PERK. Phospho eIF2α inhibits global translation except the selective translation of the mRNA encoding the transcription factor ATF4 (CREB 2). ATF4 controls the expression of various genes involved in the stress response. In addition, PERK possesses an endonuclease activity. Upon translocation to the nucleus it is involved in the induction of ER chaperones such as GRP78 and heat shock proteins. GRP78 prevents protein-protein aggregation and helps to refold the proteins. Prolonged ER stress can however result in the activation of ER-dependent apoptosis through the activation of CHOP (C/EBP homologous protein), GADD153 (growth arrest and DNA damage inducible gene 153) and caspase-12 (McCullough *et al.,* 2001; Boyce and Yuan, 2006; Sheng *et al.,* 2012; Gao *et al.,* 2013).

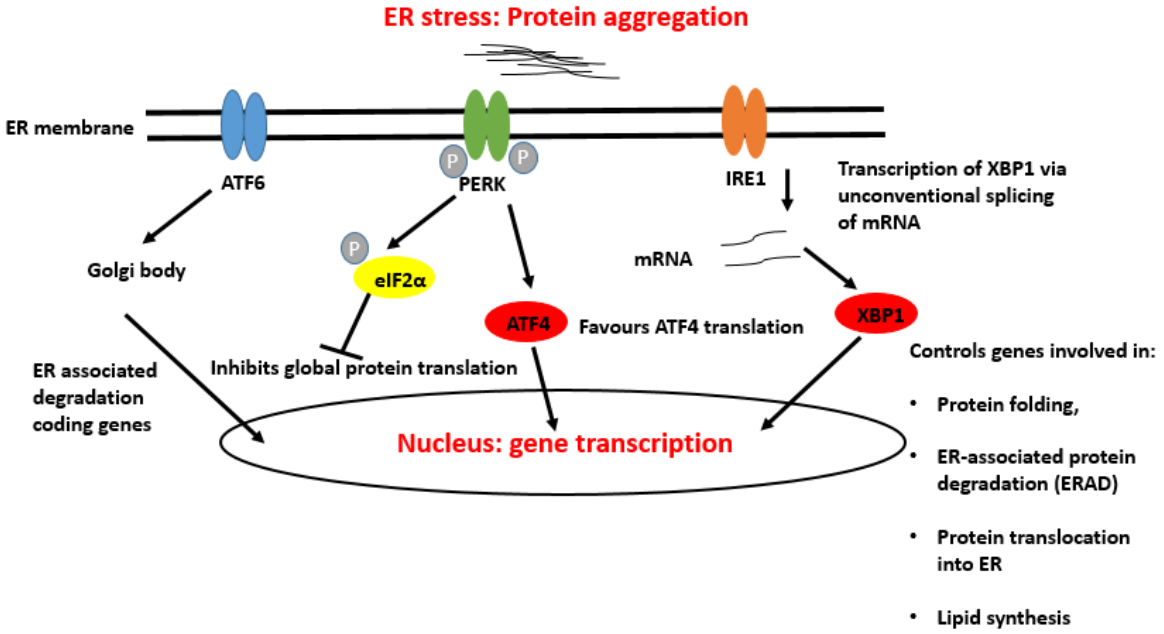

Figure 1.10 The ER Stress Response Primary function of the UPR (unfolded protein response) is to maintain and re-establish ER homeostasis. It has three stress sensors, PERK (Protein kinase RNA (PKR)-like ER kinase) (1), Inositol requiring enzyme-1 (IRE-1) (2) and Activating transcription factor 6 (ATF6) (3). ATF6 is a cell surface receptor leading to the degradation of ER-associated proteins via changes in gene transcription of the coding genes. PERK is a cell surface receptor that phosphorylates eIF2α leading to ATF4 activation of gene transcription altering protein translation of ER chaperone, redox, autophagy and amino acid metabolism proteins. IRE1 is another cell surface receptor leading to the activation of both JNK and RIDD signalling modulating autophagy and apoptosis.

1.9.1 A role for the Tuberous Sclerosis Complex in Endoplasmic Reticulum Stress

The mechanisms by which hamartin promotes neuroprotection appear to be mainly centred around the mTOR pathway and its effects on productive autophagy and energy conservation, but may also include alleviation of the deleterious effects of ER stress.

There is substantial evidence linking TSC and ER stress. Di Nardo *et al.,* (2009) use Tsc2 deficient rat hippocampal neurons, brain lysates from a TSC1 deficient mouse model and human tissue to demonstrate elevated ER and oxidative stress. The mTOR pathway has also been implicated as rapamycin abolished these stress responses. Neurons lacking TSC1/TSC2 complex have increased vulnerability to ER stress-induced cell death via the activation of the mitochondrial death pathway. TSC2 is initially inactivated in these neurons during ER stress, but is later activated (Di Nardo *et al.,* 2009).

When loss of TSC function occurs, there is uncontrolled mTOR hyperactivation that results in an increase in protein synthesis and ROS production. This overloads the cellular machinery resulting in ER and oxidative

stress responses which induce CHOP and hemeoxygenase-1 (HO-1) (Di Nardo *et al.,* 2009). Tsc2 deficient rat hippocampal neurons have increased expression of CHOP and HO-1. CHOP is a transcription factor that promotes apoptosis (Oyadomari and Mori, 2004). HO-1 is a member of heatshock family Hsp32, a marker of stress (Takahashi *et al.,* 2004). Finally, cells with mutations in either TSC1 or TSC2 are hypersensitive to ER stress and undergo apoptosis (Kang *et al.,* 2011). Therefore, the neuroprotective effects of hamartin could be produced by decreasing ER stress.

1.9.2 The link between ER stress and autophagy

If the ER experiences a perturbation in homeostasis that is not salvageable by the UPR, autophagy and cell death ensue.

The link between autophagy and ER stress is not entirely clear, with evidence for involvement in all three of the stress sensor pathways. Autophagy can be activated by both PERK and ATF6 pathways (Fang *et al.,* 2015). In SK-N-SH neuroblastoma cells, the only ER stress pathway implicated was IRE1 signalling (Ogata *et al.,* 2006). Using human cell lines and grafting onto nude mice, the PERK pathway was found to be important in increasing their survival. In several human cancer cell lines, hypoxia increased transcription of the crucial autophagy genes, microtubule-associated protein 1 light chain 3beta (MAP1LC3B) and autophagy-related gene 5 (ATG5) via phosphorylation of phosphoeIF2α and subsequent activation of the transcription factors ATF4 and CHOP (Rouschop *et al.,* 2010).

In several human cancer cell lines, hypoxia increased transcription of the crucial autophagy

A potential mechanism has been proposed whereby autophagy is enhanced via the ER-stress driven negative regulation of the AKT/TSC/mTOR pathway (Qin *et al.,* 2010b). Indeed, ER stress can be a potent stimulus of autophagy in neurons (Sheng *et al.,* 2012). ER stress has been shown to increase the formation of autophagosome via IRE1-JNK signaling pathway, and in addition, dysfunction of ERAD and autophagy and the resultant failure of protein folding make cells vulnerable to ER stress (Ogata *et al.,* 2006). 'Omegasomes' are areas on the ER that may serve as the nucleation site in mammalian cells in the induction of autophagy (Axe *et al.,* 2008).

In addition to evidence that ER stress activation can lead to autophagy, autophagy may modulate ER stress. In a permanent model of neonatal hypoxia ischaemia there was a decrease in ER stress following autophagy pre-activation. Ribosomes were also detected in autophagosomes. Limiting protein translation in this way could also be part of the neuroprotective mechanism (Carloni *et al.,* 2014). The presence of ribosomes in autophagosome has been noted using electron microscopy since the discovery of autophagy itself (Ashford and Porter, 1962).

The relationship between ER stress and autophagy is extremely complex as the ER may also have significance in the inhibition of autophagy. ER-localized Bcl-2 inhibits autophagy (Pattingre *et al.,* 2005) indeed, phosphorylated Bcl-2 localizes predominantly to the ER (Bassik *et al.,* 2004). In addition, Bcl-2 may be a target for mTOR (Wei *et al.,* 2008). Furthermore, ATF4 controls the expression of various genes involved in autophagy, apoptosis amino acid metabolism and antioxidant responses (as reviewed by Hetz and Mollereau, 2014). ATF4 is responsible for transcription of proteins that inhibit BCL-2 expression, favouring apoptosis (Nakka *et al.,* 2016).

1.10 Pharmacological manipulation of hamartin and its downstream effects

The mechanism by which hamartin confers its neuroprotective effect could hold the key to a novel therapy in the treatment of ischaemic stroke. The pharmacological manipulation of mTOR, productive autophagy and ER stress is undertaken in this thesis in order to test existing small molecules and their effect on neurons that undergo OGD. It is hoped that targeting these mechanisms with small molecules could replicate the endogenous neuroprotection observed with hamartin. The compounds appear in Table 1.2, their site of action is described in Figure 1.11 and each compound is discussed in more detail in the relevant chapter.

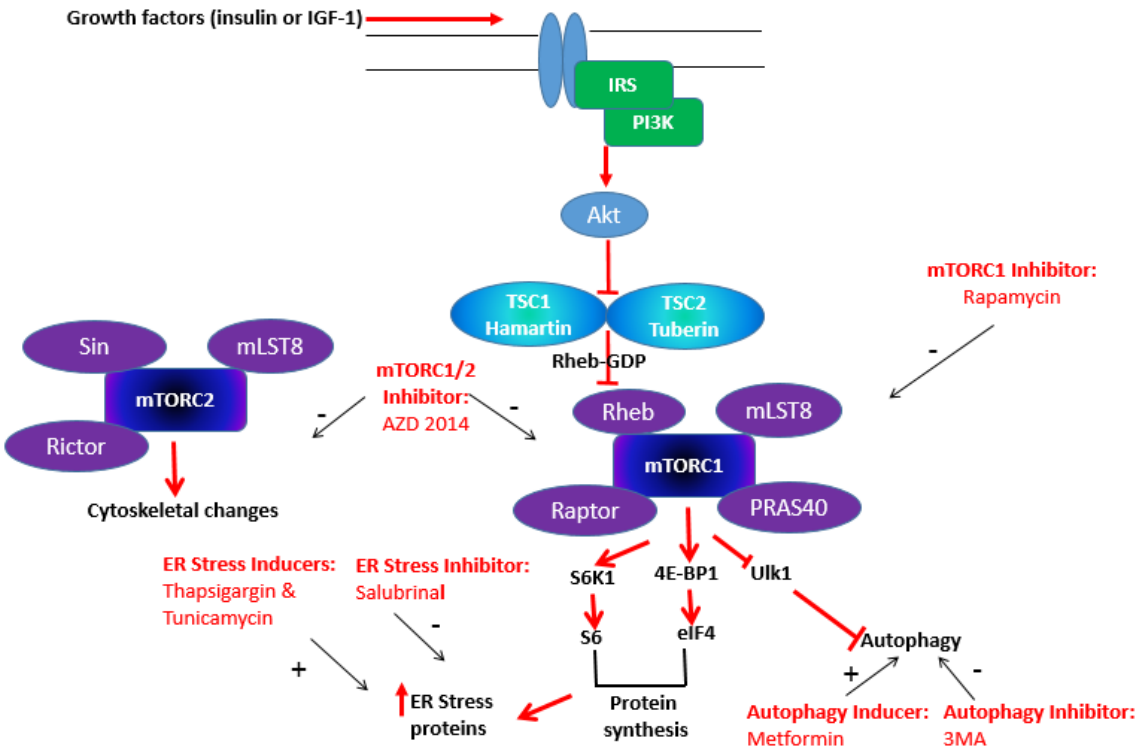

Figure 1.11 Compounds used in this thesis and their site of action

Drug	Function	Chapter used in
Rapamycin	mTORC1 inhibition	3
AZD 2014	mTORC1/2 inhibition	3
Metformin	Autophagy inducer	4 and 5
3MA	Autophagy inhibitor	4
Thapsigargin	ER stress inducer	5
Tunicamycin	ER stress inducer	5
Salubrinal	ER stress inhibitor	5

Table 1.2 Compounds used in this thesis

1.11 Hypotheses

There are several hypotheses that will be explored in this thesis:

Chapter 3:

1. CA3 neurons in the hippocampus are resistant to global cerebral ischaemia *in vivo* by altering hamartin expression, and these changes are hippocampal region and time-dependent.

2. In vitro pharmacological inhibition of the downstream mTOR pathway will replicate neuroprotection mediated by hamartin.

Chapter 4:

3. Promotion of autophagy is a mechanism responsible for the neuroprotective effect of hamartin and will be altered in the hippocampus in a region and time-dependent manner *in vivo*.

4. *In vitro* pharmacological induction of autophagy will replicate neuroprotection mediated by hamartin.

Chapter 5:

5. Inhibition of ER stress is a mechanism responsible for the neuroprotective effect of hamartin and will be altered in the hippocampus in a region and time-dependent manner *in vivo*.

6. *In vitro* pharmacological inhibition of ER stress will replicate neuroprotection mediated by hamartin.

This thesis considers downstream pathways of mTOR, productive autophagy and ER stress in order to provide mechanistic insight into hamartin's neuroprotective effect and provide putative small molecular targets based on this endogenous protective mechanism.

Chapter 2: Method Development – Exploring the Global Model of Ischaemia

2.1 Executive Summary

This chapter describes the 4-VO method of global cerebral ischaemia used throughout this thesis. The model replicates the effect of cardiac arrest on the brain and is useful for gaining mechanistic insight into how global cessation of blood flow affects the brain. In the hippocampus, the phenomenon of selective vulnerability provides an excellent experimental paradigm for studying endogenous neuroprotection – something which is not provided by focal models although they are more analogous to human ischaemic stroke. Following global ischaemia, CA1 neurons are susceptible and die, but they die slowly. The existence of compromised, yet viable neurons provides another dimension to experiments with the existence of a vital window of potential salvation (Pulsinelli *et al.,* 1982 a). Importantly, the observation that CA3 neurons are resistant to ischaemia allows us to ask the question: why do they survive? Harnessing this endogenous neuroprotection could also lead to potential neuroprotective therapies.

Blood flow during pre-4-VO and 4-VO was recorded and India ink perfusion demonstrated a lack of perfusion during 4-VO. Telemetry recordings verified ischaemic animals display increased activity (due to hippocampal damage) and increased temperature compared to sham.

In my hands, the model is appropriate to investigate the mechanism underlying endogenous neuroprotection as there exists both spatial differences in susceptibility (CA1 vs CA3) and temporal differences between hippocampal brain regions (delayed cell death in CA1). These outcomes of the model allow the investigation into the following hypotheses:

The temporal (0-24 hours) and spatial (membrane vs cytoplasm, CA1 vs CA3) expression of hamartin following global ischaemia could give mechanistic insight into endogenous neuroprotection (Chapter 3).

Differential expression of proteins associated with autophagy (Chapter 4) and ER stress (Chapter 5) will further elucidate the mechanism of endogenous neuroprotection.

2.2 Background

The place of animal studies in stroke research is a highly contentious issue. It is possible to extrapolate from animal models as many of the biochemical reactions are evolutionarily conserved and with the exception of the gerbil, many rodent species have a complete circle of Willis (Yamori *et al.,* 1976). There are also pathophysiological similarities such as the existence of an ischaemic penumbra in animal models of focal ischaemia and human models of stroke (Dirnagl and Endres, 2014). However after over 1000 preclinical studies and 100 clinical trials, with the noteworthy exception of recombinant tissue plasminogen activator (NINDS, 1995), which was initially shown to be efficacious in a rabbit model of small clot emboli (Zivin *et al.,* 1985) there has been a resounding failure for any of this research to result in licensed therapies (O'Collins *et al.,* 2006). When looking for compounds in preclinical studies to carry forward to clinical trials it is paramount to distinguish between true neuroprotective effects at the proposed target and off target effects. For example MK-801 conferred neuroprotection via hypothermia (Buchan and Pulsinelli, 1990 a) and potentially an alteration of cerebral blood flow (Buchan*,* 1992) – not through its actions at the NMDA receptor. The proposed compound may actually be having a neuroprotective effect by improving the supply of oxygen and glucose, rather than any biochemical effect preventing cell death. In addition, over recent years it has become increasingly possible to visualise changes that are happening as a result of ischaemia. Sutherland *et al.,* highlight the importance of using available imaging techniques to demonstrate causality citing the example of visualizing oxidative stress and successive mitochondrial dysfunction in multiple sclerosis using two-photon microscopy (Nikić *et al.,* 2011, Sutherland *et al,* 2012). Changes in glutathione levels between astrocytes and neurons have also been visualised in ischemic stroke (Bragin *et al.,* 2010). In addition to the neuroprotective effect of hypothermia, alterations in cerebral blood flow are often overlooked in preclinical studies. To ensure a better chance of translation of therapies from bench to bedside measuring cerebral blood flow and other physiological parameters are of paramount importance (Sutherland *et al.,* 2011).

Seventeen years ago, the Stroke Therapy Academic Industry Roundtable (STAIR) emphasized the importance of targeting multiple mechanisms and multiple cell types in the treatment of stroke (STAIR 1999). In another attempt to rectify the discrepancy between independent preclinical animal studies and clinical trials, multicentre

phase III animal trials have been suggested (Dirnagl *et al.,* 2013). Indeed, the significance of preclinical research in the development of neuroprotective strategies for treating ischaemic stroke' has been reviewed recently by Neuhaus *et al.,* (2014).

2.2.1 Development of the Global Model of Ischaemia

The differential susceptibility of hippocampal neurons to the ischaemic insult provided by the global model of ischaemia allows study of the endogenous neuroprotection displayed by CA3 at the mechanistic level. The four vessel occlusion (4-VO) method of forebrain global cerebral ischemia mimics the human clinical condition of cardiac arrest (Traystman, 2003). It results in delayed selective neuronal damage to the CA1 neurons of the hippocampus and is a useful experimental system allowing the dissection of the underlying mechanisms of delayed neuronal death, while attempting to understand why CA3 neurons survive (Kirino, 1982). It also provides an ideal platform by which to test potential agents for neuroprotection.

The model of transient global forebrain ischemia is highly successful in rodents. It is reversible and the size of the rat means that it is relatively easy to control physiological variables. The 4-VO model was first described in 1979 (Pulsinelli and Brierley, 1979). The model of 2-VO was the most popular model before the development of 4-VO, collateral circulation was reduced by hypotension or exsanguination. In addition to transient occlusion of the carotid arteries, the 4-VO model involves cauterisation of the vertebral arteries and occlusion of the collaterals in the neck.

The method was modified in 1983 to allow for the tightness of the suture occluding the collaterals in the neck muscles to be responsive to the condition of the rat. Successful ischaemia of the rat is assessed using the following clinical criteria; lack of righting response, an absence of reaction to painful stimuli, lack of corneal reflex and a running response (Pulsinelli and Duffy, 1983). The success of the model is therefore a balance between achieving the desired complete ischaemia versus the adverse outcome of respiratory arrest (Pulsinelli and Buchan 1988). The global model is advantageous as the neuronal damage produced is predictable and the occurrence of seizures is low. In mice, it is more difficult to control for the effect of collaterals and maintain physiological control.

2.2.2 Cell death after 4-VO

In this rodent model of global transient forebrain ischaemia, the CA1 neurons are vulnerable to the insult whereas the CA3 cells are resistant. CA1 neurons are vulnerable to relatively short periods of ischaemia (>4-6 min) (Kirino *et al.,* 1984; Colbourne *et al.,* 1999 b; Suguwara, 2002; Halaby, 2004) whereas CA3 damage only becomes apparent at much greater durations of ischaemia (>20 min) (Kirino *et al.,* 1984; Ordy *et al.,* 1993).

2.2.3 Delayed neuronal death

CA1 neurons do not die immediately, but exhibit 'an unusual, slowly progressing neuronal damage', first described in the gerbil hippocampus in the early 1980s (Kirino*,* 1982). Delayed neuronal death has also been observed in the rat 4-VO model (Pulsinelli *et al.,* 1982 a). It is well documented that CA1 neurons remain morphologically intact after 24 hours of reperfusion and the histological detection of cell death is not possible until at least 48 hours (Colbourne *et al.,* 1999 b), with the final morphological outcome not apparent for 3-4 days following the insult (Kirino, 2000). In addition to investigating the intrinsic differences between CA1 and CA3 regions of the hippocampus, that give rise to the selective vulnerability, it may be possible to ascertain whether this delayed cell death provides a window for 'compromised but otherwise viable neurons' to be salvaged (Pulsinelli *et al.,* 1982 a).

The pattern of cell death in CA1 is predictable. Following a latency of approximately 24 hours, there is a medial lateral spread of cell death with some properties of apoptosis (Heron *et al.,* 1993; Ferrer *et al.,* 1994; MacManus *et al.,* 1993; MacManus *et al.,* 1995; MacManus *et al.,* 1997) but eventually resulting in necrotic cell death (Kirino and Sano, 1984; Yamamoto *et al.,* 1990; Deshpande *et al.,* 1992). The morphological features of 'delayed neuronal death' include (Kirino, 2000):

1. Maintenance of the cytoplasm and cellular organelles, such as mitochondria, for the first 2 days following ischemia (unlike necrotic lesions),

2. Clumping of the nuclear chromatin, but not to the extent of typical apoptosis (evident >48 hours).

3. Accumulation of non-membrane-bound dense structures, which probably consist of cleaved structural proteins (evident >48 hours).

The process of cell death in CA1 does not appear to be completely congruous with apoptosis, although caspase 3 (executor of apoptotic cell death) is activated in CA1 neurons and inhibiting caspase-3 has been shown to have a neuroprotective effect (Kirino, 2000). The immunosuppressants cyclosporin A and FK506, known to inhibit the permeability transition pores of mitochondria, are neuroprotective (Sheardown *et al.,* 1990), but as mitochondria are also required for apoptosis this does not allude to the actual mechanism (Kirino, 2000). In addition upon examination of CA1 neurons, DNA laddering on electrophoresis and positive Terminal deoxynucleotidyl transferase dUTP nick end labelling (TUNEL) staining were demonstrated again providing potential evidence for an apoptotic mechanism, but these changes are also found in cerebral infarction following focal cerebral ischemia, where neurons undergo typical necrosis (Kirino, 2000).

In addition to H&E staining, immunohistochemistry can also be used to characterise cellular changes following global ischaemia to look for indicators of cellular damage. Neuronal markers such as NeuN can be used to quantify cell death, GFAP (a marker of astrocytes) reactivity parallels degenerative changes in CA1 (Kragh *et al.,* 1993) and there is an increase in $GFAP^+$ astrocytes following 4-VO, in both CA1 and CA3 (15 min ischaemia) (Ordy *et al.,*1993). In addition, Iba1 has been used to characterise microglia activation following 4-VO (Kragh *et al.,* 1993).

2.2.4 Physiological Consistency

2.2.4.1 Blood Flow

In the clinic, the primary therapeutic goal is rapid restoration of blood flow through recanalization, which can be achieved by thrombolytic therapy or mechanical thrombectomy (Balami *et al.,* 2013). Indeed, recently in appropriately selected patients, endovascular restoration of blood flow in the range up to 4.5 hours to 8 hours post symptom onset improved functional outcome at 90 days as measured by the modified Rankin scale (Berkhemer *et al.,* 2015; Campbell *et al.,* 2015; Goyal *et al.,* 2015; Jovin *et al.,* 2015; Saver *et al.,* 2015). Historically, during the global model of ischaemia, adequate ischaemia in rats is assessed according to the

clinical criteria described above. In the focal model, alterations in blood flow are increasingly measured at the time of surgery using laser Doppler flowmetry (LDF) to confirm occlusion has occured. In order to provide a second measure of validation to complement the H&E staining, in this chapter LDF was used to measure changes in blood flow during the global model of ischaemia. However, hippocampal blood flow was not measured, only cortical as the fibre optic probe attached to the skull measured flow only to a depth of approximately layer IV of the cortex.

2.2.4.2 Temperature and hypoglycaemia

Core temperature and regulation achieved via telemetry probe implantation is vital in global ischaemia experiments as hypothermia has been shown to be neuroprotective (Morikawa *et al.,* 1992). Indeed, in a systematic review and meta-analysis of animal models of acute ischaemic stroke, hypothermia ameliorated outcome in about one third of animals (van der Worp *et al.,* 2007). If temperature is not controlled, it can confound the results of an experiment. For example, the method of measuring temperature should also be considered as stress induced fever has been noted following post-ischaemic rectal temperature measurements in gerbils (Clark *et al.,* 2003).

In studies using telemetry, on the one hand, gerbils that are exposed to brief ischaemia display spontaneous hyperthermia (Colbourne and Corbett, 1995) and on the other hand mild hypothermia has been observed in the 4-VO model in rats (Colbourne *et al.,* 1999 a). In addition mild hypothermia was observed in rats subjected to asphyxia-induced cardiac arrest (Hickey *et al.,* 2000). In the 2-VO model there is controversy, with a delayed temperature rise in ischaemic animals from 21 to 63 hours (measured rectally) (Coimbra *et al.,* 1996) whereas other studies have shown that rats do not always develop fever (measured using telemetry) (Clark *et al.,* 2007). There are however other physiological variables that should be considered as hyperglycaemic rats displayed postischemic hyperthermia (Uchino *et al.,* 1994), whereas normoglycemic rats had slightly decreased temperature in the first 4 hours following ischaemia with subsequent hyperthermia. Again, using the 2VO model with hypotension in rats fasted overnight, the animals were hypothermic for approximately 2 hours following surgery, then becoming slightly hyperthermic compared with initial temperatures (Spencer *et al.,* 2007).

In the global forebrain model of ischaemia, rats are fasted overnight before the day of global ischemia in order to ensure low blood glucose levels, but have free access to water. Low serum glucose has been shown to reduce the severity of strokes, decrease collateral damage and focus damage on specific brain regions which include the region of interest in this study, the hippocampus (Pulsinelli and Buchan, 1988). A reduction in temperature and or lowering of the blood sugar (Tanaka *et al*., 2008) will retard cell death and can in a dose dependant way prevent it altogether. This is illustrated by the observations made on persistent neuroprotection using prolonged hypothermia following severe forebrain ischaemia (Colbourne *et al.,* 1999 a). The evidence that temperature and hypoglycaemia reduce the likelihood of cell death account for the only true neuroprotective phenomenon so far discerned. This is not limited to the laboratory setting, glucose control post ischemic stroke is paramount to improving patient outcome (Guidelines for management of ischaemic stroke and transient ischaemic attack, 2008) and there is currently a large clinical trial underway for hypothermia to treat stroke: 'A European, multicentre, randomised, phase III, clinical trial of hypothermia plus medical treatment versus best medical treatment alone for acute ischaemic stroke' (EUROHYP-1) (https://clinicaltrials.gov/show/NCT01833312; van der Worp *et al*., 2014). However, there is no clear-cut understanding of the mechanism through which this protection is afforded underlining why recent findings on endogenous neuroprotection (Papadakis *et al.,* 2013) are important.

2.2.4.3 Activity

Locomotor hyperactivity has been described as a behavioural change following transient global forebrain ischaemia (Chandler *et al.,* 1985; Gerhardt and Boast, 1988; Poignet *et al.,* 1989). As rats habituate, the frequency of these measures should decrease as demonstrated in rats following sham ischaemia, whereas ischaemic rats had an increase in locomotor activity, in keeping with the amount of neuronal loss in the pyramidal layer of the hippocampus (Mileson and Schwartz, 1991; Andersen *et al.,* 1997; Kesner, 2007).

2.3 Aims of this Chapter

The aim of this chapter is to further characterise the global model of ischaemia by assessing cortical cerebral blood flow changes, investigating cellular changes within the hippocampus and recording temperature and activity changes.

2.4 Materials and Methods

2.4.1 Reagents

All reagents were purchased from commercial suppliers unless otherwise stated in the text.

2.4.2 Animals

Adult male Wistar rats (150-200g) were obtained from Harlan, UK. Animals were provided with food and water *ad libitum.* All procedures were conducted in accordance with regulations of the 1986 Animals (Scientific Procedures) Act under a project license from the UK Home Office, experiments were approved by the Animal Care and Ethical Review committee of the University of Oxford. All animals were allowed to acclimatize for 1 week prior to the onset of experiments to account for the effects of transport stress and were housed and studied under a standard light:dark cycle (12/12 hours).

2.4.3 Global ischaemia

Experimental animals were subjected to 10 min severe global ischaemia (GI) for the animals in the time course studies in Chapters 3, 4 and 5 and 15 minutes for laser Doppler recording in chapter 2. In sham animals the vertebral arteries were electrocauterized and the carotid arteries were manipulated, but not occluded. Rats were killed at 7 days of reperfusion following severe GI. The method consists of preparatory 'pre-4-VO' surgery 24 hours before the 4-VO surgery that results in the ischaemia. For the global ischemia model a 24 hour interval is present between the preparatory surgery and the induction of ischemia/sham ischaemia to allow the animals time to recover, to limit the stress on the day from the ischemia itself and to reduce confounding factors.

2.4.3.1 General anaesthesia and pre-operative preparation

Anaesthesia was induced in the rats using isofluorane 3% v/v, mixed with 30% (v/v) O_2 and 70% (v/v) N_2O with maintenance at 1-1.5% isofluorane v/v mixed with 30% (v/v) O_2 and 70% (v/v) N_2O. Depth of anaesthesia was assessed by degree of pupil dilation and lack of pedal reflex and the breathing rate was monitored throughout the procedure. All surgeries were performed using aseptic technique. A rectal temperature probe was inserted

to monitor temperature and the rat was placed on a draped, sterile heating mat to maintain body temperature at 37°C. Buprenorphine was diluted in sterile saline (1:9) and injected subcutaneously at a dose of 0.1mg/kg.

2.4.3.2 Telemetry probe insertion

At least seven days prior to pre 4-VO surgery, under the anaesthetic regime detailed above, sterilized core telemetry probes (TA-F40, Data Sciences International) were implanted into the peritoneal cavity using aseptic technique. A midline incision was made through the skin and peritoneum and the probe was inserted. 5-0 absorbable suture was used to close the abdominal wall. Wound staples were used to close the skin, ensuring no suture was protruding. Lidocaine was applied for local analgaesia. Rats were weighed and had their wound inspected daily.

2.4.3.3 Pre-4-VO

This preparatory surgery was carried out 24 hours prior to the 4-VO (Section 2.5.3.5). The anaesthetic regime, physiological monitoring and aseptic technique described above were used for this procedure. A baseline temperature was measured – it was vital to ensure absence of fever (therefore infection) prior to proceeding. The rat was placed in a supine position on a heating blanket and covered with a sterile drape to expose the sterilised surgical field. A 1.5cm incision was made using surgical scissors in the midline of the ventral surface of the neck. Forceps were used to bilaterally dissect out the common carotid arteries. Blunt dissection was carried out along the longitudinal aspect of the central and adjacent muscular tissues (these are sternocleidomastoid, omohyoid, thyrohyoid and sternohyoid). The vagus nerve was gently separated away from the common carotid arteries. Once the common carotids arteries were separated from surrounding tissues and nerves, 3-0 braided silk suture was passed underneath while ensuring that the artery was not ligated at this point. The sutures were then left inside the neck. A spinal needle (18 GA 3.50 in 1.2x90mm) was passed behind the trachea, oesophagus, external jugular veins and common carotid arteries, but in front of the cervical and paravertebral muscles. A length of 2-0 silk suture was passed through the spinal needle. The needle was then removed taking care to ensure that the suture remains in place at either side of the neck. The neck wound was closed using wound staples.

The rat was rotated to a prone position and its head was placed in stereotaxic ear bars with the head tilted at approximately 30° to the horizontal. An incision was made in the midline behind the occipital bone directly overlying the first two cervical vertebrae. The paraspinal muscles were separated from the midline and retracted. Cauterization of the vertebral arteries occurred through the alar foramina of the first cervical vertebra using a <1 mm diameter, palladium electrode loop angled tip electrocautery needle and Geiger Thermal Cautery Unit. The inner portion of an 18G spinal needle was used to probe the vertebral foramina to check for any remaining collaterals that required further cauterisation. The muscle layer was closed using 5-0 silk suture, followed by a 5-0 silk suture for the skin. The animal recovered from anaesthesia and was returned to an individual cage for 24 hours with access to water but not food.

2.4.3.4 Sham pre-4-VO

For sham animals, the preparatory surgery for the 4-VO occlusion model was conducted as above, including cauterisation of vertebral arteries (Papadakis *et al.,* 2013).

2.4.3.5 Global ischaemia: 4-VO

Twenty-four hours following pre-4-VO, the rat was anaesthetised as described above. The neck wound was reopened and the common carotid arteries were exposed. Once exposed, aneurysm clips were placed on the arteries to completely occlude flow. The suture thread exiting both sides of the neck was tightened to restrict collateral circulation and held in place with a surgical clamp. Clinical criteria indicating ischaemia had been achieved included dilated pupils, presence of a running response, absence of corneal reflexes, absence of response to pain and loss of righting response. Ischaemia was maintained for 10 minutes at which point the neck ligature was released, the clips removed from the carotid arteries and all sutures removed. The neck wound was stapled and lidocaine cream applied.

2.4.3.6 Sham 4-VO

For sham animals, the ligature was not tightened and carotid artery occlusion did not occur, but the carotid arteries were exposed and manipulated which in itself can produce very transient occlusion.

2.4.3.7 Laser Doppler flowmetry

LDF was conducted in collaboration with Mr Ain Neuhaus in order to describe blood flow changes in the model of global ischaemia. Prior to pre-4-VO or 4-VO, rats were anaesthetised as described above and placed prone on a heating blanket. A small midline incision was made under aseptic conditions, in the skin overlying the skull. The scalp was then retracted and a surgical microdrill was used to thin a small area of the skull. For posterior circulation measurements during pre-4-VO, the area thinned was in the centre of the occipital bone. For anterior circulation measurements during 4-VO the area thinned was ~4 mm lateral and ~1.5 mm caudal to bregma. A fiberoptic probe (connected to OxyFlo 2000 or OxyLab, Oxford Optronix, Oxford, UK) was connected using cyanoacrylate. Once baseline had been established, blood flow was recorded throughout the pre-4-VO or 4-VO procedure. At the end of the ischaemic period, or once vertebral artery occlusion had occurred, the probe was disconnected and the wound was sutured.

2.4.3.8 Recovery

Animals were recovered in a 'hot box' at 30-37°C. They were carefully monitored and once they had recovered from their anaesthesia, they were returned to their cages and given free access to water and food.

For time course experiments, each rat was returned to its cage, with free access to food and water and moved to telemetry where temperature was regulated for the required number of hours. In this system, rats are free-moving and every 30 seconds, the computerised temperature control system ART-2.2 maintains their core body temperature at 37.0±0.5°C via an infrared lamp directly over the cage. In addition, activity of each rat was recorded every 30 seconds.

2.4.4 Haematoxylin and eosin staining

In order to ascertain successful ischaemia, rats were deeply anaesthetised using 5% isoflurane in 30% (v/v) O_2 and 70% (v/v) N_2O and i.m. injections of ketamine 0.1mg/kg and xylazine 0.002mg/kg at 7 days following ischaemic insult. They were killed by overdose of anaesthetic followed by transcardiac perfusion with 10% (v/v)

formalaldehyde in PBS (4 °C). Brains were removed and incubated overnight in chilled 10% (v/v) formaldehyde in PBS, before dehydration and embedding in paraffin wax (see Table 2.1).

Solution	**Time**
30% Ethanol	2 hours
50% Ethanol	2 hours
70% Ethanol	Overnight
95% Ethanol	1 hour
100% Ethanol #1	1 hour
100% Ethanol #2	1 hour
100% Ethanol #3	1 hour
100% Ethanol:Clearene 1:1	1 hour
Clearene	45 minutes
Clearene:Wax 1:1	1 hour
Infiltration Wax #1	1.5 hours
Infiltration Wax #2	1.5 hours

Table 2.1 Preparation of tissue for paraffin embedding Time indicates incubation time in each solution.

Coronal sections (10 µm) of paraffin-embedded brains were cut from 3.6–4.16 mm posterior to bregma on a microtome. Paraffin sections were dewaxed at 60-65°C for 30 minutes, washed for 2×5 minutes in a Histoclear bath and rehydrated in progressive baths of 100% → 95% → 80% → 70% ethanol. The slides were then washed in reverse osmosis water. Sections were stained with Harris' haematoxylin (Sigma-Aldrich) for 3 minutes, washed in tap water for 5 minutes, differentiated in 1% acid alcohol, washed, blued in 0.2% ammonia water, washed and stained with eosin (Sigma-Aldrich) for 1 minute. Dehydration was performed in 70% → 80% → 95% → 100% ethanol and the sections were cleared in Histoclear for 2×5 minutes. Clear glass coverslips were mounted on the slides with DePeX. A Nikon Eclipse 1000M with Nikon DS-Fi1 camera was used for imaging.

2.4.5 Immunofluorescence

2.4.5.1 Fixed brain tissue

For immunofluorescence, animals were perfused-fixed using the same method as section 2.4.4. Brains were embedded in agarose and 50μm thick hippocampal coronal sections were cut using a Leica VT1000 vibratome.These sections then underwent free-floating immunofluorescence. Serum block in 10% donkey serum occurred for 1 hour at which point coverslips were incubated in primary antibodies: NeuN(1:300), GFAP(1:500) and Iba(1:500).overnight at 4°C. Following a wash with PBS, sections were incubated in a secondary antibody solution of Alexa488-conjugated anti-goat and anti-rabbit IgG (both from Abcam, 1:400) for a period of 1 hour at room temperature. Confocal images were acquired on a Zeiss LSM 700 with a 20× water-immersion lens and appropriate excitation/emission settings.

2.5 Results

2.5.1. 4-VO induces cell death selectively in the CA1 region of the hippocampus

2.5.1.1 H&E Staining

Occlusion of the four major cerebral blood vessels (the vertebral arteries and carotid arteries) induces selective cell death within the hippocampus, with the CA1 neurons undergoing cell death while the CA3 neurons were spared. Hippocampal cell loss was demonstrated with haematoxylin-eosin staining from animals that underwent 4-VO and 7 days reperfusion (Figure 2.1).

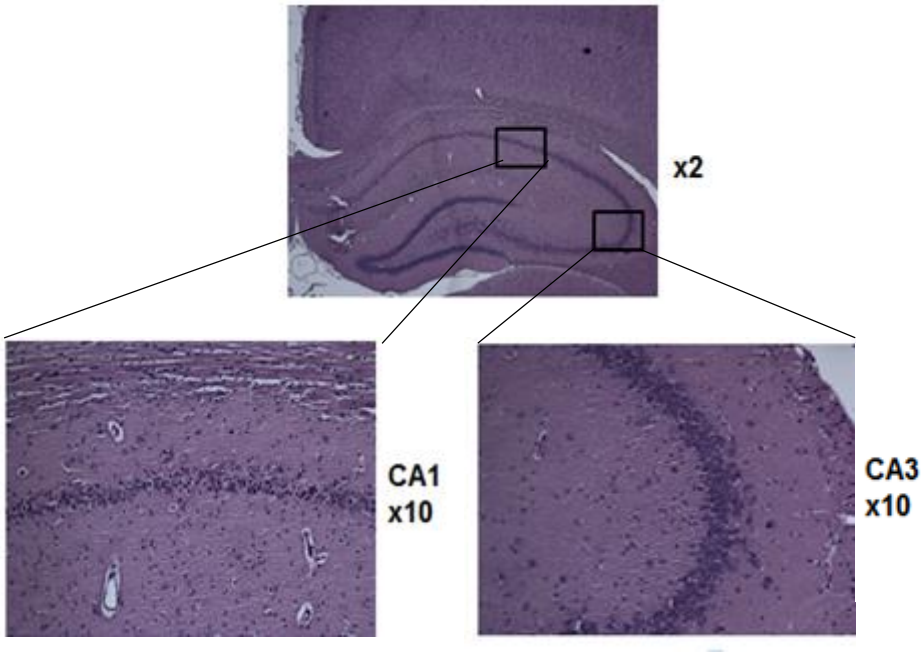

Figure 2.1 Differential cell death in CA1 and CA3 neurons 7 days following 4-VO Cells in the CA1 area demonstrate substantiall cell death when compared to CA3. Magnification x2 and x10.

2.5.1.2 Immunofluorescence

Ischaemic CA1 neuronal death could also be confirmed using NeuN, a canonical neuronal marker, while the CA3 neuronal layer remained intact. Both CA1 and CA3 neuronal layers were intact in sham animals. See Figure 2.2 for a representative image.

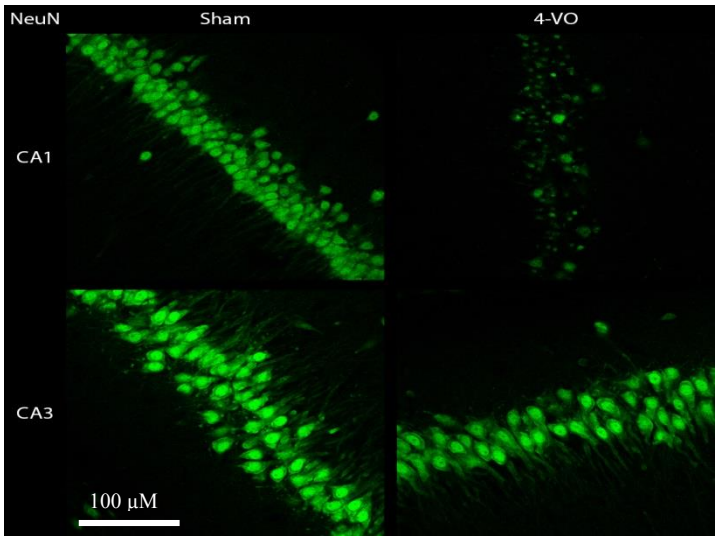

Figure 2.2: Neu-N staining in the hippocampus after 4-VO Animals underwent 4-VO surgery and were allowed to recover for 7 days prior to tissue analysis. Sham CA1 and CA3 and 4-VO CA3 regions have an intact neuronal layer, while CA1 neurons in ischaemic animals displayed neuronal death. Scale bar represents 100μmTo assess astrogliosis, GFAP reactivity was used which parallels degenerative changes in CA1. There is an increase in $GFAP^+$ astrocytes following 4-VO, in both CA1 and CA3 (Figure 2.3) compared to sham animals. Astrocytes upregulate GFAP in both CA1 and CA3, but cytoplasmic enlargement is obvious only in CA1.

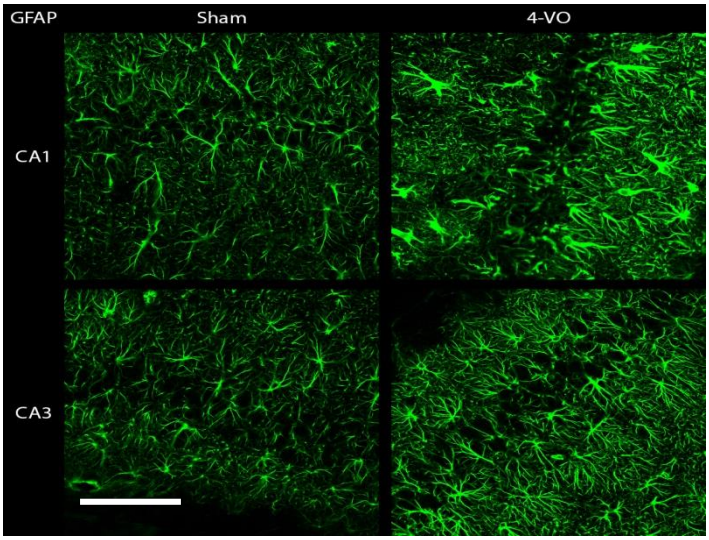

Figure 2.3: GFAP staining in the hippocampus after 4-VO Animals underwent 4-VO surgery and were allowed to recover for 7 days prior to tissue analysis. Scale bar represents 100μm.

To assess microglial activation, Iba, a marker of activated microglia was used. Microglial activation is apparent in CA1 but not CA3 at 7 days (Figure 2.4). There was no microglial activation in CA1 or CA3 in sham animals.

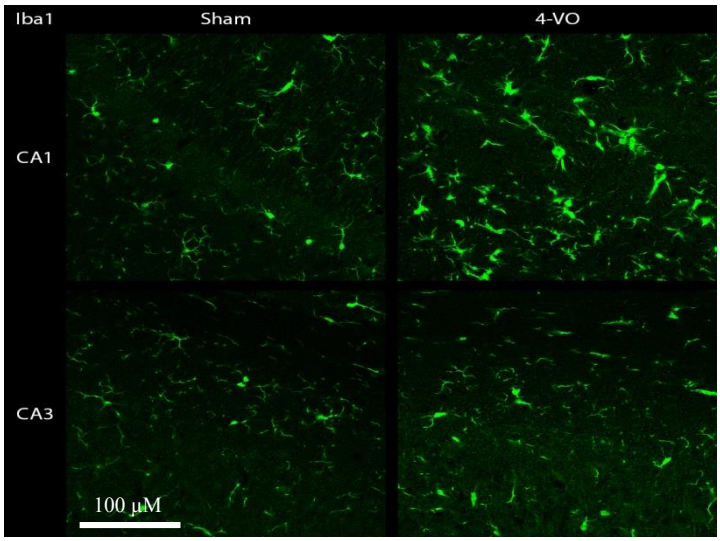

Figure 2.4: Iba1 staining in the hippocampus after 4-VO Animals underwent 4-VO surgery and were allowed to recover for 7 days prior to tissue analysis. Upregulation of Iba1 labelling was apparent in CA1 of ischaemic animals compared to CA3 of ischaemic animals and both CA1 and CA3 of sham animals. Scale bar represents 100µm.

2.5.2 Blood flow changes during Pre 4-VO and 4-VO surgery

2.5.2.1 Pre 4-VO

In order to confirm vertebral artery occlusion, a subset of animals had CBF measurements during the pre-4-VO procedure. There appears to be a gradual decrease in cerebellar blood flow upon vertebral cauterisation to about 60% of baseline (see Figure 2.5).

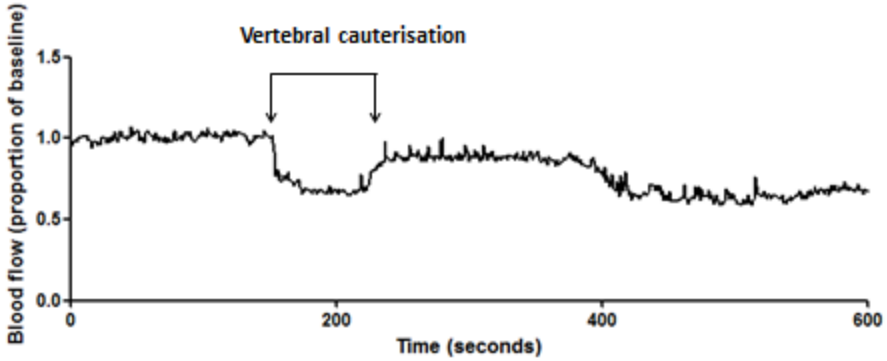

Figure 2.5: Representative LDF during preparatory Pre 4-VO surgery. There is a decrease in CBF at the point of vertebral cauterisation. The Laser Doppler probe was placed overlying the cerebellum, to monitor an area supplied by the posterior circulation.

2.5.2.2 4-VO

In order to show minimal CBF during 4-VO, a subset of animals had CBF measurements during the 4-VO procedure. Blood flow monitoring showed that CBF transiently dropped upon the manipulation of the common carotid arteries in sham animals (Figure 2.6 (A)). After placement of the clips on the common carotid arteries to produce bilateral carotid artery occlusion (BCCAO), there was a clear drop in CBF (Figure 2.6 (B)). The CBF drop remained throughout the ischaemic period and any noise observed on the trace was due to the head not being fixed and any movement caused an artefact. Figure 2.6 (C) shows that both sham (n=4) and ischaemic (n=4) animals had a sudden decrease in CBF upon occlusion of the carotids arteries. Sham animals had a very brief ischaemic period (seconds) because the arteries were manipulated but not ligated. Both sham and ischaemic animals had reperfusion back to baseline. While sham animals remained at baseline 94.2 $\pm$ 7.1 % SEM 1 minute after reperfusion, ischaemic animals had a post ischaemic hypoperfusion of 43.7% $\pm$ 9.2% SEM. One animal underwent terminal anaesthesia and was perfused with India ink with the carotid clips and suture still in place. Figure 2.6 (D) demonstrates: (i) effective prevention of perfusion to the forebrain of this animal; (ii) no perfusion of the hippocampus (the area of interest for these studies); and (iii) sections through the brain were not perfused yet the liver (bottom right handside of panel) was fully perfused.

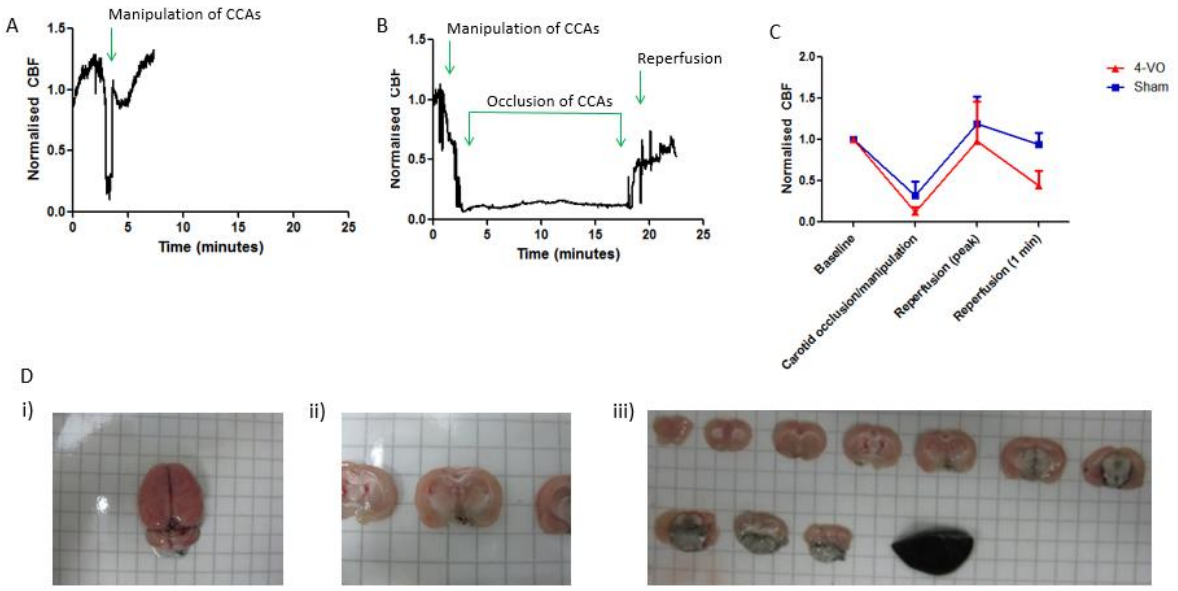

Figure 2.6 Cerebral blood flow changes in the global model of ischaemia (A) Representative trace of change in cerebral blood flow over time during sham 4-VO measured using laser Doppler. (B) Representative trace of change in blood flow over time during 4-VO measured using laser Doppler. (C) Difference in blood flow between ischaemic and sham groups according to stage of 4-VO procedure. (D) India ink perfusion to demonstrate effective cessation of blood flow. i) absence of perfusion of forebrain ii) absence of perfusion of hippocampus.and iii) coronal brain slices with absent perfusion compared to fully perfused liver (bottom right hand side of frame). CCA= Common carotid artery

2.5.3 Characterisation of temperature and activity following 4-VO

All animals used for autophagy (Chapter 4) and ER stress (Chapter 5) and experiments were placed on a telemetry system following both sham and global ischaemia. Temperature and activity recordings were recorded. Since time points of analysis were 3 and 12 hours post ischaemia, the time period 0-3 hours was reported for all animals.

2.5.3.1 Temperature following 4-VO

Sham animals had consistently lower temperatures than ischaemic animals over the first 3 hours following 4-VO (see Figure 2.7).

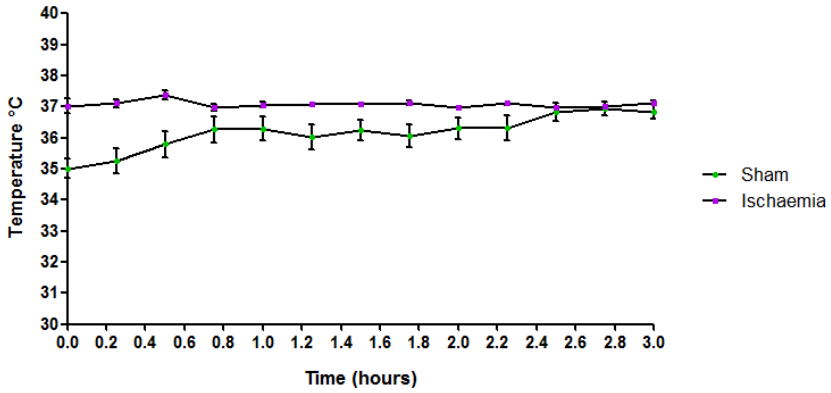

Figure 2.7: Monitoring temperature following sham and 4VO surgeries using telemetry Animals underwent sham or 4-VO surgery and were placed on telemetry immediately following the procedure. Implanted telemetry probes aimed to maintain temperature at 37ºC. Data are mean ±SEM sham n=11 vs ischaemia n=10.

2.5.3.2 Activity following 4-VO

Activity was plotted every 30 minutes for 3 hours following 4-VO. Ischaemic animals were more active than sham animals over time which reflects loss of habitual control suggesting hippocampal damage (Figure 2.8).

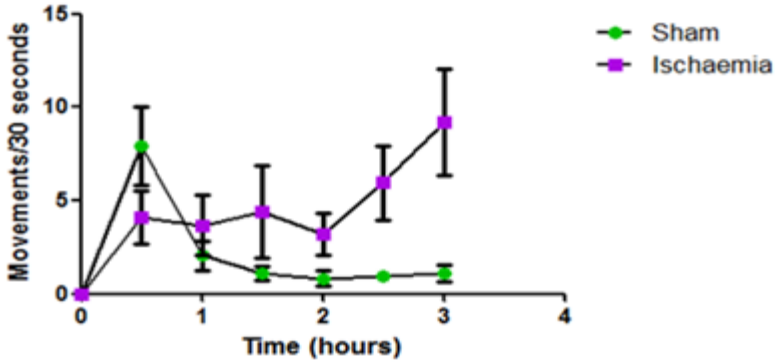

Figure 2.8 Activity immediately following sham and 4VO surgeries Animals underwent 4-VO surgery and were allowed to recover with a telemetry probe in order to monitor core body temperature and activity. Data are mean ±SEM (sham n=11, ischaemia n=10).

2.6 Discussion

The animal model of global ischaemia has the same effect as human cardiac arrest on the brain, a complete cessation of blood flow, and is used to gain mechanistic insight into ischaemic damage of the brain. Even though the model is a two day procedure, it produces a reproducible pathological outcome that allows investigation into the pathophysiology of ischaemia, as well as neuroprotection (both endogenous and exogenous).

H&E staining demonstrated the phenomenon of differential cell death in the CA1 of the hippocampus compared to CA3 (Kirino, 1982). Figure 2.1 clearly showed that animals used for 4-VO in this thesis demonstrated CA1 cell death 7 days post ischaemia. Immunohistochemistry corroborated this selective and near-complete loss of CA1 neurons without damage to CA3 confirming suitability of NeuN staining as an alternative for assessment of neuronal loss. In addition, further immunohistochemistry analysis revealed replication of an increase in GFAP staining of astrocytes (Jørgensen, 1993; Ordy *et al.,* 1993) and changes in microglial morphology following 4-VO (Jørgensen, 1993). This suggests that other cell types in the brain are reactive to the ischaemic insult and could contribute to the neuronal cell death in CA1.

Blood flow during pre-4-VO and 4-VO has been characterised using laser Doppler and clear reductions in blood flow upon vertebral artery and common carotid artery occlusions were observed. Following transient global ischaemia, there is initially hyperaemia, which is followed by post ischaemic hypoperfusion (as reviewd by Frerichs *et al.,* 1992). Pulsinelli and colleagues were the first to describe the late rise above control values in the striatum and hippocampus following post-ischaemic hypoperfusion (Pulsinelli *et al.,* 1982 b). Post ischaemic hypoperfusion may also represent the added imbalance between energy and oxygen requirements as neurons recover from the prior insult (Frerichs *et al.,* 1992). The absence of perfusion of India ink to the forebrain in this study further confirms the lack of blood flow to the brain following 4-VO.

Animals that experience 4-VO had higher temperatures and were more active in the 3 hours immediately after the ischaemic insult. Previous literature has conflicting results in this area. In studies using telemetry, on the one hand, gerbils that are exposed to brief ischaemia display spontaneous hyperthermia (Colbourne and Corbett, 1995) and on the other hand mild hypothermia has been observed in the 4-VO model in rats (Colbourne

et al., 1999 a). The ischaemic rats in these experiments may have had higher temperatures than the shams, but this did not amount to a clinical 'fever' as the 4-VO rats were only at 37°C. In the present dataset, only the first 3 hours after ischaemia was analysed as all of the animals were on telemetry for at least this duration (3 and 12 hour samples) so it was not possible to compare with studies such as Coimbra *et al.,* 1996 who observed a delayed temperature rise in ischaemic animals from 21 to 63 hours (in the 2-VO model, although these measurements were taken rectally). The data serves as a reference for others using the model and suggests that even though telemetry probes are inserted, it takes sham animals approximately 3 hours to attain 37ºC.

Locomotor hyperactivity observed in this study is in keeping with previous research (Chandler *et al.,* 1985; Gerhardt and Boast, 1988; Poignet *et al.,* 1989) where animals subjected to global ischaemia had increased activity. This increase in locomotor activity suggests that there is neuronal loss in the pyramidal layer of the hippocampus and leading to loss of habituation (Mileson and Schwartz, 1991).

It should be appreciated that after successful global ischaemia that rats usually lack activity and their body temperature drops. Telemetry is necessary as it is crucial to maintain body temperature in the normal range after ischaemia until they regain normal activity. The purpose of telemetry in these experiments was to prevent any protective effect resulting from hypothermia, therefore the rats were maintained at 37ºC. However differences can still be observed between sham and ischaemic animals as shown in this study.

2.7 Conclusion

The experiments described in this chapter showed that global ischaemia led to selective neuronal cell death in CA1 area of the hippocampus while sparing CA3 region. The CA1 region also had an increase in activated astrocytes and microglia representing an insult to this region. Global ischaemia can lead to a sharp drop in CBF and post-ischaemic hypoperfusion after reperfusion but these measurements were in the cortex and it was not known whether there were differences in blood flow between the hippocampal regions. Ischaemic animals had higher core temperature and activity within the first 3 hours after 4-VO compared to sham animals representing some degree of hippocampal neuronal loss. This model will further investigate the endogenous protective effect of hamartin (Chapter 3) and downstream effects such as autophagy (Chapter 4) and ER stress (Chapter 5).

Chapter 3: Hamartin is a novel endogenous neuroprotectant

3.1 Executive Summary

Hamartin is part of the tuberous sclerosis complex, which was previously only associated with the developmental disease, tuberous sclerosis. Upregulation of hamartin has previously been shown to provide neuroprotection in neurons following OGD. This thesis provides evidence of an *in vivo* temporal and spatial relationship between hamartin and endogenous neuroprotection demonstrated by resistant CA3 neurons compared with vulnerable CA1 neurons. There was immediate induction of hamartin expression in the membrane and a concomitant decrease in the cytoplasm following 10 minutes of global ischaemia; it is, however, not clear if this is due to transfer or translocation. Hamartin expression peaked at 12 hours in the membrane fraction of the CA3 region of the rat hippocampus and this increase in expression persisted at 24 hours following reperfusion. The temporal profile of tuberin expression did not coincide, suggesting that hamartin's effects are independent of tuberin. In CA3 there was a selective increase in the ratio of phosphotuberin to tuberin at 12 hours of reperfusion selectively in CA3, which indicates that inactivation of tuberin occured when hamartin expression peaked.

Experiments were conducted *in vitro* in order to ascertain if manipulation of the protein complex, mTOR, which is downstream of hamartin, could mimic hamartin's protective effect and afford a neuroprotection on cortical neurons. Different mTOR inhibitors had divergent effects on cell viability. Rapamycin (an mTORC1 inhibitor) applied to E18 cortical cultures for a 24 hour recovery period following 2 hours OGD did reduce cell death, but did not appear to replicate the extent to which hamartin affords neuroprotection. AZD2014, a novel mTORC1/2 inhibitor currently in clinical trials for cancer, caused increased cell death in cortical and hippocampal neurons after 24 hours OGD. There was a trend for higher expression levels of the ER stress protein ATF4 in neurons treated with AZD2014 which could explain the mechanism for the neurotoxicity this compound induced.

Hamartin is responsible for the endogenous neuroprotective phenomenon in CA3 cells of the hippocampus. Mechanistically, a temporal and spatial profile of changes in hamartin expression in the hippocampus has been elucidated. However, pharmacological modulation of the downstream targets, mTORC1 and mTORC2 has not

reproduced this protective effect. Further downstream mechanisms from hamartin will be probed in Chapter 4 (autophagy) and Chapter 5 (ER stress) in addition to a potential mechanism for the cytotoxic effects of AZD2014.

3.2 Background

3.2.1 Hamartin and mTOR

In vivo, hamartin (TSC1) and tuberin (TSC2) exist together in a structure called the tuberous sclerosis complex (TSC). TSC1 interacts and stabilises TSC2 via its coiled- coiled domain (Inoki and Guan, 2009). TSC is a tumour suppressor (Jozwiak, 2006), which inhibits the mTOR via its GTPase-activating protein (GAP) activity toward Rheb (as reviewed by Wong, 2010). When the inhibitory effect of the TSC complex is removed, mTOR is unregulated which results in uncontrolled protein synthesis and inhibition of autophagy. Hamartin is part of the PI3K/AKT pathway.which can regulate hamartin's activity based on the activation of growth factor receptors and other cell triggers.

The neuroprotective effect of mTOR is mediated not only by reducing energy consumption due to decreased protein synthesis, but also by recycling existing proteins through the austere phenomenon of productive autophagy (Gabryel *et al.,* 2012). In the ischaemic brain, neurons are not only hypoxic but lack energy and nutrients. The adaptive response of productive autophagy removes to misfolded or long-lived proteins and organelles that are damaged or surplus to requirements and recycles their constituent parts for use in this time of acute need. TSC, and therefore hamartin and mTOR, have been implicated in each of these three stresses upon the ischaemic cell. Hypoxia has been shown to affect mTOR signalling through more than one mechanism (Arsham *et al.,* 2003; DeYoung *et al.,* 2008; Huang and Manning, 2008). Any stress that depletes cellular ATP (the cell's energy source), such as oxidative stress, hypoxia and nutrient deprivation, results in the activation of AMPK which directly phosphorylates and activates part of the TSC complex (Hardie, 2004). Nutrient deprivation results in decreased availability of amino acids which has been shown to regulate the mTOR pathway (Huang and Manning, 2008).

There are two known mTOR complexes, mTOR complex 1 (mTORC1) and complex 2 (mTORC2). Downstream effectors of mTORC1 include S6K1 and 4E-BP1 leading to increased protein synthesis. mTORC1 also has an

inhibitory effect on autophagy. Activation of mTORC2 leads to PKC phosphorylation and cytoskeletal changes. Given its pivotal role in the mTOR pathway, modulation of this pathway which may be responsible for the neuroprotective effect of hamartin, could be a novel therapeutic approach for treating neurological diseases.

It is well documented CA1 neurons are morphologically intact after 24 hours of reperfusion following global ischaemia and cell death is not detected histologically until 48 hours following ischaemia whereas CA3 neurons remain resistant (Colbourne *et al.,* 1999). The differential expression of hamartin in this critical time period after ischaemia could be a factor in the selective vulnerability of CA1 neurons or the resistance of CA3 neurons and this chapter will explore changes in hamartin expression within the hippocampus following global ischaemia.

3.2.2 Pharmacology

To replicate the endogenous upregulation of hamartin resulting in the inhibition of mTOR and subsequent neuroprotection, this chapter will use pharmacological inhibitors of mTOR.

3.2.2.1 Rapamycin

The case for a neuroprotective effect lying within a pathway regulated by hamartin is strengthened by the results of a retrospective study of Mayo Clinic heart transplant patients (n=313) who were switched from cyclosporine-based therapy to the mTOR inhibitor Rapamycin (also known as Sirolimus) (n=116) and followed over a period of nearly 20 years. Not a single patient receiving Sirolimus in this inherently high-risk group had a stroke or transient ischaemic attack (van de Beek *et al.,* 2009). This study did not have an imaging component, and it may be that this group of patients maintained their incidence of ischaemic stroke (an embolic phenomenon), but the neuroprotective effect of suppressing the mTOR pathway prevented clinically detectable events and they were therefore asymptomatic. Alternatively, suppressing the mTOR pathway could be preventing embolic stroke from occurring in the first place. In a retrospective study of heart transplant patients at the same centre, not on Sirolimus, cerebrovascular events occurred in 5% of patients with perioperative stroke being quoted as being the most important neurologic complication that affects the survival of these patients in their first year post transplant (van de Beek *et al.,* 2008).

Rapamycin (Figure 3.1) is an mTORC1 inhibitor, approved by the USA Food and Drug Administration (FDA) for immunosuppression in renal transplant patients (Aspeslet and Yatscoff, 2000). Rapamycin, produced from the bacteria *Streptomyces hygroscopicus* takes its name from the island where the soil sample in which it was discovered, 'Rapa Nui' (Easter Island; as reviewed by Stipp, 2011). Although rapamycin is traditionally considered an mTORC1 inhibitor, it can affect mTORC2, but only after prolonged treatment can it affect assembly and function in some cells (Huang and Manning 2008).

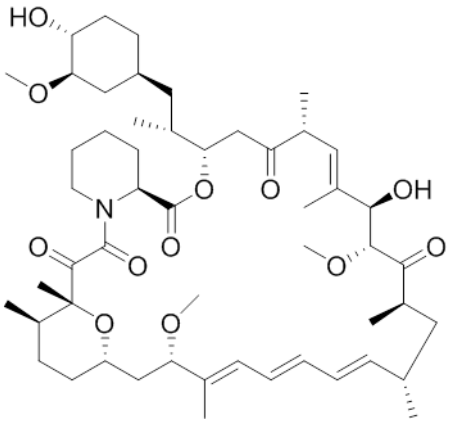

Figure 3.1 Chemical structure of rapamycin

Rapamycin has previously been shown to have neuroprotective effects in animal studies. In neonatal hypoxia-ischaemia rapamycin increased autophagy in Sprague–Dawley pup rats, reduced necrotic cell death and decreased brain injury (Carloni *et al.,* 2008). Neuronal cultures, following 1 hour of OGD and either 90 minutes or 24 hours of rapamycin treatment demonstrated increased neuronal viability. 5nM rapamycin was sufficient to achieve a 50% reduction of mTORC1 Ser-2448 phosphorylation. 20nM of rapamycin for 90 minutes caused a 21.6% +2.5% reduction in mTORC2 Ser-2481 phosphorylation, rising to 63.7% + 0.3% at 24 hours (Fletcher *et al.,* 2013). Rapamycin may ameliorate brain oedema following focal cerebral ischaemia reperfusion in rats via inhibition of matrix metalloproteinase 9 (MMP9) and aquaporin 4 (AQP4) expression (Guo *et al.,* 2014). MMPs are zinc dependent endopeptidases that participate in neuronal injury after ischaemia reperfusion and aquaporins are thought to be in part responsible for cerebral oedema as they govern water movement in and out of the brain.

Rapamycin has also been postulated to extend maximum lifespan in rodent models (Blagosklonny and Hall, 2009: Harrison *et al.,* 2009). In addition the inhibition of mTOR via rapamycin in a transgenic human (h)APP mouse model of Alzheimer's disease (AD) restores brain vascular integrity and function through NO synthase activation (Lin *et al.,* 2013). The clinical utility of rapamycin for indications other than transplantation is an emerging field, as is the role of the pathway containing hamartin and mTOR in a variety of seemingly disparate pathologies.

Rapamycin does not fully inhibit mTORC1. Initially downstream targets (S6K and 4E-BP1) are inhibited, but 4E-BP1 recovers in phosphorylation. This recovered 4E-BP1 remains rapamycin resistant but still requires mTOR, Raptor, and mTORC1's activity (Choo *et al.,* 2005). Rapamycin was used in this study to determine the beneficial effects suggested by the literature of mTOR inhibition on neuronal viability following OGD because it is the gold standard mTOR inhibitor.

3.2.2.2 AZD2014

AZD2014 (Figure 3.2) is a dual mTORC1/mTORC2 small molecule ATP-competitive inhibitor produced by Astra Zeneca. It was discovered through the optimization of AZD8055 that reduces turnover in human hepatocytes (Pike *et al.,* 2013). AZD2014 is currently undergoing a number of clinical trials in malignancy (https://clinicaltrials.gov/).

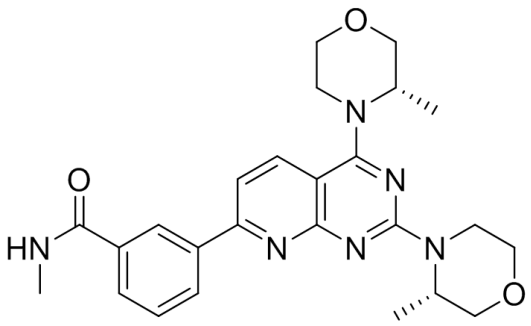

Figure 3.2: Chemical structure of AZD2014

AZD2014 was investigated as a replacement to rapamycin because rapamycin and its derivatives neither completely block mTORC1 nor offer effective inhibition of mTORC2. In the absence of mTORC2 inhibition, Akt

is activated and the negative feedback loop that usually prevents over-activation of mTORC1 becomes irrelevant, thus diminishing the antitumor activity of these drugs (Hsieh *et al.,* 2010; Pike *et al.,* 2013; Sun, 2013) (see Figure 1.7, Chapter 1). In cancer cells, the contribution of mTORC2 to the phosphorylation of AKT at Ser^{473} residue (Sarbassov *et al.,* 2005) is pivotal to the maximal activation of AKT accounting for its role in the growth, proliferation and angiogenesis of cancer cells. In human hepatocellular cancer cell (HCC) lines, AZD2014 resulted in dramatic antitumour effects (Liao *et al.,* 2014). Through measuring different substrates of mTORC1 (phosphorylation of S6K at Thr^{389} and phosphorylation of 4EBP1 at $Thr^{37/46}$) and mTORC2 (phosphorylation of AKT at Ser^{473}), it was demonstrated that AZD2014 fully inhibited mTORC1 and mTORC2 signalling and prevented the feedback activation of AKT (Liao *et al.,* 2014). AZD2014 effectively inhibited p-S6K Thr^{389} and p-4EBP1 $Thr^{37/46}$ in a concentration-dependent manner (10-1,000nM). In these particular cancer cells this phosphorylation site appeared to be resistant to rapamycin.

In further experiments, AZD2014 was found to induce apoptosis in subsets of HCC cells and a strong G1 arrest in HCC cells. Dual mTORC1/2 inhibition using AZD2014 not only induced a more profound autophagy than rapamycin but it was present in all cell lines tested (Liao *et al.,* 2014). In cultured colorectal cancer cell lines, AZD2014 (1-100nM) significantly inhibited cancer cell growth not by inducing cell apoptosis, but via inhibition of mTORC1/2 and activating autophagy. Growth inhibition occurred at concentrations >10nM and 50nM induced around 50% of cell viability loss. The investigators, translated these findings to an *in vivo* paradigm as oral AZD2014 significantly inhibited the growth of HT-29 cell xenograft in SCID mice and dramatically increased survival (Huo *et al.,* 2013).

AZD2014 has also been investigated for use in human glioblastoma. In a recent study, 1- 4μM AZD2014 was shown to enhance radiosensitivity of glioblastoma stem-like cells, both *in vitro* (using 4 neurosphere-forming cultures from human GBM surgical specimens) and *in vivo* (8-10 week old athymic female nude mice) (Kahn *et al.,* 2014). The safety and tolerability was assessed in a phase 1 dose-escalation and expansion study in 50 patients with solid tumours (Banerji *et al,.* 2012) leading to pharmacokinetic and pharmacodynamics studies in humans revealing pharmacologically relevant plasma concentrations and clinical responses (including reduced metabolism and proliferation of malignant cells) (Basu *et al.,* 2015).

AZD2014 was shown to be protective in the context of oxidative stress and inflammatory reactions produced by disturbed flow in atherosclerosis (Martin *et al.,* 2014). AZD2014 has however never been used in the context of cerebral ischaemia and it will be used in this study as a comparison with rapamycin due to its dual inhibition of mTORC1/2. AZD2014 will be referred to as AZD from this point on in the thesis.

3.3 Aims of this chapter

1. Aim to demonstrate that CA3 neurons in the hippocampus are resistant to global cerebral ischaemia *in vivo* by altering hamartin expression, and that these changes are hippocampal region and time-dependent.

2. Aim to mimic the neuroprotection mediated by hamartin *In vitro* by pharmacological inhibition of the mTOR pathway.

3.4 Materials and methods

All reagents were purchased from commercial suppliers unless otherwise stated in the text.

3.4.1 *In vivo*

3.4.1.1 Global ischaemia

This method is described in Chapter 2. For the results displayed in this chapter, the *in vivo* experiments were carried out working in collaboration with Dr Michalis Papadakis, University of Oxford.

3.4.1.2 Terminal anaesthesia and brain microdissection

Rats were killed immediately following the required period of reperfusion (0, 3, 12 and 24 hours) by deeply anaesthetising and decapitating them using a small animal guillotine. Rat brains were removed, rinsed with sterile saline and microdissected on ice. Coronal slices of approximately 2 mm were obtained using a brain matrix and surgical blade. Tissue from CA1 and CA3 regions of the hippocampus were dissected from the relevant slices with the aid of a rat brain atlas and dissecting microscope. The samples were then frozen using dry ice and kept at -80°C until processing.

3.4.1.3 Subcellular fractionation

Subcellular fractionation was carried out using a modified version of Guillemin *et al.,* 2005. This was conducted for the timepoints 0, 12 and 24 hours. Tissues were homogenised in cell lysis (CLB) buffer (10 mM 2-[4-(2-hydroxyethyl)piperazin-1-yl]ethanesulfonic acid (HEPES), 10 mM NaCl, 1 mM KH_2PO_4, 5 mM $NaHCO_3$, 5 mM ethylenediaminetetraacetic acid (EDTA), 1 mM $CaCl_2$, 0.5 mM $MgCl_2$, 250 mM sucrose, pH 7.4), supplemented with 1mM Phenylmethylsulfonyl fluoride (PMSF), protease inhibitor cocktail (Roche) or 10mM $NaVO_4$ or phosphatase inhibitor cocktail (PhosSTOP, Roche) at 4 °C. The volume of CLB buffer added was equal to 30 microlitres per milligram of tissue and this was homogenised using a glass homogenizer. The tissue was pre-homogenised by applying ten strokes with a loose pestle and incubated for 10 minutes. The sample was then further homogenised by applying 50 strokes with the loose pestle. A further volume of 10% of the CLB added

to the tissue and 2.5M sucrose was added to restore the isotonicity of the sample. The homogenates were centrifuged at 1,000*g* for 10 min. The pellet was re-suspended in CLB buffer according to original weight and centrifuged at 1,000*g* for 10 minutes. After sedimentation at 107,000*g* for 30 minutes, the resulting supernatant (cytoplasmic fraction) was stored at −80 °C. Solubilization buffer (20 mM Tris, 7 M urea, 2 M thiourea, 4% (w/v) CHAPS, pH 7.4) was added to the pellet according to weight and incubated for 1 h at 4 °C. Samples were ultracentrifuged at 120,000*g* for 3 h, and the supernatant (membrane fraction) was stored at −80 °C.

3.4.1.4 Whole Cell Homogenisation

All steps were conducted at 4 °C, and all buffers were supplemented with 1 mM PMSF, 10 mM $NaVO_4$ and a protease inhibitor cocktail (Roche Diagnostics). Tissues were homogenised in 300 µl of homogenisation buffer (50mM Tris HCl, 150mM NaCl, 1% Triton X-100, 1mM EDTA, 0.1% sodium dodecyl sulfate (SDS), pH 7.4) using a glass homogeniser with a tight glass rod using 50 strokes on ice until the solution was smooth. The homogenates were incubated for 30 minutes using a rotary platform at 4°C. The homogenates were spun at 13,000 rpm (maximum speed) for 30 minutes at 4°C. The resulting supernatant was transferred to an eppendorf tube and kept on ice. The pellet was resuspended in 200µl of homogenisation buffer by pipetting and centrifuged at 13,000 rpm (maximum speed) for 30 minutes at 4°C. The supernatant was pooled and stored at -80°C.

3.4.1.5 Protein Assay

Protein assays were carried out using a detergent compatible (DC) (Reagent A and B kit) (Bio-Rad) or bicinchoninic acid *assay* (BCA). Absorbance was determined using a microplate reader and the concentration of protein (mg/ml) in each individual sample was calculated using a standard curve.

3.4.1.6 Identification of Proteins

3.4.1.6.1 Electrophoresis

Volumes of original sample required for 25µg of protein were calculated. If the volume required exceeded the maximum volume permitted by the gel, samples were precipitated. Cytoplasmic and membrane fractions or whole-cell homogenates (20–50 µg) were precipitated using methanol/chloroform. The initial volume containing

the desired amount of protein was made up to 50µl initial volume with the appropriate solution cell lysis buffer (CLB) (for cytoplasmic fraction, solubilisation buffer for membrane fraction, homogenisation buffer for whole cell homogenate). 200 µl of methanol (x4), 50 µl of chloroform (x1) and 150 µl of deionized water (x3) was then added to each eppendorf tube and vortexed. Samples were placed into a table top centrifuge and spun at maximum speed (13,000 rpm) for 1 minute. On careful removal from the centrifuge, there was an upper layer, an interface and lower layer. The upper liquid layer was removed taking care not to disturb the interface. Methanol 200 µl (x4) was then added and the samples were spun at maximum speed again for 5 minutes. The supernatant was removed and the pellet then left to air dry.

The pellet was resuspended to a total volume of 15µl – 45ul depending on the capacity of the gel in x2 Laemmli sample buffer (Biorad), 10% 100mM dithiothreitol (DTT) and the remaining volume distilled water. Samples were heated to 95°C for 5 minutes to denature proteins.

Samples were then loaded via pipetting onto Criterion Tris-HCl Precast 7.5 or 15% gels (Biorad) (depending upon the molecular weight of the protein to be detected), in a chamber filled with running buffer (x10 stock (0.025M Tris Base, 0.2M Glycine, 0.1% (w/v) SDS in distilled water). At least one marker lane was used to determine molecular weight. The gel was then run at 110V for 2 hours before transferring to a Polyvinylidene difluoride (PVDF) membrane. The membrane was prepared for protein transfer by rehydration in methanol for 15 seconds, followed by water for 30 seconds and finally transfer buffer (0.025M Tris Base, 0.2M Glycine and 10% methanol in distilled water) until needed. The gels were removed from the electrophoresis chamber and equilibrated in transfer buffer for 5 minutes. The gel and membrane were assembled in a cassette and placed in the transfer chamber and covered with transfer buffer. A cold pack was added to reduce semi-dry transfer time and the transfer occurred over 30 minutes at a 100V.

3.4.1.6.2 Quantification of loading

Protein quantification was carried out using SYPRO® reagent (Life Technologies). The validation for this method is presented in Section 3.5.1. The membrane was left for one hour to dry completely. Washing and staining steps were conducted on a rocking platform at 30rpm. Firstly, the membrane was floated face-down in

7% acetic acid and 10% methanol made up to 50ml with deionised water and incubated for 15 minutes. The membrane was then floated in four changes of deionised water for a period of five minutes each. The membrane was then floated in SYPRO® reagent for 15 minutes. The membrane was then washed 2-3 times for 1 minute in deionised water to remove excess dye from the membrane. Six (most prominent) band analyses were conducted using the UVP Biospectrum AC imaging system (see Figure 3.4).

3.4.1.6.3 Western blotting

The membrane was blocked with constant rocking at 30 rpm with 5% w/v milk powder in phosphate buffered saline (PBS), containing 0.01M phosphate buffer, 0.0027M potassium chloride and 0.137M sodium chloride (obtained from Sigma-Aldrich and made up in deionised water), for one hour at room temperature. The membrane was then removed and placed in the appropriate primary antibody at an optimised concentration (see section 3.4.1.6.4) diluted in 5% milk in PBS and left overnight at 4°C.

The following morning, the membrane was washed for 3 changes of 5 minutes each in PBST (1ml Tween per litre of PBS). The secondary antibody was either goat-anti-rabbit, goat-anti-mouse or donkey-anti-goat horseradish peroxidase (HRP). The secondary antibody, again diluted in 5% w/v milk powder PBS was left on the rocking platform for 1 hour at room temperature, followed by five washes in PBST of 3 minutes. The membrane was then developed using enhanced chemiluminescence (ECL) (Lumigen) for 5 minutes. The excess ECL was removed and the membrane was sandwiched between transparent acetates with a tracker tape to identify corresponding standard molecular weights as dictated by the marker. The blot was exposed using the Biospectrum AC imaging system and VisionWorks software (UVP) and images were captured for analysis. The bands were quantified by densitrometry and corrected for loading using the quantified SYPRO ® data.

It was possible to probe the same membrane with more than one antibody. Membranes were stripped as follows: 5 minutes PBS-T, 10 minutes Blot Restore Solution A (Millipore), 15 minutes Blot Restore Solution B (Millipore), 5 minutes PBS-T, further blocking with 2 x 5 minutes 5% w/v milk powder PBS then placed in the required antibody at the required concentration in 5% milk PBST and left overnight at 4°C.

3.4.1.6.4 Antibody reagents for immunoblotting (IB)

Primary antibodies used: 1:1000 antibody to hamartin (rabbit) (ab25882, Abcam), 1:1000 antibody to tuberin (rabbit) (ab32554, Abcam), 1:1000 antibody to mTOR (rabbit), 1:1000 antibody to PhosmTOR (Ser2448) (rabbit) (Cell Signaling Technology), 1:1000 antibody to Phospho-S6 Ribosomal Protein (p-S6RP) Ser235/236 (rabbit) (Cell Signaling Technology).

3.4.2 *In vitro*

3.4.2.1 Cell Culture

Primary neuronal cultures were used to determine pharmacological effects on cell viability following oxygen and glucose deprivation (OGD).

For neurons to adhere to wells of a plate, plates were coated with poly-D-lysine (Sigma), coated one day prior to dissections 100µg/ml poly-D-lysine was added to each well for 1 hour. Two washes were then carried out with sterile water and plates were left to dry overnight. For plates containing coverslips for immunocytochemistry experiments, coverslips were autoclaved, soaked in ethanol for one hour and left to air dry for an hour (in the sterile hood) before they were coated with poly-D-lysine.

Hippocampal and cortical neuronal cultures were prepared from E18 rat embryos (Vogiatzi *et al*., 2008). The dam was killed via Schedule 1 and the embryos quickly removed and placed in Hanks' Balanced Salt solution (HBSS) and kept on ice. Each embryo was removed from its amniotic sac and the brain was removed. Using a dissecting microscope, the meninges were unwrapped and the cortex and the hippocampus were dissected out and placed in 1ml of NeuroBasal medium (NBM). The NBM was removed and 1ml of prewarmed trypsinisation solution (0.05% trypsin, 100µg/ml DNAse in NBM) was added, the tissue was dissociated and digested for 15 minutes at 37°C. Trypsin was inhibited by adding 3ml 10% fetal bovine serum (FBS) in NBM. The tissue was then fully dissociated with a pipette and spun at 1500rpm for 5 min. The supernatant was discarded and the cells were re-suspended in 10 ml of complete NBM medium (Gibco, containing 2% B27 serum-free supplements (Gibco), 2 mM L-glutamine**,** 1% Penicillin /Streptomycin (Sigma). Cells were then counted using trypan blue and

a haemocytometer and plated onto plates at a density of approximately 150,000cm^2 (500,000 cells per well of a 12 well plate). Cells were maintained in complete NBM in 5% CO_2/95% O_2 at 37°C and every third day half the medium was replaced with fresh medium.

Primary neuronal cultures were used to determine pharmacological effects on cell viability following oxygen and glucose deprivation (OGD).

3.4.2.2 Oxygen glucose deprivation

OGD experiments were conducted using a hypoxic chamber (Coy, USA) in cortical and hippocampal cultures that had been plated for 7-8 days, these are considered mature cells. Plates were washed twice and immersed in deoxygenated custom Neurobasal medium without without D-glucose and sodium pyruvate (Neurobasal-A, Invitrogen) at 0% O_2. The immersion solution was pre-equilibrated overnight in the hypoxic chamber, resulting in a pO_2 less than 10 mm Hg. Normoxic controls were treated similarly but with normoxic custom Neurobasal medium supplemented with 25 mM d-glucose in a standard incubator in humidified room air with 5% CO_2. Following OGD, both hippocampal and cortical cultures were recovered with fresh complete NBM for 24 h in a normoxic incubator.

3.4.2.3 Cell death assays

Cell death in primary neuronal cultures was assessed quantitatively using the LDH release Cytotox96 assay (Promega). Media was collected at the end of 2 h and 24 h recovery periods for LDH analysis. Total LDH released was determined by exposing cells to NBM containing 1% Triton x100 and incubating for 45 minutes to lyse cells. Measurements were carried out in technical triplicate for at least n = 3 biological replicates. The results were expressed as a percentage ratio of the amount of LDH released in the cell culture medium to the total LDH content, measured in the same cultures.

3.4.2.4 Preparation of samples for western blot

At 24 hours recovery, recovery media were removed and plates were washed with PBS. 250ul Cell lysis buffer (50 mM Tris-Base, 150mM NaCl, 1mM EDTA (pH to 7.4), 1% Triton, 0.1% SDS) was added to each well. The

wells were scraped with a pipette tip to detach and lyse and the cell solution was transferred to eppendorf tubes and left on ice for 30 minutes. Samples were placed in a centrifuge precooled to 4°C and spun at maximum speed (13,200 rpm) for 30 minutes. The supernatant was removed and stored at -20°C until Western blotting was carried out (see section 3.4.1.6).

3.4.2.5 Pharmacology

A rapamycin (Sigma) stock solution (2.7mM) was prepared in DMSO. Concentrations 1, 10 and 100nM were used in treatment time point experiments ('pre-treatment' 24 hours prior to 2 hours OGD or normoxia, during the 2 hour OGD or normoxia period, or 'post treatment' in the recovery media only for 24 hours following the 2 hour OGD or normoxia period. A dose range of 1nM - 10μM was used to assess protein expression during normoxia. A 10mM stock solution of AZD2014 (Astra Zeneca) was prepared in DMSO. Concentrations of 100nM and 1μM were used for treatment time points with media and DMSO controls. Concentrations of 1nM - 10μM were used to assess protein expression during normoxia.

3.4.3 Statistical analyses

Statistical analysis was carried out with GraphPad Prism 5 using a two-tailed Student's *t*-test if two groups were compared, one-way ANOVA with Bonferroni's multiple comparisons *post hoc* test for comparisons of more than two groups and two-way ANOVA with Tukey's multiple comparison *post hoc* test when two independent variables were assessed. Differences were considered significant for $P < 0.05$. Data are presented as mean $\pm$ SEM.

3.5 Results

3.5.1 Method Development

In Western blotting, although the same amount of protein is loaded into each well (in this thesis 20-25 micrograms, it is necessary to conduct a 'loading correction' to reflect the actual amount of protein loaded (some may be lost in the loading process). This ensures that the intensity of bands seen when probed for antibodies is corrected according to the amount of protein loaded. Validation of SYPRO® protein gel stain (Life Technologies) was required as earlier western blot analysis had previously used the Ponceau-S stain. When assessing protein loading, whole lane analysis (Figure 3.3 (A) and (B)) was compared with analysis of four salient bands (Figure 3.3 (C) and (D). SYPRO® Ruby stain (4-band average) provides the most accurate correction for loading in western blots (r^2=0.79) compared with whole lane analysis (r^2=0.56). For all subsequent western blot loading corrections, at least 4 individual defined bands were selected to include those corresponding to areas where the proteins of interest were expected to be found.

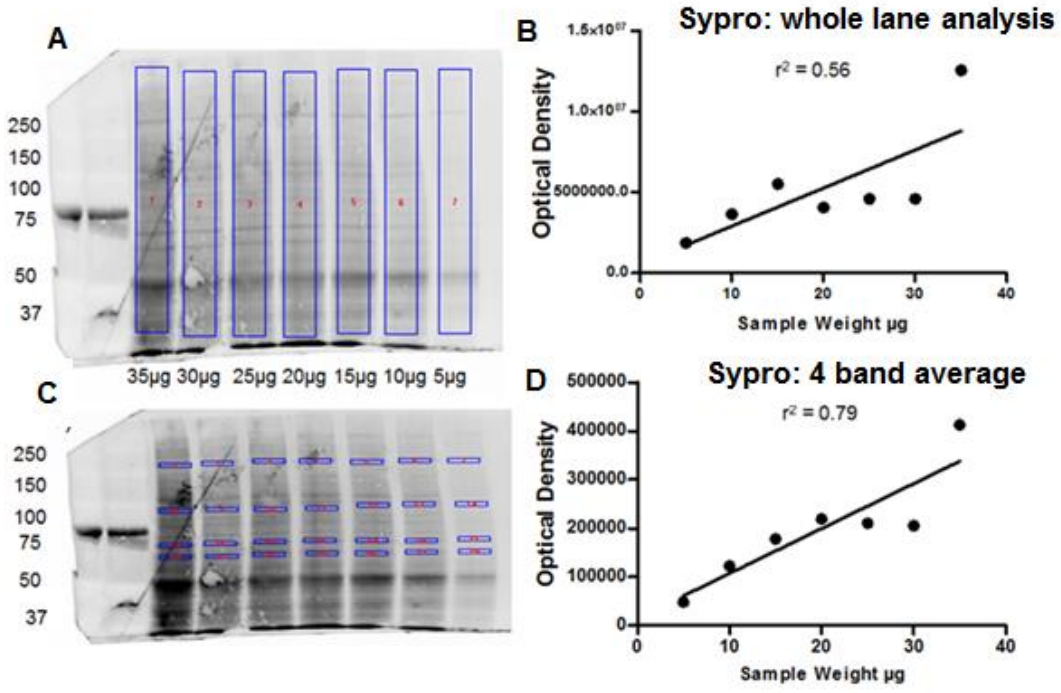

Figure 3.3 Method validation for correction of loading in Western Blot analysis using SYPRO® Analysis conducted using BioSpectrum Imaging System software (UVP). (A) 7.5 % gel, whole lane analysis using concentrations of protein (0-35µg). (B) Correlation coefficient graph for the whole lane analysis. (C) 7.5 % gel, four band analysis using concentrations of protein (0-35µg). (D) Correlation coefficient graph for the 4 band average.

3.5.2 *In vivo*

3.5.2.1 Time course of hamartin and tuberin expression following 4-VO

In order to investigate basal levels of hamartin in sham animals, CA1 and CA3 areas of the hippocampus from sham animals were dissected. Tissue was processed into membrane and cytoplasmic fractions via subcellular fractionation and material used for Western Blot analysis. There is no significant difference between hamartin expression levels in CA1 and CA3 of sham animals (Figure 3.4 (A)). There is no difference between expression of the other tuberous sclerosis protein, tuberin, and its inactivated form phosphotuberin in sham animals in either the cytomplasmic or membrane fractions of the hippocampus (Figure 3.4 (B)).

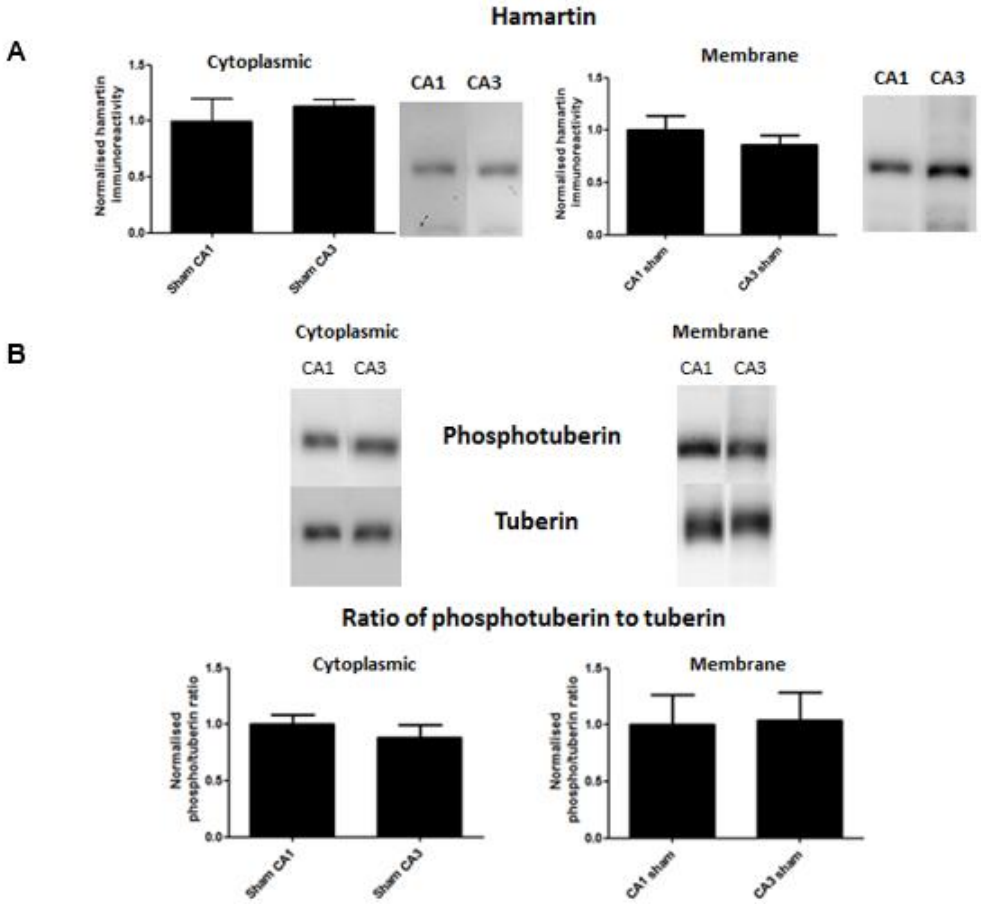

Figure 3.4 Expression levels of the proteins composing the TSC complex in the hippocampus. Levels are similar between the CA1 and CA3 regions of the hippocampus. Expression levels of (A) hamartin, (B) phosphotuberin to tuberin ratio are not significantly different between the CA1 and CA3 hippocampal areas of sham animals. n=4 all groups.

To examine whether a selective dynamic response of hamartin expression in the CA3 area could be involved in the endogenous resistance of CA3 neurons to global ischaemia, CA1 and CA3 areas of the hippocampus were dissected following 10 minutes of global cerebral ischaemia and reperfusion times of 0, 12 and 24 hours. Tissue was processed into membrane and cytoplasmic fractions via subcellular fractionation and the material was used for Western Blot analysis.

Hamartin expression in the membrane fraction of CA1 and CA3 hippocampal neurons over the time course 0-24 hours is shown in Figure 3.5 (A). In the CA3 area after 10 minutes of forebrain ischaemia, there was a 1.67 ± 0.24 fold induction of hamartin expression (p=0.0006, one-way ANOVA) in the membrane fraction compared to membrane CA3 sham levels. Hamartin expression in the CA3 membrane fraction peaked at 12h (1.94 ± 0.30 fold) and was still significantly increased compared to sham at 24h of reperfusion. Hamartin expression in cytoplasmic fraction of CA1 and CA3 hippocampal neurons is shown in Figure 3.5 (B). In the cytoplasmic fraction, there was a reduction in CA3 hamartin expression immediately after 10 minutes global ischaemia which correlated with the increase in CA3 hamartin expression in the membrane fraction. At both 12h and 24h of reperfusion hamartin expression in CA3 was decreased but not significantly compared to sham CA3. In CA1 hamartin expression remained unaffected after ischaemia and reperfusion in both membrane and cytoplasmic fractions.

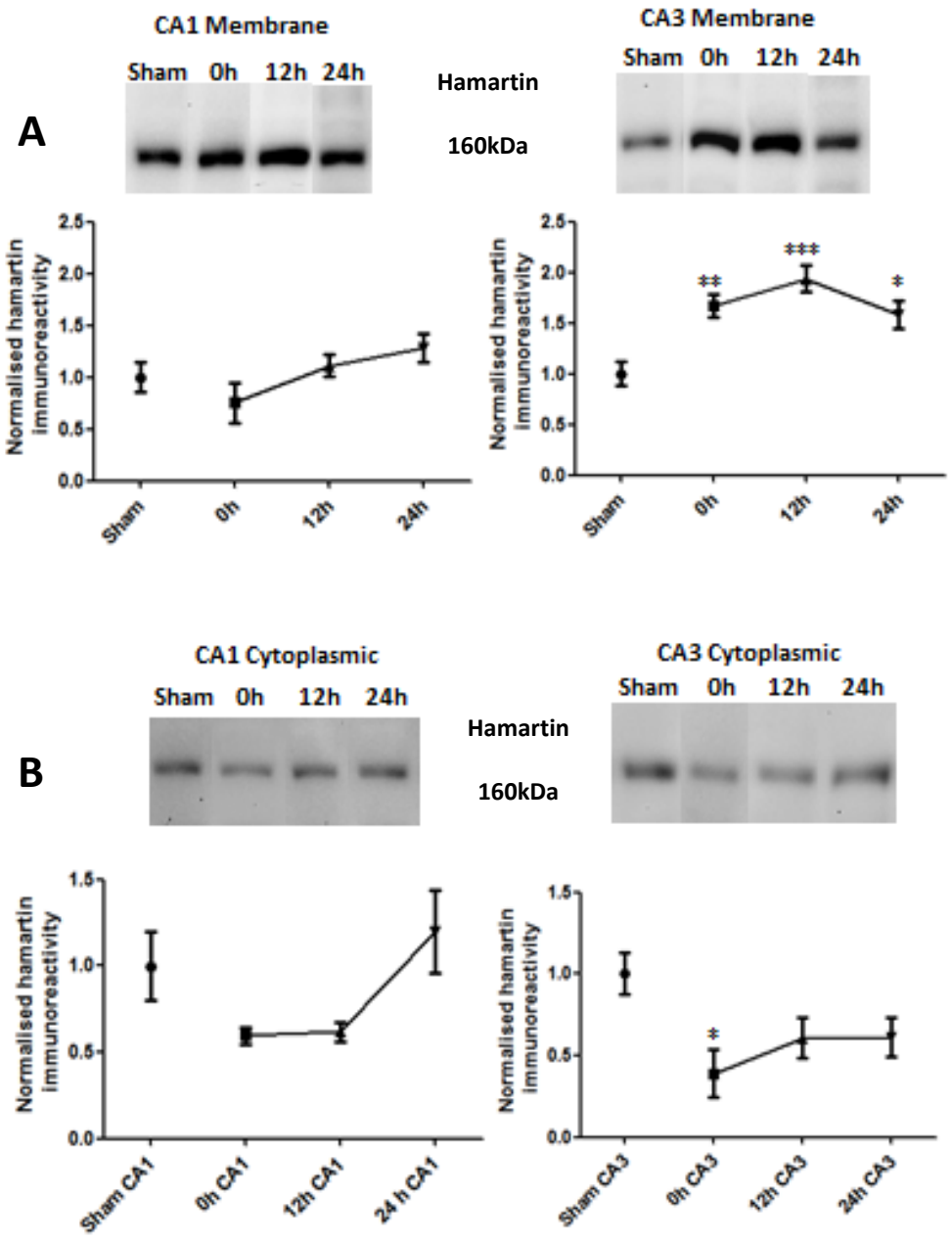

Figure 3.5 Time course of hamartin expression CA1 and CA3 neurons (A) Hamartin expression in membrane fraction of CA1 and CA3 hippocampal neurons. (B) Hamartin expression in cytoplasmic fraction of CA1 and CA3 hippocampal neurons. Upper panels show representative western blots used to produce the graphs below. Sham CA1 (n = 11) and CA3 (n = 12). After 10 min of ischemia: 0 h (n = 5), 12 h (n = 5) and 24 h (n = 10) of reperfusion in CA1 and CA3 regions. Values were corrected for total protein content, determined by Sypro staining, normalized such that the expression levels from sham ischemia samples were 1 and presented as mean ± s.e.m. (one-way analysis of variance (ANOVA), Bonferroni's *post hoc* test, *p<0.05, **p<0.01, ***p < 0.001 compared to sham ischemia. Band size of hamartin 160kDa.

The CA1 and CA3 brain regions from rats used for the autophagy (Chapter 4) and ER stress (Chapter 5) time courses were also run on Western blots to look for changes in hamartin expression. This adds a further time point to the above time course (0, 12 and 24 hours) demonstrating that at the sub-acute time point of 3 hours, levels of expression hamartin are significantly decreased in CA1 ischaemia compared to CA1 sham (p=0.003) (Figure 3.6).

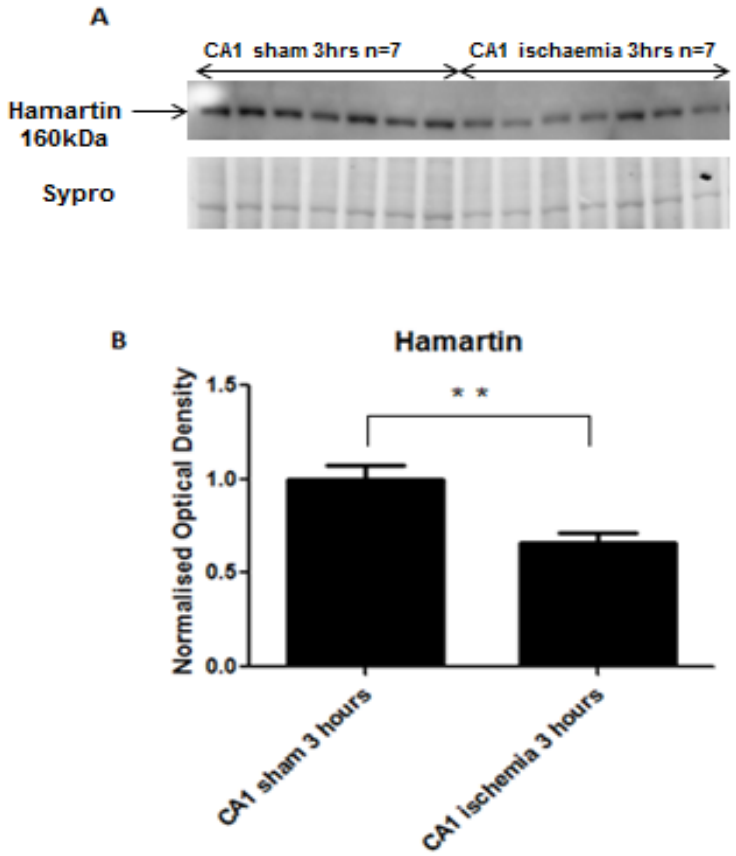

Figure 3.6 Hamartin expression in CA1 of hippocampus at 3 hours following 4-VO Upper panel (A) shows the western blots and loading correction with SYPRO® used to produce the graph (B) of hamartin immunoreactivity. (B) CA1 sham (n=7) and CA1 ischaemia (n=7). **p<0.01 Molecular weight of Hamartin: 160 kDa.

To examine whether tuberin expression in the CA3 area could also be involved in the endogenous resistance of CA3 neurons to global ischaemia, CA1 and CA3 areas of the hippocampus were dissected following 10 minutes of global cerebral ischaemia and reperfusion times of 0, 12 and 24 hours. The tissue was processed in the same manner as for hamartin assessment (Figure 3.5). There was no significant difference in the phosphotuberin (inactive version) to tuberin ratio in the cytoplasmic fraction (Figure 3.7 (A)). The phosphotuberin to tuberin ratio was significantly induced only at 12 hours following reperfusion by 2.67 ± 1.29 fold (p=0.0332, one-way ANOVA) compared to sham in the membrane fraction of the CA3 area (Figure 3.7 (B)).

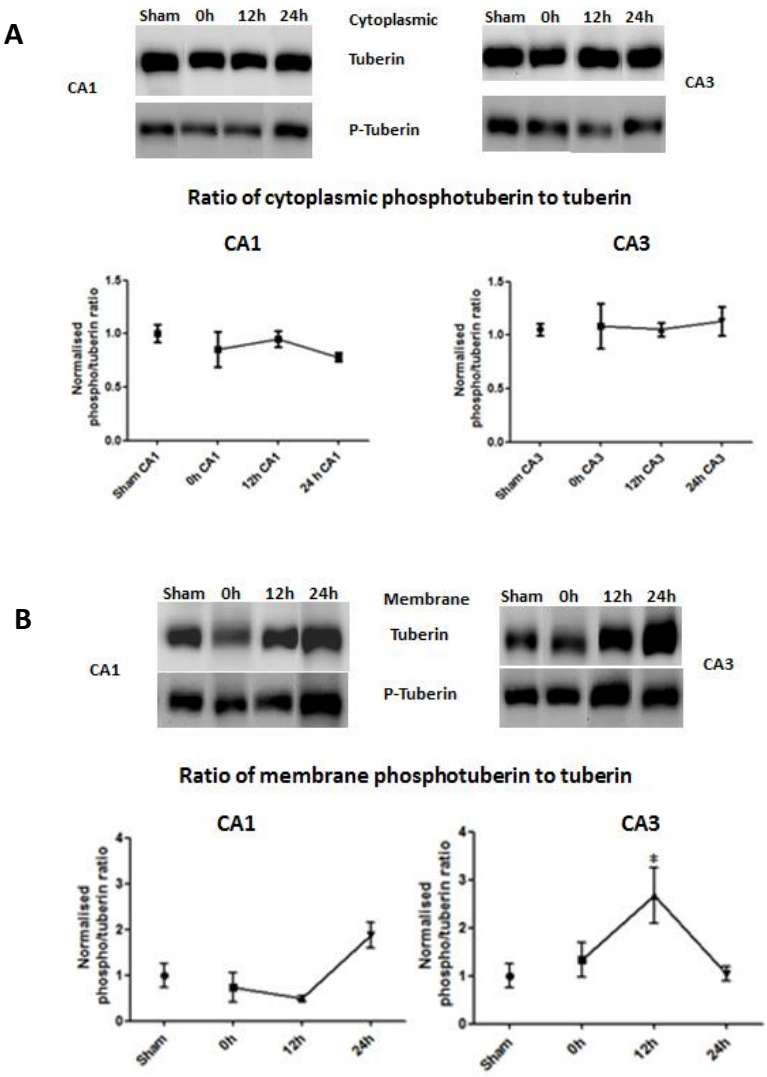

Figure 3.7 Time course of phosphotuberin to tuberin ratio following 4-VO. (A) membrane and (B) cytoplasmic fractions of the CA1 and CA3 regions of the rat hippocampus following global ischaemia. The phosphotuberin to tuberin ratio was significantly induced only at 12 hours following reperfusion compared to sham in the membrane fraction of the CA3 area. Upper panels show the western blots used to produce the graphs below of normalised phosphotuberin-tuberin ratio immunoreactivity over time. Sham CA1 (n = 11) and CA3 (n = 12). After 10 min of ischemia: 0 h (n = 5), 12 h (n = 5) and 24 h (n = 10) of reperfusion in CA1 and CA3 regions. Values were corrected for total protein content, determined by Sypro staining, normalized such that the expression levels from sham ischemia samples were 1 and presented as mean ± s.e.m. (one-way analysis of variance (ANOVA), Bonferroni's *post hoc* test, *p<0.05, **p<0.01, ***p < 0.001 compared to sham ischemia. Band size of tuberin and phosphotuberin 200kDa.

3.5.3 *In vitro*

Firstly, hippocampal (Figure 3.8) and cortical cultures (Figure 3.10) from E18 Wistar embryos were exposed to 2 hours of normoxia or OGD followed by 24 hours in recovery media in order to verify consistent levels of cell death as this method would form the basis of pharmacology experiments in Chapters 3, 4 and 5. Western blot analysis was conducted for expression levels of hamartin and tuberin.

3.5.3.1 Hippocampal Cultures

Representative images of hippocampal neuronal cultures at day 7 *in vitro* from E-18 Wistar rat embryos prior to OGD experiments in culture at day 7 are presented in Figure 3.8 (A) at x10 (i), x20 (ii) and x40 (iii) magnification. The LDH release assay was used to assess neuronal cell death following 2 h OGD and 24 H recovery, and these results are presented in Figure 3.8 (B). There is significantly more cell death in neurons following 2 h OGD (n=6) compared to normoxia (n=6) (p<0.0001). Also, there is significantly more cell death in neurons following 2 h OGD with 24 hour recovery (n=6) compared with 2 h normoxia with 24 h recovery (n=6) (p<0.0001).

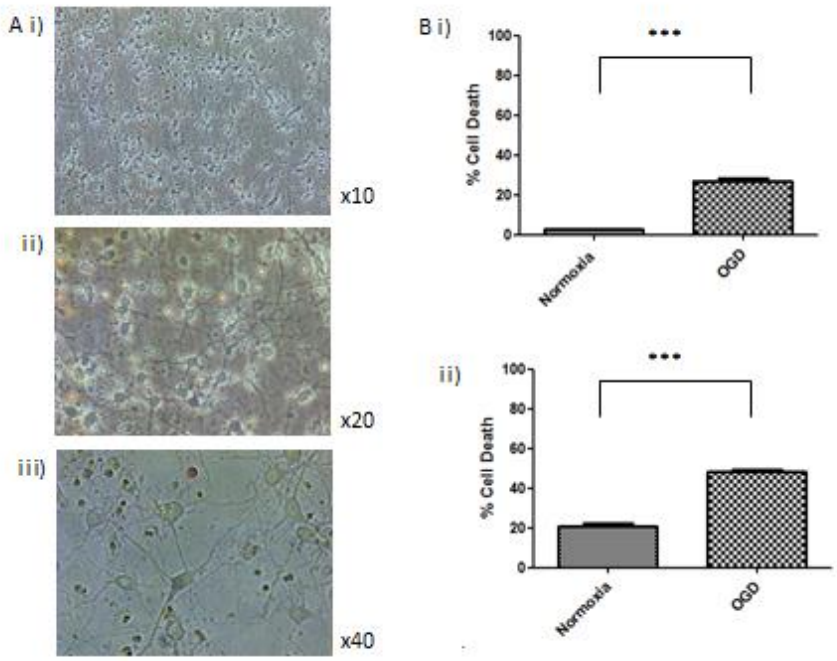

Figure 3.8 Hippocampal neuronal cultures from E-18 Wistar rats for *in vitro* OGD experiments A) Representative images of E18 hippocampal neurons in culture at day 7 at x10 (i), x20 (ii) and x40 (iii) magnification prior to OGD experiments. (B) Cell death of neuronal cultures was assessed using the LDH release assay. There is significantly more cell death in OGD neurons following (i) 2 hours OGD (n=6) compared to normoxia (n=6) and (ii) 2 hours OGD (n=6) with 24 hours recovery compared to normoxia. ***p<0.001

3.5.3.1.1. Hamartin and tuberin expression in hippocampal neurons

In Day 7 cultured hippocampal cells from E18 embryos, 2 hours of normoxia (n=6) and OGD (n=6) followed by 24 hours (n=6) of recovery resulted in significantly reduced expression levels of hamartin (p<0.006) and tuberin (p<0.0001) (Figure 3.9) in OGD samples compared to normoxia. Therefore there is a strong association between reduction in hamartin levels and increased cell death.

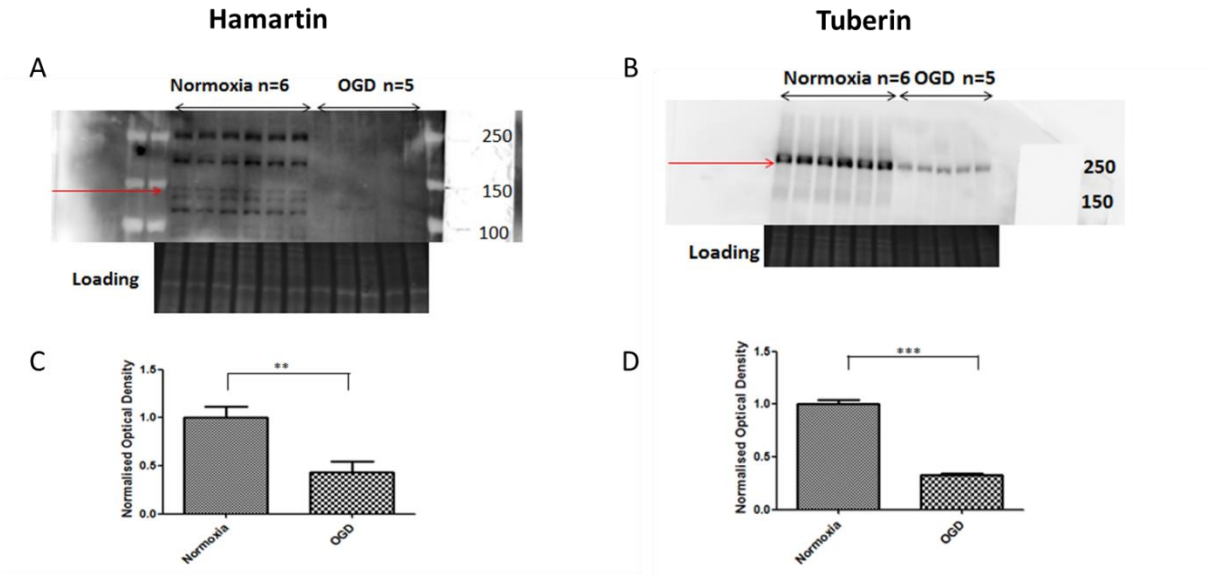

Figure 3.9 The effect of OGD on hamartin and tuberin expression in hippocampal neuronal cultures Upper panels (A and B) show the western blots and loading correction with SYPRO® used to produce the graphs of immunoreactivity for hamartin (C) and tuberin (D) below. (C) There is a significant decrease in hamartin expression levels in OGD (n=6) compared to normoxia (n=6). (D) There is a significant decrease in tuberin expression levels in OGD (n=6) compared to normoxia (n=6). Molecular weight of hamartin: 160 kDa. Molecular weight of tuberin: 200 kDa. **p<0.01 ***p<0.001.

3.5.3.2 Cortical Cultures

Representative images of cortical neuronal cultures at day 7 *in vitro* from E-18 Wistar rat embryos prior to OGD experiments are presented in Figure 3.10 (A) at x10 (i), x20 (ii) and x40 (iii) magnification. Futhermore, these cells expressed the canonical neuronal marker NeuN demonstrating these cultures were neurons (Figure 3.11). The LDH release assay was used to assess neuronal cell death following 2 h OGD and 24 h rand these results are presented in Figure 3.10 (B). There is significantly more cell death in neurons following 2 h OGD (n=6) compared to normoxia (n=6) (p<0.0002). Also, there is significantly more cell death in neurons following 2 h OGD with 24 h recovery (n=6) compared with 2 h normoxia with 24 h recovery (n=6) (p<0.0001).

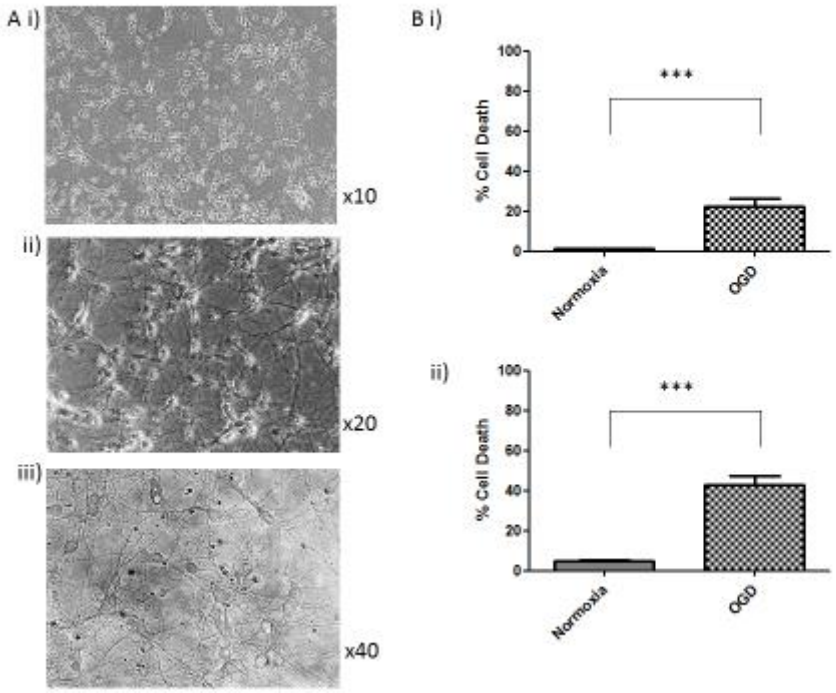

Figure 3.10 Cortical neuronal cultures from E-18 Wistar rats for *in vitro* OGD experiments A) Representaive images of E18 cortical neurons in culture at day 7 at x10 (i), x20 (ii) and x40 (iii) magnification. (B) Cell death of neuronal cultures was assessed using the LDH release assay. There is significantly more cell death in OGD neurons following (i) 2 hours OGD (n=6) compared to normoxia (n=6) and (ii) 2 hours OGD (n=6) with 24 hours recovery compared to normoxia. ***p<0.001

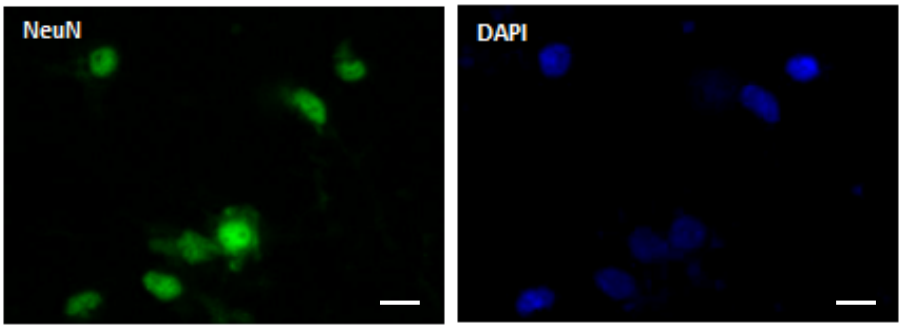

Figure 3.11: Characterization of neuronal cells by Immunofluorescence Cells were fixed and underwent immunofluorescence as described in methods with the following markers (A) NeuN (green) and (B) DAPI (blue). Scale bar = 20µm.

3.5.3.3 Pharmacology

3.5.3.3.1 Rapamycin

Rapamycin is an mTORC1 inhibitor and it is hypothesised to mimic the neuroprotective effects of hamartin.

Expression of mTOR pathway proteins with rapamycin treatment

A dose response was conducted to ascertain the effect of rapamycin on the mTOR pathway under normoxic conditions (Figure 3.12). Media and DMSO were used as controls and the following concentrations of rapamycin were administered: 1nM, 10nM, 100nM, 1μM and 10μM. All groups were n=3 except media which was n=6. Western blot analysis was used to ascertain expression levels of tuberin (Figure 3.16 (A)), hamartin (Figure 3.12 (B)), mTOR (Figure 3.12 (C)) and phosmTOR (Figure 3.12 (D)). There were no significant differences in tuberin expression between treatments (p=0.1703), although a similar downward trend in expression levels to hamartin was observed with increasing concentration of rapamycin. (B) The one way ANOVA for hamartin approached but did not reach significance (p=0.0827). There is a clear downward trend for expression with increasing dose of rapamycin. (C) There was a significant difference in mTOR expression levels (p=0.0185), with a significant difference between DMSO and 10μM rapamycin and a downward trend in expression levels at higher doses of rapamycin. There were no significant differences in phosmTOR expression between treatments (D). Levels of activated mTOR expression can be calculated by dividing phosmTOR expression levels by total mTOR expression levels (Yoshitomi *et al.,* 2011). There was no significant difference in levels of activated mTOR expression over the concentration range of rapamycin tested (E).

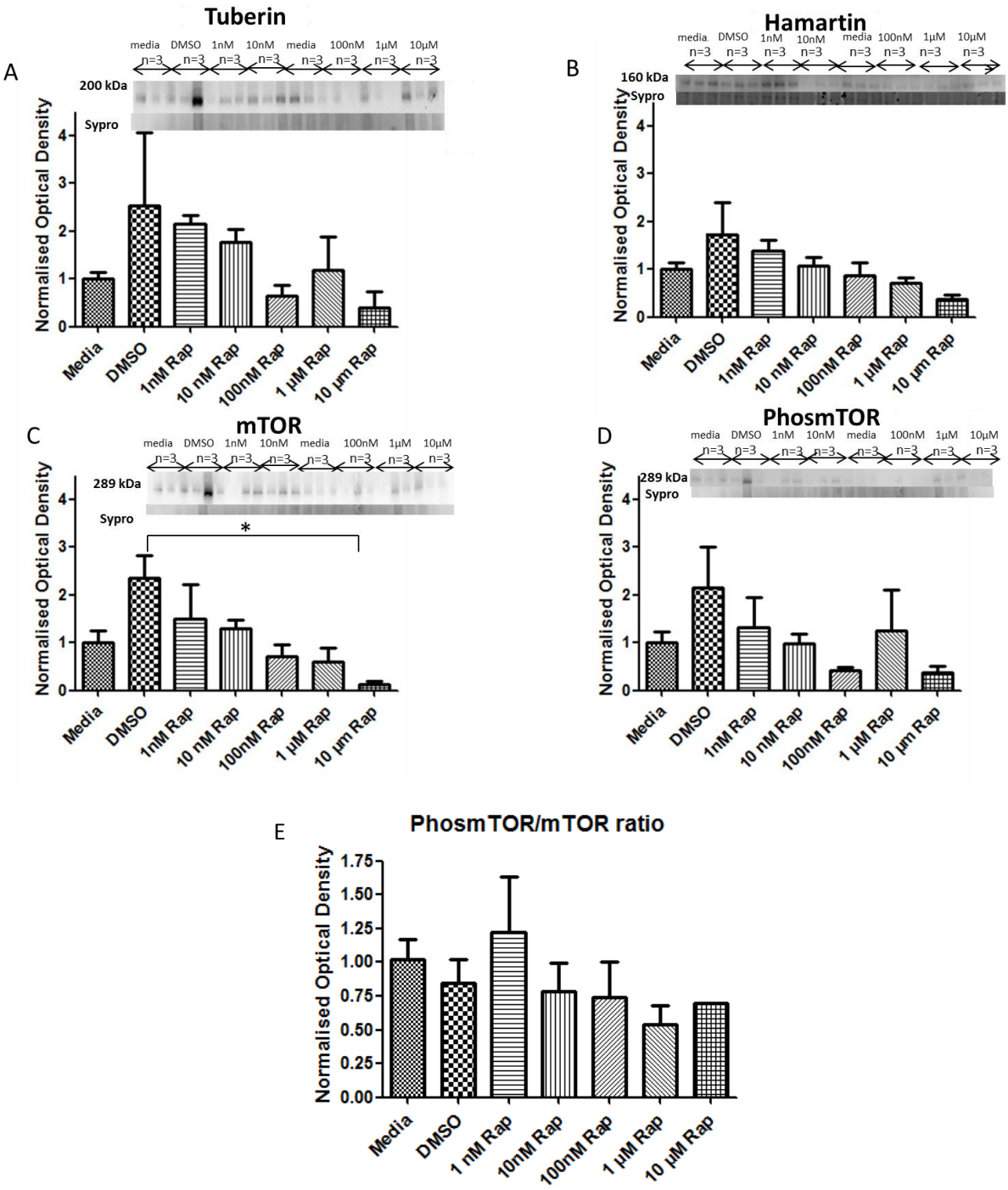

Figure 3.12 Expression levels of mTOR pathway proteins with rapamycin treatment (A) Tuberin expression levels. There were no significant differences in tuberin expression with rapamycin treatment. (B) There was no significant difference in hamartin expression levels but there was a clear downward trend with increasing doses of rapamycin. (C) mTOR expression levels were reduced with increasing levels of rapamycin which reached significance at 10µM. There were no significant differences in phosmTOR expression between with rapamycin treatment. (E) The ratio of phosmTOR (D) to total mTOR (C) indicative of mTOR activation did not differ significantly over the dose response. All groups n=3 analysed using one-way ANOVA with Bonferroni post hoc tests. Molecular weights: tuberin: 200 kDa, hamartin 160 kDa, mTOR 289 kDa, PhosmTOR 289 kDa. *p<0.05

Treatment with rapamycin during OGD

An LDH assay was conducted to determine cell viability following rapamycin treatment with different doses during OGD. Percentage cell death was measured in cortical cultures that had undergone 2 hours of normoxia or OGD (in the presence of DMSO (control) (n=3), 1 nM (n=3), 10nM (n=3) and 100nM (n=3) rapamycin) and 24 hours recovery. At 2 hours (Figure 3.13 (A)), there was a significant effect of OGD on cell death (p=0.0059) (two-way ANOVA). There was however no significant effect of treatment p=0.6970 (two-way ANOVA). At 2 hours and 24 hours recovery (Figure 3.13 (B)), there was a significant effect of OGD (p<0.0001) (two-way ANOVA). There was however no significant effect of treatment (p=0.4824) (two-way ANOVA). There was no interaction between OGD and treatment at either timepoint. Rapamycin treatment during OGD did not affect neuronal death.

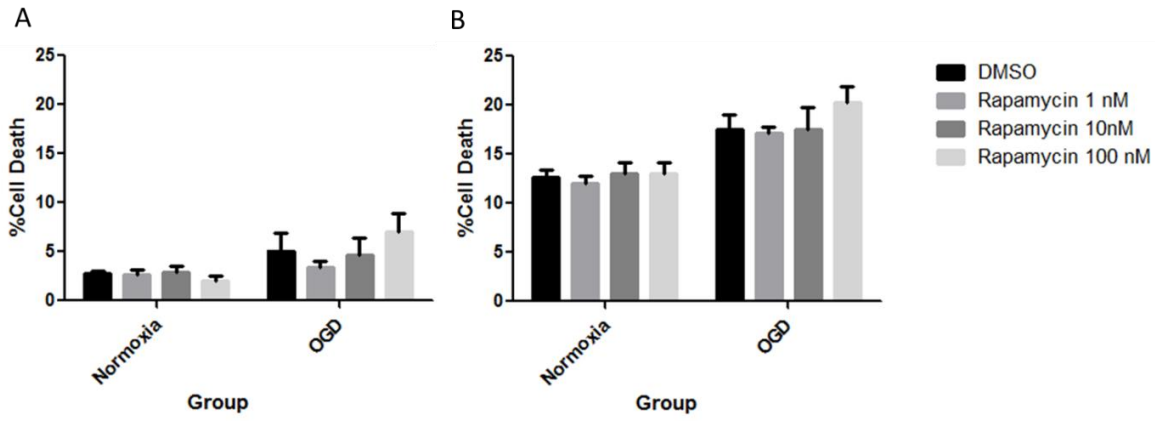

Figure 3.13 Effect of rapamycin treatment during OGD Cell death was quantified by LDH assay. Panel A shows percentage cell death following 2 hours of treatment. There was a significant effect of OGD but no significant effect of treatment. Panel B shows percentage cell death following 2 hours of treatment and 24 hours of recovery. There was a significant effect of OGD but no significant effect of treatment.

Pretreatment with rapamycin before OGD

To determine whether pre-treatment with rapamycin could reduced neuronal cell death, cortical neurons were pre-treated with media control (n=4), DMSO (n=4) or 10nM rapamycin (n=4) for 24 hours prior to undergoing 2 hours of normoxia or OGD and 24 hours recovery. Cell death was assessed using the LDH assay. At 2 hours (Figure 3.14 (A)), there was a significant effect of OGD (p<0.0001) (two-way ANOVA). There was however no significant effect of treatment p=0.2657 (two-way ANOVA). At 2 hours and 24 hours recovery (Figure 3.14 (B)), there was a significant effect of OGD (p<0.0001) (two-way ANOVA). There was however no significant effect of treatment (p=0.3727) (two-way ANOVA). There was no interaction between OGD and treatment at either timepoint. Rapamycin treatment prior to OGD did not affect neuronal survival.

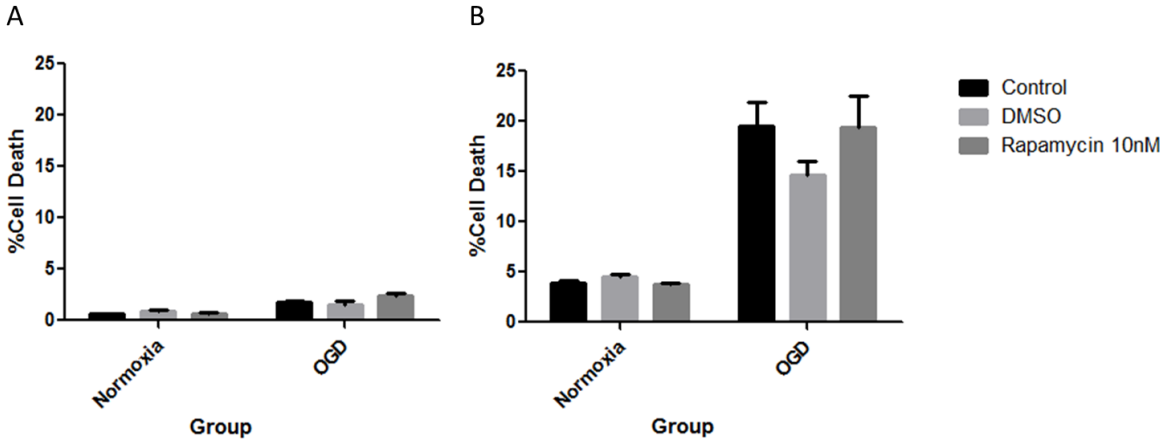

Figure 3.14 Effect of rapamycin treatment 24 hours before OGD Cell death was quantified by LDH assay. Panel A shows percentage cell death following 2 hours of treatment. There was a significant effect of OGD but no significant effect of treatment. Panel B shows percentage cell death following 2 hours of treatment and 24 hours of recovery. There was a significant effect of OGD but no significant effect of treatment.

Post treatment with rapamycin after OGD

To ascertain whether treatment with rapamycin after OGD could reduce neuronal cell death, cortical neurons underwent 2 hours of normoxia or OGD followed by 24 hours recovery. One of the following treatments were added to the recovery media: media control (n=4), DMSO (n=4) and 10nM rapamycin (n=4). Cell death was assessed using the LDH assay. At 2 hours and 24 hours recovery (Figure 3.15), there was a significant effect of OGD ($p<0.0001$) (two-way ANOVA). There was also significant effect of treatment ($p<0.0001$)) (two-way ANOVA). Tukey's multiple comparisons post hoc test demonstrated significantly less cell death in DMSO compared to control ($p<0.0001$), but also in the 10nM rapamycin group compared with control ($p<0.0001$) and DMSO ($p<0.0001$). There was a significant interaction between OGD and treatment in these neurons $p<0.0001$). Therefore 10nM rapamycin results in less cell death when added to the recovery media after OGD.

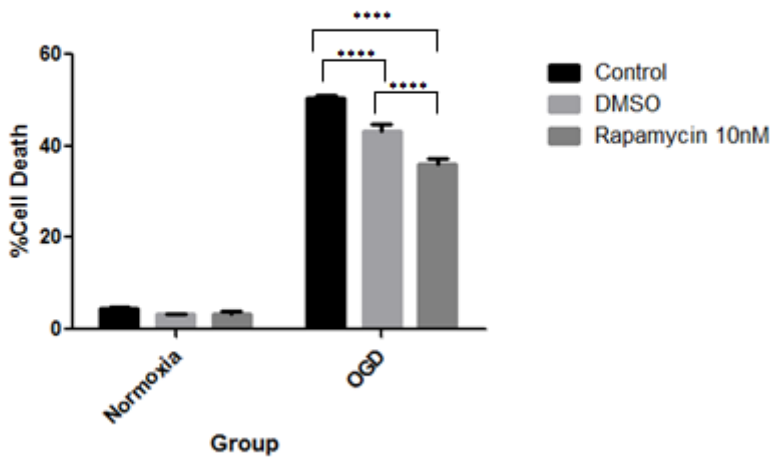

Figure 3.15 Effect of rapamycin treatment 24 hours after OGD Cell death was quantified by LDH assay. There was a significant effect of OGD and a significant effect of treatment with rapamycin treatment resulting in significantly less cell death ****$p<0.0001$

3.5.3.3.2 AZD2014

AZD2014 is a dual mTORC1/2 inhibitor currently undergoing clinical trials in cancer. Dual mTORC1/2 inhibition is more closely aligned with the biological function of hamartin and may be expected to more closely mimic its endogenous neuroprotective effect.

Expression levels of mTOR pathway proteins with AZD treatment

A dose response experiment was conducted to ascertain the effect of AZD on the mTOR pathway under normoxic conditions (Figure 3.16). Media and DMSO were used as controls and the following concentrations of AZD were administered: 1nM, 10nM, 100nM, 1μM and 10μM. All groups were n=3, except the media group which was n=6. Western blot analysis was used to ascertain expression levels of tuberin (Figure 3.16 A), hamartin (Figure 3.16 B), mTOR (Figure 3.16 C) and phosmTOR (Figure 3.16 D). Both tuberin and hamartin are upstream regulators of mTOR activity, and we found there was no significant difference in tuberin expression with AZD treatment (p=0.3082), while there was a significant decrease in hamartin expression levels (p= 0.0145) with increasing AZD concentration, with 100nM AZD providing the greatest inhibitory effect when compared to media (p=0.0303). There was also no significant difference in mTOR expression levels (p=0.0588), although there was a clear downward trend in expression levels. There was no significant difference in phosmTOR expression levels (p=0.3380). However, when calculating activated mTOR by dividing phosmTOR expression levels by total mTOR expression levels (Yoshitomi *et al*., 2011), there is a significant increase in activated mTOR with increasing concentrations of AZD (p=0.0017) (Figure 3.16 E). This suggests that AZD could be inhibiting hamartin possibly through upstream Akt inhibition which leads to the release of the inhibition of mTOR leading to its activation.

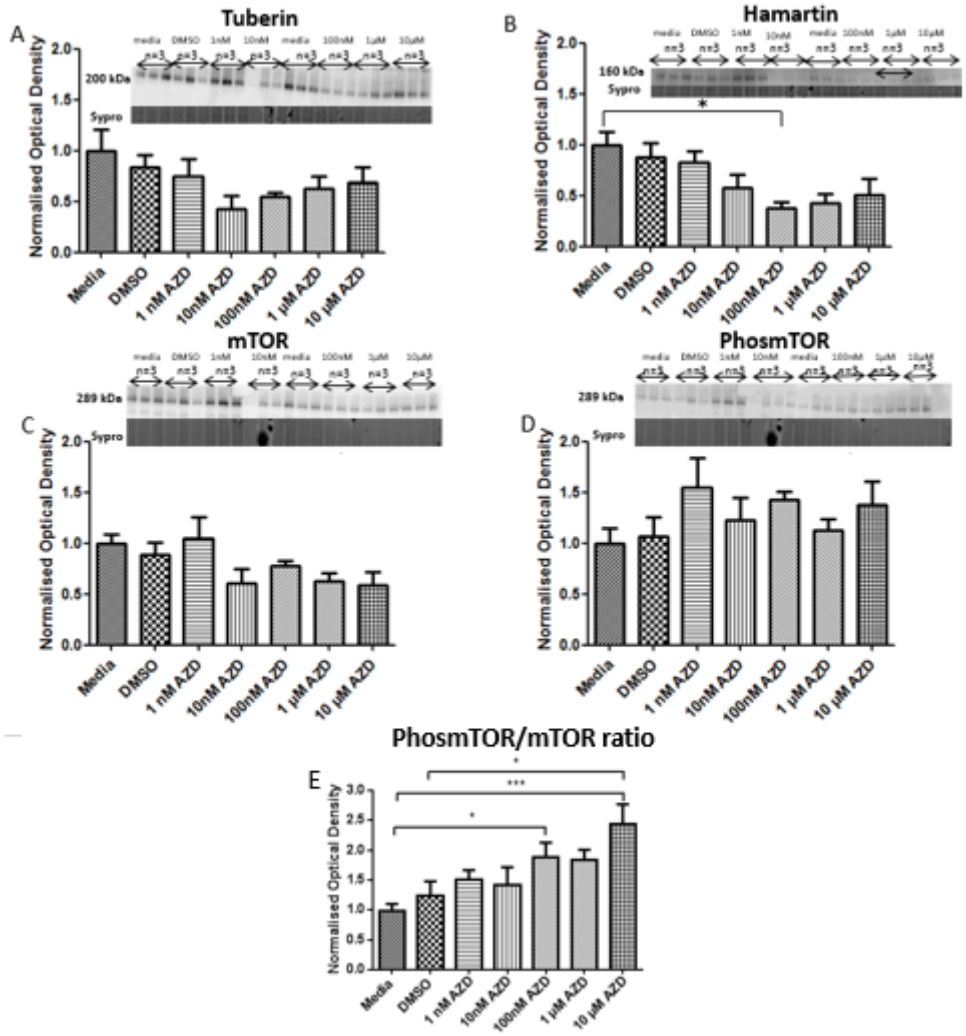

Figure 3.16 Expression levels of mTOR pathway proteins with AZD2014 treatment (A) Expression levels of tuberin following 2h exposure to 1nM-10µM AZD. (B) Expression levels of hamartin following 2h exposure to 1nM-10µM AZD. (C) Expression levels of mTOR following 2h exposure to 1nM-10µM AZD. (D) Expression levels of phosmTOR following 2h exposure to 1nM-10µM AZD. (E) The ratio of phosmTOR (D) to total mTOR (C) indicative of activated mTOR following 2h exposure to 1nm-10µM AZD. Molecular weights: tuberin: 200 kDa, hamartin 160 kDa, mTOR 289 kDa, PhosmTOR 289 kDa. Data presented as mean ± sem. n=3 per group except media which was n=6. * p<0.05;***p<0.001.

Treatment with AZD or rapamycin during OGD in cortical neurons

An LDH assay was conducted to determine cell viability following treatment with AZD or rapamycin with different doses under normoxia or OGD conditions. Percentage cell death was measured in cortical cultures that had undergone 2 hours of normoxia or OGD in the presence of media (control) (n=6) DMSO (control) (n=6), 10nM rapamycin (n=3), 100nM rapamycin (n=3), 100nM AZD (n=3) or 1µM AZD (n=3). At 2 hours (Figure 3.17 (A)), there was a significant effect of OGD (p<0.0001) (two-way ANOVA). There was also a significant effect of treatment (p<0.0001) (two-way ANOVA). Tukey's multiple comparison test demonstrated a highly significant increased levels of cell death (p<0.0001) with 100nM AZD and 1µM AZD when compared with media, DMSO and rapamycin in OGD conditions. At 2 hours and 24 hours recovery (Figure 3.17 (B)), there was a significant effect of OGD (p<0.0001) (two-way ANOVA). There was also a significant effect of treatment on cell death (p<0.0001) (two-way ANOVA). Tukey's multiple comparison test demonstrated a highly significant increased levels of cell death (p<0.0001) with 100nM AZD and 1µM AZD when compared with media, DMSO and rapamycin in the cells that had undergone OGD. There is significant interaction between OGD and treatment at 2 hours (p<0.0001) and 2 hours and 24 hours recovery (p<0.01). Therefore AZD is showing neurotoxicity following OGD whereas rapamycin had no effect.

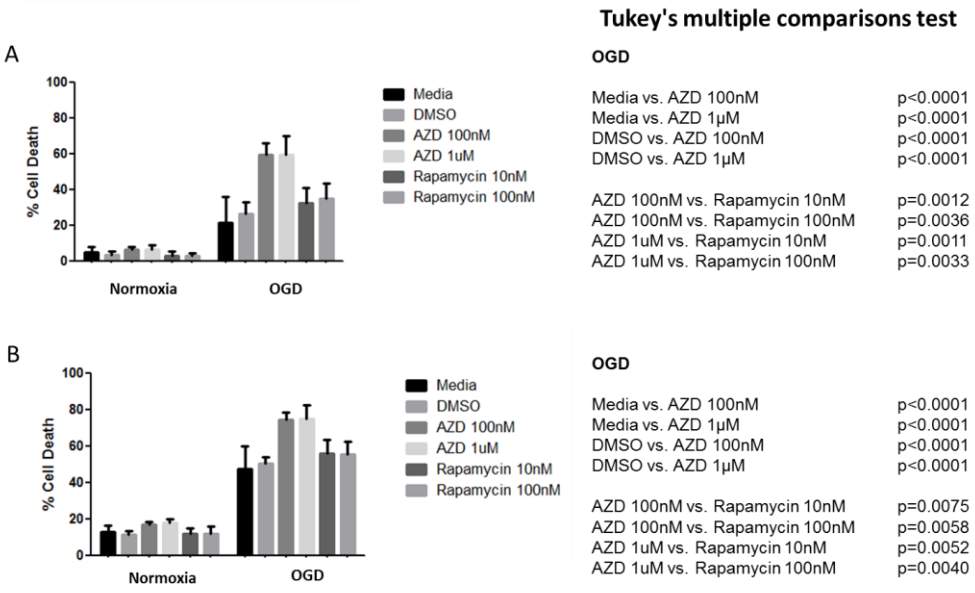

Figure 3.17 Cortical cell death following treatment with AZD2014 or rapamycin during OGD Cell death was quantified using an LDH assay. (A) At 2 hours, OGD increased cell death compared to normoxia while AZD increased cell death compared with media, DMSO and rapamycin doses in OGD conditions. (B) At 2 hours and 24 hours recovery, OGD increased cell death compared to normoxia, while AZD increased cell death compared with media DMSO and rapamycin in OGD conditions.

Treatment with AZD or rapamycin during OGD in hippocampal neurons

An LDH assay was conducted to determine cell viability following treatment with AZD or rapamycin with different doses under normoxia or OGD conditions. Percentage cell death was measured in hippocampal cultures that had undergone 2 hours of normoxia or OGD in the presence of media (control) (n=6) DMSO (control) (n=6), 10nM rapamycin (n=2), 100nM rapamycin (n=2), 100nM AZD (n=3) or 1µM AZD (n=3). At 2 hours (Figure 3.18 (A)), there was a significant effect of OGD (p<0.0001) (two-way ANOVA). There was also a significant effect of treatment (p=0.0003) (two-way ANOVA). Tukey's multiple comparison test demonstrated a highly significant increased levels of cell death with 100nM AZD and 1µM AZD when compared with media, DMSO and rapamycin in OGD conditions. At 2 hours and 24 hours recovery (Figure 3.18 (B)), there was a significant effect of OGD (p<0.0001) (two-way ANOVA). There was also a significant effect of treatment on cell death (p<0.0001) (two-way ANOVA). Tukey's multiple comparison test demonstrated a highly significant increased levels of cell death (p<0.0001) with 100nM AZD and 1µM AZD when compared with media, DMSO and rapamycin in the cells that had undergone OGD. There is significant interaction between OGD and treatment at 2 hours (p<0.001) and 2 hours and 24 hours recovery (p<0.01). AZD is showing neurotoxicity following OGD whereas rapamycin has no effect.

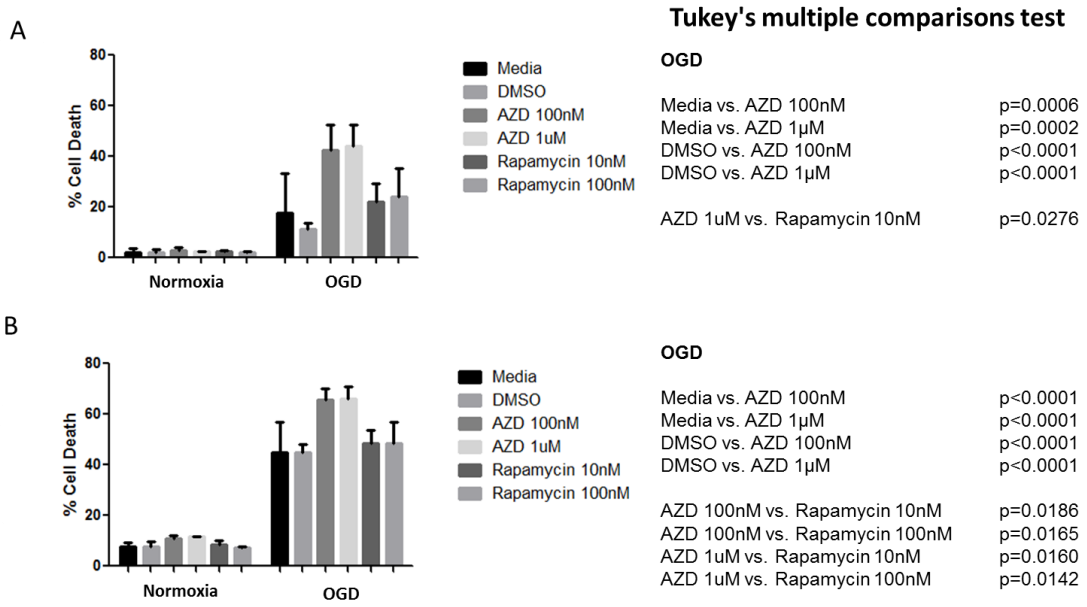

Figure 3.18 Hippocampal cell death following treatment with AZD2014 or rapamycin during OGD Cell death was quantified using an LDH assay. (A) At 2 hours, OGD increased cell death compared to normoxia while AZD increased cell death compared with media, DMSO and rapamycin in OGD conditions. (B) At 2 hours and 24 hours recovery, OGD increased cell death compared to normoxia, while AZD increased cell death compared with media, DMSO, 10nM and 100nM rapamycin in OGD conditions.

Pre-treatment with AZD before OGD in cortical neurons

Cell death was assessed using an LDH assay in cortical cultures that had undergone 2 hours of normoxia or OGD and 24 hours recovery that had been exposed to 24 hours of pretreatment with: media (n=3), DMSO (n=3), 100nM AZD (n=3) or 1μM AZD (n=3). At 2 hours (Figure 3.19 (A)), there was a significant effect of OGD ($p<0.0005$). There was however no significant effect of treatment ($p<0.4346$) (two-way ANOVA). At 2 hours and 24 hours recovery (Figure 3.19 (B)), there was a significant effect of OGD on survival ($p<0.0001$) (two-way ANOVA). There was also a significant effect of treatment ($p=0.0002$) (two-way ANOVA). Tukey's multiple comparison test demonstrated that 1μM AZD produced significantly more cell death than media ($p<0.0001$), DMSO ($p=0.0002$) and 100nM AZD ($p=0.0002$) in the cells that had undergone OGD. There was no significant interaction between OGD and treatment at 2 hours. Following 2 hours and 24 hours recovery there was a significant interaction between OGD and treatment ($p<0.001$). 1μM AZD has neurotoxic effects following OGD.

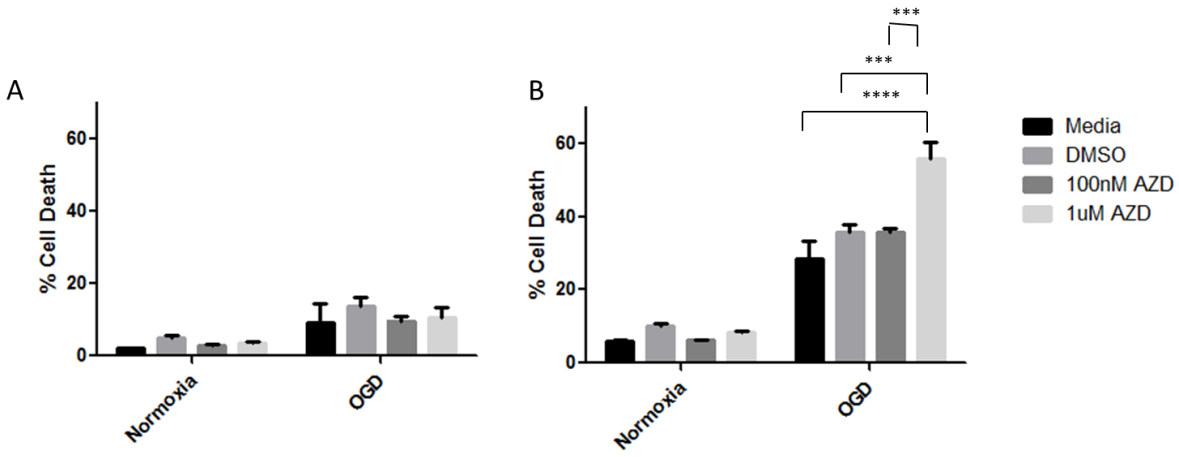

Figure 3.19 Effect of AZD2014 treatment 24 hours before OGD Cortical cell death following pretreatment with AZD2014 for 24 hours prior to 2 hours OGD and followed by 24 hours recovery. Cell death was quantified by LDH assay. (A) At 2 hours, OGD increased cell death but AZD had no effect. .(B) At 2 hours and 24 hours recovery cell death and only 1μM AZD increased cell death compared to media, DMSO and 100nM AZD following OGD. ***$p<0.001$, ****$p<0.0001$

Post treatment with AZD2014 after OGD in hippocampal and cortical neurons

Cell death was measured using an LDH assay in hippocampal cultures that had undergone 2 hours of normoxia or OGD and 24 hours recovery. The following treatment groups were added to the recovery media only: DMSO (n=3) and 100nM AZD (n=3) and 1μM AZD (n=3). Since treatment was in the recovery media, analysis of cell death was carried out during the recovery period only after 2 hours OGD or normoxia. In hippocampal neurons (Figure 3.20 (A)), there was a significant effect of OGD (p=0.0178) and treatment (p=0.0002) (two-way ANOVA). Tukey's multiple comparison test showed that normoxic cells exposed to 1μM AZD for 24 hours led to significantly more cell death when compared to DMSO (p=0.0014) and AZD 100nM (p=0.0055). In cells exposed to OGD, AZD 1μM caused significantly more cell death than DMSO (p=0.0115).

The same post-treatment experiment was also conducted in cortical neurons with the following groups added to the recovery media following 2 h OGD or normoxia: media (n=3), DMSO (n=3), 100nM AZD (n=3) and 1μM AZD (n=3). In cortical neurons (Figure 3.20 (B)), there was a significant effect of OGD and treatment (p<0.0001) (two-way ANOVA). Tukey's multiple comparison test demonstrated in cells that were in normoxic conditions for 2 hours prior to recovery, 1μM AZD caused significantly more cell death when compared to media (p=0.0047) and DMSO (p=0.0006). 1μM AZD caused significantly more cell death than 100nM AZD (p=0.0092). In cells that were in OGD conditions for 2 hours prior to recovery, 100nM AZD caused significantly more cell death when compared to media (p=0.0078), while 1μM AZD caused significantly more cell death compared to media (p<0.0001), DMSO (p<0.0001) and 100nM AZD (p=0.0083). There was no interaction between OGD and treatment in cortical or hippocampal neurons.

Therefore AZD has neurotoxic effects during the recovery period following normoxia and OGD in both hippocampal and cortical neurons.

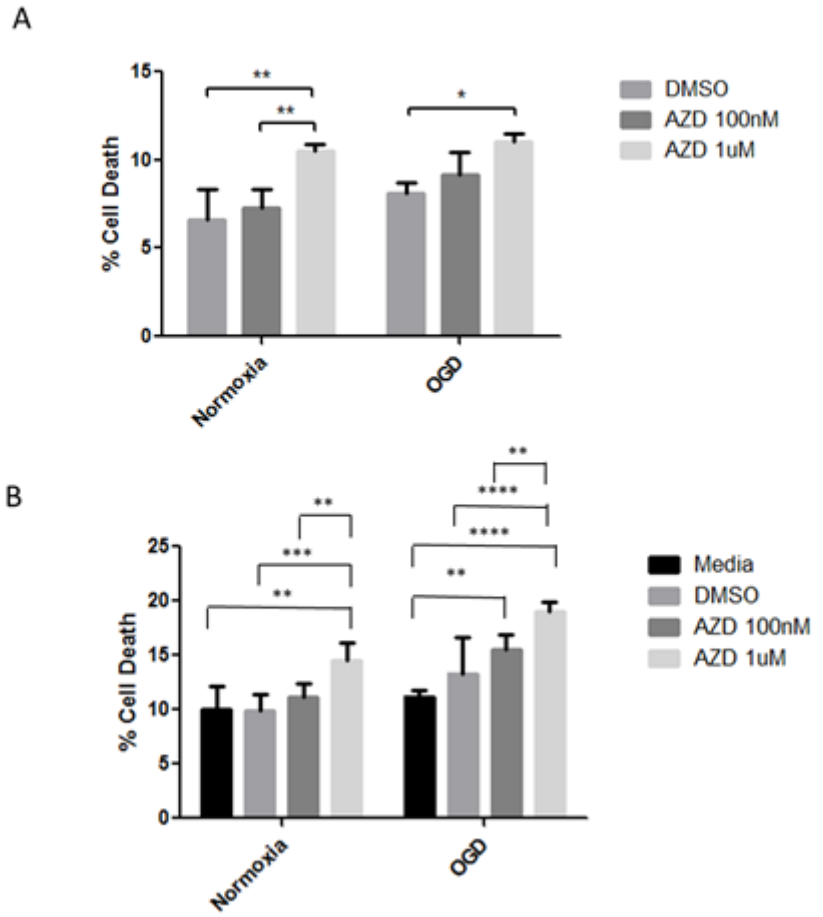

Figure 3.20 Effect of AZD2014 treatment 24 hours after OGD Cell death was quantified by LDH assay. (A) In hippocampal neurons in the 24 hour recovery period only. OGD increased cell death and AZD increased cell death following normoxia and OGD. (B) In cortical neurons in the 24 hour recovery period only, OGD increased cell death and AZD increased cell death and AZD increased cell death following normoxia and OGD. *p<0.05, **p<0.01, ***p<0.001, ****p<0.0001

The effect of rapamycin and AZD on markers of ER stress under normoxic conditions

Inhibitors of mTOR would be expected to decrease ER stress via decreased protein synthesis. A dose response was conducted to ascertain the effect of rapamycin and AZD on ATF4, a protein associated with the ER stress response under normoxic conditions (Figure 3.21). Media and DMSO were used as controls and the following concentrations of rapamycin and AZD: 1nM, 10nM, 100nM, 1µM and 10µM. The media group was n=6 all other groups n=3. Western blot analysis was used to ascertain expression levels of ATF4. There were significant differences between treatment groups for both rapamycin (p=0.0313) (Figure 3.21 (C)) and AZD (p=0.0198) (Figure 3.21 (D), one-way ANOVA). However post hoc testing did not demonstrate any significant differences between groups (Bonferroni's multiple comparisons test). There was a trend for lower expression of ATF4 with increasing rapamycin concentration, whereas the trend is for increased levels of the ER stress protein ATF4 in AZD treated neurons. This could explain the mechanism for the neurotoxicity observed following OGD with AZD (Figures 3.16-3.20). Modulation of the ER stress response is a potential mechanism accounting for hamartin's endogenous neuroprotective effect which will be further investigated in Chapter 5.

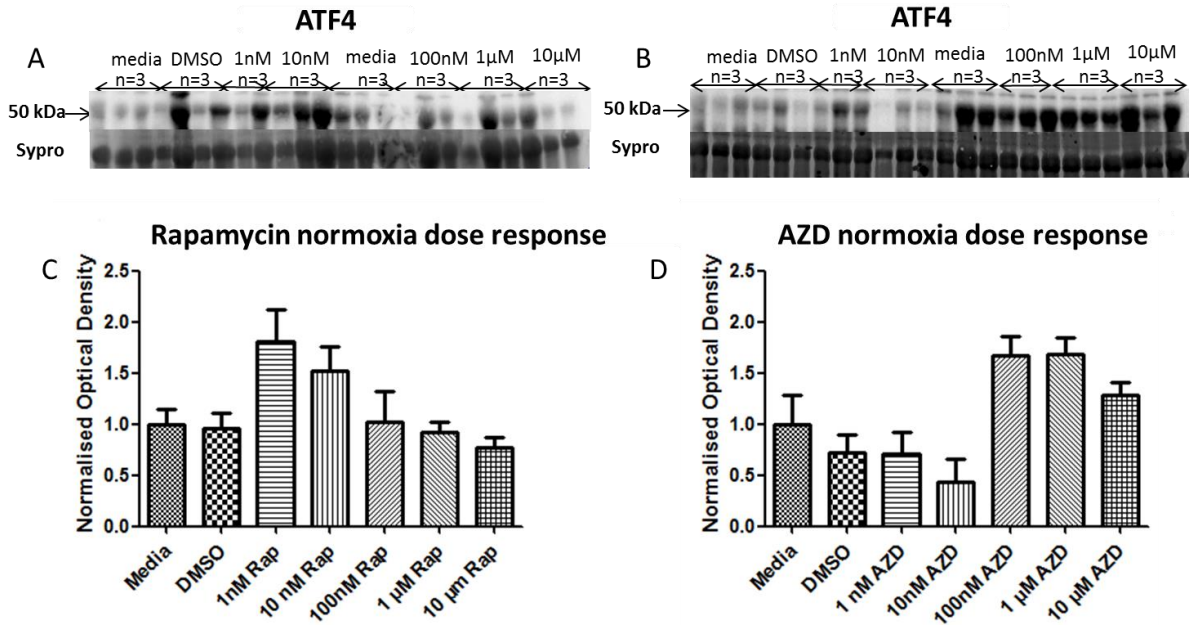

Figure 3.21 Effect of rapamycin on expression levels of the ER stress protein, ATF4 Upper panels (A) and (B) show the western blots and loading correction with SYPRO® used to produce the graphs (C) and (D). (C) The mean expression levels of ATF4 in rapamycin treated cells were significantly different but post hoc testing did not reveal any significance between specific groups. (D) The mean expression levels of ATF4 in AZD treated cells were significantly different but post hoc testing did not reveal any significance between specific groups. All groups n=3, except media which was n=6 analysed using one-way ANOVA with Bonferroni post hoc tests. Molecular weight: ATF4 50 kDa.

3.6 Discussion

It is proposed that the selective dynamic response of hamartin expression in the CA3 area observed in *in vivo* experiments is involved in the endogenous resistance of CA3 neurons to global ischaemia. Manipulation of mTOR as a downstream target using pharmacological tools *in vitro* experiments did not replicate hamartin's endogenous neuroprotective effect and the precise mechanism may be found further downstream in the pathway.

3.6.1 *In vivo* time course

Global ischaemia selectively induced hamartin expression in the membrane fraction of the CA3 region of the rat hippocampus and this peaked at 12 hours of reperfusion and persisted at 24 hours. There was immediate induction of hamartin expression in the membrane and a concomitant decrease in the cytoplasm following 10 minutes of global ischaemia. No difference in hamartin expression was observed in the CA1 neurons following global ischaemia over this time course. At the subacute timepoint of 3 hours, however, levels of expression of hamartin are significantly decreased in CA1 ischaemia compared to CA1 sham. Although this supports the hamartin time course, it should be interpreted with some caution as it is derived from whole cell homogenates and not fractionated cytoplasmic and membrane fractions like the initial cohorts. The temporal profile of tuberin expression in the CA3 did not coincide with that of hamartin, suggesting that the hamartin neuroprotective effect is independent of tuberin. The significant increase in the ratio of phosphotuberin to tuberin at 12 hours of reperfusion selectively in the CA3 suggests that inactivation of tuberin occurred when hamartin expression peaked.

From the time course results, there is a clear association between CA3 survival and hamartin expression following global cerebral ischaemia. Previous experiments in this lab have shown that when hamartin is suppressed in the CA3, these previously resistant neurons can become susceptible to ischaemic damage (Papadakis *et al.,* 2013). This is futher backed up with behavioural findings whereby rats lose their habituation response in line with a loss of hippocampal function when hamartin has been suppressed (Papadakis *et al.,* 2013). The most likely mechanism by which the induction of hamartin would produce neuroprotection would be

through the inhibition of mTOR. While specific mTOR changes following global ischaemia have not been investigated *in vivo,* there is futher evidence that hamartin's neuroprotective effects are mediated by the inhibition of mTOR as evidenced by the promotion of productive autophagy (Papadakis *et al.,* 2013, Chapter 4). Another study has used the 2-VO rat model to investigate autophagy and tauopathy related markers in cerebral ischaemia and Alzheimer's disease (Villamil-Ortiz and Cardona-Gomez, 2015). They showed that neuronal loss and tauopathy were observed at 1 and 15 days post-ischemia but reversed at 30 days. A reduction in phosphorylated mTOR activity at this time coupled with an association of Beclin-1 and Vps34, LC3B puncta and autophagolysosome formation linked this to a protective role for late stage autophagy. This mechanism was not observed in their AD model suggesting different temporal relationships between endogenous neuroprotection and neurodegeneration.

Using focal and global models of cerebral ischaemia and cobalt chloride to develop an ischaemia-reperfusion injury *in vitro* in HT22 cells suggested that Beclin-1 and mTOR might demonstrate coordinated regulation in ischaemia stages but not in reperfusion stages. In ischaemia, inhibiting mTOR (with rapamycin) may result in Beclin-1 expression therefore inducing autophagy, such 'cross-talk' is not demonstrated in the reperfusion stage (Yang *et al.,* 2015). Cell death analysis suggested that autophagy may play different roles depending on which stage of ischaemia-reperfusion; autophagy can increase rate of cell death in the ischaemic stage but stimulate neuronal survival in the reperfusion stage. In the current study, the early changes in hamartin expression may implicate endogenous neuroprotection but the times at which these changes take place may be critical for the success of neuroprotection.

3.6.2 *In vitro*

In hippocampal cultures, 2 hours of OGD followed by 24 hours recovery resulted in significantly reduced expression levels of hamartin and tuberin compared to normoxia. This could not be attributed to cell death in OGD as SYPRO® protein loading correction was used meaning that hamartin expression was normalized to the total protein level in each sample. It is not possible to comment on CA1 vs CA3 effects as they were not separated, but demonstrates the effect of ischaemia in the proteins of interest. However, what is clear is that

the hamartin decrease is associated with increased cell death providing further evidence for neurprotective effects of hamartin.

3.6.2.1 Rapamycin

In cortical neurons, a rapamycin dose response was conducted to look at expression of proteins associated with hamartin demonstrated a significant decrease in mTOR (although not phosmTOR) levels and hamartin with increasing doses of rapamycin. There was no significant difference in levels of activated mTOR expression levels over the concentration range of rapamycin tested. This is in contrast with AZD (discussed below) which is indicative of different mechanisms of action between the two compounds. The endogenous neuroprotection is associated with CA3 area of the hippocampus. Since, like CA1, the cortex is susceptible to ischaemia, protein expression associated with any endogenous neuroprotective pathway may cast more light onto why CA3 neurons demonstrate inherent resistance compared to vulnerable cells.

Cortical cultures that were pretreated with rapamycin however, had no effect of treatment using cell death assays. It could be that OGD dysregulates mTOR and since protein expression is measured after 24 hour recovery period that any modulation that occurred pre OGD is not sufficient to overcome this response. There was also no effect of treatment with rapamycin given during 2 hours normoxia or OGD on cell death. Again, any detrimental effect of mTOR is likely to happen after this period with the effects of protein translation coming into play.

With post treatment rapamycin, LDH assays demonstrated that 10 nM rapamycin results in less cell death compared to both media and DMSO controls when added to the recovery media following OGD. This is in agreement with previous studies, where in neonatal hypoxia-ischaemia rapamycin increased autophagy in Sprague–Dawley pup rats, reduced necrotic cell death and decreased brain injury (Carloni *et al.,* 2008). In E17 neuronal cultures following 1 hour of OGD and either 90 minutes or 24 hours of 5nM and 20nM rapamycin treatment demonstrated increased neuronal viability (Fletcher *et al.,* 2013). Although the clinical utility of rapamycin beyond transplant medicine is an emerging field, there are inherent side effects with an essentially immunosuppressant drug. In addition, rapamycin does not precisely replicate the effects of hamartin as it is an

mTORC1 inhibitor that only inhibits mTORC2 at very high concentrations which are likely to be detrimental in a clinical context.

3.6.2.2 AZD2014

AZD2014 was obtained from Astra Zeneca in order to test whether this existing therapy in cancer trials could be extended to ischaemic stroke. It was investigated to evaluate whether its dual mTORC1 and mTORC2 inhibition would prove superior to rapamycin as a potential neuroprotectant.

A dose response was conducted to ascertain the effect of AZD on the mTOR pathway under normoxic conditions. There was a significant decrease in hamartin expression levels in neurons exposed to 100nM AZD compared to media. There was also no significant difference in mTOR expression levels or phosmTOR expression levels. High doses of AZD decreased hamartin expression which acts upstream of mTOR and would act to further activate mTOR. This was supported by increasing AZD concentrations significantly enhancing phosphorylated mTOR expression (active conformation) as a ratio of total mTOR. This is contrary to the proposed mTOR inhibitory properties of AZD, but this could be explained by its hamartin inhibition. In addition, mTORC2 negates the feedback loop that ordinarily allows high levels of mTORC1 acitivation to feedback via phosphorylation of S6K1 activating of Akt that results with mTORC1 inhibition (Guertin and Sabatini, 2007; Wan *et al.,* 2007). Inhibiting the negative feedback loop would also lead to high levels of activated mTOR. The exact mechanism of AZD2014 is not known and it could have multiple effects - the downregulation of hamartin may be as a result of a direct effect or as a result of an indirect effect via Akt or at a multitude of points in this complicated pathway. It is however very interesting that a compound that was very neurotoxic under OGD conditions *in vitro* had the specific effect of decreasing hamartin expression – the protein that is robustly associate with CA3 neuronal survival following global ischaemia *in vivo.*

The effects of AZD on cell death following OGD were compared to those of rapamycin. Again, rapamycin did not produce a protective effect in this model following 2 hours normoxia or OGD and 24 hours recovery compared to control and DMSO (NB rapamycin's effect was only seen when treated post-OGD in this thesis). AZD 100nM and 1μM reproducibly resulted in more cell death in cortical and hippocampal neurons. In pre and

post treatment with AZD in cortical neurons, AZD produced significantly greater levels of cell death. It was hoped that a dual mTORC1/2 inhibitor would provide a solution to the problem of incomplete mTORC1 inhibition. mTORC2 negates the feedback loop that would oridinarily attenuate PI3K-Akt signalling as a result of high levels of S6K1 phosphorylation, directlydownstream of mTORC1 (Guertin and Sabatini, 2007; Wan *et al.,* 2007). The finding that rapamycin, the gold standard mTOR inhibitor, did not affect neuronal cell death suggests that there is indeed a difference in the mechanism of action between the two drugs.

The AZD2014 literature is mainly on survival effects in cancer models. In human hepatocellular cancer cell (HCC) lines, AZD2014 resulted in dramatic antitumour effects (Liao *et al.,* 2014) and in cultured colorectal cancer cell lines, AZD2014 (1-100nM) significantly inhibited cancer cell growth not by inducing cell apoptosis, but via inhibition of mTORC1/2 and activating autophagy. AZD2014 has also been shown to enhance radiosensitivity of glioblastoma stem-like cells (Kahn *et al.,* 2014). Although never previously used in cerebral ischaemia, AZD2014 was shown to be protective in the context of oxidative stress and inflammatory reactions produced by disturbed flow in atherosclerosis (Martin *et al.,* 2014).

Increased activation of mTOR results in an increase in protein synthesis and ROS production. This overloads the cellular machinery designed to keep these processes in check, resulting in ER and oxidative stress responses (Di Nardo *et al.,* 2009). There was a trend for lower expression of ATF4 with increasing rapamycin concentration, whereas there was a trend is for increased levels of the ER stress protein ATF4 in AZD2014-treated neurons. In cancer therapy cell death is a desirable outcome and the effect on ER stress in normoxia may give a mechanistic insight to the efficacy of AZD2014 in cancer studies (Huo *et al.,* 2013; Kahn *et al.,* 2014; Liao *et al.,* 2014). However, in the context of ischaemia, AZD2014's neurotoxic effects by inducing ER stress would be detrimental to stroke outcome.

AZD2014 is currently undergoing clinical trials in humans for cancer and already has safety and tolerability data *in vivo* and would have been an ideal candidate to carry forward if neuroprotective efficacy had been shown. However, OGD experiments clearly revealed cytotoxic effects which is in line with its antitumour actions. The main mechanism for this cytotoxic effect is likely to be due to increased hamartin leading to overactivation of mTOR and subsequent increased ER stress. If AZD2014 was ever to be used as a long term therapy,

neurotoxicity would be a very concerning feature. Patients on this drug who have an ischaemic stroke could potentially have much worse outcomes than they would otherwise.

3.7 Conclusions

It is proposed that the selective dynamic response of hamartin expression in the CA3 area of the hippocampus is involved in the endogenous resistance of CA3 neurons to global ischaemia. *In vivo,* following global ischaemia, hamartin expression immediately increased in the membrane fraction of CA3 neurons, an effect that peaks at 12 hours and persists at 24 hours (Table 3.1). Manipulation of this downstream pathway through understanding the exact mechanism of endogenous neuroprotection could hold the key to a novel therapeutic approach to stroke.

Time Course (hours) 10 min global ischaemia	**0**	**12**	**24**
CA1	No difference in hamartin expression.	No difference in hamartin expression.	No difference in hamartin expression.
CA3	Hamartin expression induced (membrane) and decreased (cytoplasm)	Peak hamartin expression (membrane).	Persistant hamartin expression (membrane).

Table 3.1 *In vivo* summary of results

The available pharmacological inhibitors failed to replicate hamartin's endogenous neuroprotective effect (Table 3.2). Although post treatment rapamycin did prove to offer some neuroprotective effects *in vitro*, it is not an ideal drug candidate owing to side effects and furthermore as it is only an mTORC1 inhibitor at usual concentrations it does not replicate hamartin's mechanism of action exactly. The cytotoxic effects of AZD2014 may not however be exclusively linked to its dual mTORC1/2 inhibition, with AZD2014 having a potential effect of inhibiting upstream regulators such as hamartin, and inducing stress responses such as ER stress. While cytotoxic actions of these drugs would be desirable in cancer, this is not the case for ischaemic stroke where survival of cells is paramount. Therefore, it appears that exclusively targeting mTOR inhibition does not hold the key to

endogenous neuroprotection. This leads to the hypotheses that targeting downstream pathways sucas productive autophagy (Chapter 4) and ER stress (Chapter 5) could further elucidate hamartin's endogenous neuroprotective effect.

Drug	Function	Summary of treatment effect
Rapamycin	mTORC1 inhibition	Pre: No effect During: No effect Post: 10nM **improved neuronal survival** (OGD)
AZD 2014	mTORC1/2 inhibition	Pre: **Increased neuronal death** (OGD) During: **Increased neuronal death** (OGD) Post: **Increased neuronal death** (hippocampal and cortical, normoxia and OGD).

Table 3.2 *In vitro* summary of results

Chapter 4: Autophagy and hamartin's endogenous protective mechanism

4.1 Executive summary

Autophagy removes misfolded or long-lived proteins and organelles that are damaged or surplus to requirements and is an adaptive response to provide nutrients and energy following cellular stress. There remains controversy over whether productive autophagy is beneficial or detrimental in the context of cerebral ischaemia. In order to further probe the downstream molecular mechanisms from hamartin, productive autophagy was investigated.

In vivo experiments conducted over a time course revealed that at 3 hours post global ischaemia, beclin-1 levels (involved in early autophagosome formation) were significantly lower in CA3 regions compared to sham, and lower levels of p62 (a marker of impaired flux and hence productive autophagy if present at low levels) in ischaemic CA3 regions compared to CA3 sham regions. At 12 hours, LC3 (autophagosomal membrane marker) expression is significantly lower in CA3 ischaemia compared to sham while CA1 had increased LC3 in response to ischaemia.

Lenitiviral experiments in hippocampal neurons *in vitro* demonstrated that overexpression of hamartin was neuroprotective whereas shRNA knock down of hamartin was detrimental, with protection due to enhancement of productive autophagy. *In vitro* experiments confirmed that the inhibitor of autophagy, 3MA resulted in increased cell death. Metformin, a drug currently in wide clinical use and known to be an inducer of autophagy failed to replicate hamartin's endogenous neuroprotective effect.

Overall, it appears that hamartin is producing its neuroprotective effect by inducing autophagy but pharmacologically inducing autophagy did not replicate this protection. Therefore there may be a number of factors involved in CA3 endogenous neuroprotection with autophagy being one of multiple influences.

4.2 Background

4.2.1 mTOR, a regulator of the autophagic pathway

mTORC1 is an inhibitor of autophagy, a catabolic process implicated in ischemic pathophysiology (Gabryel *et al.,* 2012). Autophagy degrades damaged organelles and protein aggregates, enclosing them inside autophagosomes and digesting them with hydrolases after autophagosome fusion with lysosomes. Efficient completion of this cascade is termed productive autophagy (Gabryel *et al.,* 2012). As hamartin indirectly inhibits mTORC1 activity, hamartin's neuroprotective mechanism could be through induction of productive autophagy. Upon induction of autophagy, microtubule-associated protein 1 light chain 3 (LC3) is processed from a 16-kDa form (LC3-I) to a 14-kDa form (LC3-II), which is recruited to autophagosomes and is an indicator of autophagosome formation (Klionsky *et al.,* 2008). Under oxygen deprivation conditions, mTORC1 becomes inhibited which initiates the autophagy process (Kim *et al.,* 2011). AMPK is a heterotrimeric serine/threonine kinase that is phosphorylated and activated in times of cellular austerity manifested by an increase in the ratio of AMP to ATP. mTOR and AMPK have been shown to directly phosphorylate ULK1 (mammalian autophagy-initiating kinase) (Kim *et al.,* 2011). Under conditions of glucose starvation, AMPK promotes autophagy by directly phosphorylating and activating Ulk1 on Ser^{317} and Ser^{777}. When the supply of nutrients is sufficient, high mTOR activity prevents Ulk phosphorylation inhibiting autophagy. The activation of AMPK and subsequent induction of autophagy has been demonstrated to be effective in other body tissues, including the heart (Xie *et al,* 2011; Matsui *et al.,* 2007), kidney (Wang *et al.,* 2013) and muscle (Pauly *et al.,* 2012). However, there remains controversy over the neuroprotective nature of autophagy in the brain. For example, in a rodent model of neonatal hypoxia-ischaemia a protective role for autophagy was demonstrated (Carloni *et al.,* 2008) whereas using a rat model of permenant focal cerebral ischaemia, the activation of autophagy was shown to contribute to ischemic neuronal injury (Wen *et al.,* 2008).

4.2.2 Measuring autophagy

Proteins that can be used to evaluate the process of autophagy include Beclin-1, LC3-II and p62. Beclin-1 is a component of the PI3K complex involved in the early stage of autophagosome formation and vital for recruitment

of Atg proteins to the expansion step. Beclin-1 interacts with Bcl-2 via its BH3 domain. In times of nutrient abundance, the interaction is strong, preventing autophagy whereas it is weak under starvation conditions promoting autophagy (as reviewed by Carloni *et al.,* 2008). It has been suggested that beclin-mediated autophagy may be responsible for the protective effect induced by the preconditioning provided by hyperbaric oxygen therapy (reviewed by Wang *et al.,* 2010). Amino acids can inhibit Beclin-1 via two methods, first by mTOR activation and second by reducing Beclin1-associated PI3K class III activity due to increased binding of Beclin 1 by Bcl-2 which is not sensitive to rapamycin (Meijer and Codogno, 2006). Microtubule-associated protein 1 light chain 3 (LC3-II) is recruited to autophagosomes and is an indicator of autophagosome formation. After synthesis, pro-LC3 is cleaved by ATG4 protease and becomes the 16–18 kDa LC3-I. Upon activation of autophagy, LC3-I is conjugated with phosphatidylethanolamine (PE, lipidated) which is referred to as LC3-II (Kabeya *et al.,* 2000, Kabeya *et al.,* 2004). Measuring LC3 alone is not sufficient to determine productive autophagy as there should be some indication of autophagic flux (Gustafsson and Gottlieb, 2008). Sequestosome-1 (p62) is a marker of autophagic flux as it is degraded by lysosomes and only accumulates following impairments in autophagy. Under normal conditions, basal autophagy continuously clears p62 from the cytoplasm. Where autophagy is deficient, p62 and its associated cargo accumulates in the cytoplasm (Rusten and Stenmark, 2010) and is used as a marker of autophagic flux. See Figure 1.9 for an explanation of the autophagic process and the proteins involved.

4.2.3 The importance of time on the effect of autophagy

The conundrum as to whether autophagy is protective or harmful following ischaemic damage could be solved by considering the time at which it becomes active. Using primary cortical neurons from Sprague–Dawley rats and SH-SY5Y, 3-MA caused increased neuronal death when administered during six hours of OGD and 24 hours of reperfusion whereas after 48 and 72 hours of reperfusion, 3-MA demonstrated a neuroprotective effect (Shi *et al.,* 2012). This finding is corroborated by rodent studies where 3-MA caused reduction in lesion volume and blocked ischaemia-related LC3-II expression even when given more than four and a half hours following the induction of the ischaemia (Puyal and Clarke, 2009). In neonatal hypoxic ischaemic brains, beclin-1 was upregulated in the cortex as late as 7 days postischemia (Shi *et al.,* 2012).

Using slice cultures (the preparation of which results in intrinsic stress) comparing cortical and hippocampal regions demonstrated higher steady levels of autophagy in hippocampal slices than cerebral cortex slices (Pérez-Rodríguez *et al.,* 2014). In cortical slices the whole autophagic process was observed 3 hours after OGD. By contrast, autophagy induction in the hippocampus may not be detectable within the first 3 hours following ischaemia. *In vivo* studies have detected induction of autophagy in the hippocampus at 12 hours (Cui *et al.,* 2013) and 24 hours (Ruan *et al.,* 2012). Using a 10 minute 2VO and hypotension model of I/R injury *in vivo*, a time course of autophagy protein expression was established (with animals killed at 1.5, 3, 6, 12 and 24 hours following the insult and also compared to a sham group) in the hippocampus. There was an upregulation of the LC3-II/LC3-I expression ratio starting at 3 hours and peaking at 12 hours while beclin-1 levels increased 6–24 hours following the insult ($P < 0.01$) (Cui *et al.,* 2013). As the hippocampus was not separated into CA1 and CA3, it is not possible to make exact predictions for differences that would be observed between these hippocampal subfields. In the 4-VO model in male Wistar rats, it was found that that autophagy could phagocytose synaptic structures following ischemia with the frequency of autophagosomes observed escalating from 12 to 48 hours following ischemia in CA1. Again, there was no CA3 comparison but in this study it was demonstrated that ischaemia increases the presence of asymmetric synapses as well as synaptic autophagy (Ruan *et al.,* 2012)

4.2.4 Pharmacology

4.2.4.1 Inhibition of Autophagy: 3-methyadenine (3MA)

The drug, 3MA (Figure 4.1) is a selective inhibitor of the class III PI3K and inhibits beclin-1-dependent autophagy in various disease models (Kihara *et al.,* 2001) and has been used to determine the neurotoxic vs neuroprotective role of autophagy in cerebral ischaemia. 3MA has been shown to abolish the protective effect of IPC in a rat focal model (Sheng *et al*., 2010). In a neonatal model of hypoxia ischaemia in Sprague–Dawley pup rats 3MA blocks autophagosome formation. In a neonatal model of hypoxia ischaemia in Sprague–Dawley pup rats 3MA was administered 10 min after rapamycin resulting in Bax and Bad translocation to the mitochondria. However neither cytochrome c release nor caspase-3 activation occurred. Inhibition of rapamycin

induced autophagy resulted in cells dying in a necrotic fashion (Carloni *et al.,* 2008). 3MA will be used as a tool to further elucidate hamartin's endogenous protective mechanism.

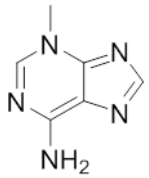

Figure 4.1 Chemical structure of 3-MA

4.2.4.2 Induction of Autophagy: Metformin

Metformin (Figure 4.2) is biguanide molecule used for type 2 diabetes treatment and is in wide clinical use. Metformin activates both protein kinase, AMP-activated (PRKA) and sirtuin (silent mating type information regulation 2 homolog) 1 (SIRT1). It could therefore induce autophagy via either of its signalling pathways: PRKA-MTOR-ULK1 or SIRT1-FOXO (Song *et al.,* 2015). In male Sprague-Dawley rats using pMCAO, a single dose of pretreatment metformin (10 mg/kg intraperitoneally) conferred neuroprotection against focal cerebral ischemia by pre-activation of AMPK-dependent autophagy (Jiang *et al.,* 2014). The underlying mechanism has been postulated to be either via mTOR (Zhang *et al.,* 2013) or via direct phosphorylation of ULK1 by AMPK (Kim *et al.,* 2011). Metformin may also afford neuroprotection by modulating inflammatory and antioxidant pathways via induction of AMPK (Ashabi *et al.,* 2015). A recent study using tMCAO in mice has demonstrated that metformin reduces blood-brain barrier disruption via down-regulation of ICAM-1 (Liu *et al.,* 2014).

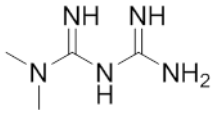

Figure 4.2 Chemical structure of metformin

Metformin will be used as an inducer of autophagy and since this is a drug that is already in wide clinical use with established safety and tolerability, any neuroprotective effect would be highly significant.

4.3 Aims of this Chapter

The aim of this chapter is to study hamartin's effect on autophagy as a downstream mechanism for its neuroprotective effect.

1. Aim to determine the temporal profile of autophagy-related protein expression *In vivo:* following global ischaemia in CA1 and CA3 areas of the hippocampus.

2. Aim to genetically alter hamartin expression to determine effects on productive autophagy and pharmacologically manipulate autophagy to assess neuroprotection.

4.4 Materials and Methods

All materials were obtained from commercial suppliers unless otherwise stated in the text. There are several methods in this chapter which are common to other chapters in the thesis. Where the methods appear in another chapter in full, this is indicated below.

4.4.1 *In vivo*

4.4.1.1 Global Forebrain Ischemia

This method is described in Chapter 2.

4.4.1.2 Terminal anaesthesia and brain microdissection

This method is described in Chapter 3, section 3.4.1.2. The reperfusion time points following 10 minutes global ischaemia used in this chapter were 3 and 12 hours.

4.4.1.3 Whole Cell Homogenisation

This method is described in Chapter 3, section 3.4.1.4

4.4.1.4 Protein Assay

This method is described in Chapter 3, section 3.4.1.5

4.4.1.5 Identification of proteins

This method is described in Chapter 3, section 3.4.1.6

4.4.1.5.1 Electrophoresis

This method is described in Chapter 3, section 3.4.1.6.1

4.4.1.5.2 Quantification of loading

This method is described in Chapter 3, section 3.4.1.6.2

4.4.1.5.3 Western Blotting

This method is described in Chapter 3, section 3.4.1.6.3

4.4.1.5.4 Antibody reagents for immunoblotting (IB)

Primary antibodies used: anti-rabbit to p62 (MABC32, Millipore), 1:100; anti-mouse antibody to LC3 (5F10, Nanotools Antikoepertechnik), 1:200, anti-rabbit antibody to beclin-1 1:1000 (3738, Cell Signalling).

4.4.2 *In vitro*

The method of cell culture of hippocampal and cortical neurons from E18 rats is described in Chapter 3, section 3.4.2.1. The lentiviral transduction and overexpression cell culture experiments were carried out working in collaboration with Dr Michalis Papadakis, University of Oxford and Dr Kostas Vekrellis, Biomedical Research Foundation of the Academy of Athens, Athens, Greece.

4.4.2.1 Primary hippocampal cultures and lentiviral transduction.

Hippocampal and cortical cultures were prepared from E18 rat embryos, as described in Chapter 3, section 3.4.2.1. For lentiviral experiments, cells were transduced with lentiviral vectors at a multiplicity of infection of 10–20, 7 days *in vitro* (DIV) for shRNA studies and at 11 DIV for overexpression studies. In these experiments, rapamycin (10nM) or 3MA (10mM) or vehicle were added 24 h before normoxia or OGD.

4.4.2.2 Oxygen glucose deprivation.

For the pharmacology experiments with 3MA and metformin, OGD experiments were performed as described in Chapter 3, section 3.4.2.2. See section 4.4.2.5 for the compounds used in this study. For lentiviral experiments, hippocampal cultures were washed twice and immersed in 500 µl deoxygenated custom Neurobasal medium without glucose, aspartate, glutamate, glutamine or pyruvate (Invitrogen) to induce OGD.

Oxygen was removed by bubbling the immersion solution for 30 min with a premixed gas (85% N_2, 10% H_2, 5% CO_2). Cultures were sealed inside a modular chamber (Billups-Rothenberg) which was flushed for 10 min with the same premixed gas and placed inside an incubator for 3 h. Anoxia was confirmed using disposable anaerobic indicator strips (GasPak, BD Biosciences). Control cultures were treated similarly but with normoxic custom Neurobasal medium supplemented with 25 mM d-glucose in a normoxic incubator.

4.4.2.3 Cell death assays.

Cell death was assessed following OGD using the LDH release Cytotox96 assay (Promega) as described in Chapter 3, section 3.4.2.3. For the lentiviral experiments, the necrotic/healthy cells detection kit (PromoKine) was used. Cells were co-stained with Hoechst 33342 and ethidium homodimer III and fluorescence visualised using a fluorescent microscope (NIKON) with a ×20 lens. At least 500 neurons were counted and images were acquired using Simple-PCI software (Digital Pixel). The data were expressed as a percentage of the number of neurons stained with ethidium homodimer III to the number stained with Hoechst 33342.

4.4.2.4 Lentiviral vectors

Lentiviral work was conducted in collaboration with Dr Michalis Papadakis. Lentiviral vectors (Sigma-Aldrich) used were pLKO.1 TSC1 shRNA (5'- CCG GCC GGG AGC TGT TCC GTA ATA ACT CGA GTT ATT ACG GAA CAG CTC CCG GTT TTT G-3'), which targets nucleotides 2,262–2,282 of the rat TSC1 mRNA (GenBank accession number NM021854)); pLKO.1 control shRNA (5'-CCG GCA ACA AGA TGA AGA GCA CCA ACT CGA GTT GGT GCT CTT CAT CTT GTT GTT TTT- 3'), which contains a scrambled sequence that does not target any known rat genes; pLKO.1 TurboGFP, which contains the TurboGFP gene.

Recombinant lentiviral particles encoding rat *Tsc1*-eGFP, human *TSC1* or a control eGFP plasmid were generated by co-transfection of human embryonic kidney (HEK) 293T cells with each expression plasmid (pEZ-Lv201 vector) together with the GeneCopoeia Lenti-Pac HIV Expression Packaging Kit, according to manufacturer's instructions (Lifesciences, Source Bioscience). HEK 293T cells were cultured in DMEM (Invitrogen) supplemented with 10% FBS and 1% penicillin-streptomycin. Two days before transfection, 1.5 × 10^6 cells were plated onto 10-cm dishes. For transfection, 2.5 µg of vector DNA (rat or human *TSC1*, or control

eGFP plasmid) and 2.5 µg of Lenti-Pac HIV mix were added in 293T cells in the presence of the Endofectin Lenti transfection reagent (GeneCopoeia). After 16 h, the medium was removed, and the cells were washed twice with PBS and returned to the normal culture medium supplemented with 1:500 volume of the Titer Boost reagent. Medium was collected containing recombinant lentiviral particles 48 h after transfection and centrifuged (400*g*, 10 min, 4 °C) to remove debris. After filtration through a 0.45-µm filter unit (Millipore, USA) the supernatant was centrifuged at 46,100*g* for 4.5 h at 4 °C in a SS34 rotor (Sorvall). The viral particles were resuspended in 50 µl per tube of PBS supplemented with 0.5% BSA, aliquoted them and stored them at −80 °C. Lentiviral titres were determined by seeding HeLa cells in 12-well plates at 5 × 104 cells per well, 3–4 h before infection with serial dilutions of the concentrated viral stock. After incubation for 2 d, the medium was removed and the eGFP-expressing cells were identified by FACS. Titers ranged from 4 × 108 to 2.5 × 109 infectious units (IU ml−1). The human *TSC1* mRNA sequence contains six nucleotide mismatches compared to the rat *Tsc1* mRNA base pairs 2,262–2,282, making it resistant to TSC1 shRNA knockdown.

4.4.2.5 Pharmacology

A 3MA stock solution of 200mM was prepared in DMSO with concentrations of 0.1µM, 1 µM and 10 µM were used in this thesis. Metformin hydrochloride (Fluka analytical, Sigma-Aldrich) was prepared in DMSO giving a stock solution of 25mM with concentrations of 20 µM, 50 µM, 200 µM and 500 µM used in this thesis. Timings of drug administration were: 'pre-treatment' 24 hours prior to 2 hours OGD or normoxia, during the 2 hour OGD or normoxia period, or 'post treatment' in the recovery media only for 24 hours following the 2 hour OGD or normoxia period.

4.4.3 Statistical analyses

Statistical analysis was carried out with GraphPad Prism 5 using a two-tailed Student's t-test if two groups were compared, one-way ANOVA with Bonferroni's multiple comparisons post hoc test for comparisons of more than two groups and two-way ANOVA with Bonferroni's post hoc test when two independent variables were assessed. Differences were considered significant for $P < 0.05$. Data presented as Mean $\pm$ SEM.

4.5 Results

4.5.1 *In vivo*

Hippocampal sub-regions CA1 and CA3 were investigated at 3 and 12 hours post-global ischaemia. Western blotting was conducted for expression levels of beclin-1 as a marker of autophagy induction, microtubule-associated protein 1 light chain 3 (LC3-II) as a marker of autophagosome formation and sequestosome-1 (p62) as a marker of autophagic flux.

4.5.1.1 Autophagy time course: 3 hours post global forebrain ischaemia

4.5.1.1.1 Expression levels of Beclin-1

Beclin-1 was present in sham operated animals. There was no significant difference in beclin-1 expression levels between CA1 regions in sham and ischaemic animals (p= 0.8516) or between in CA1 and CA3 regions in sham animals (p=0.6733). There were significantly lower levels of beclin-1 in the CA3 region of ischaemic animals at 3 hours compared to the CA3 region in sham animals (p=0.0031) (Figure 4.3).

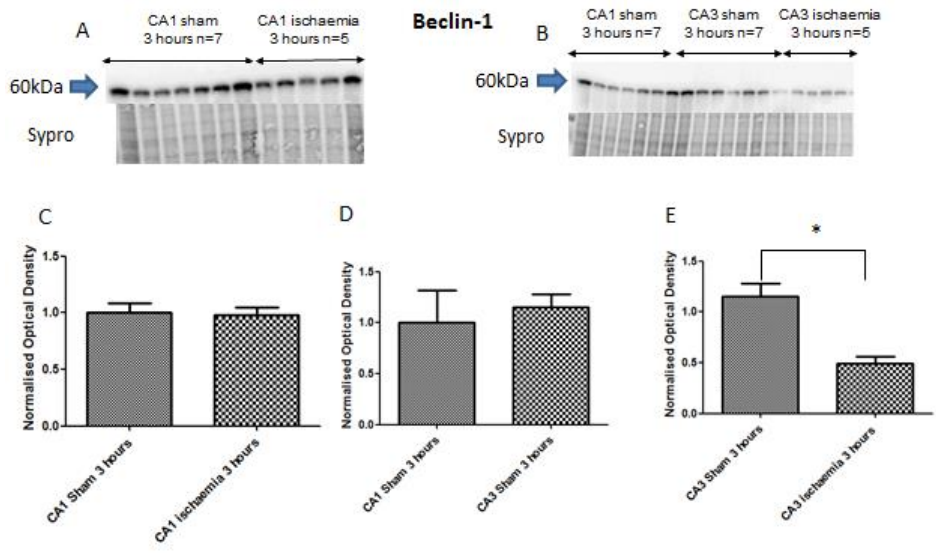

Figure 4.3 Beclin-1 expression at 3 hours following 10 minutes of global cerebral ischaemia Upper panels (A and B) show the western blots and loading correction with SYPRO® used to produce the graphs (C), (D) and (E) below of Beclin-1 immunoreactivity. (C) CA1 sham (n=7) and CA1 ischaemia (n=5) had no significant difference in beclin-1 expression levels. (D) There was no significant difference in beclin-1 expression levels between CA1 sham (n=7) and CA3 sham (n=7). (E) There were significantly lower levels of beclin-1 in CA3 at 3 hours following ischaemia (n=5), compared to sham (n=7). Molecular weight of beclin-1: 60 kDa. *p<0.05

4.5.1.1.2 Expression levels of LC3

LC3 was present in sham-operated animals. There was no significant difference between CA1 regions of sham animals and ischaemic animals (p=0.5701), between CA1 and CA3 regions in sham animals (p=0.3030) and CA3 regions of sham animals compared to ischaemic animals (Figure 4.4).

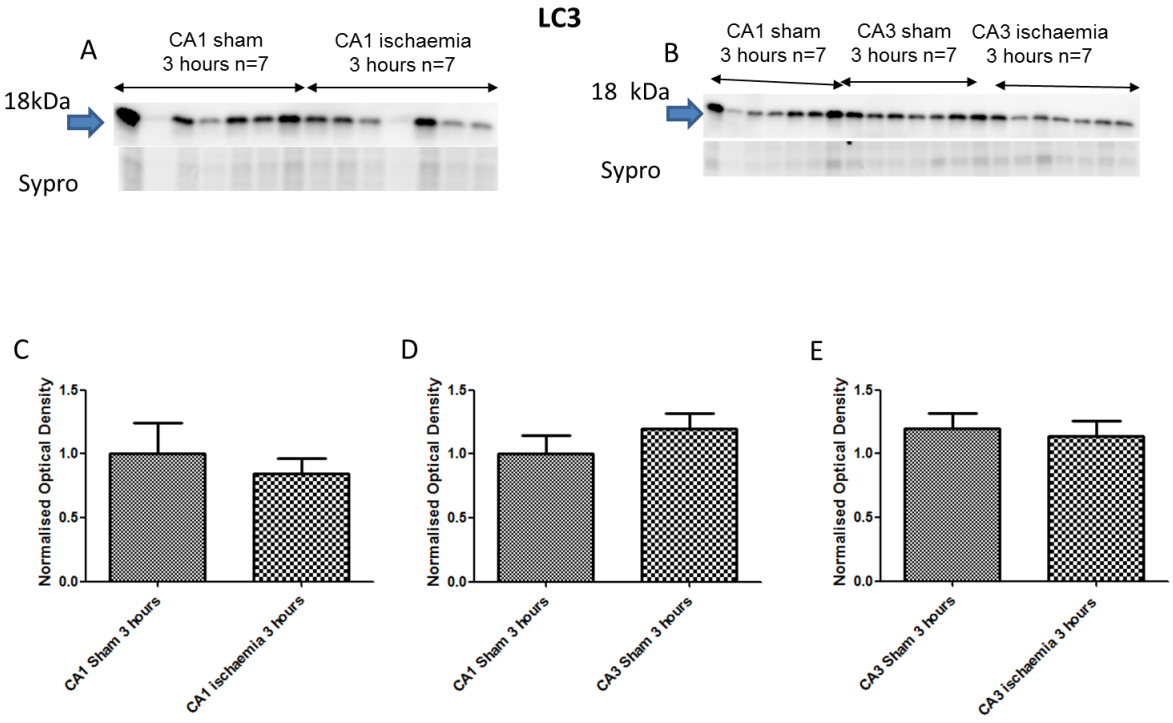

Figure 4.4 LC3 expression at 3 hours following 10 minutes of global cerebral ischaemia Upper panels (A and B) show the western blots and loading correction with SYPRO® used to produce the graphs (C), (D) and (E) below of LC3 immunoreactivity. (C) CA1 sham (n=7) and CA1 ischaemia (n=7) showed no significant difference. (D) There was no significant difference in LC3 expression levels between CA1 sham (n=7) and CA3 sham (n=7). (E) There was no significant difference between CA3 sham (n=7) and CA3 ischaemia (n=7). Molecular weight of LC3: 16-18 kDa.

4.5.1.1.3 Expression levels of p62

At 3 hours there was no difference expression of p62 between CA1 regions in sham animals and CA1 regions in ischaemic animals (p=0.1004) nor between CA1 and CA3 regions in sham animals (p=0.5029) (Figure 4.5). There was a significantly reduced expression of p62 in the CA3 region in ischaemic animals compared to the CA3 regions in sham animals (p=0.0006).

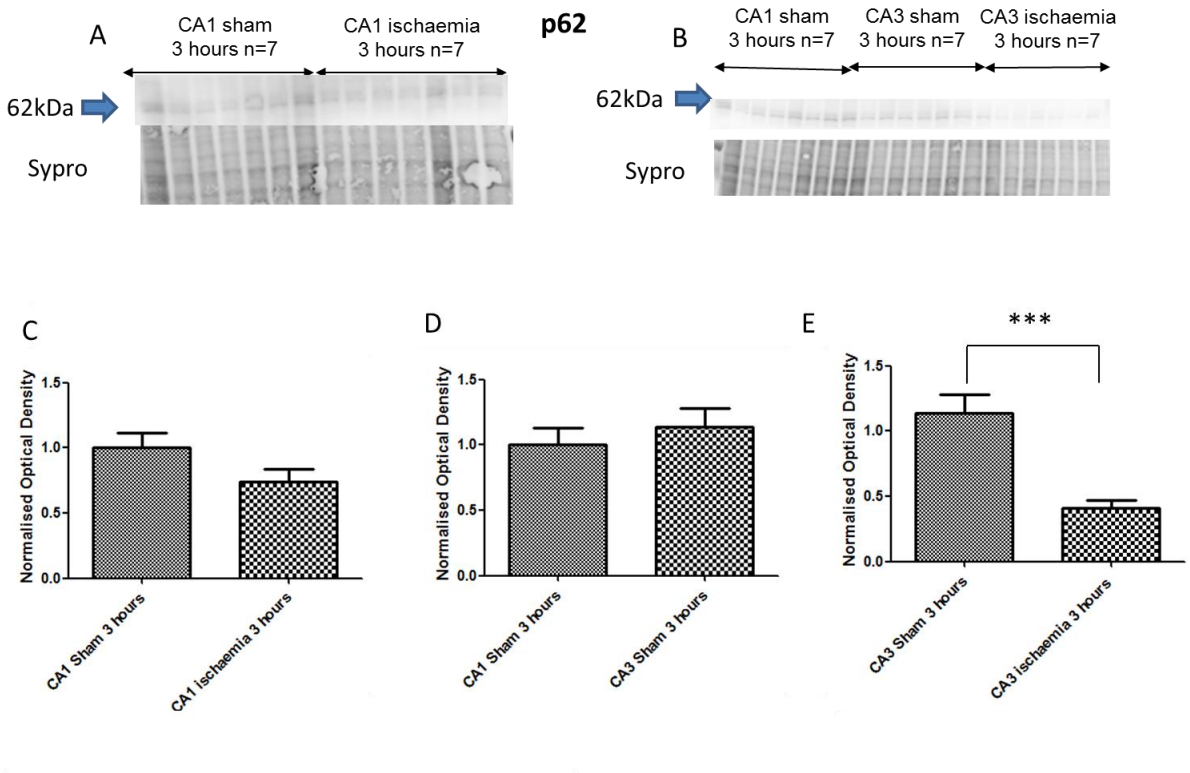

Figure 4.5 p62 expression at 3 hours following 10 minutes of global cerebral ischaemia Upper panels (A and B) show the western blots and loading correction with SYPRO® used to produce the graphs (C), (D) and (E) below of p62 immunoreactivity. (C) CA1 sham (n=7) and CA1 ischaemia (n=7) showed no significant difference. (D) There was no significant difference in p62 expression levels between CA3 sham (n=7) and CA1 sham (n=7). (E) There were significantly lower levels of p62 in CA3 at 3 hours following ischaemia (n=7) compared to CA3 sham (n=7). Molecular weight of p62: 62 kDa. ***p<0.001

4.5.1.2 Autophagy time course: 12 hours post global forebrain ischaemia

4.5.1.2.1 Expression levels of Beclin-1

There was no significant difference in beclin-1 expression levels between CA1 regions in sham and ischaemic animals (p=0.7637). There was a significant difference between levels of beclin-1 between CA1 and CA3 regions in sham animals (p=0.0179). There was no significant difference in beclin-1 levels in CA3 regions in ischaemic compared to sham animals (p=0.2717) (Figure 4.6).

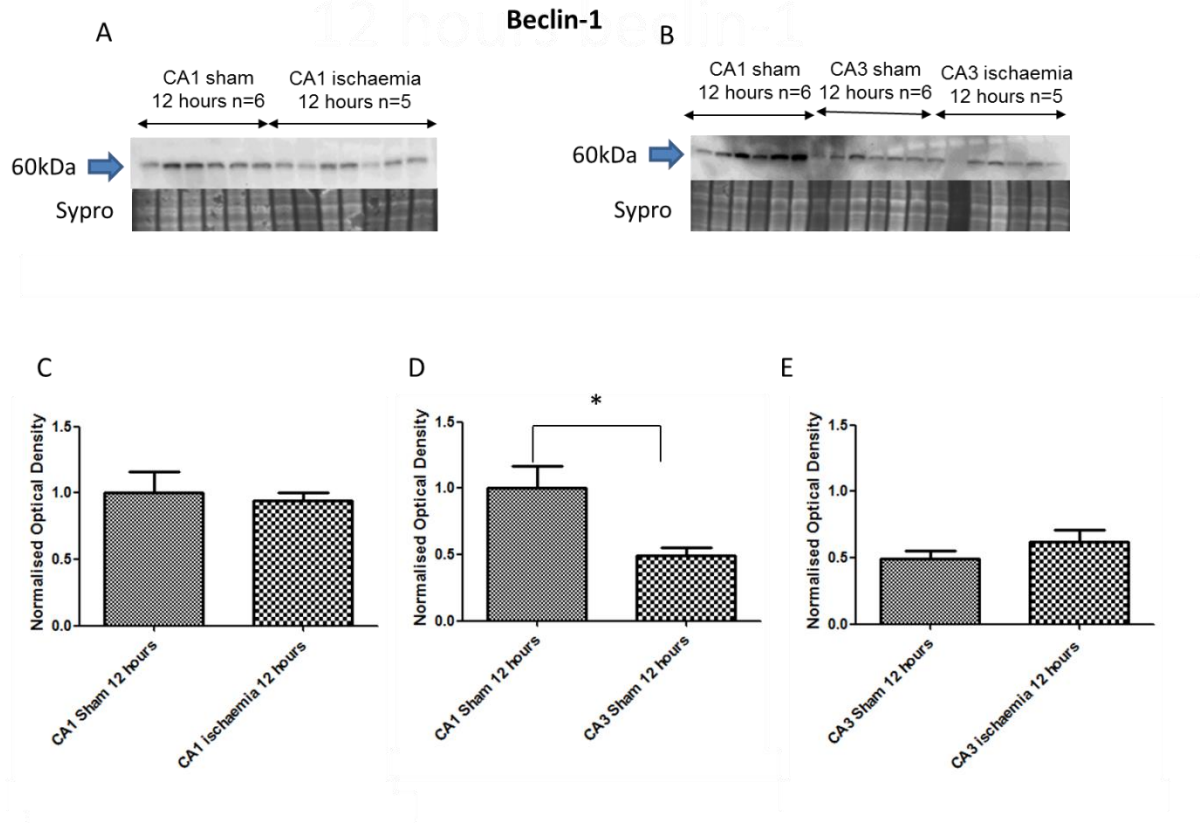

Figure 4.6 Beclin-1 expression at 12 hours following 10 minutes of global cerebral ischaemia Upper panels (A and B) show the western blots and loading correction with SYPRO® used to produce the graphs (C), (D) and (E) below of beclin-1 immunoreactivity. (C) CA1 sham (n=6) and CA1 ischaemia (n=5) had no significant difference in expression levels. (D) There was a significant difference in beclin-1 expression levels between CA1 sham (n=6) and CA3 sham (n=6). (E) There was no significant difference in beclin-1 levels in CA3 at 12 hours following ischaemia (n=5) compared to CA3 sham (n=6). Molecular weight of beclin-1: 60 kDa. *p<0.05

4.5.1.2.2 Expression levels of LC3

There was no significant difference in LC3 levels between CA1 regions in sham and ischaemic animals (p=0.0553), however the trend was highly suggestive of higher LC3 levels in CA1 ischaemic areas compared to sham. There was no significant difference in LC3 levels in the CA3 region of sham animals compared to sham CA1 region (p=0.6376). There was a significant decrease in LC3 levels in the CA3 regions in ischaemic animals compared to sham (p=0.0453) (Figure 4.7).

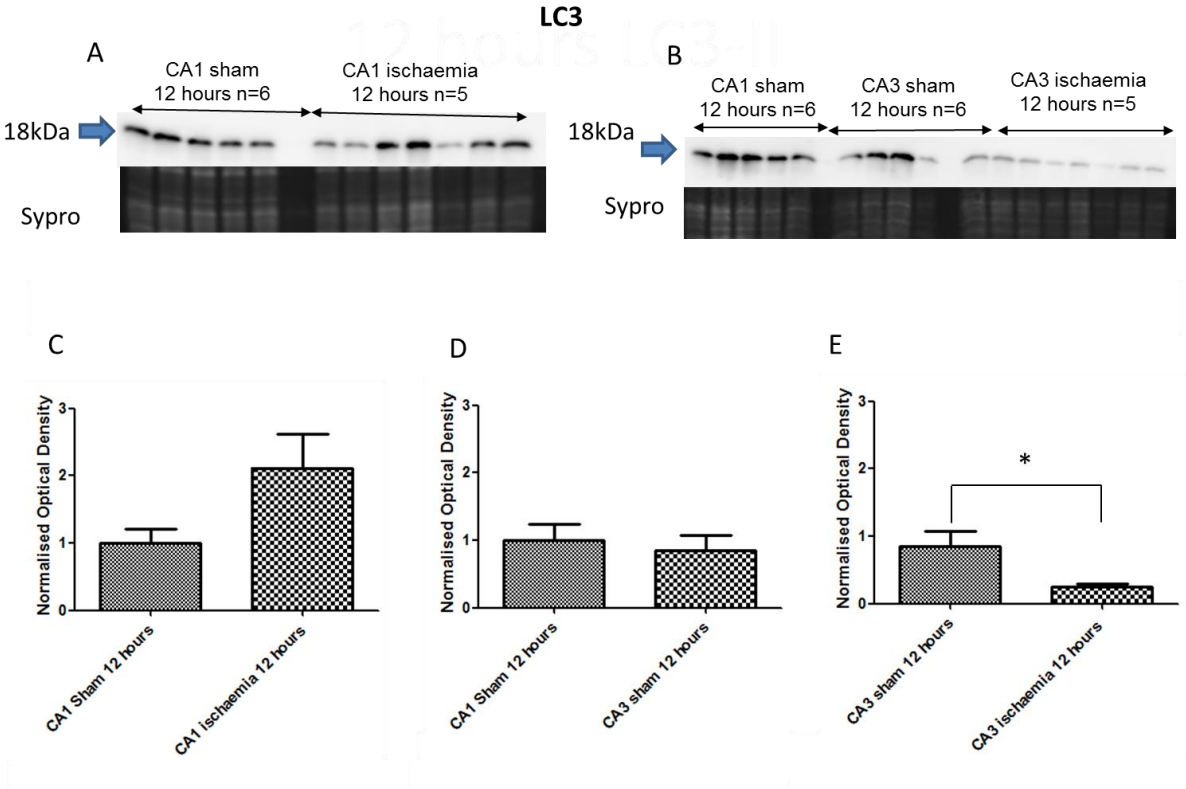

Figure 4.7 LC3-I expression at 12 hours following 10 minutes of global cerebral ischaemia Upper panels (A and B) show the western blots and loading correction with SYPRO® used to produce the graphs (C), (D) and (E) below of LC3-I immunoreactivity. (C) CA1 sham (n=6) and CA1 ischaemia (n=5) showed no significant difference in expression levels. (D) There was no significant difference in LC3-I expression levels between CA1 sham (n=6) and CA3 sham (n=6). (E) There were significantly lower levels of LC3-I in CA3 at 12 hours following ischaemia (n=5) compared to CA3 sham (n=6). Molecular weight of LC3-I: 18 kDa. *p<0.05

4.5.1.2.3 Expression levels of p62

There was no difference in p62 levels in CA1 regions in sham animals compared to ischaemic animals (p=0.0809). There was also no difference in p62 levels between CA1 and CA3 regions of sham animals (p=0.6579) or CA3 regions in sham animals compared to ischaemic animals (p=0.5239) (Figure 4.8).

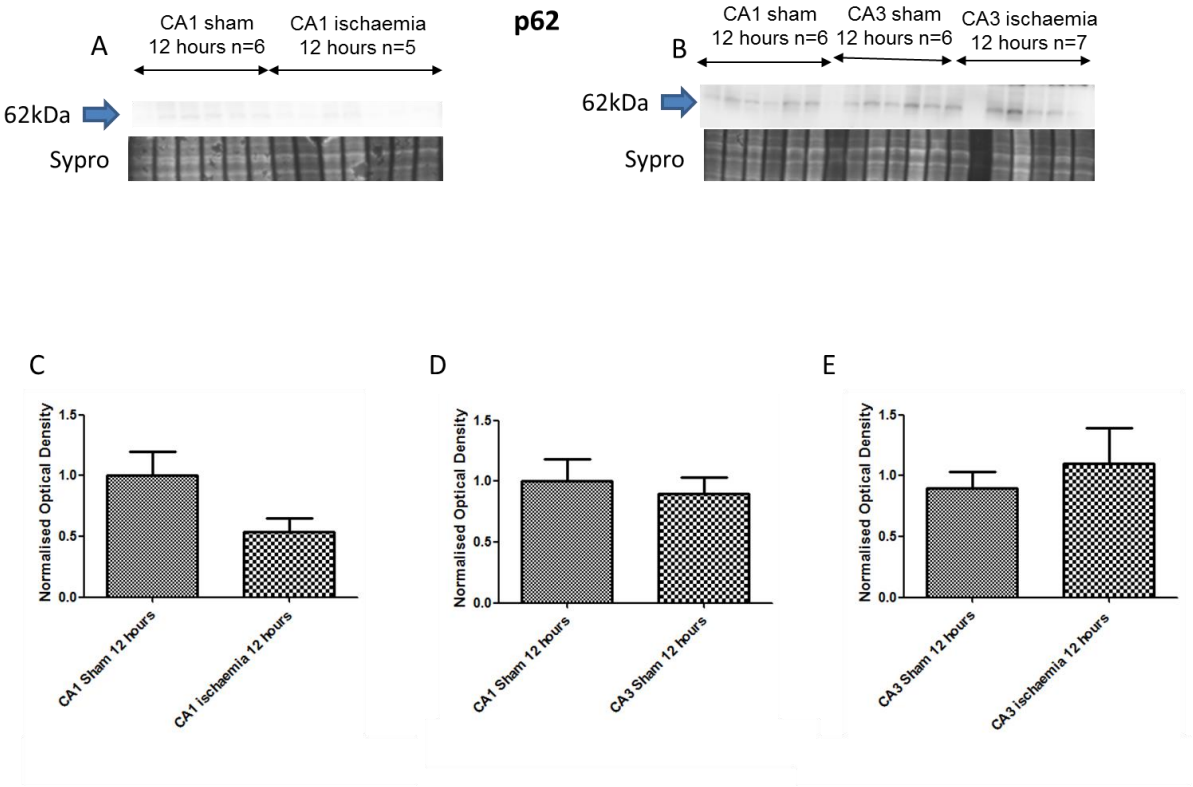

Figure 4.8 p62 expression at 12 hours following 10 minutes of global cerebral ischaemia Upper panels (A and B) show the western blots and loading correction with SYPRO® used to produce the graphs (C), (D) and (E) below of p62 immunoreactivity. (C) CA1 sham (n=6) and CA1 ischaemia (n=5) showed no significant difference in p62 expression levels. (D) There was no significant difference in p62 expression levels between CA1 sham (n=6) and CA3 sham (n=6). There was also no difference in expression levels of p62 in CA3 at 3 hours following ischaemia (n=5) compared to CA3 sham (n=6). Molecular weight of p62: 62 kDa.

4.5.1.3 Summary of autophagy time course

The *in vivo* autophagy protein expression time course is summarised in Figure 4.9 below.

	Beclin	LC3	p62
CA1 sham vs CA1 ischaemia	↔	↔	↔
CA1 sham vs CA3 sham	↔	↔	↔
CA3 sham vs CA3 ischaemia	↓ (CA3 ischaemia)	↔	↓ (CA3 ischaemia)

	Beclin	LC3	p62
CA1 sham vs CA1 ischaemia	↔	↔ (trend for↑ CA1 ischaemia)	↔
CA1 sham vs CA3 sham	↓ (CA3 sham)	↔	↔
CA3 sham vs CA3 ischaemia	↔	↓ (CA3 ischaemia)	↔

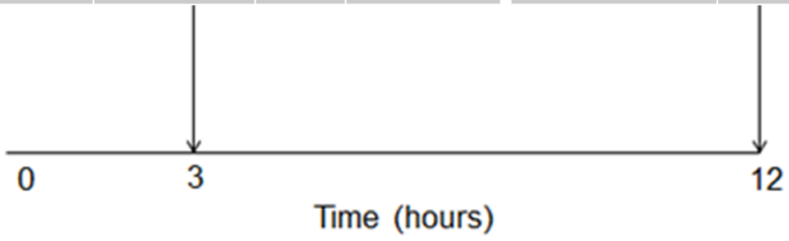

Figure 4.9: Timecourse of protein expression for markers of autophagy following 4-VO

4.5.2 *In vitro*

4.5.2.1 Lentiviral experiments

Lentiviral experiments were conducted to assess whether hamartin expression alters neuronal vulnerability to ischemia and if this is related to productive autophagy.

LC3-II expression was significantly higher in TSC1 shRNA–transduced compared to control shRNA–transduced rat hippocampal cultures following both normoxia and OGD indicative of greater autophagosome formation (Figure 4.10 A, B). Expression of p62 protein was significantly increased by suppression of hamartin compared to control shRNA–transduced rat hippocampal cultures following both normoxia and OGD showing greater impairment in autophagic flux (Figure 4.10 A, B). Rapamycin restored this autophagic flux demonstrated by decreased levels of p62. The autophagy inhibitor 3-methyladenine (3MA) was used to dissect the macroautophagy component of lysosomal activity. During normoxia, TSC1 shRNA–transduced neurons

showed significantly less macroautophagy-dependent degradation (down 53 ± 10% as compared to control shRNA–transduced cultures), which was completely diminished after OGD (Figure 4.10 C). Hamartin therefore promotes neuronal survival by inhibiting mTORC1 and inducing productive autophagy as autophagy is impaired (indicated by increased p62 levels) in the absence of hamartin.

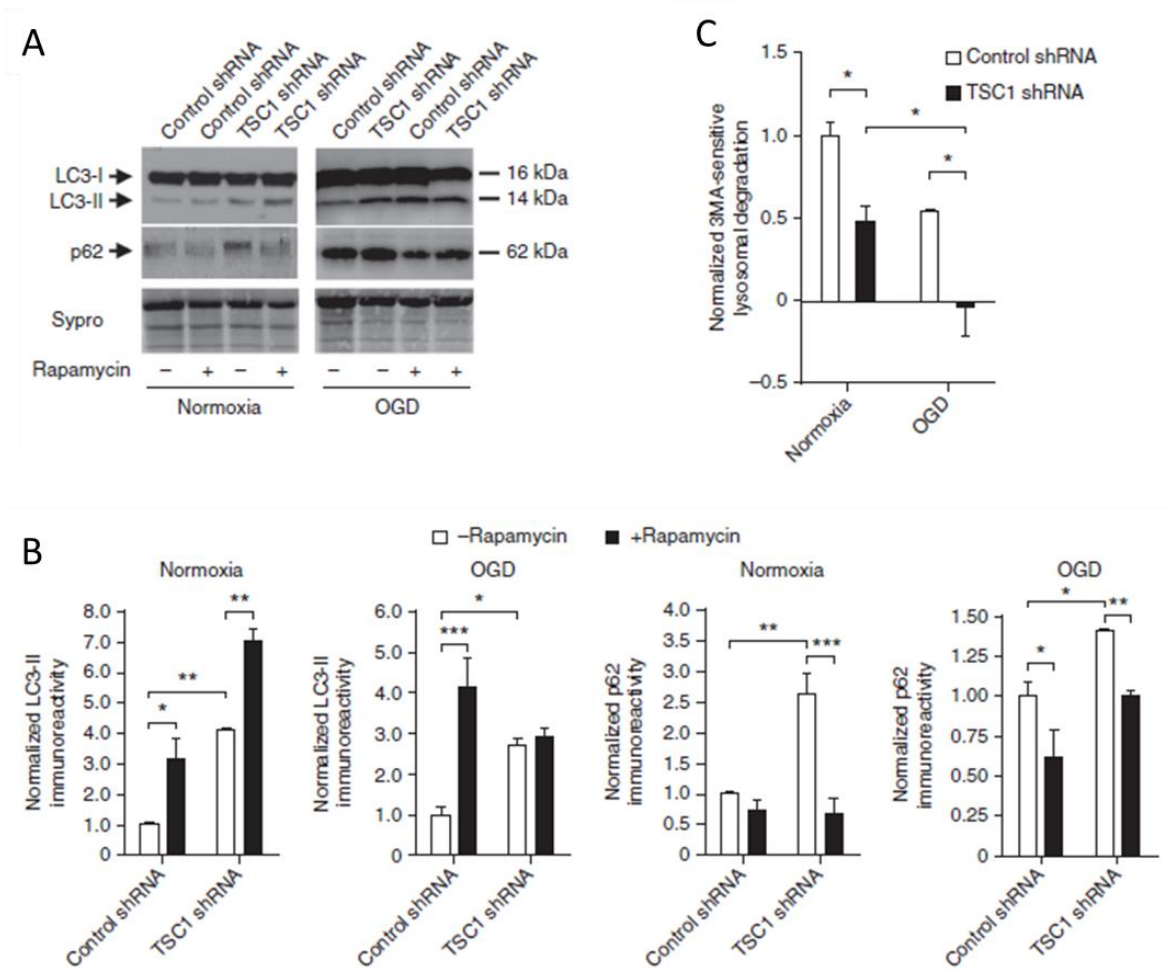

Figure 4.10 Hamartin promotes neuronal survival by inhibiting mTORC1 and inducing productive autophagy: **Knock down experiments** (A), (B) Representative immunoblots depicting LC3-I, LC3-II and p62 expression (A) and quantification of LC3-II and p62 levels (B) in the hippocampal cultures described in (A) (*n* = 3). (C) Quantification of macroautophagy-dependent (3MA-sensitive) lysosomal degradation in control transduced– and TSC1 shRNA–transduced cultures (*n* = 3). For B, data were normalized to control shRNA–treated levels. SYPRO® staining was used as loading control. For (C), data were normalized to 3MA-sensitive degradation from control shRNA–transduced cultures following normoxia. Values are mean ± s.e.m. of *n* = 3 independent experiments (two-way ANOVA with Bonferroni's post hoc test (B), (C), **p*< 0.05, ***p*< 0.01, ****p*< 0.001).

Overexpression of *Tsc1* in rat hippocampal neurons upregulated LC3-II expression, suppressed p62 expression by 44 ± 7% in normoxia and OGD and increased 3MA-sensitive degradation 340 ± 40% compared to GFP-transduced cultures after OGD (Figure 4.11 A-C). Inhibition of autophagy in rat TSC1-transduced cultures with 3MA abolished the protection conferred by overexpression of rat TSC1, reducing neuronal survival to 23 ± 2% from 47 ± 3% for untreated cultures overexpressing hamartin ($p < 0.001$; Figure 4.11). Hamartin therefore promotes neuronal survival by inhibiting mTORC1 and inducing productive autophagy as autophagy is unimpaired in overexpression experiments indicated by decreased p62 levels. This effect is negated in the presence of the autophagy inhibitor 3MA.

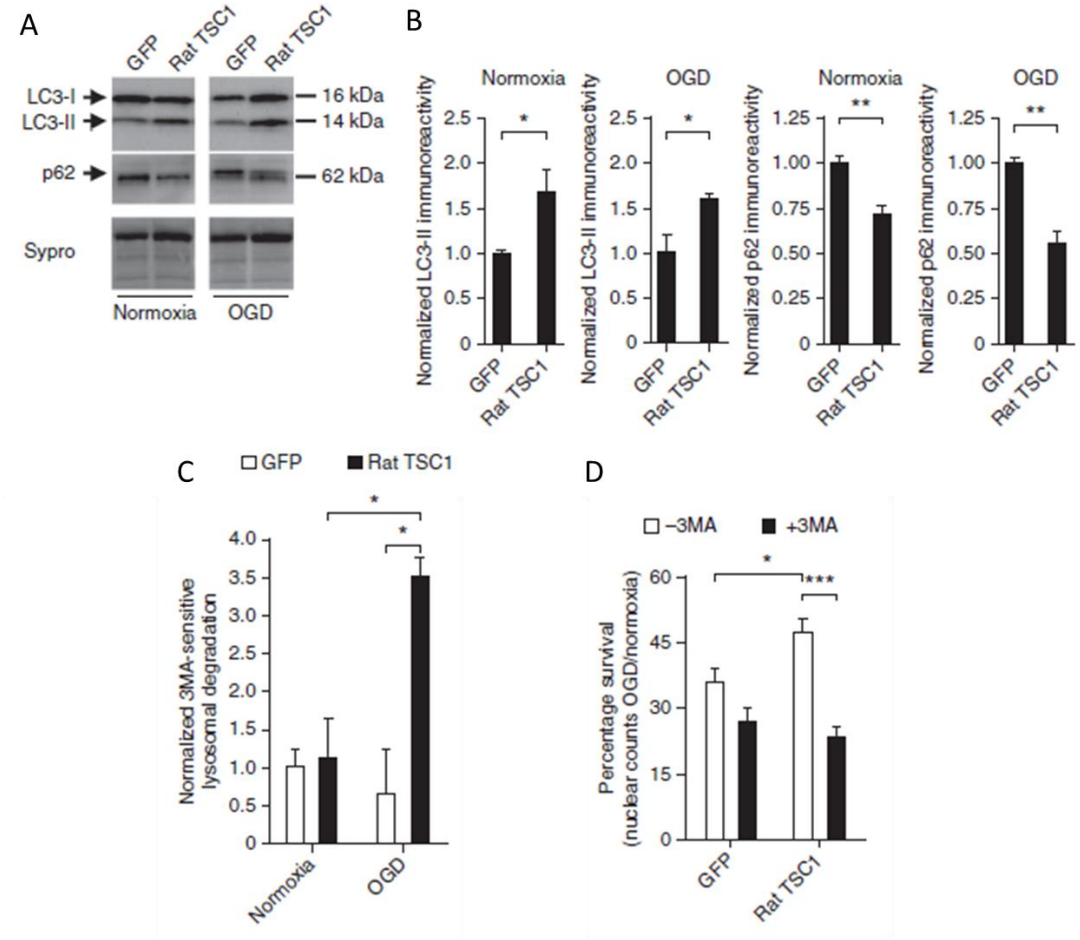

Figure 4.11 Hamartin promotes neuronal survival by inhibiting mTORC1 and inducing productive autophagy: **Overexpression experiments** (A),(B) Representative immunoblots of LC3-I, LC3-II and p62 expression (A) and quantification of LC3-II and p62 expression (B) from GFP– and rat TSC1–transduced cultures exposed to normoxia or OGD ($n = 3$). (C) Quantification of macroautophagy-dependent lysosomal degradation in GFP– and rat TSC1–transduced cultures ($n = 3$). Quantification of percentage survival (OGD to normoxia nuclear count ratio) of GFP– and rat TSC1–transduced cultures with or without 3MA (10 mM). For (B), data were normalized to control shRNA–treated levels. SYPRO® staining was used as loading control. For (C), data were normalized to 3MA-sensitive degradation from control shRNA–transduced cultures following normoxia. Values are mean ± s.e.m. of $n = 3$ independent experiments, (two-way ANOVA with Bonferroni's *post hoc* test (C), (D) or two tailed *t*-test (B), *$p < 0.05$, **$p < 0.01$, ***$p < 0.001$).

4.5.2.2 Pharmacology

4.5.2.2.1 3MA

3MA is an inhibitor of autophagy often used to decipher the effect of autophagy in cerebral ischaemia.

Treatment with 3MA during ischaemia

The effect of a dose response of 3MA on cortical neuron viability was assessed using an LDH assay (Figure 4.12). Percentage cell death was measured in cortical cultures that had undergone 2 hours of normoxia or OGD (in the presence of media control (n=3), DMSO (n=3), 0.1μM 3MA (n=6), 1μM 3MA (n=6), 10μM 3MA (n=6)) followed by 24 hours recovery. At 2 hours (Figure 4.12 (A)), there was a significant effect of OGD (p=0.0002) and treatment (p=0.0010) (two-way ANOVA). Tukey's multiple comparison test demonstrated significant differences between 10μM and all groups (media (p=0.0003), DMSO (p=0.0004), 0.1μM 3MA (p=0.0026), and 1μM (p=0.0301) in OGD samples (see Figure 4.12 (A)). At 2 hours and 24 hours recovery (Figure 4.12 (B)), there was a significant effect of OGD (p<0.0001) and treatment (p<0.0001) (two-way ANOVA). Tukey's multiple comparison test demonstrated significant differences between 10μM 3MA compared with media (p=0.0026), 0.1μM 3MA (p=0.0014) and 1μM 3MA (p=0.0253) in samples that had undergone normoxia. In OGD samples there were significant differences between 10μM 3MA and all groups (media, DMSO, 0.1μM 3MA, 1μM 3MA (p<0.0001)). There was a significant interaction between OGD and treatment at 2 hours (p<0.05) and 2 hours followed by 24 hours recovery (p<0.05). Increasing 3MA concentration causes increased cell death in a dose dependent fashion with greater levels of cell death following OGD conditions. Therefore inhibiting autophagy appears to have neurotoxic effects following OGD.

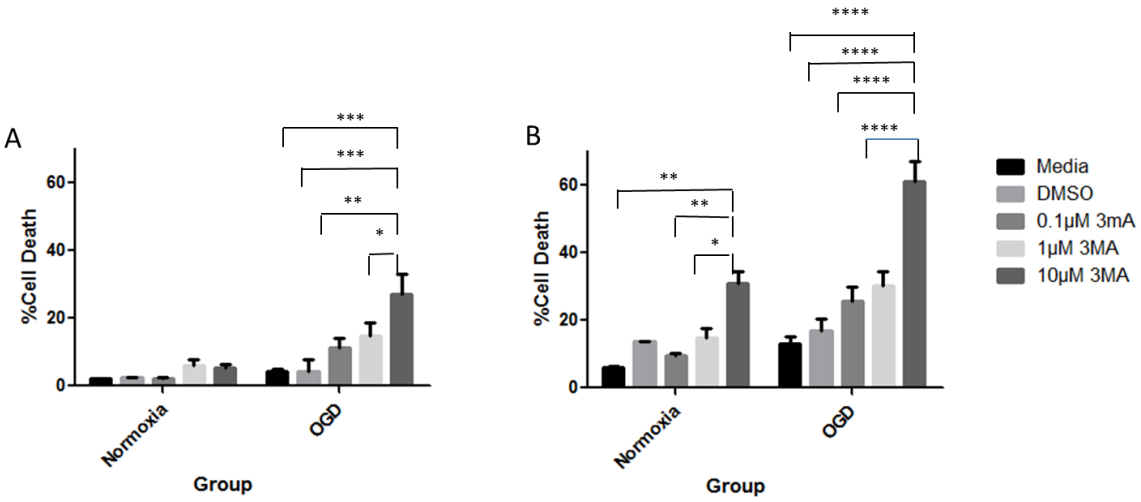

Figure 4.12 Effect of 3MA treatment during OGD Cell death was quantified by LDH assay. (A) Following 2 hours OGD there was a significant effect of OGD and treatment with augmented cell death with increasing concentrations of 3MA. (B) Following 2 hours normoxia and OGD followed by 24 hours recovery there was a significant effect of OGD and treatment with enhanced cell death with increasing concentrations of 3MA. **p*<0.05, ***p*<0.01, ****p*<0.001, *****p*<0.0001

Post treatment with 3MA after OGD

The effect of various doses of 3MA on neuron viability was measured using an LDH assay in cortical cultures that had undergone 2 hours of normoxia or OGD followed by 24 hours recovery (Figure 4.13). Post-treatment recovery media contained control (media only) (n=3), DMSO (n=3), 0.1µM 3MA (n=3) or 10µM 3MA (n=3). In cortical neurons (Figure 4.13), there was a significant effect of OGD (p<0.0001) and treatment (p<0.0001) (two-way ANOVA). Tukey's multiple comparison test demonstrated in cells that all treatment groups had greater cell death during the recovery period compared to media following 2 h normoxia (DMSO (p=0.0016), 0.1µM 3MA (p=0.0163) and 10µM 3MA (p<0.0001) or 2h OGD (DMSO (p=0.0029), 0.1µM 3MA (p=0.0038) and 10µM 3MA (p<0.0001)). In addition, 10µM 3MA had significantly more cell death during the recovery period following 2 h normoxia (DMSO (p<0.0001) and 0.1µM 3MA (p<0.0001) and 2 h OGD (DMSO (p<0.0001) 0.1µM 3MA (p<0.0001). There was a significant interation between OGD and treatment (p<0.01).

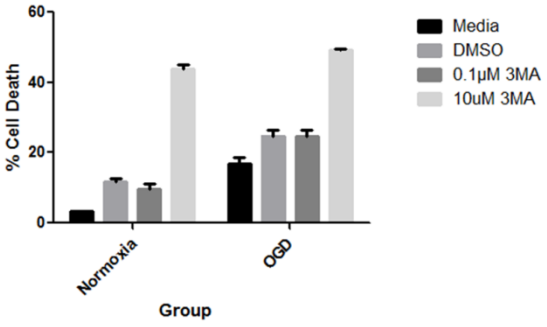

Tukey's multiple comparisons test

Normoxia	
Media vs. DMSO	**
Media vs. 0.1µM 3MA	*
Media vs. 10µM 3MA	****
DMSO vs. 10µM 3MA	****
0.1µM 3MA vs. 10uM 3MA	****
OGD	
Media vs. DMSO	**
Media vs. 0.1µM 3MA	**
Media vs. 10µM 3MA	****
DMSO vs. 10µM 3MA	****
0.1µM 3MA vs. 10µM 3MA	****

Figure 4.13 Effect of 3MA treatment 24 hours after OGD Cell death was quantified by LDH assay. There was a significant effect of OGD and treatment with augmented cell death with increasing concentrations of 3MA.*p<0.05, **p<0.01, ****p<0.0001.

4.5.2.2.2 Metformin

Metformin is drug in wide clinical use mainly for type 2 diabetes. It has been shown to activate autophagy via a number of mechanisms and so will be used as a tool to induce autophagy while being a widely used agent clinically.

Treatment with metformin during OGD

The effect of a dose response of metformin on cortical neuron viability was assessed using an LDH assay (Figure 4.16). Percentage cell death was measured in cortical cultures that had undergone 2 hours of normoxia or OGD (in the presence of media control (n=3), DMSO (n=6), 20 μM metformin (n=9), 200 μM metformin (n=9), 500 μM metformin (n=9)), followed by 24 hours recovery. At 2 hours (Figure 4.16 (A)), there was a significant effect of OGD (p=0.0080) but no significant effect of treatment p=0.1182 (two-way ANOVA). At 2 hours and 24 hours recovery (Figure 4.16 (B)), there was a significant effect of OGD (p=0.0231) no significant effect of treatment (p=0.1432) (two-way ANOVA). There was no interaction between OGD and treatment at either timepoint.

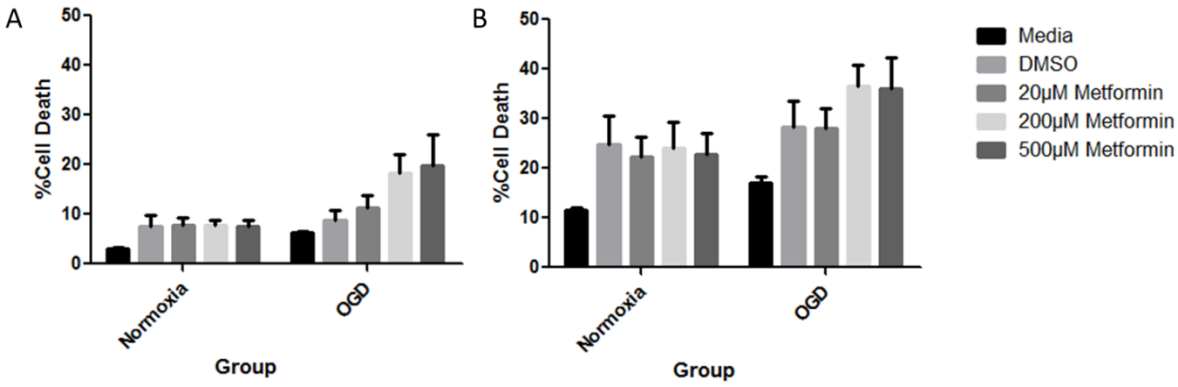

Figure 4.14 Effect of metformin treatment during OGD Cell death was quantified by LDH assay. (A) Following 2 hours OGD, there was a significant effect of OGD but not treatment. (B) Following 2 hours and 24 hours recovery there was a significant effect of OGD but not treatment.

Pre-treatment with metformin before OGD

The effect of various doses of metformin on neuron viability was measured using an LDH assay in cortical cultures that had undergone 2 hours of normoxia or OGD followed by 24 hours recovery (Figure 4.15). Pretreatment was administered 24 hours prior to normoxia or OGD: media (n=3), DMSO (n=3) and 50μM metformin (n=3) and 500μM metformin (n=3). At 2 hours (Figure 4.15 (A)), there was a significant effect of OGD (p<0.0001) and treatment (p<0.0001) (two-way ANOVA). Tukey's multiple comparison test demonstrated that 500μM metformin produced significantly more cell death than media (p<0.0001) and DMSO (p=0.0257) in the cells that had undergone OGD. 50μM metformin (p<0.0001) and DMSO (p<0.0001) also produced significantly more cell death than media. At 2 hours and 24 hours recovery (Figure 4.15 (B)), there was a significant effect of OGD (p<0.0001) and treatment (p<0.0001) (two-way ANOVA). Tukey's multiple comparison test demonstrated that 500μM metformin produced significantly more cell death than media (p<0.0001), DMSO (p<0.0001) and 50μM metformin (p<0.0001) in the cells that had undergone normoxic conditions. Following OGD conditions, post hoc testing demonstrated that 500μM metformin produced significantly more cell death compared to media (p<0.0001), DMSO (p<0.0001) and 50μM metformin (p<0.0001) and 50μM metformin (p=0.0022) and DMSO (p=0.0427) also produced significantly more cell death than media. There was a strong effect of interaction between OGD and treatment at both timepoints (p<0.0001).

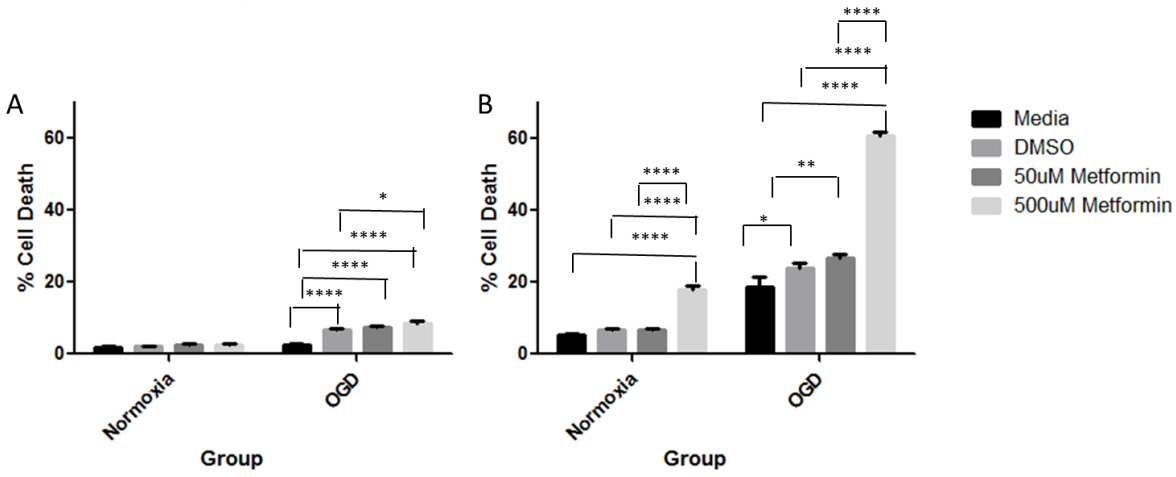

Figure 4.15 Effect of metformin treatment 24 hours before OGD Cell death was quantified by LDH assay. (A) At 2 hours there was a significant effect of OGD and treatment with 500μM metformin produced significantly more cell death. (B) Following 2 hours and 24 hours recovery there was a significant effect of OGD and treatment with 500μM metformin demonstrating significantly more cell death. *p<0.05, **p<0.01, ****p<0.0001

4.6 Discussion

Global ischaemia selectively induced hamartin expression in the membrane fraction of the CA3 region of the rat hippocampus which peaked at 12 hours of reperfusion and persisted at 24 hours (Chapter 3) and is thought to contribute to the endogenous neuroprotective phenomenon displayed by these neurons. One of the downstream mechanisms is autophagy which occurs due to the inhibition of mTOR by TSC. The role of autophagy in cerebral ischemia is contentious, with some studies showing that activation of autophagy is detrimental (Wen *et al.,* 2008; Zheng *et al.,* 2009) and others supporting a neuroprotective role (Carloni *et al.,* 2012; Wang *et al.,* 2012).

In vivo studies using beclin-1 (a component of the PI3K complex involved in the early stage of autophagosome formation, LC3 an indicator of autophagosome formation) and p62 (an indicator of flux through the pathway), demonstrated that at 3 hours following global cerebral ischaemia, early autophagosome formation is reduced in CA3 but is accompanied by an increase in autophagic flux. At 12 hours there was an increase in autophagosome formation in CA1 but a decrease in CA3, these were not accompanied by any changes in autophagic flux.

In vitro lentiviral experiments confirmed that productive autophagy was associated with increased neuronal survival as when hamartin was silenced, flux decreased through the autophagic pathway (an increase in p62) and cell death increased. When hamartin was overexpressed, flux increased through the autophagic pathway (a decrease in p62) and cell death decreased. Further *in vitro* experiments were used to pharmacologically probe autophagy specifically. Increasing 3MA (an autophagy inhibitor) concentration caused increased cell death in a dose dependent fashion with greater levels of cell death following OGD conditions. However, pre-treatment with metformin (an autophagy inducer) also increased cell death following normoxia or OGD.

4.6.1 *In vivo* time course

At 3 hours, beclin-1 expression was significantly lower in CA3 ischaemia compared to sham. This is consistent with a time course involving slice experiments showing that autophagy induction may not be detectable for 3 hours following OGD (Pérez-Rodríguez *et al.,* 2014). The preparation of slice cultures, however does involve

intrinsic stress so caution should be exercised when extrapolating these findings. The time course observed in this study does however appear to be corroborated by an *in vivo* study, using the 2VO model and hypotension where an increase in beclin-1 levels was not seen until 6-12 hours post ischaemia. It is not possible to directly compare this study with the results in this thesis as the investigators did not separate out the CA1 and CA3 regions of the hippocampus (Cui *et al.,* 2013). At the 3 hour time point, there was no difference in LC3 levels between any groups and p62 levels were significantly decreased in ischaemic CA3 regions compared to sham, which could be consistent with the time point being too early to detect autophagy or equally productive autophagy via a beclin-1 independent mechanism. The lower levels of p62 in the ischaemic CA3 region compared to CA3 sham region is indicative of either increased flux through basal autophagy or a lower level of autophagy taking place. There was no significant difference in beclin-1, LC3 or p62 expression when comparing CA1 sham and ischaemic regions which may indicate a time point too early to detect any autophagy changes, completely different level of basal autophagy or a fundamental difference in the process between areas of the hippocampus. It is known that upon induction of autophagy, microtubule-associated protein 1 light chain 3 (LC3) is processed from a 16-kDa form (LC3-I) to a 14-kDa form (LC3-II), which is recruited to autophagosomes and is an indicator of autophagosome formation (Klionsky *et al.,* 2008) and a ratio from two bands that appear is calculated to give an indication of activity. In these experiments, LC3 appeared as a single band at 16-18 KDa. A single band has however, been reported in the literature, using the same antibody (Schapansky *et al.,* 2014) and is likely a real result. The lack of a second band could be due to the antibody, the processing of samples or the point of the time course following ischaemia at which the samples were collected.

At 12 hours, no trend was observed for increased beclin-1 in the CA3 area of the hippocampus, which is what has been previously detected in the literature. Cui *et al.,* 2013, have shown that beclin 1 levels increased 6–24 hours following ischaemia ($p< 0.01$). A more comprehensive time course with later time points would be required to fully corroborate this. There was also a significant difference in beclin-1 levels between sham CA1 and CA3 regions, being lower in CA3 sham regions which again could demonstrate fundamental differences in the process of autophagy and the potential role for a beclin independent mechanism, equally this could also be an erroneous result as one would not expect any changes to be observed at any time point following sham surgery (no ischaemia). LC3 expression was significantly higher in the CA1 ischaemic region compared to CA1

sham region, leading to greater autophagosome formation but CA1 did not have any changes in flux as there was no difference between p62 expression levels. LC3 expression was significantly lower in CA3 ischaemic than sham regions which is in disagreement with Cui *et al.,* (2013), which showed an upregulation of the LC3-II/LC3-I starting at 3 hours ($p < 0.05$) and peaking at 12 hours in the hippocampus ($p < 0.01$). However, as CA1 and CA3 regions were not separated in their study, this could be consistent with expression as a whole. There was no significant difference in p62 levels at 12 hours. The two time points in this study were selected to take a hyperacute time point (differences in membrane expression of hamartin compared to the cytoplasm were clear at time 0 following global ischaemia (Chapter 3)) and a time point at which protein translation had a chance to occur (12 hours). It may be that altering the mechanism of productive autophagy at these time points is too early to have a beneficial effect as it may not have reached its full potential.

4.6.2 *In vitro*

4.6.2.1 Lentiviral experiments

LC3-II expression was significantly higher in TSC1 shRNA–transduced compared to control shRNA–transduced rat hippocampal cultures following both normoxia and OGD. As suppression of hamartin expression activated mTORC1 which should inhibit autophagy, these results suggested that autophagosome accumulation results from impaired autophagic flux (fusion and degradation of autophagosomes with lysosomes). Expression of sequestosome-1 (p62) protein, which is degraded by lysosomes and accumulates following impairments in autophagy, was significantly increased by suppression of hamartin compared to control shRNA–transduced rat hippocampal cultures following both normoxia and OGD. Further evidence for impaired autophagy was found by measuring lysosomal degradation of long-lived proteins during macroautophagy, by using the autophagy inhibitor 3MA to dissect the macroautophagy component of lysosomal activity. During normoxia, TSC1 shRNA–transduced neurons showed significantly less macroautophagy-dependent degradation (down 53 ± 10% as compared to control shRNA–transduced cultures), which was completely diminished after OGD. Therefore, suppression of hamartin expression results in the accumulation of autophagosomes and impaired autophagic flux both in normoxia and OGD in hippocampal neurons.

Overexpression of *Tsc1* in rat hippocampal neurons upregulated LC3-II expression, suppressed p62 expression by 44 ± 7% and increased 3MA-sensitive degradation by 340 ± 40% compared to GFP-transduced cultures after OGD, which was associated with increased neuronal survival. Inhibition of autophagy in rat TSC1-transduced cultures with 3MA abolished the protection conferred by overexpression of rat TSC1, reducing neuronal survival to 23 ± 2% from 47 ± 3% for untreated cultures overexpressing hamartin. Taken together, these findings suggest that overexpression of hamartin conferred protection of hippocampal neurons to OGD by inducing efficient autophagic flux.

In a recent study, loss of Tsc2 in neuronal cultures resulted in autophagic activity via AMPK-dependent activation of ULK1 on Ser^{555} resulting in autophagic flux and accumulation of autolysosomes (Di Nardo *et al.,* 2014). In addition, the group looked at brain tissues of the Tsc1c/c;NestinCre and the Tsc1c/c;L7Cre conditional knockout mice and cortical tubers from TSC patients finding a similar dysfunction of autophagy (Di Nardo *et al.,* 2014). Therefore the link between hamartin and autophagy appears to be critical for neuronal survival following cerebral ischaemia.

4.6.2.2 3MA

The drug 3MA is a selective inhibitor of the class III PI3K and indeed inhibits beclin-1-dependent autophagy in various disease models (Kihara *et al.,* 2001). Increasing 3MA concentration caused increased cell death in a dose dependent fashion with greater levels of cell death following OGD conditions when given at the time of normoxia and OGD and in the recovery period. This corroborates the protective effect of autophagy that has been seen in other studies. 3MA abolished the protective effect of IPC in a rat focal model (Sheng *et al.,* 2010) and in a neonatal model of hypoxia ischaemia in Sprague–Dawley rat pups, 3MA inhibition of rapamycin-induced autophagy resulted in cells dying in a necrotic fashion (Carloni *et al.,* 2008).Therefore, inhibition of autophagy with 3-MA appears to have neurotoxic effects.

4.6.2.3 Metformin

Metformin is widely used clinically for type 2 diabetes so the direct effect on neurons is very relevant in the context of stroke. Metformin results in pre-activation of AMPK-dependent autophagy in male Sprague-Dawley

rats using pMCAO (Jiang *et al.,* 2014). 100μM metformin administered to primary cortical neurons showed that it was neuroprotective (El-Mir *et al.,* 2008). Another study showed that 200 μM metformin was pharmacologically active in rodent hippocampal cells (Amato *et al.,* 2011). In this chapter, cell death was not reduced relative to control with treatment during OGD. Pre-treatment with metformin produced a significantly increased level of cell death in a dose dependent fashion suggesting that metformin may affect neurons in multiple ways depending on conditions. Metformin has a number of molecular mechanisms which could account for its divergent effects on neurons following OGD. Metformin has previously been demonstrated to afford neuroprotection by modulating inflammatory and antioxidant pathways via induction of AMPK (Ashabi *et al*., 2015). A recent study using tMCAO in mice has demonstrated that metformin reduces blood-brain barrier disruption via down-regulation of ICAM-1 (Liu *et al*., 2014). In addition, the anti-tumour effects of metformin in cancer are regulated by both AMPK-dependent or -independent mechanisms culminating in the inhibition of mTOR signalling. The mechanism of action for its primary clinical use is thought to be transient inhibition of the mitochondrial respiratory-chain complex 1, acutely decreasing hepatic glucose production (Rena *et al.,* 2013). In addition to effects on glucose metabolism, metformin also decreases microvascular and macrovascular complications of type 2 diabetes, reduces fatty liver and restores ovarian function in polycystic ovary syndrome (Rena *et al.,* 2013). An alternative autophagy inducer that could be used in future experiments is [4'-(N-diethylamino) butyl]-2-chlorophenoxazine (10-NCP), an Akt inhibitor which upregulated autophagy in a primary neuronal model of Huntington's disease (Tsvetkov *et al.,* 2010).

4.7 Conclusions

While hamartin overexpression leads to neuronal survival, pharmacological manipulation of autophagy has not yielded a specific target for therapy. There remains equipoise in the literature as to whether autophagy is beneficial or detrimental in the context of cerebral ischaemia. The results here show that autophagy appears to be in a state of flux at 3 hours which does not persist to 12 hours which varies between hippocampal regions (Table 4.1). Autophagy is a dynamic process that shows changes over time and space within the experimental paradigms tested. Understanding the key to the mechanism that makes autophagy protective at certain times and detrimental at others is pivotal in understanding endogenous neuroprotection. Hamartin may confer

neuroprotection against ischaemia by inducing autophagy however, the time course examined in this thesis has not demonstrated the point of intervention where inducing productive autophagy through an as yet undefined mechanism increases cell survival. Autophagy is an incredibly dynamic process and would require monitoring at much more frequent intervals to fully elucidate its role. Indeed, if autophagy is the underlying explanation for neuroprotective phenomena such as hypothermia, this would make sense as interventions after 6 hours become much less effective (Colbourne *et al*., 1999). However, evidence from this thesis has shown that manipulating autophagy with specific modulators has not replicated the neuroprotective effect demonstrated by hamartin (Table 4.2). There is however, a link between autophagy and ER stress and indeed both are downstream of hamartin and mTOR. As a result, the ER stress pathway is further considered in Chapter 5.

Autophagy Protein	**3 hours**	**12 hours**
Beclin-1	Decreased levels in CA3 ischaemia compared to CA3 sham	No difference in levels
LC3	No difference in levels	Decreased levels in CA3 ischaemia compared to CA3 sham
p62	Decreased levels in CA3 ischaemia compared to CA3 sham	No difference in levels

Table 4.1 *In vivo* summary of results

Drug	**Function**	**Summary of treatment effect**
Metformin	Autophagy inducer	Pre: **Increased neuronal death** (normoxia and OGD) During: No effect
3MA	Autophagy inhibitor	During: **Increased neuronal death** (normoxia and OGD) Post: **Increased neuronal death** (normoxia and OGD)

Table 4.2 In vitro summary of results

Chapter 5: ER stress and hamartin's endogenous protective mechanism

5.1 Executive summary

The ER is responsible for protein folding within the cell. Under conditions of stress, where the build-up of proteins exceeds the capacity of the machinery, a stress response occurs. Modulation of the ER stress response as a downstream action of TSC has been postulated with links to autophagy also suggested.

In this thesis, *in vivo* studies demonstrated a significant attenuation of the ER stress response in CA3 ischaemic regions compared to sham regions at 3 hours post global ischaemia. At 12 hours post global ischaemia, there was a significantly increased ER stress response in CA1 regions compared to sham regions. This could partially explain the selective vulnerability within the hippocampus and associated with the endogenous protective response of hamartin.

In vitro experiments failed to demonstrate neuroprotection with an ER stress inhibitor or small doses of an ER stress inducer prior to 2 hours of OGD, in fact these showed neurotoxicity. Due to described links between ER stress and autophagy, an ER stress inhibitor and autophagy inducer were tried in combination and it was found that autophagy induction could prevent the neurotoxic effects of the ER stress inhibitor.

Further studies are required to ascertain when ER stress becomes detrimental to neurons and whether modulation of ER stress pharmacologically is a viable therapeutic strategy for cerebral ischaemia.

5.2 Background

Physiologically, the endoplasmic reticulum (ER) is responsible for folding proteins in the cell. Under pathophysiological conditions, for example an ischaemic insult, the protein-folding machinery in the cell is overwhelmed and misfolded proteins accumulate, triggering a stress response. The unfolded protein response (UPR) is a homeostatic mechanism by which cells regulate levels of misfolded proteins in the ER. It has three specialized stress sensors located at the ER membrane: inositol-requiring enzyme 1 (IRE1), activating transcription factor 6 (ATF6) and protein kinase RNA-like ER kinase (PERK) (Figure 1.10).

5.2.1 ER stress and mTOR

TSC has been implicated in neuronal stress responses, as neurons lacking TSC have increased vulnerability to ER stress-induced cell death via the activation of the mitochondrial death pathway (Di Nardo *et al.,* 2009). With loss of TSC function, there is uncontrolled mTOR hyperactivation that results in an increase in protein synthesis and ROS production. This overloads the cellular machinery resulting in ER and oxidative stress responses which induce CHOP and hemeoxygenase-1 (HO-1) (Di Nardo *et al.,* 2009). In a study using MEFs (mouse embryonic fibroblasts), cells with mutations in either TSC1 or TSC2 are hypersensitive to ER stress and undergo apoptosis (Kang *et al.,* 2011). In the absence of TSC, greater cell death is observed in response to ER stress and so mTOR inhibition is a possible strategy to curb ER stress.

5.2.2 ER stress and autophagy

Like autophagy, ER stress is also finely balanced. Significant ER stress involving GADD153/CHOP and CASP12/caspase 12 activation are detrimental to the cell (Nakagawa et al., 2000; Hetz et al., 2006). In addition to condemning cells to die via an apoptotic pathway, there is emerging evidence that ER stress activation can lead to autophagy (Yorimitsu *et al.,* 2006; Sakaki and Kaufman, 2008). If the ER experiences a perturbation in homeostasis that is not salvageable by the UPR, autophagy and cell death ensue.

Mild ER stress however, (or 'preconditioning') leads to preferential activation of the X box binding protein (XBP1) resulting in cellular protection (Lin *et al.,* 2007; Mendes *et al.,* 2009). The mechanism underlying this protective effect is thought to be due to autophagy (Bernales *et al.,* 2006). Using *Drosophila* and mouse models of Parkinson disease, it has recently been demonstrated that mild ER stress is neuroprotective via autophagy (Fouillet *et al.,* 2012). A mechanism was proposed whereby caspase-8 regulates an ATG7-beclin 1 programme of cell death (Yu *et al.,* 2004). There is a link with ER stress as autophagy induced by IPC reduces apoptosis by suppressing excess ER stress during the subsequent ischaemia (Sheng *et al.,* 2012). This benefit is abolished by the ER stress inhibitor salubrinal (Gao *et al.,* 2013). This phenomenon of the protective effect of ER stress induced autophagy is also observed in the heart (Petrovski *et al.,* 2011).

5.2.3 ER stress following ischaemia

ER stress is activated following cerebral ischaemia. In a rodent cardiac arrest model (10 min global brain ischemia and four hours reperfusion), PERK activation and downstream eIF2α phosphorylation inhibited protein synthesis although there was no concomitant increase in downstream CHOP or ATF4. In addition, the other two pathways in the UPR, IRE1 and ATF6 were not activated (Kumar *et al.,* 2003). Using 8 minutes of global brain ischaemia via bilateral carotid occlusion and hypotension it was demonstrated that PERK activation and downstream phosphorylation of eIF2α was unrelated to nascent protein load in the ER, potentially suggesting that an alternative method other than the UPR was responsible for activating PERK (Sanderson *et al.,* 2010). A decrease in cellular energy status (depleted of ATP) stimulates PERK and eIF2alpha phosphorylation in pancreatic beta cells, independently of both unfolded proteins in the ER and IRE1 (Gomez *et al.,* 2008). The absence of the canonical ER stress response in neurons and lack of IRE1 and ATF6 transcription factor initiation may tip the balance in favour of cell death (Sanderson *et al.,* 2015). The UPR temporarily slows accumulation of new proteins in the ER lumen, at the same time as up-regulating transcription of genes for ER resident chaperones and enzymes that ablate the effects of ER stress (Kumar *et al.,* 2003). If however, this machinery is overwhelmed by proteins created as a result of the ischaemic insult, cell death ensues.

5.2.4 ER stress protein expression in the hippocampus

Learning and memory a key hippocampal function involves the important ER stress proteins, eIF2α and ATF4. Phosphorylation of eIF2α results in a generalized attenuation of translation and selective expression of ATF4, which promotes the inhibition of cyclic AMP-responsive element-binding protein (CREB) and, as a consequence, reduced expression of synaptic plasticity and memory genes. (Hetz and Mollereau, 2014).

Using a five minute global brain ischemia model in wild-type and copper/zinc superoxide dismutase (SOD1) transgenic rats, Hayashi *et al.,* (2003) found that phosphoeIF2α and phosphoPERK were increased in CA1 neurons in the wild-type, rather than in the transgenic animals. They link production of ROS with modification of ER stress protein and implicate ER stress in neuronal cell death. Roberts *et al.,* (2007) carried out a 2VO/HT model (10 minutes) in rats with non-ischaemic controls (NIC); (sham operated but no carotid clamping and blood

withdrawal) and reperfusion durations (10 minutes - 72 hours). Following microdissection and homogenisation of CA1 and CA3 the ER stress response was found to be stronger in CA1 than CA3. Current literature would suggest that expression levels of ER stress proteins are likely to be higher in CA1 than CA3 following ischaemia which could possibly be associated with their differential survival following an ischaemic insult.

5.2.5 Pharmacological manipulation of ER Stress

5.2.5.1 Inducer of ER Stress: Thapsigargin

Thapsigargin (Figure 5.1) is an ER stress inducer that functions by blocking Ca^{2+} ATPase. Release of calcium stores could be responsible for excitotoxic cell death (Szydlowska and Tymianski, 2010). During calcium-induced calcium release, the sarcoplasmic/endoplasmic reticulum calcium ATPase (SERCA) pump sends calcium into the ER. It is released back into the cytosol by the inositol trisphosphate receptor (IP3R or ITPR) in response to extracellular signals, and by the ryanodine receptors (Roussel *et al.,* 2013). Thapsigargin inhibits the SERCA pump and is used to induce ER stress experimentally (Nguyen *et al.,* 2002). In a study investigating the neurotoxicity of agents that disrupt calcium homeostasis in E18 rat cortical neurons, thapsigargin was applied at 0.001-1 μM (Ringler *et al.,* 2008) which formed the basis for the concentrations used in this thesis.

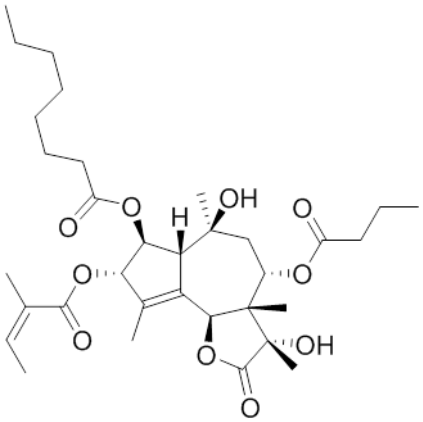

Figure 5.1 Chemical structure of thapsigargin

The effect of thapsigargin on neuronal survival appears to be dose-dependent. Thapsigargin (TG) was intracerebroventricularly injected prior to MCAO and 24 hours post-surgery, Thapsigargin within the range of 2 to 20 ng was shown to reduce the brain infarct. Maximal protection was achieved at 20 ng, but 200ng was

detrimental. The protective mechanism postulated involved ER-stress reduced PARK2-dependent mitophagy (Zhang *et al.,* 2014b).

5.2.5.2 Inducer of ER Stress: Tunicamycin

Tunicamycin (Figure 5.2) is an ER stress inducer and inhibits of N-glycosylation. In a study using E18 neuronal cultures from Wistar rats, investigating the protective effects of S-allyl-L-cysteine against ER stress, tunicamycin was used at 10 µg/mL (11.9 µM) (Imai *et al*., 2014) which formed the basis for the doses selected in this thesis.

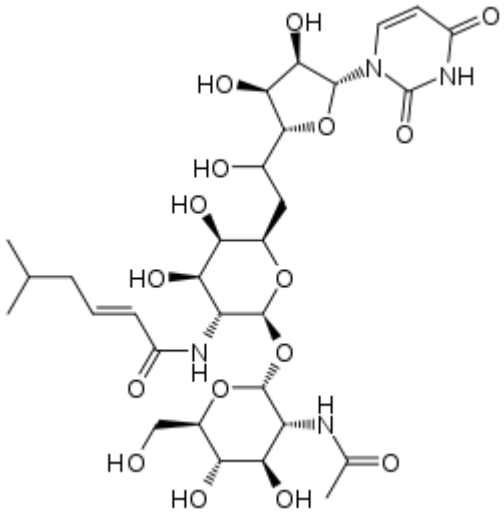

Figure 5.2 Chemical structure of tunicamycin

Again, the effect of tunicamycin on neuronal survival is conflicting. Tunicamycin (0.3-3 µg) has also shown protection of the brain by intracerebral injection prior to MCAO with maximal protection achieved at 3µg but 30µg was detrimental. As with thapsigargin (section 5.6.1), the protective mechanism postulated involved ER-stress induced PARK2-dependent mitophagy (Zhang *et al.,* 2014b).

5.2.5.3 Inhibitor of ER Stress: Salubrinal

Salubrinal (Figure 5.3) is a small molecule ER stress inhibitor that prevents formation of GADD34/PP1 complex therefore reducing the dephosphorylation of phosphoeIF2α (Boyce *et al.,* 2005). Salubrinal has been used experimentally and decreased neuronal death in rodent models of excitotoxicity, epilepsy and focal ischemia (Sokka *et al.,* 2007; Nakka *et al.,* 2010). Salubrinal was found to be protective against cytotoxic neuronal injury in E17 rat hippocampal neurons when used at 50 μM and also in vivo in a rat model using glutamate receptor stimulation via kainite (Sokka *et al.,* 2007).

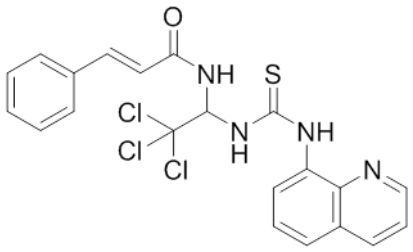

Figure 5.3 Chemical structure of salubrinal

While inhibiting ER stress may reduce neuronal cell death, in isolation it may not provide overall neuroprotection to the brain and salubrinal may have other effects aside from inhibition of ER stress. In a study looking at β-amyloid-induced neuronal death and microglial activation in E17 primary rat neurons, salubrinal used at concentrations 25, 50 and 100μM attenuated cell death by inhibiting NF-κB pathway rather than inhibition of ER stress (Huang *et al*., 2011). However, salubrinal could have detrimental effects. The inhibition of ER stress induced autophagy as a protective mechanism was abolished in the presence of salubrinal using an *in vivo* focal rodent stroke model (Gao *et al.,* 2013).

5.2.5.4 Pharmacology summary

From the literature it has emerged that ER stress is a complex process. Mild ER stress can be neuroprotective and this mechanism may involve autophagy. Excess ER stress is detrimental to the cell and apoptotic cell death ensues. Therefore the compounds that act on this pathway may have dose dependent effects and their effects

may depend on the extent of ER stress. Indeed, by inducing a small amount of ER stress, thapsigargin and tunicamycin may be neuroprotective. Salubrinal may be neurotoxic by virtue of inhibiting protective mild ER stress. As the link between ER stress and autophagy is highly complex, an autophagy inducer, metformin (see section 4.2.6.2) was also used in combination with an ER stress inhibitor to ascertain if there are any synergistic beneficial effects not observed in these compounds when used alone.

5.3 Aims of this chapter

The aim of this chapter is to investigate ER stress as a downstream mechanism for hamartin's neuroprotective effect.

1. Aim to determine the temporal profile of ER stress-related protein expression *in vivo:* following global ischaemia in CA1 and CA3 areas of the hippocampus.

2. Aim to pharmacologically manipulate ER stress *in vitro* following ischaemia and to mimic the neuroprotection mediated by hamartin and to ascertain a potential link with autophagy.

5.4 Materials and Methods

All materials were obtained from commercial suppliers unless otherwise stated in the text. There are several methods in this chapter which are common to other chapters in the thesis. Where the methods appear in another chapter in full, this is indicated below.

5.4.1 *In vivo*

5.4.1.1 Global Forebrain Ischemia

This method is described in Chapter 3, section 3.4.1.2.

5.4.1.2 Terminal anaesthesia and brain microdissection

The reperfusion timepoints used following 10 minutes global ischaemia in this chapter were 3 and 12 hours, the same time points used for *in vivo* Chapter 4.

This method is described in Chapter 3, section 3.4.1.2

5.4.1.3 Whole Cell Homogenisation

This method is described in Chapter 3, section 3.4.1.4

5.4.1.4 Protein Assay

This method is described in Chapter 3, section 3.4.1.5

5.4.1.5 Identification of proteins

This method is described in Chapter 3, section 3.4.1.6

5.4.1.5.1 Electrophoresis

This method is described in Chapter 3, section 3.4.1.6.1

5.4.1.5.2 Quantification of loading

This method is described in Chapter 3, section 3.4.1.6.2

5.4.1.5.3 Western Blotting

This method is described in Chapter 3, section 3.4.1.6.3

5.4.1.5.4 Antibody reagents for immunoblotting (IB)

Primary antibodies used in this chapter were: anti-rabbit to ATF4/CREB-2 (C-20) (sc-200, Santa Cruz), 1:600, and anti-rabbit to phosphoeIF2alpha (Ser^{51}) 1:1000 (9721, Cell Signalling).

5.4.2 *In vitro:*

5.4.2.1 Cell Culture

The method of cell culture of hippocampal and cortical neurons from E18 rats is described in Chapter 3, section 3.4.2.1.

5.4.2.2 Oxygen glucose deprivation

This method is described in Chapter 3, section 3.4.2.2.

5.4.2.3 Cell death assays

This method is described in Chapter 3, section 3.4.2.3.

5.4.2.4 Pharmacology

All stock solutions were prepared in DMSO. Metformin (see section 4.6.2.4), stock 25mM (used at 20μM, 200μM and 500μM) for combination experiments. Thapsigargin (Sigma), stock 500 μM (used at concentrations of 0.001μM, 0.01μM, 0.1μM, 1μM and 10μM). Tunicamycin (Sigma), stock 5mM (used at concentrations of 0.01μM, 0.1μM and 1μM). Salubrinal (Santa Cruz Biotechnology) stock 5mM (used at concentrations of 25μM, 50μM and 100μM). Timings of drug administration were: 'pre-treatment' 24 hours prior to 2 hours OGD or

normoxia, during the 2 hour OGD or normoxia period, or 'post treatment' in the recovery media only for 24 hours following the 2 hour OGD or normoxia period.

5.4.3 Statistical analyses

Statistical analysis was carried out with GraphPad Prism 5 using a two-tailed Student's t-test if two groups were compared, one-way ANOVA with Bonferroni's multiple comparisons post hoc test for comparisons of more than two groups and two-way ANOVA with Tukey's multiple comparisons post hoc test when two independent variables were assessed. Differences were considered significant for $p < 0.05$. Data are presented as mean $\pm$ SEM.

5.5 Results

5.5.1 *In vivo*

5.5.1.1 Method development- Effect of sham procedure on ER Stress

A validation experiment was conducted to verify that the sham or vertebral cauterization step of the global model of ischaemia did not significantly affect ER stress levels. Four groups were tested: sham (anaesthesia, vertebral cauterization, common carotid artery manipulation but no occlusion); naïve (no procedure, just anaesthesia); sham without vertebral cauterization (anaesthesia, no vertebral cauterization, common carotid artery manipulation but no occlusion); and 4 vessel occlusion ischaemia (anaesthesia, veretebral cauterisation, common carotid artery occlusion for 10 minutes). All brains were assessed at 3 hours reperfusion. Measurement of PhosphoeiF2α at 3 hours post global ischaemia in CA3 revealed no significant difference between sham, naïve or sham without the vertebral cauterization step (p= 0.4533) (one-way ANOVA). The levels of the ER stress protein phosphoeiF2α observed at 3 hours following sham or global ischaemia are independent of the vertebral cauterisation step of the global model of ischaemia.

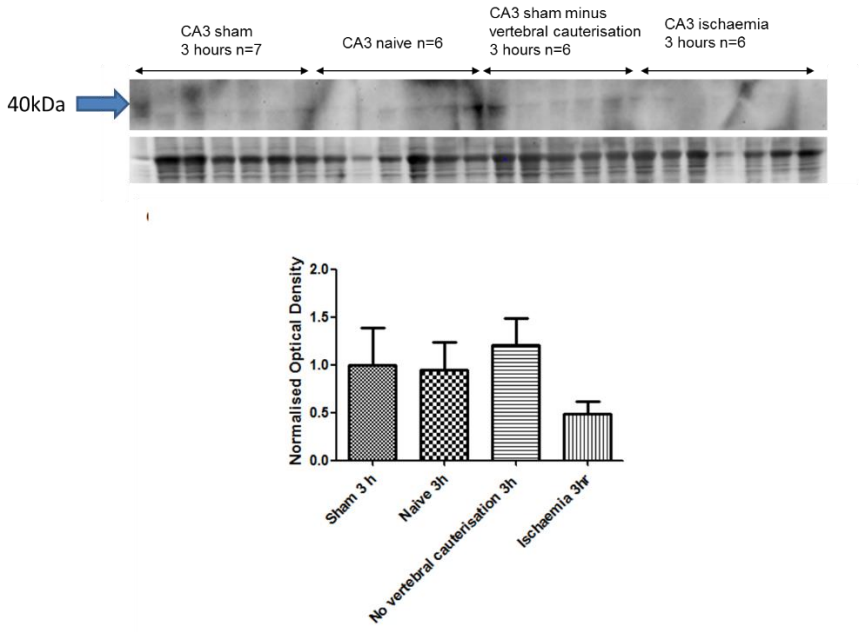

Figure 5.4: Effect of sham procedure on ER Stress protein expression Groups: sham (anaesthesia, vertebral cauterisation with common carotid artery manipulation, no occlusion n=7), naïve (no procedure, just anaesthesia n=6), sham without vertebral cauterization (anaesthesia, common carotid artery manipulation, no occlusion and no vertebral cauterization n=6), and 4 vessel occlusion ischaemia (anaesthesia, veretebral cauterisation, common carotid artery occlusion for 10 minutes), n=6). There was no significant difference of any group compared to ischaemia. 3 hours reperfusion.

5.5.1.2 ER stress time course: 3 hours post global forebrain ischaemia

To examine the role of ER stress in the endogenous resistance of CA3 neurons to global ischaemia, CA1 and CA3 areas of the hippocampus were dissected following 10 minutes of global cerebral ischaemia and an initial reperfusion time of 3 hours. *ATF4 and* phosphoeiF2α protein expression was used to assess ER stress levels.

Expression levels of ATF4 (CREB 2)

There was no significant difference in ATF4 (CREB 2) expression between CA1 sham and CA1 ischaemia (p=0.1106) (Figure 5.5 C) or between CA1 sham and CA3 sham (p=0.6343) (Figure 5.5 D) after 10 minutes of global ischaemia followed by 3 hours of reperfusion. There were significantly lower ATF4 (CREB 2) levels in CA3 at 3 hours following ischaemia compared to sham (Figure 5.5 B, E) (p=0.0396).

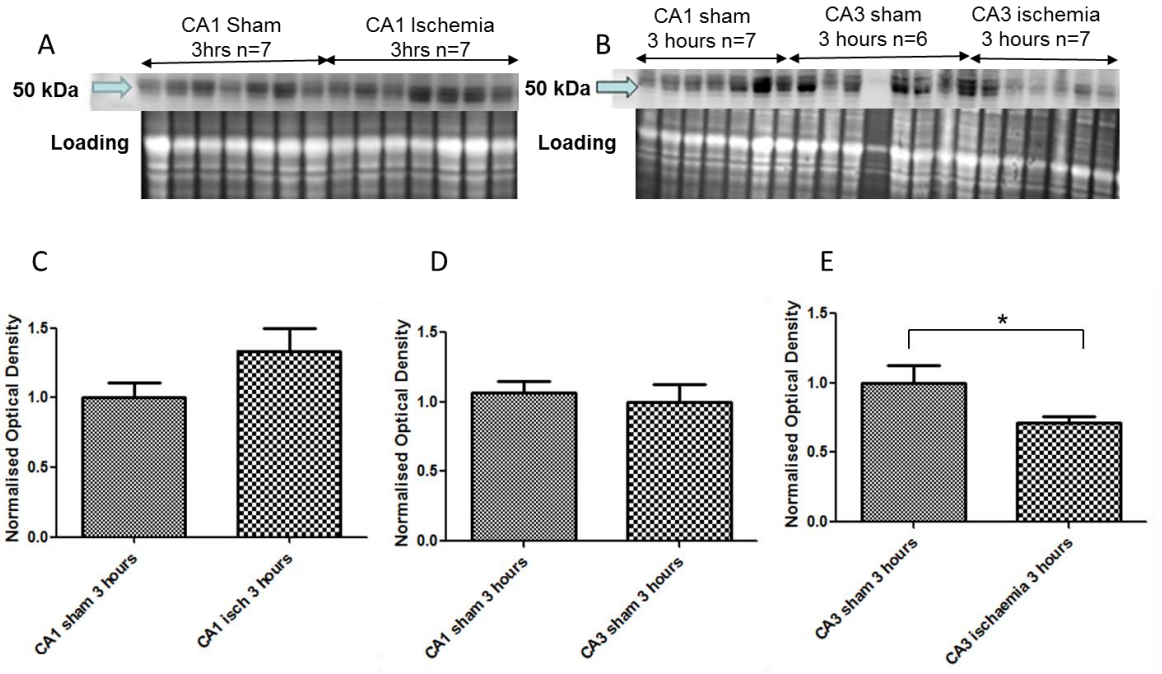

Figure 5.5: ATF4 (CREB 2) expression at three hours following 10 minutes of 4-VO Upper panels (A) and (B) show the western blots and loading correction with SYPRO® used to produce the graphs (C), (D) and (E) below of normalised ATF4 (CREB 2) immunoreactivity. (C) There was no significant difference in expression levels of ATF4 between CA1 sham and CA1 ischaemia. (D) There was no significant difference in expression levels of ATF4 between CA1 sham and CA3 sham. (E) There were significantly lower ATF4 (CREB 2) levels in CA3 at 3 hours following ischaemia compared to sham. Molecular weight of ATF4 (CREB 2): 50 kDa. * $p < 0.05$.

Expression levels of Phosphoeif2α

There was no significant difference in phosphoeif2α expression between CA1 sham and CA1 ischaemia (p=0.8053) (Figure 5.6 C) or between CA1 sham and CA3 sham (p=0.0597) (Figure 5.6 D) after 10 minutes of global ischaemia followed by 3 hours of reperfusion. There were significantly lower phosphoeif2α levels in CA3 at 3 hours following ischaemia compared to sham (Figure 5.6 C) (p=0.0206) (Figure 5.6E).

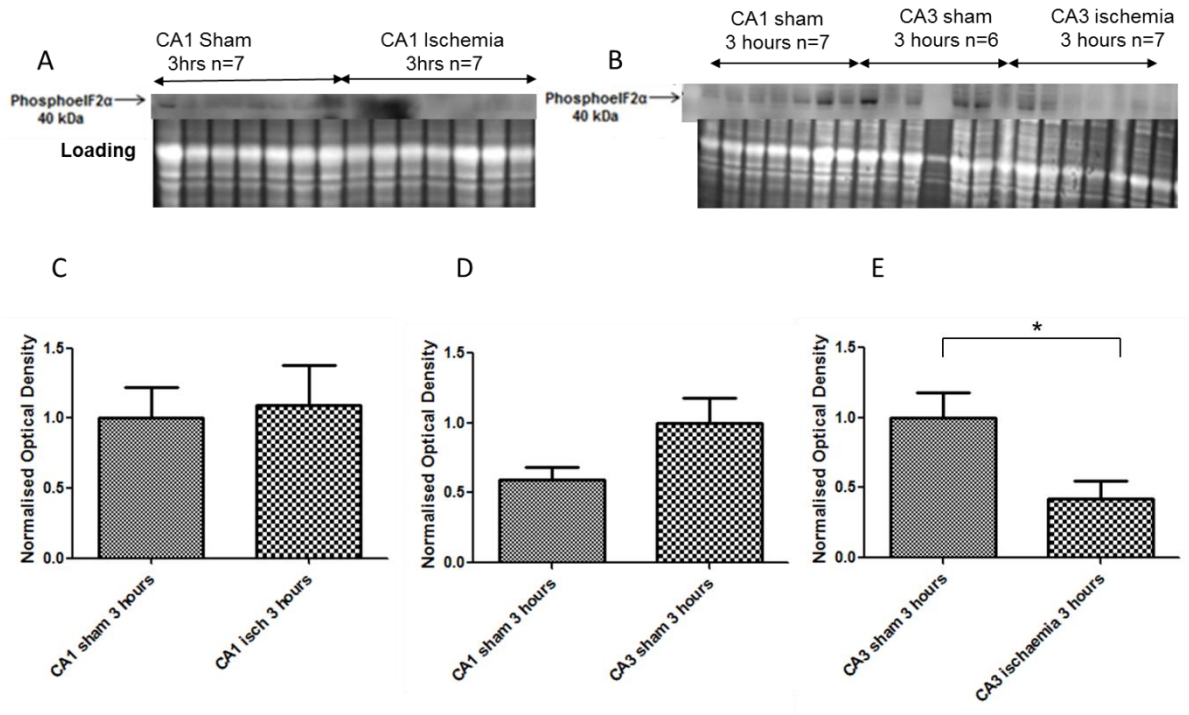

Figure 5.6: Phosphoeif2α expression at three hours following 10 minutes of 4-VO Upper panels (A) and (B) show the western blots and loading correction with SYPRO® used to produce the graphs (C), (D) and (E) below of normalised phosphoeif2α immunoreactivity. (C) There was no significant difference in expression levels of phosphoeif2α between CA1 sham and CA1 ischaemia or (D) CA1 sham and CA3 sham. (E) There were significantly lower phosphoeif2α levels in CA3 at 3 hours following ischaemia compared to sham. Molecular weight of Phosphoeif2α: 40 kDa. * $p < 0.05$.

5.5.1.3 ER stress time course: 12 hours post global forebrain ischaemia

Expression Levels of ATF4 (CREB2)

There was no significant difference in ATF4 expression between CA1 sham and CA3 sham (p=0.6403) nor CA3 sham and CA3 ischaemia (p=0.6158) at 12 hours timepoint. There were significantly higher ATF4 (CREB 2) levels in CA1 at 12 hours following ischaemia compared to sham (Figure 5.7 C) (p=0.0142).

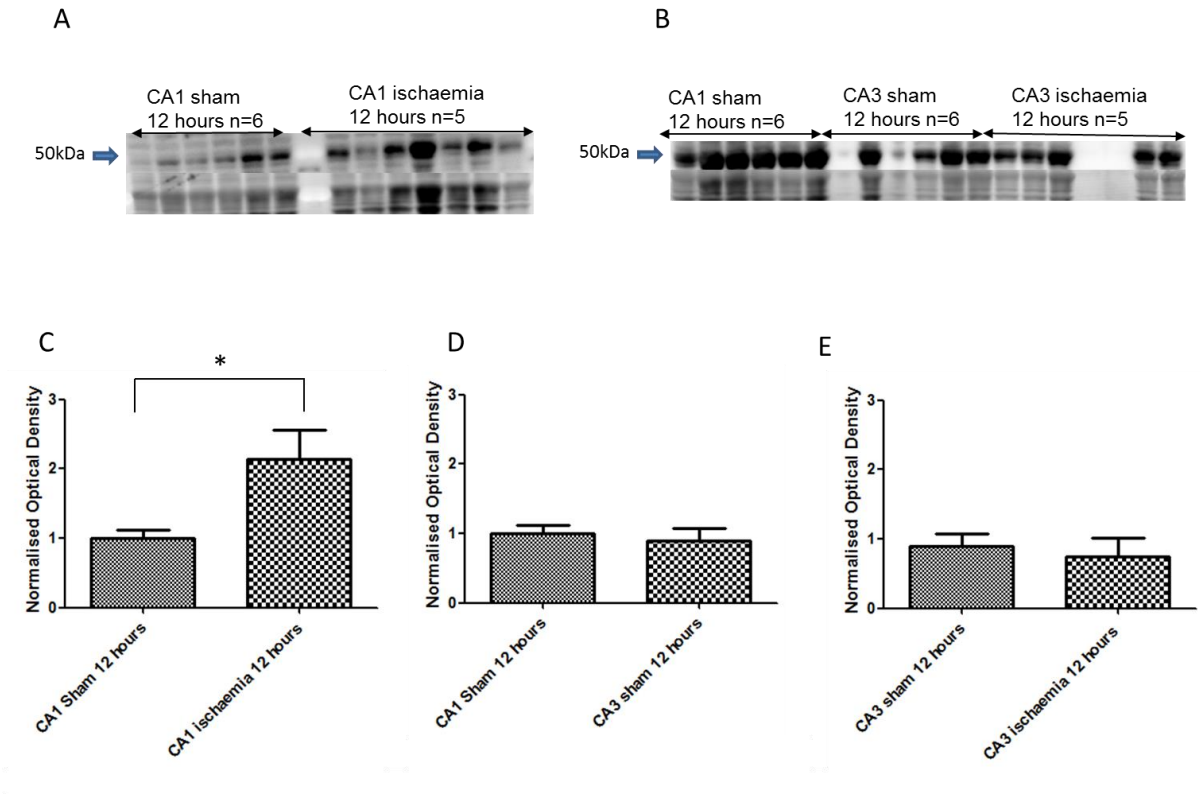

Figure 5.7: ATF4 (CREB 2) expression at 12 hours following 10 minutes of 4-VO Upper panels (A) and (B) show the western blots and loading correction with SYPRO® used to produce the graphs below of normalised ATF4 (CREB 2) immunoreactivity (C), (D) and (E). There were significantly higher ATF4 (CREB 2) levels in CA1 at 12 hours following ischaemia (n=5) compared to sham (n=6) (C). There is no significant difference between CA1 sham and CA3 sham (D) and CA3 sham and CA3 ischaemia (E). Molecular weight of ATF4 (CREB 2): 50 kDa. * $p < 0.05$.

Expression levels of Phosphoeif2α

There was no significant difference in phosphoeif2α expression between CA1 sham and CA3 sham (p= 0.2023) nor CA3 sham and CA3 ischaemia (p=0.9042) at the 12 hour timepoint. There were significantly higher phosphoeif2α levels in CA1 at 12 hours following ischaemia compared to sham (Figure 5.8 B) (p=0.015).

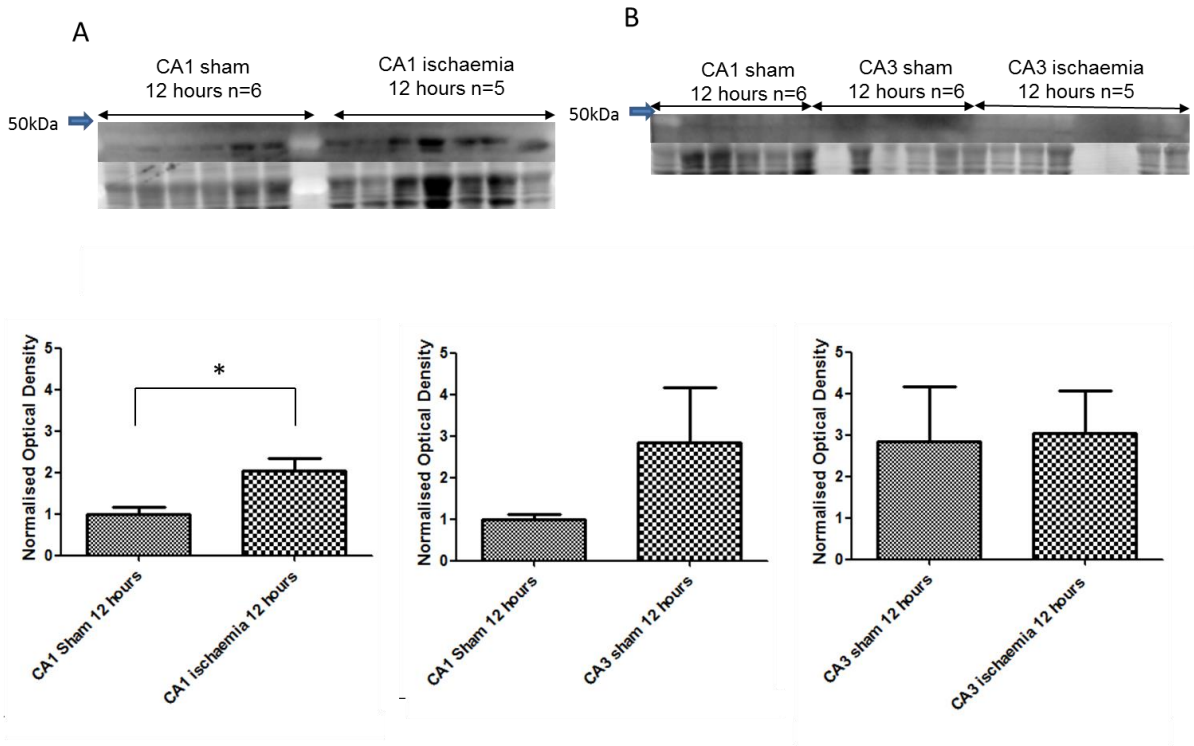

Figure 5.8: Phosphoeif2α expression at 12 hours following 10 minutes of 4-VO Upper panels (A) and (B) show the western blots and loading correction with SYPRO® used to produce the graphs (C), (D) and (E) below of normalised phosphoeif2α immunoreactivity. There were significantly higher phosphoeif2α levels in CA1 at 3 hours following ischaemia (n=5) compared to sham (n=6) (C). There was no significant difference between CA1 sham and CA3 sham (D) and CA3 sham and CA3 ischaemia (E). Molecular weight of Phosphoeif2α: 40 kDa. * $p < 0.05$.

5.5.1.4 Summary of *in vivo* studies

At 3 hours following global ischaemia (Figure 5.9), CA3 had reduced ER stress levels compared to sham while there was no change in CA1. At 12 hours following global ischaemia, CA1 had increased ER stress levels. while levels in CA3 had returned to sham levels. These data suggest that early (3 hour) reduction of ER stress is associated with protection in CA3 cells while an increase in ER stress 12 hours after the insult is associated with increased cell death in CA1 cells.

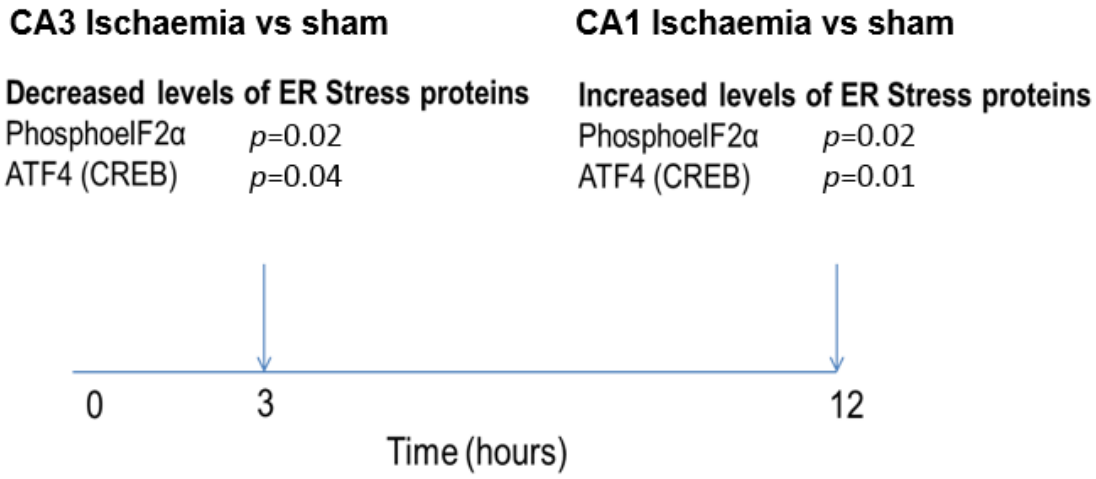

Figure 5.9 Timecourse of protein expression for markers of ER stress following 4-VO

5.5.2 *In vitro*

5.5.2.1 ER stress inducers

5.5.2.1.1 Thapsigargin

Thapsigargin is an ER stress inducer that blocks Ca^{2+} ATPase, triggering Ca^{2+} release and activating ER stress.

Treatment with thapsigargin during OGD

The effect of a dose response of thapsigargin on cortical neuron viability was assessed using an LDH assay (Figure 5.10). Percentage cell death was measured in cortical cultures that had undergone 2 hours of normoxia

or OGD in the presence of DMSO (n=9), 0.001µM thapsigargin (n=3), 0.01µM thapsigargin (n=6), 0.1µM thapsigargin (n=6), 1µM thapsigargin (n=6) or 10µM thapsigargin (n=3) followed by 24 hours recovery. At 2 hours (Figure 5.10 (A)), there was a significant effect of OGD (p< 0.0001) and treatment (p< 0.0001) (two-way ANOVA). Tukey's Multiple Comparison Test demonstrated significant differences in cell death between groups following 2 hours of OGD, with the highest concentration of thapsigargin leading to substantial neurotoxicity (for specific group differences and p-values, see Figure 5.10 A).

At 2 hours and 24 hours recovery (Figure 5.10 (B)), there was a significant effect of OGD (p<0.0001) and treatment (p<0.0001) (two-way ANOVA). Tukey's Multiple Comparison Test demonstrated in cells that had remained in normoxic conditions 10µM thapsigargin caused significantly more cell death than other groups. Similarly in cells that had undergone OGD, 10µM thapsigargin caused significantly more cell death than other groups. There was a significant interaction between OGD and treatment at both time points (p<0.0001).

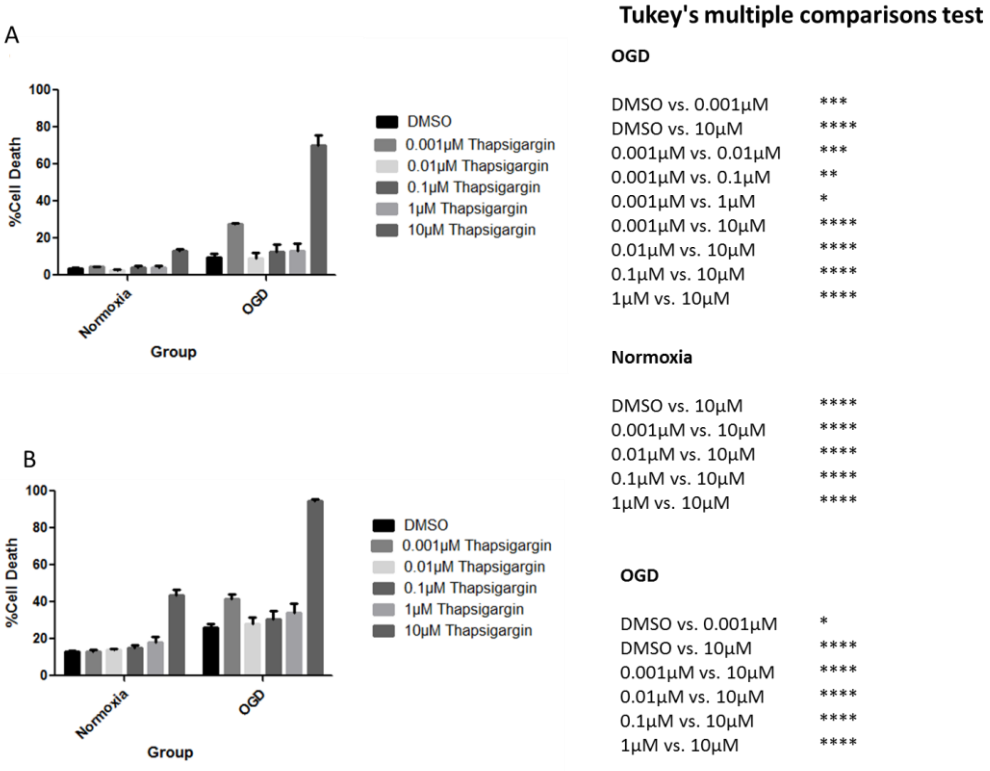

Figure 5.10 Effect of thapsigargin treatment during OGD Cell death was quantified by LDH assay. (A) At 2 hours there was a significant effect of OGD and treatment with increasing concentrations of thapsigargin leading to increased cell death. (B) Following 2 hours and 24 hours recovery there was a significant effect of OGD and treatment with 10µM thapsigargin caused significantly more cell death under both normoxic and OGD conditions. *p<0.05, **p<0.01, ***p<0.001, ****p<0.0001

Pre-treatment with thapsigargin before OGD

The effect of various doses of thapsigargin on neuron viability was measured using an LDH assay in cortical cultures that had undergone 2 hours of Normoxia or OGD followed by 24 hours recovery (Figure 5.11). Pre-treatment was administered 24 hours prior to normoxia or OGD: media (n=3), DMSO (n=3), 0.1μM thapsigargin (n=3) and 10μM thapsigargin (n=3). At 2 hours following normoxia or OGD (Figure 5.11 (A)), there was a significant effect of OGD (p=0.0008) and treatment (p=0.0026) (two-way ANOVA). Tukey's Multiple Comparison Test demonstrated that 10μM thapsigargin produced significantly more cell death than 0.1μM thapsigargin (p=0.0233) in the cells that had undergone normoxic conditions. At 2 hours and 24 hours recovery (Figure 5.11 (B)), there was a significant effect of OGD (p<0.0001) and treatment (p<0.0001) (two-way ANOVA). Tukey's Multiple Comparison Test demonstrated that 10μM thapsigargin produced significantly more cell death than media, DMSO and 0.1μM thapsigargin and 0.1μM thapsigargin produced significantly more cell death than media and DMSO in the cells that had undergone normoxic and OGD conditions (for specific group comparisons and p-values, (Figure 5.11 (B))). There was no interation between OGD and treatment at either timepoint. This suggests that ER stress induction with thapsigargin increases cell death.

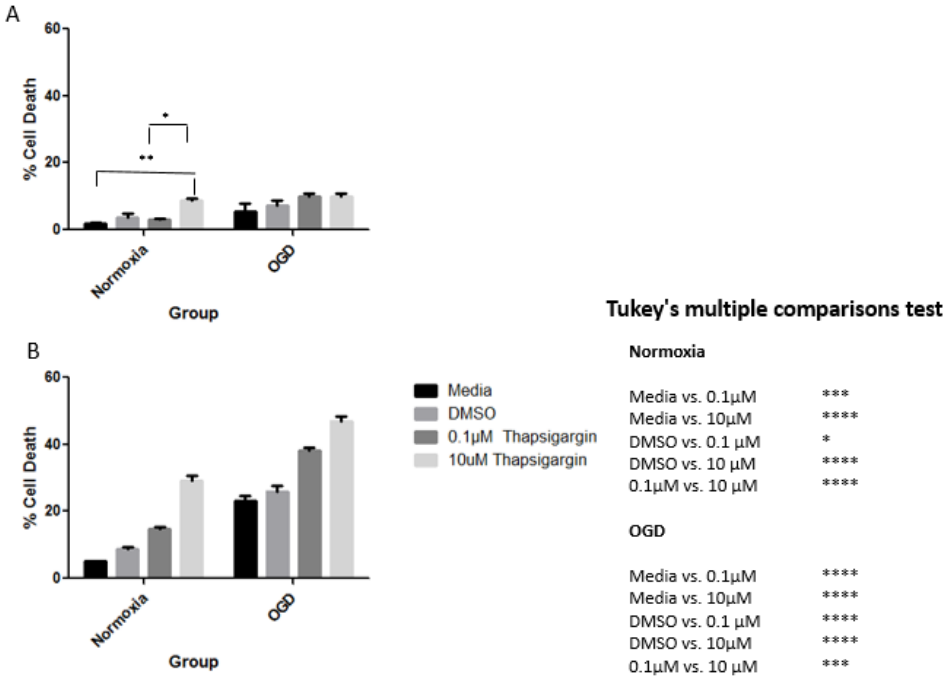

Figure 5.11: Effect of thapsigargin treatment 24 hours before OGD Cell death was quantified by LDH assay. (A) At 2 hours there was a significant effect of OGD and treatment with 10μM thapsigargin producing significantly more cell death after normoxia. (B) At 2 hours and 24 hours recovery, there was a significant effect of OGD and treatment with increasing concentrations of thapsigargin augmenting cell death. *p<0.05, **p<0.01, ***p<0.001, ****p<0.0001.

5.5.2.1.2 Tunicamycin

Tunicamycin is an ER stress inducer by acting as an inhibitor of N-glycosylation inhibition.

Treatment with tunicamycin during OGD

The effect of a dose response of tunicamycin on cortical neuron viability was assessed using an LDH assay (Figure 5.12). Percentage cell death was measured in cortical cultures that had undergone 2 hours of normoxia or OGD in the presence of DMSO (n=3), 0.01µM tunicamycin (n=3), 0.1µM tunicamycin (n=3) or 1µM tunicamycin (n=3), followed by 24 hours recovery. At 2 hours (Figure 5.12 (A)), there was a significant effect of OGD (p=0.0042) and a significant effect of treatment (p=0.0044) (two-way ANOVA). Tukey's Multiple Comparison Test demonstrated significant differences between 1µM tunicamycin and DMSO (p=0.0176) and 0.01µM tunicamycin (p=0.0294) following OGD with the higher concentrations of tunicamycin causing greater levels of cell death. At 2 hours and 24 hours recovery (Figure 5.12 (B)), there was a significant effect of OGD (p=0.0360) (two-way ANOVA) and treatment (p=0.0233) (two-way ANOVA). However, Tukey's Multiple Comparison Test showed that there were no significant differences between groups. There was no interation between OGD and treatment at either timepoint.

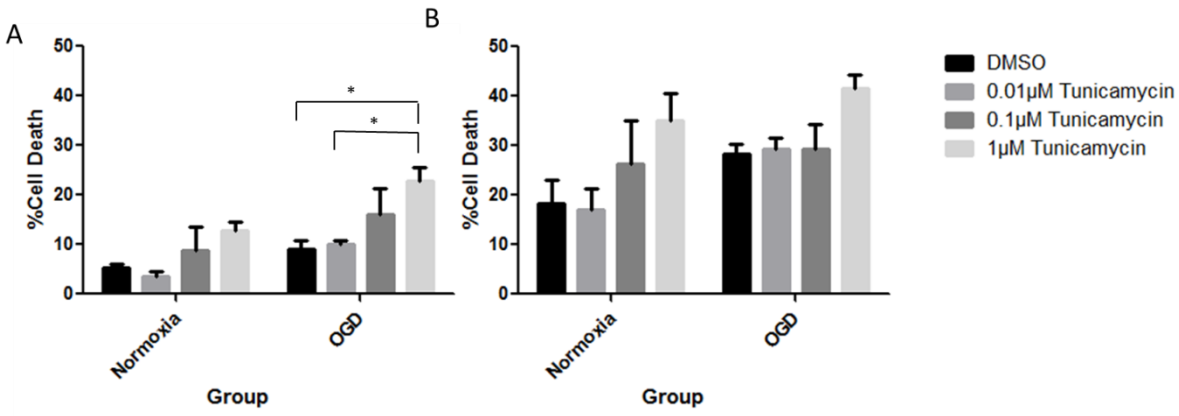

Figure 5.12: Effect of tunicamycin treatment during OGD Cell death was quantified by LDH assay. (A) At 2 hours there was a significant effect of OGD and treatment with higher concentrations of tunicamycin causing greater levels of cell death. (B) At 2 hours and 24 hours recovery there was a significant effect of OGD and treatment but there were no significant differences between groups. *p<0.05

5.5.2.2 ER stress inhibitors

5.5.2.2.1 Salubrinal

Salubrinal is a small molecule ER stress inhibitor that prevents formation of GADD34/PP1 complex therefore reducing the dephosphorylation of phosphoeIF2α.

Treatment with salubrinal during OGD

The effect of a dose response of salubrinal on cortical neuron viability was assessed using an LDH assay (Figure 5.13). Percentage cell death was measured in cortical cultures that had undergone 2 hours of normoxia or OGD in the presence of DMSO (n=3), media (n=3) 10μM salubrinal (n=3), 25μM salubrinal (n=9), 50μM salubrinal (n=9), 100μM salubrinal (n=9), 200μM salubrinal (n=3) or 500μM salubrinal (n=3), followed by 24 hours recovery. At 2 hours (Figure 5.13 (A)), there was a significant effect of OGD (p<0.0001) and treatment (p=0.0033) (two-way ANOVA). Tukey's Multiple Comparison Test demonstrated significant differences between media and 50μM, 100μM and 500μM salubrinal following OGD with the higher concentrations of salubrinal causing greater levels of cell death. At 2 hours and 24 hours recovery (Figure 5.13 (B)), there was a significant effect of OGD (p<0.0001) and treatment (p<0.0001) (two-way ANOVA). Tukey's Multiple Comparison Tests demonstrated that higher concentrations of salubrinal led to greater levels of cell death (for specific group comparisons and p-values, see Figure 5.13 (B)). There was no interation between OGD and treatment at either timepoint.

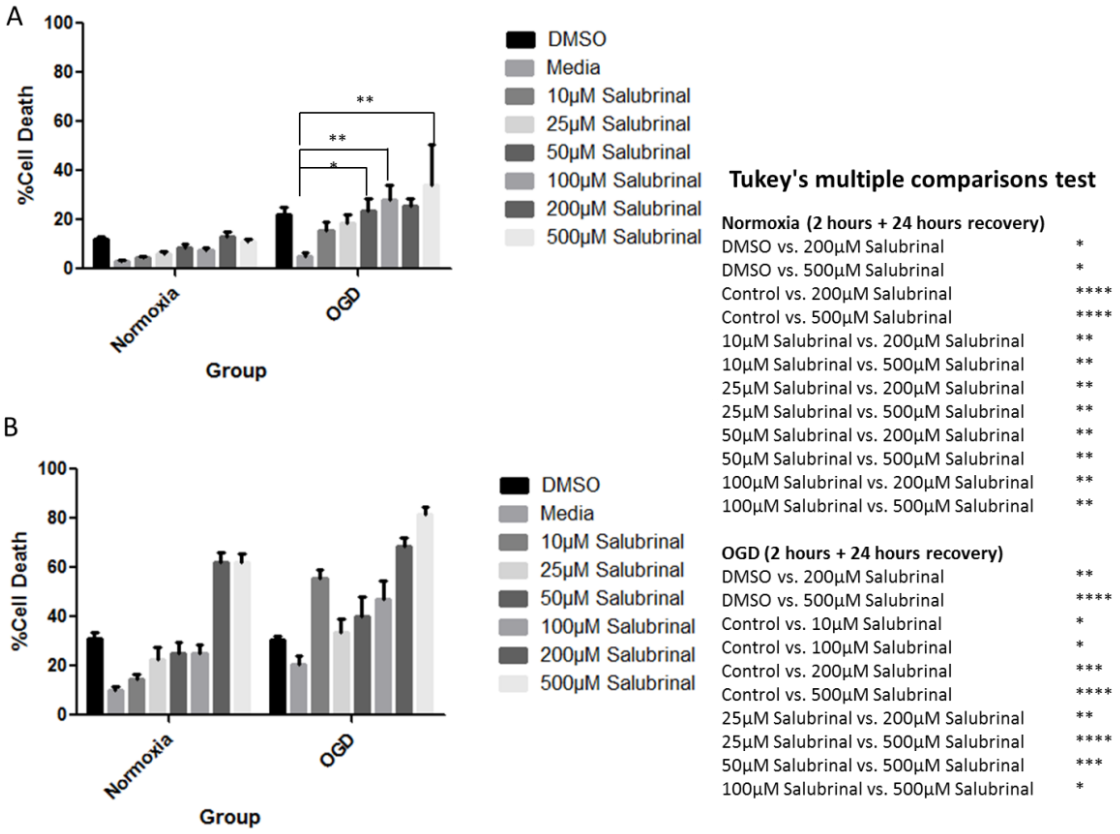

Figure 5.13 Effect of salubrinal treatment during OGD Cell death was quantified by LDH assay. (A) At 2 hours there was a significant effect of OGD and treatment with higher concentrations of salubrinal causing greater levels of cell death during OGD. (B) At 2 hours and 24 hours recovery there was a significant effect of OGD and treatment with higher concentrations of salubrinal leading to greater levels of cell death. *p<0.05, **p<0.01, ***p<0.001, ****p<0.0001

Pre-treatment with salubrinal before OGD

The effect of various doses of salubrinal on neuron viability was measured using an LDH assay in cortical cultures that had undergone 2 hours of OGD and 24 hours recovery with 24 hours pretreatment with salubrinal: DMSO (n=2) and 50μM salubrinal (n=2). At 2 hours (Figure 5.14 (A)), there was no significant difference between groups (p= 0.1231). At 2 hours and 24 hours recovery (Figure 5.14 (B)), there was a significant difference with salubrinal cells demonstrating a higher level of cell death (p=0.0011). These results are for OGD conditions only.

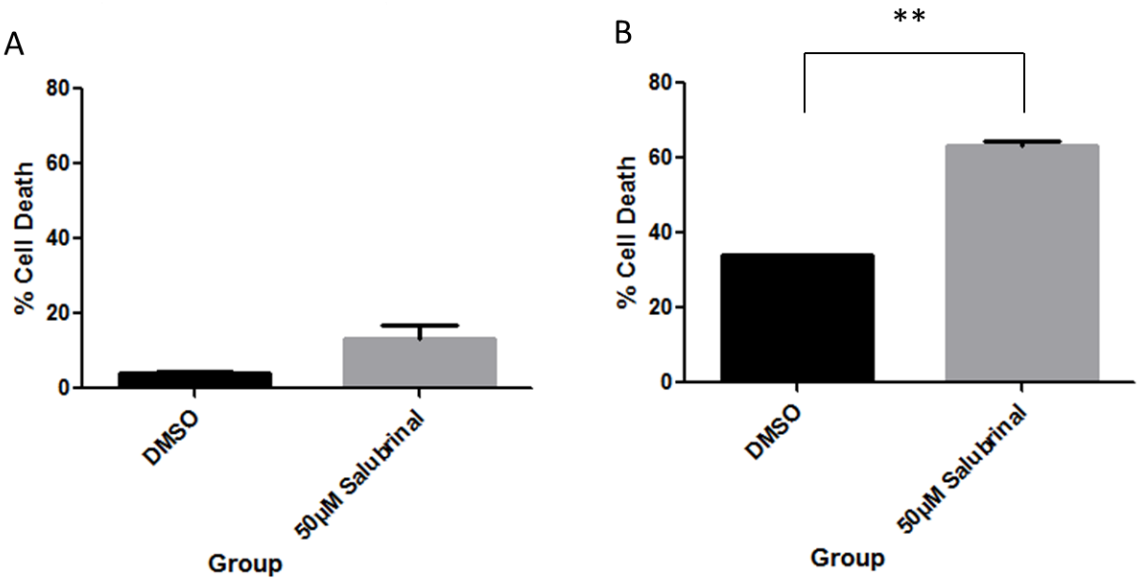

Figure 5.14 Effect of salubrinal treatment 24 hours before OGD Cell death was quantified by LDH assay. (A) At 2 hours, there was no significant difference between groups. (B) At 2 hours and 24 hours recovery, salubrinal treatment significantly increased cell death. *p<0.01

5.5.2.3 Combining Autophagy Inducer and ER stress Inhibitor

The previous results showed that treatment with the ER stress inhibitor, salubrinal unexpectedly caused neurotoxicity. Previous studies have shown that mild ER stress can be protective through the production of autophagy (Bernales *et al.,* 2006) and so here an autophagy inducer (metformin was used to try and prevent the detrimental effects of inhibiting ER stress.

Combination treatment with salubrinal and metformin during OGD

The effect of many concentrations of both salubrinal and metformin on cortical neuron viability was assessed using an LDH assay (Figure 5.15). Percentage cell death was measured in cortical cultures that had undergone 2 hours of normoxia or OGD in the presence of DMSO (n=3), 25μM salubrinal and 20μM metformin (n=3), 50μM salubrinal and 200μM metformin (n=3), or 100μM salubrinal and 500μM metformin (n=3)) followed by 24 hours recovery. At 2 hours (Figure 5.15 (A)), there was a significant effect of OGD (p<0.0001) but no significant effect of treatment (p=0.0955) (two-way ANOVA). At 2 hours and 24 hours recovery (Figure 5.15 (B)), there was a significant effect of OGD (p<0.0001) but there was no significant effect of treatment (p=0.0506) (two-way ANOVA). There was no interation between OGD and treatment at either timepoint. Considering Figures 5.13 and 5.14 showed a neurotoxic effect with salubrinal, adding metformin to the treatment blocked any detrimental effect of salubrinal.

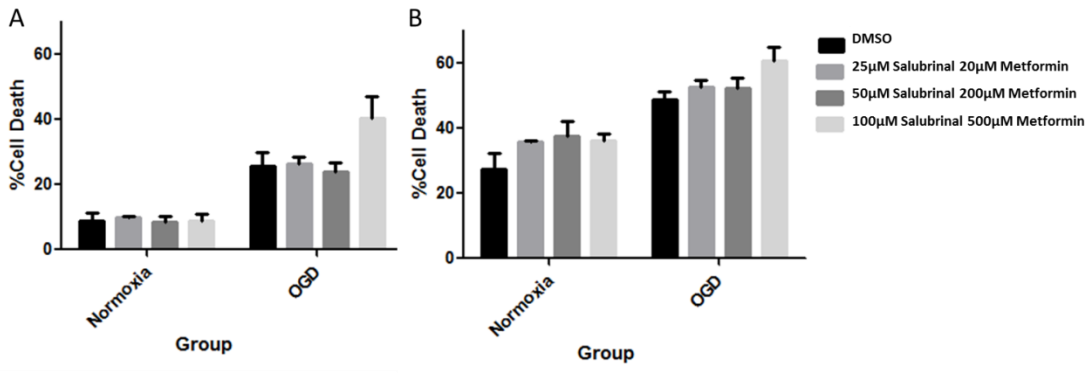

Figure 5.15 Effect of combining an ER stress inhibitor and an autophagy inducer during OGD Cell death was quantified by LDH assay. (A) At 2 hours there was a significant effect of OGD but no significant effect of treatment. (B) At 2 hours and 24 hours recovery there was a significant effect of OGD but no significant effect of treatment.

5.6 Discussion

Physiologically, the ER is involved in the synthesis and processing of intracellular proteins. The induction of ER stress results from ROS following ischaemia. A depletion of ATP, lowering of intraluminal calcium levels and inhibition of protein glycosylation occurs resulting in the build-up of unfolded proteins within the ER lumen, disturbing the equilibrium. The UPR temporarily slows accumulation of new proteins in the ER lumen, at the same time as up-regulating transcription of genes for ER resident chaperones and enzymes that ablate the effects of ER stress (Kumar *et al.,* 2003).

Di Nardo *et al.,* (2009) provided the first evidence that TSC was implicated in neuronal stress responses in an mTOR-dependent manner. Neurons lacking TSC1/TSC2 complex have increased vulnerability to ER stress-induced cell death via the activation of the mitochondrial death pathway. TSC2 is initially inactivated in these neurons during ER stress, but is later activated (Di Nardo *et al.,* 2009). The work in this chapter explored how global ischaemia altered ER stress spatially and temporally and whether ER stress modulation could influence neuronal survival and form part of the mechanism for hamartin's endogenous neuroprotective effect.

5.6.1 *In vivo* time course

There was a differential ER stress response to 10mins of global ischaemia. Following 3 hours reperfusion there was a significant decrease in phosphoeIF2α and ATF4 selectively in the CA3 region compared to sham with no significant difference following 12 hours reperfusion. This suggests that a decrease in ER stress at 3 hours is associated with neuronal survival, but this decrease is not sustained. This is in keeping with current literature. In a 2VO/HT model (10 mins) in rats compared to NIC (non-ischaemic controls), following microdissection and homogenisation of CA1 and CA3, the ER stress response was found to be stronger in CA1 than CA3 (Roberts *et al.,* 2007). The temporal association between increased hamartin expression and decreased ER stress levels in CA3 neurons may contribute to the mechanism of hamartin's endogenous protective effect.

Corroborating previous studies, there was a significant increase in CA1 phosphoeIF2α and ATF4 expression following 12hrs reperfusion, indicating ER stress activity which was not present at 3 hours reperfusion. This delayed ER stress response could be associated with the neuronal death that eventually occurs in CA1. This is

in line with previous findings that ER stress markers phosphoeIF2α and PERK were increased in CA1 neurons following ischaemia in a rodent model (Hayashi *et al.,* 2003). ATF4 is known to be activated by severe ER stress and both ATF4 and ER stress play a role in apoptosis (Hayashi *et al.,* 2003). In wild-type and human copper/zinc superoxide dismutase transgenic rats, following global ischemia, increased levels of ATF4 and CHOP were measured in CA1 neurons that would undergo apoptotic cell death (Hayashi *et al.,* 2005). In the gerbil model of transient forebrain ischemia, ER stress is also implicated in the neuronal cell death demonstrated in the CA1 region of the hippocampus (Oida *et al.,* 2008).

Overall, the divergent ER stress response between CA1 and CA3 neurons of the hippocampus following ischaemia is associated with the differential effects of hamartin expression and neuronal survival.

5.6.2 *In vitro*

Given the *in vivo* results revealing an association between hamartin expression, ER stress downregulation and neuronal survival in the CA3 region of the hippocampus following global ischaemia, a prudent approach would be to use small molecule modulators of ER stress to isolate the effects of ER stress in ischaemic neurons and replicate hamartin's neuroprotective effect.

5.6.2.1 Thapsigargin

As expected, the ER stress inducer, thapsigargin resulted in increased cell death when added to cortical neurons during two hours of normoxia or OGD. 24 hour pre-treatment with thapsigargin was also investigated as mild ER stress has been suggested to be neuroprotective via autophagy (Fouillet *et al.,* 2012) and autophagy induced by IPC reduces apoptosis by suppressing excess ER stress during the subsequent ischaemia (Sheng *et al.,* 2012). However, a dose dependent increase in cell death was observed in normoxic and OGD treated cells meaning even pretreatment of ER stress induction did not provide protection.

5.6.2.2 Tunicamycin

Treatment with tunicamycin, another ER stress inducer also resulted in a dose dependent increase in cell death, supporting previous findings (Imai *et al.,* 2014) and in a similar manner to thapsigargin. The results from both

ER stress inducers supports the notion that ER stress is detrimental to neuronal cell survival following ischaemia.

5.6.2.3 Salubrinal

While it was expected that an ER stress inhibitor would afford neuroprotection, treatment with salubrinal (an ER stress inhibitor) dose dependently increased of cell death following 2 hours of normoxia and OGD. A previous study has shown detrimental effects of salubrinal by abolishing the protection by ER stress-induced autophagy in an *in vivo* focal rodent stroke model (Gao *et al.,* 2013). However, other studies have shown that salubrinal decreased neuronal death in experimental rodent models of excitotoxicity, epilepsy and focal ischemia (Sokka *et al.,* 2007; Nakka *et al.,* 2010). While previous literature is conflicting, it was clear in these experiments that salubrinal was neurotoxic potentially by abolishing any protective effects of ER stress induced autophagy.

5.6.2.4 Combination of an ER stress inhibitor and an autophagy inducer

There is emerging evidence that ER stress activation can lead to autophagy (Yorimitsu *et al.,* 2006; Sakaki and Kaufman, 2008) including in neurons (Sheng *et al.,* 2012). Salubrinal alone appeared to increase neuronal cell death following OGD, possibly due to the inhibition of ER stress induced autophagy. Therefore it was attempted to prevent salubrinal toxicity by combining it with an autophagy inducer such as metformin. This experiment revealed that metformin could prevent salubrinal neurotoxicity suggesting that salubrinal was preventing autophagy. Metformin alone was also not enough to produce neuroprotection by inducing autophagy (Chapter 4), but these combination treatment results reveal a clear link between ER stress and autophagy.

There exists a complicated interplay between ER stress and autophagy. The protective effect of mild ER stress (preconditioning) is thought to be due to autophagy (Bernales *et al.,* 2006). The link between autophagy and ER stress is however not entirely clear, with evidence for involvement in all three of the stress sensor pathways. Autophagy can be activated by both PERK and ATF6 pathways (Ogata *et al.,* 2006; Rouschop *et al.,* 2010). A potential mechanism has been proposed whereby autophagy is enhanced via the ER stress-driven negative regulation of the AKT/TSC/mTOR pathway (Qin *et al.,* 2010b). To further complicate the relationship, autophagy may also modulate ER stress (Carloni *et al.,* 2014) and the ER may inhibit autophagy (Bassik *et al.,* 2004;

Pattingre *et al.,* 2005). Furthermore, ATF4 controls the expression of various genes involved in autophagy, apoptosis, amino acid metabolism, and antioxidant responses (as reviewed by Hetz and Mollereau, 2014). It is clear that a greater mechanistic understanding of the particular points at which ER stress and productive autophagy switch from detrimental effects to beneficial effects or vice versa in the context of neuronal ischaemia is required in order to harness any endogenous neuroprotection.

5.7 Conclusions

The temporal association between increased hamartin expression and decreased ER stress levels in CA3 neurons may contribute to the mechanism of hamartin's endogenous protective effect.

The ER stress response is attenuated in resistant CA3 neurons at 3 hours and there is greater expression of ER stress proteins in vulnerable CA1 neurons at 12 hours which could be a manifestation of uncontrolled protein synthesis via uncontrolled mTOR activation (Table 5.1).

ER Stress Protein Expression	3 hours	12 hours
PhosphoeIF2α	Decreased in CA3 ischaemia	Increased in CA1 ischaemia
ATF4	Decreased in CA3 ischaemia	Increased in CA1 ischaemia

Table 5.1 *In vivo* summary of results

Table 5.2 summarises the *in vitro* pharmacology in this Chapter. Inducing ER stress had the expected result of increasing neuronal death, a more precise time course and more comprehensive dosing range may have demonstrated any potential effect of pharmacological preconditioning leading to protection which was not observed here. Salubrinal did not afford neuroprotection at dosing intervals used in this study but instead produced neurotoxicity, possibly via prevention of ER stress induced autophagy. In these experiments metformin was not found to replicate neuroprotective effects associated with autophagy. The combination of salubrinal with metformin prevented salubrinal neurotoxicity by inducing autophagy, but metformin alone was

not neuroprotective. Overall, and rather disappointingly, pharmacological manipulation of ER stress has not yielded a specific target for therapy and did not replicate hamartin's neuroprotective effects.

Drug	Function	Summary of treatment effect
Thapsigargin	ER stress inducer	Pre: **Increased neuronal death** (normoxia and OGD) During: **Increased neuronal death** (normoxia and OGD)
Tunicamycin	ER stress inducer	During: **Increased neuronal death** (normoxia at 2 hours)
Salubrinal	ER stress inhibitor	Pre: **Increased neuronal death** (OGD) During: **Increased neuronal death** (normoxia and OGD)
Combination (salubrinal/ metformin)	ER stress inhibitor /autophagy inducer	During: No effect (NB neurotoxic effect of salubrinal treatment prevented by addition of metformin)

Table 5.2 *In vitro* summary of results

In Chapter 6, the results of this thesis will be summarised and the mechanisms behind hamartin's neuroprotective effects considered. In addition, some speculation will focus on the relationship between hamartin and its downstream mechanisms on neuronal function in relation to other diseases well as aging. Emerging themes in neuroprotection as a result of this thesis will also be completed in the context of cerebral ischaemia and other neurodegenerative diseases.

Chapter 6: General Discussion

6.1 Executive Summary

Manipulating the mechanism by which hamartin 'fine-tunes' the brain's endogenous neuroprotective response could ultimately lead to the identification of a small molecular target. This compound could offer the pharmacological modulation endogenously provided by hamartin and prove to be the neuroprotectant yet to be discovered and extrapolated to the clinic. 'Time is brain' (Saver, 2006) and any small molecule that could be given in the ambulance with the aim of targeting the ischaemic cascade at source without increasing the risk in haemorrhagic would increase the chances of improved functional outcome for stroke patients. Harnessing endogenous protective mechanisms could indeed bring a cure from within that could not only benefit stroke patients, but extend to a multitude of neurodegenerative diseases which will be explored in this general discussion.

The key findings in this thesis are summarised in Figure 6.1. The early increase in hamartin expression in the resistant hippocampal CA3 region following global cerebral ischaemia (Chapter 3) corroborates recent findings that hamartin has a neuroprotective effect (Papadakis *et al.,* 2013). The key function of hamartin is the inhibition of mTOR which implicates this mechanism in neuroprotection. However, there are a number of downstream effector pathways that inhibition of mTOR by hamartin could also influence such as the promotion of productive autophagy (Chapter 4) and the inhibition of the ER stress pathway (Chapter 5). Indeed, the expression of autophagy proteins was differentially altered in both CA1 and CA3 regions of the hippocampus following global ischaemia, and hamartin inhibition prevented productive autophagy. Furthermore, decreased levels of ER stress proteins were observed in CA3 while increased protein expression was found in CA1 after global ischaemia. There is a complex interplay between autophagy and ER stress and pharmacological manipulation with mTOR, autophagy or ER stress modulators did not manage to replicate hamartin's endogenous neuroprotective effect (Table 6.1). Interestingly, a novel mTORC1/2 inhibitor and promising candidate currently in cancer trials AZD2014 significantly increased neuronal cell death in the context of neuronal ischaemia. A dose response experiment with AZD2014 demonstrated that increased ER stress proteins may play a role in this detrimental

effect and questions whether AZD2014 is solely acting on the mTOR complex. This leaves uncertainty whether long term administration of mTOR inhibitors in cancer would place brain cells at risk.

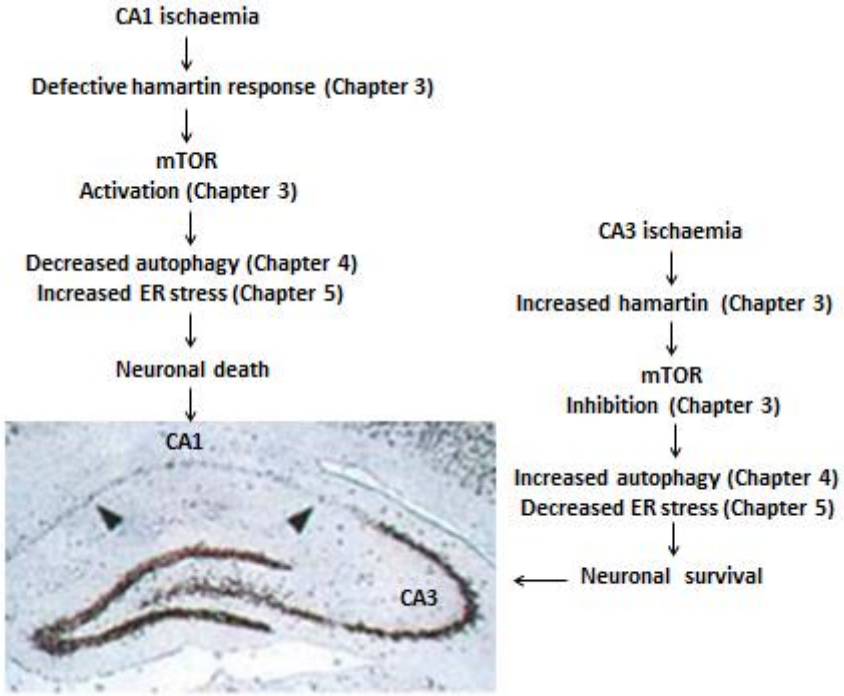

Figure 6.1 Pathways associated with selective hippocampal vulnerability in this thesis

Drug	Function	Chapter	Summary of treatment effect
Rapamycin	mTORC1 inhibition	3	Pre: No effect During: No effect Post: 10nM **improved neuronal survival** (OGD)
AZD 2014	mTORC1/2 inhibition	3 & 5	Pre: **Increased neuronal death** (OGD) During: **Increased neuronal death** (OGD) Post: **Increased neuronal death** (hippocampal and cortical, normoxia and OGD).
Metformin	Autophagy inducer	4	Pre: **Increased neuronal death** (normoxia and OGD) During: No effect
3MA	Autophagy inhibitor	4	During: **Increased neuronal death** (normoxia and OGD) Post: **Increased neuronal death** (normoxia and OGD)
Thapsigargin	ER stress inducer	5	Pre: **Increased neuronal death** (normoxia and OGD) During: **Increased neuronal death** (normoxia and OGD)
Tunicamycin	ER stress inducer	5	During: **Increased neuronal death** (normoxia at 2 hours)
Salubrinal	ER stress inhibitor	5	Pre: **Increased neuronal death** (OGD) During: **Increased neuronal death** (normoxia and OGD)
Combination (salubrinal/ metformin)	ER stress inhibitor /autophagy inducer	5	During: No effect (NB neurotoxic effect of salubrinal treatment prevented by addition of metformin)

Table 6.1 Summary of *in vitro* pharmacology results in this thesis. Findings refer to cortical neurons unless otherwise stated. The timing of drug administration was with respect to normoxia/OGD.

6.2 Hamartin and downstream mechanisms

6.2.1 Hamartin

It is becoming clear that subcellular localisation is the key to elucidating the precise temporal and spatial endogenous neuroprotective effect of hamartin (Papadakis *et al.,* 2013). In Chapter 3, experiments were described showing an immediate increase in hamartin expression in the membrane fraction following 10 minutes of global ischaemia in the CA3 area of the hippocampus which persisted to 24 hours was and associated with a concomitant decrease in the cytoplasmic fraction. This suggests that hamartin is translocated to a membrane surface within the cell in response to ischaemia. A recent study demonstrated that upon growth factor withdrawal, the tuberous sclerosis complex (TSC) translocates to the lysosomal surface where it inhibits mTORC1 by promoting guanosine 5'-triphosphate (GTP) hydrolysis and inactivation by Rheb (Menon *et al.,* 2014). Further experiments would need to decipher whether in stroke, it is at the lysosome where hamartin is initiating its protective effects.

The main function of intracellular hamartin is to bind to its binding partner tuberin and inhibit the mTOR complex (Gao and Pan, 2001). The regulation of this process is complicated with a number of upstream pathways influencing expression and activity of hamartin, and feedback loops from mTOR and downstream pathways can alter these upstream pathways leading to variations in hamartin's activity. It is unknown how these regulatory systems for hamartin are altered in ischaemia, but it is clear that preserving hamartin expression and its probable translocation to the lysosomal membrane is responsible for this beneficial effect. Preserving hamartin activity leads to the inhibition of mTOR which results in a number of cellular processes including the promotion of productive autophagy and the inhibition of the ER stress pathway. These downstream effects could provide the clue to the mechanism through which hamartin could be producing neuroprotection and provide a novel therapeutic target for a small molecule.

While mTOR inhibition is the most likely candidate for hamartin's neuroprotection, the use of specific mTOR inhibitors did not reveal any beneficial effects in primary neurons following OGD (Chapter 3). In fact, some neurotoxicity was even observed questioning the use of these agents clinically, especially for long term therapy.

This suggests two things: 1) the mTOR inhibitors commercially available are not necessarily specific for mTOR, evidenced by changes in upstream pathways with these drugs; 2) hamartin's neuroprotection is not solely due to mTOR inhibition. Further research is required to delineate the complete mechanism of hamartin's neuroprotection and no small molecule tested so far can replicate this.

6.2.2 Productive autophagy

Autophagy, the process of recycling cellular components, can have beneficial and detrimental effects in neurons. There appears to be a differential expression of markers of autophagosome formation and autophagic flux between the vulnerable CA1 region and resistant CA3 region following global ischaemia that is time-dependent (Chapter 4). This varied autophagic response in the hippocampus correlates with differences in hamartin expression, and further genetic modification of hamartin in neuronal cultures showed that protection of neurons following ischaemia was through induction of autophagy, presumably by hamartin inhibiting mTOR. The finding that hamartin confers neuroprotection against ischemia by inducing productive autophagy (Chapter 4) has recently been corroborated by a group studying Tsc1/2 deficient cells. Lack of Tsc2 leads to autophagic activity via AMPK-dependent activation of ULK1 on Ser^{555} which results in autophagic flux and accumulation of autolysosomes (Di Nardo *et al*., 2014). Therefore, promotion of productive autophagy appears to be one of the mechanisms by which hamartin can protect neurons following an ischaemic insult.

If productive autophagy is implicit in the neuroprotective response by hamartin, ideally an autophagy inducer would provide similar neuroprotective effects to hamartin. However, neuronal OGD experiments where autophagy modulators were administered revealed that autophagy inducers alone could not provide protection to neurons (Chapter 4). This suggests that hamartin produces its protection via multiple mechanisms and not just through the process of productive autophagy alone.

6.2.3 ER stress

The cell responds to oxidative stress by activating the ER stress pathway. The unfolded protein response (UPR) temporarily slows accumulation of new proteins in the ER lumen, at the same time upregulating transcription of genes for ER resident chaperones and enzymes that ablate the effects of ER stress (Kumar *et al.,* 2003). There

was a differential effect in ER stress between the resistant CA3 and vulnerable CA1 regions of the hippocampus in response to global cerebral ischaemia. ER stress increased in the CA1 region while it was downregulated in CA3 within the first 12 hours following global ischaemia (Chapter 5). Given the link between mTOR and ER stress, the upregulation of hamartin in CA3 over a similar time frame following global ischaemia could be causing the decrease in ER stress and subsequent protection of CA3 neurons. This opens up the possibility that the inhibition of the ER stress response could be targeted as a specific mechanism by which hamartin could provide neuroprotection.

Modulation of ER stress within primary neurons however, could not replicate hamartin's protective effects. Both inducers and inhibitors of ER stress actually increased neuronal death in response to OGD. Interestingly, the neurotoxicity observed with the ER stress inhibitor could be prevented when an autophagy inducer was administered (Chapter 5). Mild ER stress has been shown to lead to autophagy (Yorimitsu *et al* 2006; Sakai & Kaufman 2008) and the inhibition of ER stress could prevent autophagy and subsequent neurotoxicity. This reveals the complex interplay between ER stress and autophagy and there is fine balance between its beneficial and detrimental effects to neurons. The lack of replication of hamartin's neuroprotective effect with an ER stress inhibitor alone suggests that there are multiple mechanisms of hamartin's neuroprotection including the inhibition of ER stress and that one small molecule may not be able to replicate this. The precise mechanism of endogenous neuroprotection is likely to be complex and further studies are required to delineate the precise mechanisms of how hamartin is producing neuroprotection and whether the inhibition of ER stress is involved in this process.

6.3 The wider clinical relevance of endogenous neuroprotection

6.3.1 Hamartin and austerity

mTOR inhibition affords neuroprotection, not only by cutting down on energy consumption through inhibiting protein synthesis, but also via the austere phenomenon of recycling proteins that already exist through 'productive autophagy' (Gabryel *et al.,* 2012). Autophagy or 'self-eating' was first described in 1963 by Christian de Duve who won a Nobel Prize in 1974 for work on lysosomes (De Duve, 1963). This economical utilization of

bio-recycling proteins is highly relevant to the dearth of energy in the ischaemic brain as an adaptive response to provide nutrients and energy, in addition to removing misfolded or long-lived proteins and organelles that are damaged or surplus to requirements. The austere environment inhabited by neurons in the post-ischemic stroke brain not only lacks oxygen (hypoxic), but is energy depleted and nutrient deprived. The tuberous sclerosis complex, therefore hamartin and mTOR have been implicated in all of these three stresses upon the ischaemic cell. Hypoxia has been shown to affect mTOR signalling through more than one mechanism (Arsham *et al.,* 2003; DeYoung *et al.,* 2008; Huang and Manning 2008). Any stress that depletes cellular ATP (the cell's energy source), such as oxidative stress, hypoxia, nutrient deprivation and metabolic poisoning, results in the activation of AMPK which directly phosphorylates and activates part of the TSC complex (Hardie, 2004). Nutrient deprivation results in decreased availability of amino acids which has been shown to regulate the mTOR pathway (Huang and Manning, 2008).

A short, sharp period of "austerity" might induce tolerance of the cells to ischaemia (Papadakis *et al.,* 2013) and in keeping with recent studies demonstrating that nutritional deprivation induces longevity through mTOR (Blagosklonny and Hall, 2009; Harrison *et al.,* 2009). The up-regulation of hamartin-induced mTOR inhibition with preconditioning could provide the underlying mechanism entirely consistent with the idea that hypothermia, deafferentation (Buchan and Pulsinelli, 1990 b), hypoglycaemia and nutritional depletion might result in increased tolerance of brain cells following ischemia.

Extreme stress is pathophysiological, however previous exposure (or 'preconditioning') can afford protection (Dirnagl *et al.,* 2009). In ischemic stroke could upregulation of hamartin, inhibition of mTOR and induction of protective autophagy be the underlying mechanism that explains the enigma surrounding the protective phenomena of IPC (a taste of the austerity to come that serves to prepare and protect), hypoglycaemia (Guidelines for management of ischaemic stroke and transient ischaemic attack 2008) and hypothermia (Colbourne *et al.,* 1999)? After all, physiologically minor insults make the body stronger as illustrated by the build-up of muscle in response to repeat exercise (Moyer, 2013). This may therefore explain the paradoxical implication that immediately following ischaemia, a reduction in energy consumption through protein synthesis

(and therefore repair) might actually be advantageous. Induction of autophagy, through efficient recycling of damaged proteins and organelles, might be the secret to staying alive.

6.3.2 mTOR and aging

Humans are living longer, indeed life expectancy has increased by approximately 25 years over the past 100 years (Kirkwood, 2010). The vast majority of us are no longer killed by childhood pneumonia, childbirth and raging sepsis, largely due to the discovery of antibiotics and improvement of sanitation. Similarly disease of middle age, such as cardiovascular disease have much lower incidence and mortality rates due to an appreciation and management of risk factors. The corollary of this is that we are getting diseases that our ancestors rarely lived to develop – primarily those of neurodegeneration (see Section 6.3.3).

Perhaps we can learn something from the 'older old'? The naked mole-rat and humans that reach the age of 100 reveal that longevity is not necessarily linked to late-life disability and disease (Fontana and Partridge, 2015). In the majority of the population, however, our mind is currently leagues behind our bodies in achieving relative morbidity-free ageing.

In a recent review, the link between metabolism and ageing is probed, through considering pathways that sense nutrient availability (such as mTOR) and the role of mitochondria (Finkel, 2015). Current attempts at turning aging into a 'pharmacologically modifiable condition' (Finkel, 2015) have largely concentrated on the mTOR inhibitor, rapamycin. Although it has been dubbed the 'elixir of life' in the respect that it can increase '*maximum* life span' (the mean life span of the longest-lived 10% percent of a given population) (Stipp, 2012), its side effects if taken long-term preclude its general use.

In mice and rats lifespan can be extended as much as 50% using caloric restriction compared to *ad libitum*–fed animals (Speakman and Mitchell, 2011). Caloric restriction results in a host of metabolic changes such as a decrease in respiratory exchange ratio, decreased temperature and a decrease in white adipose tissue resulting in increased metabolic flexibility, decreased age-related diseases and increased stem cell function and DNA repair (Speakman and Mitchell, 2011; Finkel, 2015). Simulation of production of molecular chaperones such as

GRP78 (relevant to ER stress) also occurs (Fontana and Partridge, 2015). Decreased inflammation has been seen in non-human primates (Willette *et al.,* 2013).

The effects of dietary restriction were first recorded in rats in the 1930s (McCay *et al.,* 1935). The beneficial effects of dietary restriction include resistance to certain stressors such as chemotherapeutic agents and ischaemic reperfusion injury in several organs (Harputlugil *et al.,* 2014). Especially relevant is neuroprotection conferred by short-term preoperative dietary restriction in a rodent focal stroke model (Varendi *et al.,* 2014). Harputlugil *et al* (2014) make the distinction between caloric restriction and dietary restriction that concerns specific macronutrients such as amino acids whose benefits exceed their calorific value. Indeed, dietary protein intake is a key regulator of the IGF-1/mTOR network (Efeyan, *et al.,* 2012). Furthermore, mTOR activation is affected by different amino acids (particularly branched-chain amino acids) in a tissue-specific manner (Efeyan, *et al.,* 2012). Although caloric restriction has been shown to extend lifespan across species (mice (Lamming *et al.,* 2012), worms (Vellai *et al.,* 2003) and flies (Kapahi *et al.,* 2004)), there are species-specific effects. In small rodents there can be a difference in body temperature of several degrees (Speakman and Mitchell, 2011) of caloric restriction which is minimal or negligible in humans (as reviewed by Finkel 2015). mTOR is a key nutrient sensor, activated by growth factor signals and availability of amino acids and downstream effects in addition to regulation of protein synthesis include inhibition of autophagic flux, effects on mitochondrial function and insulin signalling. Observations that adding an mTOR inhibitor to a regime of caloric restriction does not increase life span yet further suggest that the pathways may be linked (Finkel, 2015).

AMPK is also a nutrient sensor, postulated to be linked to longevity which also has the effect of inducing autophagy and indeed this effect is mimicked by metformin, a drug in wide clinical use. Epidemiological clinical data exists where there is a 30-50% decrease in expected cancer incidence in patients taking metformin (Kasznicki *et al.,* 2014). Low-level ROS can actually have life extending effects which refutes the free radical theories of aging (Finkel 2015). Indeed, in *C. elegans* lifespan is extended by ROS that increase HIF-1 activity (Lee *et al.,* 2010b).

The question also arises as to what the evolutionary advantage of caloric restriction could possibly be? Why would something that prevents 'late-life decline' in a multitude of species, (admittedly sometimes in an artificial

laboratory setting) be preserved (Stipp, 2012)? It could be to enable animals to get through lean times in order to reproduce or perhaps it is just a by-product of other responses that have evolved that are unrelated to aging. Rapamycin, caloric restriction and specific genes just 'happen' to interfere with aging (Blagosklonny *et al.*, 2009) via mTOR or is there an independent evolutionary advantage? Afterall, the 'older old' reveal that longevity is not necessarily linked to late-life disability and disease (Fontana and Partridge, 2015).

The tuberous sclerosis complex itself has been linked with longevity (Kapahi *et al.,* 2004), where overexpression of TSC1 and TSC2 in *Drosophila* extends lifespan via decreased mTORC1 signalling. Recently, in mice the two significant benefits of protein restriction, first improved hepatic insulin sensitivity and second stress resistance, required the tuberous sclerosis complex (Harputlugil *et al.,* 2014).

6.3.3. Cancer

In human xenograft models, dietary protein restriction and substitution of plant for animal proteins inhibits tumour growth (Fontana *et al*., 2013).

In general, the longer one lives, the greater the chance of developing cancer. However, neurons are some of the most long lived cells in the body and their incidence of developing malignant disease is low (Siegel *et al*., 2014). What is it about neurons that make them resistant to developing cancer? Interestingly, in the disease tuberous sclerosis, where patients have a deficient hamartin/tuberin complex meaning mTOR is unregulated, patients can develop neuronal and cardiac tumours (Crino *et al*., 2006). While unrestricted mTOR can lead to increased protein synthesis and cell differentiation, explaining the tumour formation, why are the tumours specific for certain cell types? The regulation of mTOR by hamartin is critical for maintaining function and protection specifically of neurons because without this controlling switch, neurons are adversely affected.

A decreased chance of developing cancer is one of the listed benefits of dietary restriction. Young adult rhesus monkeys who start early dietary restriction have reduced risk of developing cancer (Fontana and Partridge 2015). The effect of intermittent fasting on cancer progression is said to be beneficial, but there is controversy as cancer initiation and promotion has also been suggested (as reviewed by Fontana and Partridge 2015). Short-term fasting (24-48 hours) prior to chemotherapy has demonstrated to be beneficial concerning some

side effects by protecting normal cells but not cancer cells (Safdie *et al.,* 2009). The timing of meals could also be important as epidemiological studies have suggested increased cancer rates in shift workers (Wang *et al.,* 2011b).

Dysregulation of the mTOR pathway has been implicated in cancer, but unfortunately so far, mTOR inhibitors have not been very successful in clinical trials. mTOR inhibitors are used in advanced renal cancer and there are currently three classes of mTOR inhibitor that have undergone preclinical testing or made it to clinical trial. The first class was rapamycin and its analogs called "rapalogs", the second class were dual inhibitors of PI3K and mTORC1/2, the third class were ATP-competitive, 'active-site' mTORC1/mTORC2 inhibitors (Charini *et al*., 2015).

6.3.4 Neurodegenerative diseases

In the UK in 2013, there were 815,827 people with diagnosed dementia (Dementia UK: second edition as cited by Alzheimer's Society, 2014). At current rates this would represent a projected increase of 156% over the next 38 years (Alzheimer's Society, 2014). A common theme in these pathways can be summarised as a build-up of protein (spatial) in the aging brain (temporal), in Parkinson's disease α- synuclein in the basal ganglia, amyloid proteins in cortical regions in Alzheimer's disease and stress-related proteins in ischaemic stroke in an arterial territory. TSC is emerging as pivotal to reduce the common pathology of superfluous protein accumulation and aggregation following ischaemia and neurodegeneration via induction of productive autophagy. Defective autophagy could underlie some of the pathological processes in neurodegenerative diseases (Bove *et al.,* 2011). Rapamycin restored autophagocytic flux (enhanced lysosomal biogenesis, increased autophagosome-lysosomal fusion and increased autophagosomal clearance) in an 1-methyl-4-phenyl-1,2,3,6-tetrahydropyridine (MPTP) model of Parkinson's disease (Dehay *et al.,* 2010) . In a murine model of Huntingdon's disease, inhibition of mTOR induced autophagy and reduced toxicity of polyglutamine expansions (Ravikumar *et al.,* 2004). Some mTOR activation is necessary for learning and memory, but hyperactivity leads to the cognitive defects of Alzheimer's disease (Bove *et al*., 2011). Rapamycin decreases toxicity mediated by mutant tau in transgenic flies (Khurana *et al.,* 2006). Genetic enhancement of lysosomal activity in a transgenic mouse model of AD decreased intraneuronal Aβ levels, and extracellular amyloid deposition which prevented defective

learning and memory in the animals (Yang *et al.,* 2011). Other disorders that may also be amenable to treatment by manipulation of hamartin-regulated mechanisms include spinocerebellar ataxia type 3 and amyotrophic lateral sclerosis (Bove *et al.,* 2011). In murine models suppressing basal autophagy in neural cells leads to neurodegenerative disease (Hara *et al*., 2006). ER stress has also been observed in neurodegenerative diseases such as Parkinson's and Alzheimer's (Roussel *et al*., 2013). Therefore, mTOR dysfunction could play a vital role in neurodegenerative disease and also shows the critical influence of downstream pathways such as autophagy and ER stress in brain function. Acting upstream via hamartin could be a potential mechanism by which to prevent neurodegenerative effects in these diseases.

6.3.5 Epilepsy

In addition to offering a potential therapeutic strategy for the neurodegeneration associated with increasing age, hamartin could also provide neuroprotection in diseases of younger people. This is evidenced by the fact that mTOR has a role in the development of epilepsy, a disease afflicted in young people. Mice in which TSC1 (hamartin) is knocked out had dysplastic and ectopic neurons, reduced myelination, seizure activity, and limited survival (Meikle *et al.,* 2007). In epilepsy models, the use of mTOR inhibitors can reverse some epileptogenic processes (Galanopoulou *et al.,* 2012), with effectiveness depending on time, dose and model. Impaired neuronal autophagy has been causally linked to epileptogenesis in a murine model using a forebrain-specific conditional TSC1 and phosphatase and tensin homlog knock-out mice (McMahon *et al*., 2012). Altered glutamate receptor expression has also been observed in human cortical tubers (Talos *et al.,* 2008). These results suggest that mTOR could have a critical role in epilepsy and a small molecule that could act like hamartin by inhibiting mTOR and promoting autophagy could be a potential therapeutic strategy for this disease.

6.3.6 Other pathologies

The protein complex, mTOR and its downstream effectors have also been associated with a number of other diseases. It has been shown to be cardioprotective and to suppress the inflammatory response (Aoyagi *et al.,* 2012) and cardiomyocyte death has been shown to be due to impaired autophagosome clearance (Ma *et al.,*

2012). In addition, mTOR is acutely sensitive to the macrolide, rapamycin, better known clinically as the immunosupressant, Sirolimus used post-transplant and also to prevent coronary restenosis (Das *et al*., 2012)

Dysregulated autophagy has also been implicated in HIV-associated neurocognitive disorder (HAND) (Fields *et al.,* 2015). The cancer prone disease ataxiatelangiectasia (AT) has yielded an important insight into the subcellular localisation of further effects of TSC (Alexander *et al.,* 2010). The gene mutation in AT (the cellular damage sensor, Ataxia-telangiectasia mutated (ATM)) attenuates this protein kinase and the response of cells to insults that cause double-stranded breaks in DNA (such as ionising radiation). Using studies in mice, it was demonstrated that a cytoplasmic pathway existed where ATM responded to ROS independently of double-stranded DNA breaks, acting via LKB1 and AMPK to activate TSC2, inhibit mTOR and induce autophagy (Alexander *et al.,* 2010).

6.3.7 The clinical importance of endogenous neuroprotection

Statins have pleiotropic effects, beyond their lipid lowering ability. A recent systematic review cites a dearth of controlled trials to confirm a definite beneficial neuroprotective effect in the context of human ischaemic stroke (Hong and Lee, 2015). Animal studies have demonstrated synaptogenesis, angiogenesis and neurogenesis following acute cerebral ischaemia adding a further neurorestorative angle to the suggestions of neuroprotection (Chen *et al.,* 2003).

The gold standard in treating ischaemic stroke for eligible patients, however remains, rt-PA. The underlying pathophysiological cause of the damage is lack of blood flow to the brain. Indeed the role of interventional radiology is, based on recent trials highly likely to form part of any future 'gold standard' of care (Balami *et al*., 2015). Patients that do not have strokes in hospital will have inherent delay in getting to the emergency room and the CT scanner. Any small molecule compound that does not have the potential side effect of exacerbating a haemorrhage would buy the patient time by stalling the ischaemic cascade leading to a more favourable prognosis when given clot busting treatment. The proposed mechanism for harnessing an endogenous protective mechanism is decreasing the production of (stress proteins) and increasing the removal of superfluous proteins (productive autophagy), which mTOR is intimately involved in. The underlying

pathophysiology is similar to diseases of neurodegeneration which raises the possibility of one therapeutic strategy being effective across a number of diseases. In an aging population, the prevalence of age-related disease such as stroke and neurogeneration is increasing, and so identifying mechanisms such as endogenous neuroprotection that could lead to benefit in these patient populations is critical.

6.4 Limitations and future studies

6.4.1 Limitations

There are a number of limitations that arise from the experiments in this thesis. The endogenous protective effect of hamartin is observed in hippocampal neurons and any beneficial effect in the human condition of ischaemic stroke would need to be possible in cortical neurons and the effects studied in focal models of ischaemia. Further studies in focal models will highlight the relevance of hamartin as a neuroprotectant.

The time course investigated does not completely span the time period over which the final morphological outcome in delayed neuronal death in CA1 occurs (2-3 days). Timepoints within the first 24 hours following global ischaemia were chosen as it was thought that the pathways would be altered early post-ischaemia. In order to fully elucidate potential points to intervene to halt neuronal death a more comprehensive time course covering immediately post-ischaemia to subsequent neuronal death would help to fully delineate the mechanisms of selective vulnerability and endogenous neuroprotection.

The pharmacological experiments were carried out in an *in vitro* setting. In order to map a more physiologically relevant time course of effects it would be necessary to conduct *in vivo* experiments of any promising compounds. The compounds used in the experiments were in relatively high concentrations in DMSO and although DMSO controls are used, this could still confound results. In clinical settings drugs are unlikely to be applied directly to the brain in the context of ischaemic stroke and so for any *in vivo* experiments, drugs would need to be administered using a clinically relevant dose and method.

6.4.2 Future studies

This promising area of research has opened up a number of possibilities for future studies. One major question is to which specific membrane hamartin is translocating to in order to elicit its protective effect. Immunoprecipitation of membrane markers or immunofluorescence colocalisation studies should be carried out before and after ischaemia to determine the precise location of hamartin's immediate translocation following ischaemia. In addition, revisiting the original proteomics data may demonstrate membrane proteins that are also significantly associated at the pathway and network level that could provide new leads for experimentation.

The specificity of compounds used in this thesis was not absolute, although based on existing literature or taken from those already in clinical use (e.g. metformin), alternatives could be sought. For example, 10-NCP is an alternative inducer of autophagy (Tsvetkov *et al.,* 2010) and could be used in future experiments. In addition, the time at which therapies are applied is likely to be key. For example, autophagy may increase the rate of death during ischaemia but stimulate survival during reperfusion, which may account for disagreement in the literature as to whether autophagy is neuroprotective (Carloni *et al.,* 2008, Wang *et al.,* 2012).or neurotoxic (Wen *et al.,* 2008; Zheng *et al.,* 2009). A comprehensive dose range of an ER stress inducer and autophagy inducer may provide an as yet elusive synergistic pharmacological neuroprotective effect when applied at the optimal point in the time course of any ischaemic insult as small amounts of ER stress are known to induce autophagy (Qin *et al*., 2010). The reasons behind the failure of the dual mTORC1/2 inhibitor, AZD2014 could be explained by effects on lysosomal permeability which could be further investigated with an appropriate assay. Interestingly, AZD2014 already has safety and tolerability data *in vivo* and has been used pre-clinically in mice (Zheng *et al*., 2015). The effects on isolated neuronal cultures which not only lack astrocytes but also the complexities of the mammalian brain may not be indicative of the effects on a model of stroke. An *in vivo* pilot study investigating the effects of AZD2014 following ischaemic stroke, taking into account the principles of replacement, reduction and refinement (3Rs in animal research), could further reconcile the effects of mTOR inhibition on stroke outcome.

The ability to translate findings from the rodent hippocampus to humans is key to show that these effects are conserved across species. Since the global model of ischaemia is analogous to the human condition of cardiac

arrest, a request was made to the Oxford Brain Bank for post-mortem samples from human cardiac arrest patients. Investigating changes in TSC, mTOR and downstream pathways such as autophagy (including mitophagy-related changes) and ER stress could help to determine whether these pathways would provide a suitable therapeutic target. Optimisation of calnexin (an ER membrane marker), LC3-II and hamartin staining in brain sections from rodents exposed to global ischaemia is ongoing and will also be used in human tissue. This will provide translational relevance of the hamartin signalling pathway in human brain ischaemia.

Although the global model of ischaemia provides mechanistic insight into the effects of ischaemia on hippocampal neurons, the focal model of cerebral ischemia more closely approximates the human clinical condition of ischaemic stroke. Focal ischaemia involves the occlusion of a single artery in the brain, where particular brain regions are affected depending on which artery is occluded, resulting in an infarct with a core and penumbra. The intraluminal filament model of middle cerebral artery occlusion (MCAO) (Longa *et al.,* 1989) will be used to test the hypothesis that cellular expression of hamartin and downstream mTOR proteins is altered following focal ischaemia. Translation of this work will utilise post-mortem tissue of human ischaemic stroke patients from the Oxford Brain Bank. Following this, a gene-targeted strategy will be used to assess whether upregulation of hamartin could confer neuroprotection and suppression of hamartin will be detrimental using an *in vivo* MCAO model.

The importance of preclinical research in the development of neuroprotective strategies for ischemic stroke (Neuhaus *et al*., 2014), has recently been underlined due to recent overwhelming evidence for endovascular therapy in ischaemic stroke (Balami *et al.,* 2015; Goyal *et al.,* 2016; NICE interventional procedure guidance [IPG548], 2016). Any successful therapy in acute ischaemic stroke would likely be a combination of a reperfusion strategy (thrombolysis or endovascular thrombectomy) coupled with a neuroprotectant to 'buy time' and delay the ischaemic cascade. The transient focal model provides the ideal system within which to test any potential neuroprotectants as it mimics the blood flow changes and the pathophysiology associated with thrombectomy (Sutherland *et al*., 2016) and could potentially allow researchers to 'revisit' compounds that previously lacked efficacy, as in combination with restoration of blood flow, a significant effect may be found.

Selective vulnerability of pyramidal neurons in CA1 and CA3 hippocampal regions is common to neurodegenerative conditions including Alzheimer's disease and epilepsy in addition to cardiac arrest (Mattson *et al.,* 1989). Further studies will determine whether differences in mTOR-related protein expression is associated with neuronal survival of CA3 neurons in patients with varying degrees of cognitive impairment ranging from none through to Alzheimer's disease.

Extending the findings of this thesis to wider themes of aging and neurodegeneration could use a wide variety of experimental models as the pathway is evolutionarily conserved. Human TSC1 demonstrates sequence homology with the fission yeast (*Schizosaccharomyces pombe*) TSC1 (Matsumoto *et al*., 2002). Indeed, the first 3D structure of TSC1 has recently been published in yeast (Sun *et al*., 2013) with the most conserved region being the hTSC1 region which spans the N-terminal domain (approximately 265 residues) (Sun *et al*., 2013). Studying mutations in Drosophila melanogaster homologues (dTsc1 and dTsc2) demonstrated an increase in cell and organ size (Gao and Pan 2001; Potter *et al* 2001; Tapon *et al* 2001). Significantly, a mouse model has been described in the literature (Meikle *et al*., 2007). The transgenic mouse containing TSC1 $^{\text{null-neuron}}$ Synapsin I promoter-driven cre allele was used to generate a neuronal model of TSC1 in which recombination and loss of the TSC1 gene occurs in differentiating neurons. The phenotype expressed enlarged ectopic cells, with prominent dysplasia, high level expression of pS6 and reduced myelination.

The naked mole-rat (*Heterocephalus glaber*) would be another potential model when considering hypoxia and longevity. Naked mole rats live nine times longer than laboratory mice of a similar size, demonstrating attenuated age-associated acceleration in mortality risk. Indeed, in a retrospective study of a zoo population, the most common cause of death was bite wounds and secondary complications (Delaney *et al.,* 2013). Naked mole rats also reproduce into their third decade and have an absence of characteristic signs of age related deterioration in physiological or biochemical function, until very close to their maximum lifespan. Futhermore, they exhibit good health into old age (Buffenstein, 2008). Naked mole rats do not spontaneously develop cancer and their cells demonstrate resistance to transformation (Delaney *et al.,* 2013). Naked mole rats appear to have evolved to withstand sustained periods of hypoxia and even anoxia of the brain. They live in underground colonies in low oxygen and high carbon dioxide environments, partially due to poor gas exchange in their colonies (Bennett and Faulkes, 2000). Recording of evoked activity from hippocampal slices, demonstrated that

isolated brain tissue from the naked mole-rat is remarkably tolerant to hypoxia and anoxia (Larson and Park. 2009). In addition, hippocampal slices from ground squirrels (*Citellus tridecemlineatus)* also demonstrate resistance to glucose and oxygen deprivation in the context of hibernation. It should be noted that that these animals will also be hypothermic, which can be in itself neuroprotective. The conservation of the TSC/mTOR pathway from yeast to mammals and the existence of mammals that have endogenous resistance to hypoxic injury provide exciting avenues for the further investigation of the phenomenon of endogenous neuroprotection and potential application to ischaemic stroke.

6.5 Conclusion

This thesis considers the exciting prospect that hamartin, a protein linked to an aberration of neuronal growth and development in the clinical condition of tuberous sclerosis, could be harnessed to treat a devastating disease of the brain in later life, ischaemic stroke.

Rapamycin may not be the elixir of life due to the risks of long term immunosuppression – the sterile conditions inhabited by the laboratory rats who reached a great age do not translate to the constant challenges of the immune system in everyday life. However, the mTOR pathway may indeed hold the key to diseases which blight humans in later life. Only by further dissecting the mechanism and identifying a more specific target, amenable to the design of a small molecule, will a more satisfactory answer be obtained that can be extrapolated to the clinic. For ischaemic stroke, a small molecule inhibitor would likely be used in combination therapy with clot-busing treatment, as it is the restoration of perfusion that will ultimately prevent damage within the ischaemic brain. Any small molecule that could prevent the ischaemic cascade and increase the amount of time available to image, treat, and restore blood flow to the brain would vastly improve functional outcome for ischaemic stroke patients.

The key to understanding the underlying processes of longevity and endogenous neuroprotection appear to be multifaceted. Caloric restriction and the effect of mTOR are intertwined, yet autophagy is not sufficient to explain the extended lifespan. Although clearly involved, autophagy is also not sufficient to completely explain the endogenous neuroprotection elicited by hamartin. Hamartin remains a candidate as a potential common

denominator in the not so disparate and increasingly important phenomena of morbidity-free longevity and endogenous neuroprotection, but further research is necessary to discover the complex mechanisms by which hamartin is producing these effects.

References

Abila, B., Cunningham, E. and Simeoni, M. (2013). First-time-in-human study with GSK249320, a myelin-associated glycoprotein inhibitor, in healthy volunteers. *Clin Pharmacol Ther.* **93**:163–169.

Abraham, R.T. (2015). Cell biology. Making sense of amino acid sensing. *Science* **347**(6218):128-9.

Adhami, F., Liao, G., Morozov, Y.M., Schloemer, A., Schmithorst, V.J., Lorenz, J.N., Dunn, R.S., Vorhees, C.V., Wills-Karp, M., Degen, J.L., Davis, R.J., Mizushima, N., Rakic, P., Dardzinski, B.J., Holland, S.K., Sharp, F.R. and Kuan, C.Y. (2006). Cerebral ischemia-hypoxia induces intravascular coagulation and autophagy. *Am J Pathol.***169**:566–583.

Alexander, A., Cai, S.L., Kim, J., Nanez, A., Sahin, M., MacLean, K.H., Inoki, K., Guan, K.L., Shen, J., Person, M.D., Kusewitt, D., Mills, G.B., Kastan, M.B. and Walker, C.L. (2010). ATM signals to TSC2 in the cytoplasm to regulate mTORC1 in response to ROS. *Proc Natl Acad Sci U S A.* **107**(9):4153-8.

Amaro, S. and Chamorro, Á. (2011) Translational stroke research of the combination of thrombolysis and antioxidant therapy. *Stroke* **42**(5):1495-9.

Amato, S., Liu, X., Zheng, B., Cantley, L., Rakic, P. and Man, H.Y. (2011). AMP-activated protein kinase regulates neuronal polarization by interfering with PI 3-kinase localization. *Science* **332**(6026):247-51.

Ames, A. 3rd., Wright, R.L., Kowada, M., Thurston, J.M. and Majno, G. (1968). Cerebral ischemia. II. The no-reflow phenomenon. *Am J Pathol.* **52**(2):437-53.

Andersen, M.B., Zimmer, J. and Sams-Dodd, F. (1997). Postischemic hyperactivity in the Mongolian gerbil correlates with loss of hippocampal neurons. *Behav Neurosci.* **111**(6):1205-16.

Aoyagi, T., Kusakari, Y., Xiao, C.Y., Inouye, B.T., Takahashi, M., Scherrer-Crosbie, M., Rosenzweig, A., Hara, K. and Matsui, T. (2012). Cardiac mTOR protects the heart against ischemia-reperfusion injury. Am J Physiol Heart Circ Physiol. **303**(1): H75-85.

Arai, K., Lok, J., Guo, S., Hayakawa, K., Xing, C. and Lo, E.H. (2011). Cellular mechanisms of neurovascular damage and repair after stroke. *J Child Neurol.* **26**(9):1193-8.

Arsham, A.M., Howell, J.J. and Simon, M.C. (2003). A novel hypoxia-inducible factor-independent hypoxic response regulating mammalian target of rapamycin and its targets. *The Journal of biological chemistry* **278**(32): 29655-60.

Aronowski, J., Strong, R. and Grotta, J.C. (1997). Reperfusion injury: demonstration of brain damage produced by reperfusion after transient focal ischemia in rats. *J Cereb Blood Flow Metab*. **17**(10):1048-56.

Ashabi, G., Khalaj, L., Khodagholi, F., Goudarzvand, M. and Sarkaki, A. (2015). Pre-treatment with metformin activates Nrf2 antioxidant pathways and inhibits inflammatory responses through induction of AMPK after transient global cerebral ischemia. *Metab Brain Dis.* **30**(3):747-54.

Ashford,T.P. and Porter, K.R. (1962). Cytoplasmic components in hepatic cell lysosomes. *J Cell Biol.* **12**:198-202.
Aspeslet, L.J. and Yatscoff, R.W. (2000). Requirements for therapeutic drug monitoring of sirolimus, an immunosuppressive agent used in renal transplantation. *Clin Ther.* **22** Suppl B:B86-92.

Astrinidis, A. and Henske, E.P. (2005). Tuberous sclerosis complex: linking growth and energy signaling pathways with human disease. *Oncogene* **24**:7475-81.

Astrinidis, A., Senapedis, W. and Henske, E.P. (2006). Hamartin, the tuberous sclerosis complex 1 gene product, interacts with polo-like kinase 1 in a phosphorylation-dependent manner. *Hum Mol Genet* **15**:287-97.

Astrup, J., Siesjö, B.K. and Symon, L. (1981). Thresholds in cerebral ischemia - the ischemic penumbra. *Stroke* **12**(6):723-5.

Astrup, J., Symon, L., Branston, N.,M. and Lassen, N.A. (1977). Cortical evoked potential and extracellular K^+ and H^+ at critical levels of brain ischaemia. *Stroke* **8**: 51-7.

Avruch. J., Long, X., Ortiz-Vega, S., Rapley, J., Papageorgiou, A. and Dai, N. (2009). Amino acid regulation of TOR complex 1. *Am J Physiol Endocrinol Metab* **296**:E592-602.

Axe, E.L., Walker, S.A., Manifava, M., Chandra, P., Roderick, H.L., Habermann, A., Griffiths, G. and Ktistakis, N.T. (2008). Autophagosome formation from membrane compartments enriched in phosphatidylinositol 3-phosphate anddynamically connected to the endoplasmic reticulum. *J Cell Biol.* **182**(4):685-701.

Balami, J.S., Hadley, G., Sutherland, B.A., Karbalai, H. and Buchan, A.M. (2013). The exact science of stroke thrombolysis and the quiet art of patient selection. *Brain* **136**(Pt 12):3528-53.

Balami, J.S., Sutherland, B.A., Edmunds, L.D., Grunwald, I.Q., Neuhaus, A.A., Hadley, G., Karbalai, H., Metcalf, K.A., DeLuca, G.C. and Buchan, A.M. (2015). A systematic review and meta-analysis of randomized controlled trials of endovascular thrombectomy compared with best medical treatment for acute ischemic stroke. *Int J Stroke* **10**(8):1168-78.

Banerji, U., Dean, E. and Gonzalez, M. (2012). First in-human phase I trial of the dual mTORC1 and mTORC2 inhibitor AZD2014 in solid tumors. *Journal of Clinical Oncology* **30** (suppl 3004).

Barbay, S., Plautz, E.J., Zoubina, E., Frost, S.B., Cramer, S.C. and Nudo, R.J. (2015). Effects of postinfarct myelin-associated glycoprotein antibody treatment on motor recovery and motor map plasticity in squirrel monkeys. *Stroke* **46**(6):1620-5.

Bassik, M.C., Scorrano, L., Oakes, S.A., Pozzan, T. and Korsmeyer, S.J. (2004). Phosphorylation of BCL-2 regulates ER Ca2+ homeostasis and apoptosis. *EMBO J.* **23**:1207–1216.

Basu, B., Dean, E., Puglisi, M., Greystroke, A., Ong, M., Burke, W.M., Cavallin, M., Bigley, G., Womack, C., Harrington, E.A., Green, S., Oelmann, E., de Bono, J.S., Ranson, M.R. and Banerji, U. (2015). First-in-human pharmacokinetic and pharmacodynamic study of the dual m-TORC 1/2 inhibitor, AZD2014. *Clin Cancer Res.* **21**(15):3412-9.

Bennett, N.C. and Faulkes, C.G. (2000). African mole-rats: ecology and eusociality. Cambridge: Cambridge University Press.

Benvenuto, G., Li, S., Brown, S.J., Braverman, R., Vass, W.C., Cheadle, J.P., Halley, D.J., Sampson, J.R., Wienecke, R. and DeClue, J.E. (2000). The tuberous sclerosis-1 (TSC1) gene product hamartin suppresses cell growth and augments the expression of the TSC2 product tuberin by inhibiting its ubiquitination. *Oncogene* **19**(54):6306-16.

Berkhemer. O.A., Fransen, P.S., Beumer, D., van den Berg, L.A., Lingsma, H.F., Yoo, A.J., Schonewille, W.J., Vos, J.A., Nederkoorn, P.J., Wermer, M.J., van Walderveen, M.A., Staals, J., Hofmeijer, J., van Oostayen, J.A., Lycklama à Nijeholt, G.J., Boiten, J., Brouwer, P.A., Emmer, B.J., de Bruijn, S.F., van Dijk, L.C., Kappelle, L.J., Lo, R.H., van Dijk, E.J., de Vries, J., de Kort, P.L., van Rooij, W.J., van den Berg, J.S., van Hasselt, B.A., Aerden, L.A., Dallinga, R.J., Visser, M.C., Bot, J.C., Vroomen, P.C., Eshghi, O., Schreuder, T.H., Heijboer, R.J., Keizer, K., Tielbeek, A.V., den Hertog, H.M., Gerrits, D.G., van den Berg-Vos, R.M., Karas, G.B., Steyerberg, E.W., Flach, H.Z., Marquering, H.A., Sprengers, M.E., Jenniskens, S.F., Beenen, L.F., van den Berg, R., Koudstaal, P.J., van Zwam, W.H., Roos, Y.B., van der Lugt, A., van Oostenbrugge, R.J., Majoie, C.B. and Dippel, D.W.; MR CLEAN Investigators. (2015). A randomized trial of intraarterial treatment for acute ischemic stroke. *N Engl J Med.* **372**(1):11-20.

Bernales, S., McDonald, K.L. and Walter, P. (2006). Autophagy counterbalances endoplasmic reticulum expansion during the unfolded protein response. *PLoS Biol.* **4**(12):e423.

Blagosklonny, M.V. and Hall, M.N. (2009). Growth and aging: a common molecular mechanism. *Aging* **1**(4): 357-62.

Bourneville, D. (1880). Sclérose tubéreuse des circonvolutions cérébrales: Idiotie et épilepsie hemiplégique. [Tuberous sclerosis of the cerebral cortex: intellectual disability and hemiplegic epilepsy]. *Archives de neurologie, (Paris). **1**: 81–91.*

Bove, J., Martinez-Vicente, M. and Vila, M. (2011). Fighting neurodegeneration with rapamycin: mechanistic insights. *Nat Rev Neurosci.* **12**(8): 437-52.

Boyce, M., Bryant, K.F., Jousse, C., Long, K., Harding, H.P., Scheuner, D., Kaufman, R.J., Ma, D., Coen, D.M., Ron, D. and Yuan, J. (2005). A selective inhibitor of eIF2alpha dephosphorylation protects cells from ER stress. *Science* **307**(5711):935-9.

Boyce. M. and Yuan, J. (2006). Cellular response to endoplasmic reticulum stress: a matter of life or death. *Cell Death Differ.***13**: 363–73.

Bragin, D.E., Zhou, B., Ramamoorthy, P., Müller, W.S., Connor, J.A. and Shi, H. (2010). Differential changes of glutathione levels in astrocytes and neurons in ischemic brains by two-photon imaging. *J Cereb Blood Flow Metab*. **30(**4):734-8.

Broderick, J.P., Palesch, Y.Y., Demchuk, A.M., Yeatts, S.D., Khatri, P., Hill, M.D., Jauch, E.C., Jovin, T.G., Yan, B., Silver, F.L., von Kummer, R., Molina, C.A., Demaerschalk, B.M., Budzik, R., Clark, W.M., Zaidat, O.O., Malisch, T.W., Goyal, M., Schonewille, W.J., Mazighi, M., Engelter, S.T., Anderson, C., Spilker, J., Carrozzella, J.,

Ryckborst, K.J., Janis, L.S., Martin, R.H., Foster, L.D. and Tomsick, T.A.; Interventional Management of Stroke (IMS) III Investigators. (2013). Endovascular therapy after intravenous t-PA versus t-PA alone for stroke. *N Engl J Med.* **368**(10):893-903.

Brown. E.J., Albers, M.W., Shin, T.B., Ichikawa, K., Keith, C.T., Lane, W.S. and Schreiber, S.L. (1994). A mammalian protein targeted by G1-arresting rapamycin-receptor complex. *Nature* **369**:756-8.

Brugarolas, J. and Kaelin, W.G., Jr. (2004). Dysregulation of HIF and VEGF is a unifying feature of the familial hamartoma syndromes. *Cancer Cell* **6**:7-10.

Brugarolas, J., Lei, K., Hurley, R.L., Manning, B.D., Reiling, J.H., Hafen, E., Witters, L.A., Ellisen, L.W. and Kaelin, W.G., Jr. (2004). Regulation of mTOR function in response to hypoxia by REDD1 and the TSC1/TSC2 tumor suppressor complex. *Genes Dev* **18**:2893-904.

Buchan, A.M. (1992). Do NMDA antagonists prevent neuronal injury? No. *Arch Neurol.* **49**(4):420-1.

Buchan, A.M. and Pulsinelli, W.A. (1990 a). Hypothermia but not the N-methyl-D-aspartate antagonist, MK-801, attenuates neuronal damage in gerbils subjected to transient global ischemia. *J Neurosci.* **10**(1):311-6.

Buchan AM, and Pulsinelli WA. (1990 b). Septo-hippocampal deafferentation protects CA1 neurons against ischemic injury. *Brain Res.* **512**(1): 7-14.

Buckley, K.M., Hess, D.L., Sazonova, I.Y., Periyasamy-Thandavan, S., Barrett, J.R., Kirks, R., Grace, H., Kondrikova, G., Johnson, M.H., Hess, D.C., Schoenlein, P.V., Hoda, M.N. and Hill, W.D. (2014). Rapamycin up-regulation of autophagy reduces infarct size and improves outcomes in both permanent MCAL, and embolic MCAO, murine models of stroke. *Exp Transl Stroke Med.*;**6**:8

Buffenstein R. (2008). Negligible senescence in the longest living rodent, the naked mole-rat: insights from a successfully aging species. *J Comp Physiol B.* **178**(4):439-45.

Cai, S.L., Tee, A.R., Short, J.D., Bergeron, J.M., Kim, J., Shen, J., Guo, R., Johnson, C.L., Kiguchi, K. and Walker, C.L. (2006). Activity of TSC2 is inhibited by AKT-mediated phosphorylation and membrane partitioning. *J Cell Biol.* **173**:279-89.

Calcagnotto, M.E., Paredes, M.F., Tihan, T., Barbaro, N.M. and Baraban, S.C. (2005) Dysfunction of synaptic inhibition in epilepsy associated with focal cortical dysplasia. *J Neurosci.* **25**:9649-57.

Campbell, B.C., Mitchell, P.J., Kleinig, T.J., Dewey, H.M., Churilov, L., Yassi, N., Yan, B., Dowling, R.J., Parsons, M.W., Oxley, T.J., Wu, T.Y., Brooks, M., Simpson, M.A., Miteff, F., Levi, C.R., Krause, M., Harrington, T.J., Faulder, K.C., Steinfort, B.S., Priglinger, M., Ang, T., Scroop, R., Barber, P.A., McGuinness, B., Wijeratne, T., Phan, T.G., Chong, W., Chandra, R.V., Bladin, C.F., Badve, M., Rice, H., de Villiers, L., Ma, H., Desmond, P.M., Donnan, G.A. and Davis SM; EXTEND-IA Investigators (2015). Endovascular therapy for ischemic stroke with perfusion-imaging selection. *N Engl J Med.* **372**(11):1009-18.

Cao, Y., Kamioka, Y., Yokoi, N., Kobayashi, T., Hino, O., Onodera, M., Mochizuki, N. and Nakae J. (2006). Interaction of FoxO1 and TSC2 induces insulin resistance through activation of the mammalian target of rapamycin/p70 S6K pathway. *J Biol Chem.* **281**:40242-51.

Carloni, S., Albertini, M.C., Galluzzi, L., Buonocore, G., Proietti, F. and Balduini, W. (2014). Increased autophagy reduces endoplasmic reticulum stress after neonatal hypoxia-ischemia: role of protein synthesis and autophagic pathways. *Exp Neurol.* **255**:103-12.

Carloni, S., Buonocore, G. and Balduini, W. (2008). Protective role of autophagy in neonatal hypoxia-ischemia induced brain injury. *Neurobiol Dis.* **32**(3):329-39.

Carloni, S., Buonocore, G., Longini, M., Proietti, F., Balduini, W. (2012). Inhibition of rapamycin-induced autophagy causes necrotic cell death associated with Bax/Bad mitochondrial translocation. *Neuroscience* **203**:160-9.

Cervós-Navarro, J. and Diemer, N.H. (1991). Selective vulnerability in brain hypoxia. *Crit Rev Neurobiol.* **6**(3):149-82.

Chandler, M.J., DeLeo, J. and Carney, J.M. (1985). An unanesthetized-gerbil model of cerebral ischemia-induced behavioral changes. *J Pharmacol Methods* **14**(2):137-46.

Chen, J., Nagayama, T., Jin, K., Stetler, R.A., Zhu, R.L., Graham, S.H. and Simon, R.P. (1998). Induction of caspase-3-like protease may mediate delayed neuronal death in the hippocampus after transient cerebral ischemia. J Neurosci. **18**(13):4914-28.

Chen J, Zhang ZG, Li Y, Wang Y, Wang L, Jiang H, Zhang, C., Lu, M., Katakowski, M., Feldkamp, C.S., Chopp, M.(2003). Statins induce angiogenesis, neurogenesis, and synaptogenesis after stroke. *Ann Neurol.* **53**:743–751.

Cherra, S.J. and Chu, C.T. (2008). Autophagy in neuroprotection and neurodegeneration: A question of balance. *Future Neurol* **3**:309-23.

Chiarini, F., Evangelisti, C., McCubrey, J.A. and Martelli, A.M. (2015). Current treatment strategies for inhibiting mTOR in cancer. *Trends Pharmacol Sci.* **36**(2):124-35.

Chiu. M.I., Katz, H. and Berlin, V. (1994). RAPT1, a mammalian homolog of yeast Tor, interacts with the FKBP12/rapamycin complex. *Proc Natl Acad Sci U S A* **91**:12574-8

Choi, Y.J., Di Nardo, A., Kramvis, I., Meikle, L., Kwiatkowski, D.J., Sahin, M., He, X. (2008). Tuberous sclerosis complex proteins control axon formation. *Genes Dev.* **22**(18):2485-95.

Chong-Kopera, H., Inoki, K., Li, Y., Zhu T., Garcia-Gonzalo, F.R., Rosa, J.L., Guan, K.L. (2006). TSC1 stabilizes TSC2 by inhibiting the interaction between TSC2 and the HERC1 ubiquitin ligase. *J Biol Chem.* **281**:8313-6

Choo, A.Y., Yoon, S.O., Kim, S.G., Roux, P.P. and Blenis, J. (2008). Rapamycin differentially inhibits S6Ks and 4E-BP1 to mediate cell-type-specific repression of mRNA translation. *Proc Natl Acad Sci U S A.* 2008 **105**(45):17414-9.

Ciccone, A., Valvassori, L., Nichelatti, M., Sgoifo, A., Ponzio M., Sterzi, R. and Boccardi, E; SYNTHESIS Expansion Investigators. (2013). Endovascular treatment for acute ischemic stroke. *N Engl J Med.* **368**(10):904-13.

Clark, D.L., DeBow, S.B., Iseke, M.D., and Colbourne, F. (2003). Stress induced fever after postischemic rectal temperature measurements in the gerbil. *Can. J. Physiol. Pharmacol.* **81**: 880–883.

Clark D.L., DeButte-Smith M. and Colbourne F. (2007). Spontaneous temperature changes in the 2-vessel occlusion model of cerebral ischemia in rats. *Can J Physiol Pharmacol.* **85**(12):1263-8.

Clarke, P.G.H. (1990). Developmental cell death: morphological diversity and multiple mechanisms. *Anat Embryol (Berl)* **181**:195–213.

Clinical Trials.gov website: https://clinicaltrials.gov/ Accessed 13/01/16

Coimbra, C., Boris-Moller, F., Drake, M., and Wieloch, T. (1996). Diminished neuronal damage in the rat brain by late treatment with the antipyretic drug dipyrone or cooling following cerebral ischemia. *Acta Neuropathol. (Berl.)* **92**: 447–453.

Colbourne, F. and Corbett, D. (1995). Delayed postischemic hypothermia: a six month survival study using behavioral and histological assessments of neuroprotection. *J Neurosci.* **15**(11):7250-60.

Colbourne, F., Li H. and Buchan, A.M.(1999 a). Indefatigable CA1 sector neuroprotection with mild hypothermia induced 6 hours after severe forebrain ischemia in rats. Journal of cerebral blood flow and metabolism. **19**(7): 742-9.

Colbourne F., Li, H., Buchan, A.M. and Clemens, J.A. (1999 b) Continuing postischemic neuronal death in CA1: influence of ischemia duration and cytoprotective doses of NBQX and SNX-111 in rats. *Stroke* **30**(3): 662-8.

Cramer, S.C., Abila, B., Scott, N.E., Simeoni, M. and Enney, L.A. MAG111539 Study Investigators. (2013). Safety, pharmacokinetics, and pharmacodynamics of escalating repeat doses of GSK249320 in patients with stroke. *Stroke* **44**(5):1337-42.

Crino, P.B. (2004). Molecular pathogenesis of tuber formation in tuberous sclerosis complex. *J Child Neurol*. **19**(9):716-25.

Crino, P.B., Nathanson, K.L. and Henske, E.P. (2006) The tuberous sclerosis complex. *N Engl J Med* 355:1345-56

Cui, D.R., Wang, L., Jiang, W., Qi, A.H., Zhou, Q.H. and Zhang, X.L. (2013). Propofol prevents cerebral ischemia-triggered autophagy activation and cell death in the rat hippocampus through the NF-κB/p53 signaling pathway. *Neuroscience* **246**:117-32.

Curatolo, P., Bombardieri, R. and Jozwiak, S. (2008). Tuberous sclerosis. *Lancet* **372**(9639):657-68.

Das, A., Salloum, F.N., Durrant, D., Ockaili, R. and Kukreja, R.C. (2012). Rapamycin protects against myocardial ischemia-reperfusion injury through JAK2-STAT3 signaling pathway. *J Mol Cell Cardiol.* **53**(6): 858-69.

Damme. M., Suntio, T., Saftig, P. and Eskelinen, E.L. (2015). Autophagy in neuronal cells: general principles and physiological and pathological functions. *Acta Neuropathol.* **129**(3):337-62.

De Duve, C. (1963). The lysosome. *Sci Am.* **208**: 64-72.

Dehay, B., Bove, J., Rodriguez-Muela, N., Perier, C., Recasens, A., Boya P. and Vila, M. (2010). Pathogenic lysosomal depletion in Parkinson's disease. J Neurosci. **30**(37): 12535-44.

Del Bene, A., Palumbo, V., Lamassa, M., Saia, V., Piccardi, B. and Inzitari, D. (2012). Progressive lacunar stroke: review of mechanisms, prognostic features, and putative treatments. *Int J Stroke* **7**:321-329

Del Zoppo, G.J. (2013). Toward the neurovascular unit. A journey in clinical translation: 2012 Thomas Willis Lecture. Stroke **44**(1):263-9.

Delaney, M.A., Nagy, L., Kinsel, M.J. and Treuting, P.M. (2013). Spontaneous histologic lesions of the adult naked mole rat (*Heterocephalus glaber*): a retrospective survey of lesions in a zoo population. *Vet Pathol.* **50**(4):607-21.

Denton, D., Shravage, B., Simin R., *Mills, K., Berry, D.L.,* Baehrecke, E.H. and Kumar, S. (2009). Autophagy, not apoptosis, is essential for midgut cell death in *Drosophila. Curr Biol*. **19**:1741–1746.

Deshpandem J,, Bergstedt, K., Linden, T., Kalimo, H. and Wieloch, T. (1992). Ultrastructural changes in the hippocampal CA1 region following transient cerebral ischemia: evidence against programmed cell death. Experimental brain research Experimentelle Hirnforschung Experimentation cerebrale. **88**(1): 91-105.

DeYoung, M.P., Horak, P., Sofer, A., Sgroi, D. and Ellisen, L.W. (2008). Hypoxia regulates TSC1/2-mTOR signaling and tumor suppression through REDD1-mediated 14-3-3 shuttling. *Genes Dev.* **22**:239-51

Di Nardo, A., Kramvis, I., Cho, N., Sadowski, A., Meikle, L., Kwiatkowski, D.J. and Sahin, M. (2009). Tuberous sclerosis complex activity is required to control neuronal stress responses in an mTOR-dependent manner. J Neurosci. **29**(18): 5926-37.

Di Nardo A., Wertz, M.H., Kwiatkowski, E., Tsai, P.T., Leech, J.D., Greene-Colozzi, E,, Goto, J., Dilsiz, P., Talos, D.M., Clish, C.B., Kwiatkowski, D.J. and Sahin M. (2014). Neuronal Tsc1/2 complex controls autophagy through AMPK-dependent regulation of ULK1. *Hum Mol Genet.* **23**(14):3865-74.

Dibble, C.C., Elis, W., Menon, S., Qin, W., Klekota, J., Asara, J.M., Finan, P.M., Kwiatkowski, D.J., Murphy, L.O. and Manning, B.D. (2012). TBC1D7 is a third subunit of the TSC1-TSC2 complex upstream of mTORC1. *Mol Cell*. **47**(4):535-46.

Diener, H.C., Lees, K.R., Lyden, P., Grotta, J., Davalos, A., Davis, S.M., Shuaib, A., Ashwood, T., Wasiewski, W., Alderfer, V., Hårdemark, H.G. and Rodichok, L; SAINT I and II Investigators. (2008). NXY-059 for the treatment of acute stroke: pooled analysis of the SAINT I and II Trials. *Stroke* **39**(6):1751-8.

Demetriades, C, Doumpas, N. and Teleman, A.A. (2014). Regulation of TORC1 in response to amino acid starvation via lysosomal recruitment of TSC2. *Cell* **156**(4):786-99.

Dirnagl, U., Becker, K. and Meisel, A. (2009). Preconditioning and tolerance against cerebral ischaemia: from experimental strategies to clinical use. *Lancet Neurol.* **8**: 398–412

Dirnagl, U. and Endres, M. (2014). Found in translation: preclinical stroke research predicts human pathophysiology, clinical phenotypes, and therapeutic outcomes. *Stroke* **45**(5):1510-8.

Dirnagl, U., Hakim, A., Macleod, M., Fisher, M., Howells, D., Alan, S.M., Steinberg, G., Planas, A., Boltze, J., Savitz, S., Iadecola, C. and Meairs, S. (2013). A concerted appeal for international cooperation in preclinical stroke research. Stroke **44**(6):1754-60.

Duvernoy, H.M., Cattin, F., Naidich, T.P., Raybaud, C. P., Risold, P.Y., Salvolini,, U., Scarabine, U. (2005). *The Human Hippocampus: Functional Anatomy, Vascularization and Serial Sections with MRI,* 3rd edition New York: Springer-Verlag.

Efeyan, A., Zoncu, R., and Sabatini, D.M. (2012). Amino acids and mTORC1:from lysosomes to disease. *Trends Mol. Med.* **18**, 524–533.

Eklöf, B. and Siesjö, B.K. (1972). The effect of bilateral carotid artery ligation upon the blood flow and the energy state of the rat brain. *Acta Physiol Scand.* **86**(2):155-65.

El-Mir. M.Y., Detaille, D., R-Villanueva, G., Delgado-Esteban, M., Guigas, B., Attia, S., Fontaine, E., Almeida, A. and Leverve, X. (2008). Neuroprotective role of antidiabetic drug metformin against apoptotic cell death in primary cortical neurons. *J Mol Neurosci.* **34**(1):77-87.

Eltzschig, H.K. and Eckle, T. (2011). Ischemia and reperfusion—from mechanism to translation. *Nat Med.* **17**(11):1391-401.

European Chromosome 16 Tuberous Sclerosis Consortium Identification and characterization of the tuberous sclerosis gene on chromosome 16. (1993). *Cell* **75**(7): 1305-15.

European Stroke Organisation (ESO) Executive Committee; ESO Writing Committee. Guidelines for management of ischaemic stroke and transient ischaemic attack. (2008). *Cerebrovasc Dis.* **25**(5):457-507.

Fang, Y., Tan, J. and Zhang, Q. (2015). Signaling pathways and mechanisms of hypoxia-induced autophagy in the animal cells. *Cell Biol Int.* **39**(8):891-8.

Ferrer, I., Tortosa, A., Macaya, A., Sierra, A., Moreno, D., Munell, F., Blanco, R., and Squier, W. (1994). Evidence of nuclear DNA fragmentation following hypoxia-ischemia in the infant rat brain, and transient forebrain ischemia in the adult gerbil. *Brain Pathol.* **4**(2): 115-22.

Fields, J., Dumaop, W., Elueteri, S., Campos, S., Serger, E., Trejo, M., Kosberg, K., Adame, A., Spencer, B., Rockenstein, E., He, J.J., Masliah, E. (2015). HIV-1 Tat alters neuronal autophagy by modulating autophagosome fusion to the lysosome: implications for HIV-associated neurocognitive disorders. *J Neurosci.* **35**(5):1921-38.

Finkel, T. (2015). The metabolic regulation of aging. *Nat Med.* **21**(12):1416-23.

Fletcher. L., Evans, T.M., Watts, L.T., Jimenez, D.F. and Digicaylioglu, M. (2013). Rapamycin treatment improves neuron viability in an in vitro model of stroke. *PLoS* **8**(7):e68281.

Fontana, L., Adelaiye, R.M., Rastelli, A.L., Miles, K.M., Ciamporcero, E., Longo, V.D., Nguyen, H., Vessella, R. and Pili, R. (2013). Dietary protein restriction inhibits tumor growth in human xenograft models. *Oncotarget.* **4**(12):2451-61.

Fontana, L. and Partridge, L (2015). Promoting health and longevity through diet: from model organisms to humans. *Cell* **161**(1):106-18.

Fouillet, A., Levet, C., Virgone, A., Robin, M., Dourlen, P., Rieusset, J., Belaidi, E., Ovize, M., Touret, M., Nataf, S. and Mollereau, B. (2012). ER stress inhibits neuronal death by promoting autophagy. **8**(6):915-26.

Freilinger, A., Rosner, M. and Hengstschläger, M. (2006). Tuberin negatively affects BCL-2's cell survival function. *Amino Acids* **30**(4):391-6.

Frerichs, K.U. and Hallenbeck, J.M. (1998). Hibernation in ground squirrels induces state and species-specific tolerance to hypoxia and aglycemia: an *in vitro* study in hippocampal slices. *J Cereb Blood Flow Metab.* **18**(2):168-75.

Frerichs, K.U., Sirén, A.L., Feuerstein, G.Z. and Hallenbeck, J.M. (1992). The onset of postischemic hypoperfusion in rats is precipitous and may be controlled by local neurons. *Stroke* **23**(3):399-406.

Friede, RL (1966) The histochemical architecture of the Ammon's horn as related tom its selective vulnerability. *Acta Neuropathol.* **6**:1-13.

Fukuda, T., Kobayashi, T., Momose, S., Yasui, H. and Hino, O. (2000) Distribution of Tsc1 protein detected by immunohistochemistry in various normal rat tissues and the renal carcinomas of Eker rat: detection of limited colocalization with Tsc1 and Tsc2 gene products in vivo. *Lab Invest* **80**:1347-59.

Gabryel, B., Kost, A. and Kasprowska, D. (2012). Neuronal autophagy in cerebral ischemia--a potential target for neuroprotective strategies? Pharmacol Rep. **64**(1):1-15.

Galanopoulou, A.S., Gorter, J.A. and Cepeda, C. (2012). Finding a better drug for epilepsy: the mTOR pathway as an antiepileptogenic target. *Epilepsia* **53**(7): 1119-30.

Gao, B., Zhang, X.Y., Han, R., Zhang, T.T., Chen, C., Qin, Z.H. and Sheng, R. (2013). The endoplasmic reticulum stress inhibitor salubrinal inhibits the activation of autophagy and neuroprotection induced by brain ischemic preconditioning. *Acta Pharmacol Sin.* **34**(5):657-66.

Gao, X. and Pan, D. (2001). TSC1 and TSC2 tumor suppressors antagonize insulin signaling in cell growth. *Genes Dev.* **15**(11):1383-92.

Gerhardt, S.C. and Boast, C.A. (1988). Motor activity changes following cerebral ischemia in gerbils are correlated with the degree of neuronaldegeneration in hippocampus. *Behav Neurosci.* **102**(2):301-3, 328.

Gidday, J.M. (2006). Cerebral preconditioning and ischaemic tolerance. *Nat Rev Neurosci.* **7**(6):437-48.

Ginet, V., Pittet, M.P., Rummel, C., Osterheld, M.C., Meuli, R., Clarke, P.G., Puyal, J. and Truttmann, A.C. (2014). Dying neurons in thalamus of asphyxiated term newborns and rats are autophagic .*Ann Neurol* **76**(5):695-711.

Gomez, E., Powell, M.L., Bevington, A., Herbert, T.P. (2008). A decrease in cellular energy status stimulates PERK-dependent eIF2alpha phosphorylation and regulates protein synthesis in pancreatic beta-cells. *Biochem J.* **410**(3):485-93.

Gong, G., Hu, L., Liu, Y., Bai, S., Dai, X., Yin, L., Sun, Y., Wang, X. and Hou, L. (2014). Upregulation of HIF-1α protein induces mitochondrial autophagy in primary cortical cell cultures through the inhibition of the mTOR pathway. *Int J Mol Med.* **34**(4):1133-40.

Goyal, M., Demchuk, A.M., Menon, B.K., Eesa, M., Rempel, J.L., Thornton, J., Roy, D., Jovin, T.G., Willinsky, R.A., Sapkota, B.L., Dowlatshahi, D., Frei, D.F., Kamal, N.R., Montanera, W.J., Poppe, A.Y., Ryckborst, K.J., Silver, F.L., Shuaib, A., Tampieri, D., Williams, D., Bang, O.Y., Baxter, B.W., Burns, P.A., Choe, H., Heo, J.H., Holmstedt, C.A., Jankowit,z B., Kelly, M., Linares, G., Mandzia, J.L., Shankar, J., Sohn, S.I., Swartz, R.H., Barber, P.A., Coutts, S.B., Smith, E.E., Morrish, W.F., Weill, A., Subramaniam, S., Mitha, A.P., Wong, J.H., Lowerison, M.W., Sajobi, T.T. and Hill, M.D; ESCAPE Trial Investigators. (2015). Randomized assessment of rapid endovascular treatment of ischemic stroke. *N Engl J Med.* **372**(11):1019-30.

Goyal, M., Menon, B.K., van Zwam, W.H., Dippel, D.W., Mitchell, P.J., Demchuk, A.M., Dávalos, A., Majoie, C.B., van der Lugt, A., de Miquel, M.A., Donnan, G.A., Roos, Y.B., Bonafe, A., Jahan, R., Diener, H.C., van den Berg, L.A., Levy, E.I., Berkhemer, O.A., Pereira, V.M., Rempel, J., Millán, M., Davis, S.M., Roy, D., Thornton, J., Román, L.S., Ribó, M., Beumer, D., Stouch, B., Brown, S., Campbell, B.C., van Oostenbrugge, R.J., Saver, J.L., Hill, M.D., Jovin, T.G. (2016) HERMES collaborators. Endovascular thrombectomy after large vessel ischaemic stroke: a metaanalysis of individual patient data from five randomised trials. *Lancet* Feb 18. pii: S0140-6736(16)00163-X. doi: 10.1016/S0140-6736(16)00163-X. [Epub ahead of print]

Guertin, D.A. and Sabatini, D.M. (2007). Defining the role of mTOR in cancer. *Cancer Cell* **12**(1):9-22.

Guidelines for management of ischaemic stroke and transient ischaemic attack 2008. *Cerebrovasc Dis*. (2008); **25**(5): 457-507.

Guillemin,I., Becker, M., Ociepka, K., Friauf, E. and Nothwang, H.G. (2005). A subcellular prefractionation protocol for minute amounts of mammalian cell cultures and tissue. *Proteomics* **5**: 35-45.

Gürsoy-Ozdemir, Y, Can, A. and Dalkara, T. (2004). Reperfusion-induced oxidative/nitrative injury to neurovascular unit after focal cerebral ischemia. *Stroke* 35(6):1449-53.

Gustafsson, A., B. and Gottlieb, R.A. (2008). Eat your heart out: Role of autophagy in myocardial ischemia/reperfusion. *Autophagy* **4**(4):416-21.

Gutmann, D.H., Zhang, Y., Hasbani, M.J., Goldberg, M.P., Plank, T.L. and Petri Henske E. (2000). Expression of the tuberous sclerosis complex gene products, hamartin and tuberin, in central nervous system tissues. *Acta Neuropathol.* **99**(3):223-30.

Guo., W, Feng, G, Miao, Y., Liu, G. and Xu, C. (2014). Rapamycin alleviates brain edema after focal cerebral ischemia reperfusion in rats. *Immunopharmacol Immunotoxicol.* **36**(3):211-23.

Hafting, T., Fyhn, M., Molden, S., Moser, M.B., and Moser, E.I. (2005). Microstructure of spatial map in the entorhinal cortex. *Nature* **436**, 801-806.

Halaby, I.A., Takeda, Y., Yufu, K., Nowak, T.S. Jr. and Pulsinelli, W.A. (2004). Depolarization thresholds for hippocampal damage, ischemic preconditioning, and changes in gene expression after global ischemia in the rat. *Neurosci Lett.* **372**(1-2):12-6.

Hall, C.N., Reynell, C., Gesslein, B., Hamilton, N.B., Mishra, A., Sutherland, B.A., O'Farrell, F.M., Buchan, A.M., Lauritzen, M. and Attwell, D. (2014). Capillary pericytes regulate cerebral blood flow in health and disease. *Nature* **508**(7494):55-60.

Han, J.M. and Sahin, M. (2011). TSC1/TSC2 signaling in the CNS. *FEBS Lett.* **585**(7):973-80.

Hara, T., Nakamura, K., Matsui, M., Yamamoto, A., Nakahara, Y., Suzuki-Migishima, R., Yokoyama, M., Mishima, K., Saito, I., Okano, H. and Mizushima, N. (2006). Suppression of basal autophagy in neural cells causes neurodegenerative disease in mice. *Nature* **441**(7095): 885-9.

Hardie, D.G. (2004). The AMP-activated protein kinase pathway--new players upstream and downstream. Journal of cell science **117**(Pt 23): 5479-87.

Harputlugil, E., Hine, C., Vargas, D, Robertson, L., Manning, B.D. and Mitchell, J.R. (2014). The TSC complex is required for the benefits of dietary protein restriction on stress resistance in vivo. *Cell Rep.* **8**(4):1160-70.

Harrington, L.S., Findlay, G.M., Gray, A., Tolkacheva, T., Wigfield, S., Rebholz, H., Barnett, J., Leslie, N.R., Cheng, S., Shepherd, P.R., Gout, I., Downes, C.P. and Lamb, R.F. (2004). The TSC1-2 tumor suppressor controls insulin-PI3K signaling via regulation of IRS proteins. *J Cell Biol.* **166**(2):213-23.

Harrington, L.S., Findlay, G.M. and Lamb, R.F. (2005). Restraining PI3K: mTOR signalling goes back to the membrane. *Trends Biochem Sci.* **30**(1):35-42.

Harrison, D.E., Strong, R., Sharp, Z.D., Nelson, J.F., Astle, C.M., Flurkey, K., Nadon, N.L, Wilkinson, J.E., Frenkel, K., Carter, C.S., Pahor, M., Javors, M.A., Fernandez, E. and Miller, R.A. (2009). Rapamycin fed late in life extends lifespan in genetically heterogeneous mice. *Nature* **460**(7253): 392-5.

Hayashi, T., Saito, A., Okuno, S., Ferrand-Drake, M., Dodd, R.L., Chan, P.H. (2005). Damage to the endoplasmic reticulum and activation of apoptotic machinery by oxidative stress in ischemic neurons. *J Cereb Blood Flow Metab.* **25**(1): 41-53.

Hayashi, T., Saito, A., Okuno, S., Ferrand-Drake, M., Dodd, R.L., Nishi, T., Maier, C.M., Kinouchi, H., Chan, P.H. (2003). Oxidative damage to the endoplasmic reticulum is implicated in ischemic neuronal cell death. *J Cereb Blood Flow Metab.* **23**(10):1117-28.

Heitman, J., Movva, N.R. and Hall, M.N. (1991). Targets for cell cycle arrest by the immunosuppressant rapamycin in yeast. *Science* **253**:905-9

Heron, A., Pollard, H., Dessi, F., Moreau, J., Lasbennes, F., Ben-Ari, Y. and Charriaut-Marlangue, C. (1993). Regional variability in DNA fragmentation after global ischemia evidenced by combined histological and gel electrophoresis observations in the rat brain. Journal of neurochemistry. **61**(5): 1973-6.

Hetz, C., Bernasconi, P., Fisher, J., Lee, A.H., Bassik, M.C., Antonsson, B., Brandt, G.S., Iwakoshi, N.N., Schinzel, A., Glimcher, L.H. and Korsmeyer, S.J. (2006). Proapoptotic BAX and BAK modulate the unfolded protein response by a direct interaction with IRE1alpha. *Science* **312**(5773):572-6.

Hetz, C. and Mollereau, B. (2014). Disturbance of endoplasmic reticulum proteostasis in neurodegenerative diseases. *Nat Rev Neurosci.* **15**(4):233-49.

Hickey, R.W., Ferimer, H., Alexander, H.L., Garman, R.H., Callaway, C.W., Hicks, S., Safar, P., Graham, S.H. and Kochanek, P.M. (2000). Delayed, spontaneous hypothermia reduces neuronal damage after asphyxial cardiac arrest in rats. *Crit. Care Med.* **28**:3511–3516.

Hong, K.S. and Lee, J.S. (2015). Statins in Acute Ischemic Stroke: A Systematic Review. *J Stroke.* **17**(3):282-301.

Hoogeveen-Westerveld, M., Exalto, C., Maat-Kievit, A., van den Ouweland, A., Halley, D., Nellist, M. (2010). Analysis of TSC1 truncations defines regions involved in TSC1 stability, aggregation and interaction. *Biochim Biophys Acta* **1802**(9):774-81.

Hossmann, K.A. (1997). Reperfusion of the brain after global ischemia: hemodynamic disturbances. *Shock* **8**(2):95-101; discussion 102-3.

Hsieh, A.C., Costa, M., Zollo, O., Davis, C., Feldman, M.E, Testa, J.R., Meyuhas, O, Shokat, K.M., Ruggero, D. (2010). Genetic dissection of the oncogenic mTOR pathway reveals druggable addiction to translational control via 4EBP-eIF4E. *Cancer Cell* **17**:249–261.

Huang. J. and Manning, B.D. (2008). The TSC1-TSC2 complex: a molecular switchboard controlling cell growth. *Biochem J* **412**:179-90.

Huang, X., Chen, Y., Zhang, H., Ma, Q., Zhang, Y.W. and Xu, H. (2012). Salubrinal attenuates β-amyloid-induced neuronal death and microglial activation by inhibition of the NF-κB pathway. *Neurobiol Aging* **33(**5):1007.e9-17.

Huo, H.Z., Zhou, Z.Y., Wang, B., Qin, J., Liu, W.Y. and Gu, Y. (2014). Dramatic suppression of colorectal cancer cell growth by the dual mTORC1 and mTORC2 inhibitor AZD-2014. Biochem Biophys Res Commun. **443**(2):406-12.

Hyman, B.T., Van Hoesen, G.W., Damasio, A.R. and Barnes, C.L. (1984). Alzheimer's disease: cell-specific pathology isolates the hippocampal formation. *Science* **225**(4667):1168-70.

Imai, T., Kosuge, Y., Endo-Umeda, K., Miyagishi, H., Ishige, K., Makishima, M. and Ito, Y. (2014). Protective effect of S-allyl-L-cysteine against endoplasmic reticulum stress-induced neuronal death is mediated by inhibition of calpain. *Amino Acids* **46**(2):385-93.

Inoki, K., Corradetti, M.N. and Guan, K.L. (2005). Dysregulation of the TSC-mTOR pathway in human disease. *Nat Genet.* **37**(1):19-24.

Inoki, K. and Guan, K.L. (2009). Tuberous sclerosis complex, implication from a rare genetic disease to common cancer treatment. *Hum Mol Genet.* **18**(R1):R94-100.

Inoki, K., Ouyang, H., Zhu, T., Lindvall, C., Wang, Y., Zhang, X., Yang, Q., Bennett, C., Harada, Y., Stankunas, K., Wang, C.Y., He, X., MacDougald, O.A., You, M., Williams, B.O. and Guan, K.L. (2006). TSC2 integrates Wnt and energy signals via a coordinated phosphorylation by AMPK and GSK3 to regulate cell growth. *Cell* **126**:955-68

Inoki, K., Zhu, T. and Guan, K.L. (2003). TSC2 mediates cellular energy response to control cell growth and survival. *Cell* **115**(5):577-90.

Inoue, H., Ndong, M., Suzuki, T., Kazami, M., Uyama, T., Kobayashi, K., Tadokoro, T. and Yamamoto, Y. (2009). Hamartin-Hsp70 interaction is necessary for Akt-dependent tuberin phosphorylation during heat shock. *Biosci Biotechnol Biochem.* 73(11):2488-93.

Inoue, H., Uyama, T., Suzuki, T., Kazami, M., Hino, O., Kobayashi, T., Kobayashi, K., Tadokoro, T. and Yamamoto, Y. (2010). Phosphorylated hamartin-Hsp70 complex regulates apoptosis via mitochondrial localization. *Biochem Biophys Res Commun.* **391**(1):1148-53.

Irving, E.A., Vinson, M., Rosin, C., Roberts, J.C., Chapman, D.M., Facci, L., Virley, D.J., Skaper, S.D., Burbidge, S.A., Walsh, F.S., Hunter, A.J. and Parsons, A.A. (2005). Identification of neuroprotective properties of anti-MAG antibody: a novel approach for the treatment of stroke? *J Cereb Blood Flow Metab.* **25**(1):98-107.

Ji, J. and Maren, S. (2008). Differential roles for hippocampal areas CA1 and CA3 in the contextual encoding and retrieval of extinguished fear. *Learn Mem.* **15**(4):244-51.

Jiang, T., Yu, J.T., Zhu, X.C., Wang, H.F., Tan, M.S., Cao, L., Zhang, Q.Q., Gao, L., Shi, J.Q., Zhang, Y.D. and Tan, L. (2014) Acute metformin preconditioning confers neuroprotection against focal cerebral ischemia by pre-activation of AMPK-dependent autophagy. *Br J Pharmacol.* **171**(13):3146-57.

Johnson, M.W., Kerfoot, C., Bushnell, T., Li, M. and Vinters HV. (2001). Hamartin and tuberin expression in human tissues. *Mod Pathol.* **14**(3):202-10.

Jørgensen, M.B., Finsen, B.R., Jensen, M.B., Castellano, B., Diemer, N.H. and Zimmer, J. (1993). Microglial and astroglial reactions to ischemic and kainic acid-induced lesions of the adult rat hippocampus. *Exp Neurol.* **120**(1):70-88

Jovin, T.G., Chamorro, A., Cobo, E., de Miquel, M.A., Molina, C.A., Rovira, A., Román, L.S., Serena, J., Abilleira, S., Ribó, M., Millán, M., Urra, X., Cardona, P., López-Cancio, E., Tomasello, A., Castaño, C., Blasco, J., Aja, L., Dorado, L., Quesada, H., Rubiera, M., Hernandez-Pérez, M., Goyal, M., Demchuk, A.M., von Kummer, R., Gallofré, M. and Dávalos, A.; REVASCAT Trial Investigators. (2015). Thrombectomy within 8 Hours after Symptom Onset in Ischemic Stroke. *N Engl J Med.* **372**(24):2296-306.

Jozwiak, J. (2006). Hamartin and tuberin: working together for tumour suppression. *Int J Cancer* **118**(1):1-5.

Jozwiak, J., Jozwiak, S., Grzela, T. and Lazarczyk, M. (2005). Positive and negative regulation of TSC2 activity and its effects on downstream effectors of the mTOR pathway. *Neuromolecular Med.* **7**(4):287-96.

Kaasik, A., Rikk, T., Piirsoo, A., Zharkovsky T. and Zharkovsky, A. (2005). Up-regulation of lysosomal cathepsin L and autophagy during neuronal death induced by reduced serum and potassium. *Eur J Neurosci.* **22**(5):1023-31.

Kabeya, Y., Mizushima, N., Ueno, T., Yamamoto, A., Kirisako, T., Noda, T., Kominami, E., Ohsumi, Y. and Yoshimori, T. (2000). LC3, a mammalian homologue of yeast Apg8p, is localized in autophagosome membranes afterprocessing. *EMBO J.* **19**(21):5720-8.

Kabeya, Y., Mizushima, N., Yamamoto, A., Oshitani-Okamoto, S., Ohsumi, Y. and Yoshimori, T. (2004). LC3, GABARAP and GATE16 localize to autophagosomal membrane depending on form-II formation. *J Cell Sci*. **117**(Pt 13):2805-12.

Kahn, J., Hayman, T.J., Jamal, M., Rath, B.H., Kramp, T., Camphausen, K., Tofilon, P.J. (2014). The mTORC1/mTORC2 inhibitor AZD2014 enhances the radiosensitivity of glioblastoma stem-like cells. *Neuro Oncol.* **16**(1):29-37.

Kang, Y.J., Lu, M.K., and Guan, K.L. (2011). The TSC1 and TSC2 tumor suppressors are required for proper ER stress response and protect cells from ER stress-induced apoptosis. *Cell Death Differ.* **18**(1):133-44.

Kapahi, P., Zid, B.M., Harper, T., Koslover, D., Sapin, V. and Benzer, S. (2004).Regulation of lifespan in *Drosophila* by modulation of genes in the TOR signaling pathway. *Curr. Biol.* **14**:885–890.

Kasznicki, J., Sliwinska, A. and Drzewoski, J. (2014). Metformin in cancer prevention and therapy. *Ann. Transl. Med.* **2**:57.

Kesner, R.P. (2007). Behavioral functions of the CA3 subregion of the hippocampus. *Learn Mem.* **14**(11):771-81.

Khurana, V., Lu, Y., Steinhilb, M.L., Oldham, S., Shulman, J.M., Feany, M.B. (2006). TOR-mediated cell-cycle activation causes neurodegeneration in a *Drosophila* tauopathy model. *Curr Biol.* **16**(3): 230-41.

Kidwell, C.S., Jahan, R., Gornbein, J., Alger, J.R., Nenov, V., Ajani, Z., Feng, L., Meyer, B.C., Olson, S., Schwamm, L.H., Yoo, A.J., Marshall, R.S., Meyers, P.M., Yavagal, D.R., Wintermark, M., Guzy, J., Starkman, S. and Saver, J.L.; MR RESCUE Investigators. (2013). A trial of imaging selection and endovascular treatment for ischemic stroke. *N Engl J Med.* **368**(10):914-23.

Kihara, A., Kabeya, Y., Ohsumi, Y. and Yoshimori, T. (2001). Beclin-phosphatidylinositol 3-kinase complex functions at the trans-Golgi network. *EMBO Rep.* **2**:330–335.

Kim, J., Kundu, M., Viollet, B and Guan, K.L. (2011). AMPK and mTOR regulate autophagy through direct phosphorylation of Ulk1. *Nat Cell Biol.* **13**(2):132-41.

Kirino, T. (1982). Delayed neuronal death in the gerbil hippocampus following ischemia. *Brain Res.* **239**(1):57-69.

Kirino, T. (2000). Delayed neuronal death. *Neuropathology* **20** Suppl:S95-7.

Kirino, T. and Sano, K. (1984). Fine structural nature of delayed neuronal death following ischemia in the gerbil hippocampus. *Acta neuropathologica* **62**(3): 209-18.

Kirino, T., Tamura, A. and Sano, K. (1984). Delayed neuronal death in the rat hippocampus following transient forebrain ischemia. *Acta Neuropathol.* **64**(2):139-47.

Kirkwood, T. (2010). Why can't we live forever? *Sci Am.* **303**(3):42-9.

Kitagawa, K., Matsumoto, M., Tagaya, M., Hata, R., Ueda, H., Niinobe, M., Handa, N., Fukunaga, R., Kimura, K., Mikoshiba, K. and Kamada, T. (1990). 'Ischemic tolerance' phenomenon found in the brain. *Brain Res.* **528**(1):21-4.

Klionsky, D.J. *et al.* (2008). Guidelines for the use and interpretation of assays for monitoring autophagy in higher eukaryotes. *Autophagy* **4**:151–175.

Koike, M., Shibata, M., Tadakoshi M., Gotoh, K., Komatsu, M., Waguri, S., Kawahara, N., Kuida, K., Nagata, S., Kominami, E., Tanaka, K. and Uchiyama, Y. (2008). Inhibition of autophagy prevents hippocampal pyramidal neuron death after hypoxic-ischemic injury. *Am J Pathol.* **172**:454–469.

Komatsu, M., Waguri, S., Chiba, T., Murata, S., Iwata, J., Tanida, I., Ueno, T., Koike, M., Uchiyama, Y., Kominami, E. and Tanaka, K. (2006). Loss of autophagy in the central nervous system causes neurodegeneration in mice. *Nature* **441**(7095):880-4.

Korennykh, A. and Walter, P. (2012). Structural basis of the unfolded protein response. *Annu Rev Cell Dev Biol.* **28**:251-77.

Kragh, J., Bolwig, T.G., Woldbye, D.P. and Jørgensen, O.S. (1993). Electroconvulsive shock and lidocaine-induced seizures in the rat activate astrocytes as measured by glial fibrillary acidic protein. *Biol Psychiatry* **33**(11-12):794-800.

Kulbe, J.R., Mulcahy Levy, J.M., Coultrap, S.J., Thorburn, A. and Bayer, K.U. (2014). Excitotoxic glutamate insults block autophagic flux in hippocampal neurons. *Brain Res.* **1542**:12-9.

Kumar, R., Krause, G.S., Yoshida, H., Mori, K. and DeGracia, D.J (2003). Dysfunction of the unfolded protein response during global brain ischemia and reperfusion. *J Cereb Blood Flow Metab*. **23**(4):462-71.

Lamb, R.F., Roy, C., Diefenbach, T.J., Vinters, H.V., Johnson, M.W., Jay, D.G. and Hall, A. (2000) The TSC1 tumour suppressor hamartin regulates cell adhesion through ERM proteins and the GTPase Rho. *Nat Cell Biol* **2**:281-7

Lamming, D.W. Ye, L., Katajisto, P., Goncalves, M.D., Saitoh, M., Stevens, D.M., Davis, J.G., Salmon, A.B., Richardson, A., Ahima, R.S., Guertin, D.A., Sabatini, D.M. and Baur, J.A. (2012). Rapamycin-induced insulin resistance is mediated by mTORC2 loss and uncoupled from longevity. *Science* **335**:1638–1643.

Lapchak, P.A. (2010). A critical assessment of edaravone acute ischemic stroke efficacy trials: is edaravone an effective neuroprotective therapy? *Expert Opin Pharmacother.* **11**(10):1753-63.

Larson, J. and Park, T.J. (2009). Extreme hypoxia tolerance of naked mole-rat brain. *Neuroreport.* **20**(18):1634-7.

Lee, B.J., Egi, Y., van Leyen K., Lo, E.H. and Arai, K. (2010a). Edaravone, a free radical scavenger, protects components of the neurovascular unit against oxidative stress in vitro. *Brain Res.* **1307**:22-7.

Lee, D.F., Kuo, H.P., Chen, C.T., Hsu, J.M., Chou, C.K., Wei, Y., Sun, H.L., Li, L.Y., Ping, B., Huang, W.C., He, X., Hung, J.Y., Lai, C.C., Ding, Q., Su, J.L., Yang, J.Y., Sahin, A.A., Hortobagyi, G.N., Tsai, F.J., Tsai, C.H. and Hung, M.C. (2007). IKK beta suppression of TSC1 links inflammation and tumor angiogenesis via the mTOR pathway. *Cell* **130**(3):440-55.

Lee, S.J., Hwang, A.B. and Kenyon, C. (2010b) Inhibition of respiration extends C. elegans life span via reactive oxygen species that increase HIF-1 activity. *Curr. Biol.* **20**:2131–2136.

Li, S. and Carmichael, S.T. (2006). Growth-associated gene and protein expression in the region of axonal sprouting in the aged brain after stroke. *Neurobiol Dis*. **23**:362–373.

Liao, H., Huang, Y., Guo, B., Liang, B., Liu, X., Ou, H., Jiang, C., Li, X. and Yang, D. (2014). Dramatic antitumor effects of the dual mTORC1 and mTORC2 inhibitor AZD2014 in hepatocellular carcinoma. *Am J Cancer Res.* **5**(1):125-39.

Lin, A.L., Zheng, W., Halloran, J.J., Burbank, R.R., Hussong, S.A., Hart, M.J., Javors, M., Shih, Y.Y., Muir, E., Solano Fonseca, R., Strong, R., Richardson, A.G., Lechleiter, J.D., Fox, P.T. and Galvan, V. (2013). Chronic rapamycin restores brain vascular integrity and function through NO synthase activation and improves memory in symptomatic mice modeling Alzheimer's disease. *J Cereb Blood Flow Metab.* **33**(9):1412-21.

Lin, J.H., Li, H., Yasumura, D., Cohen, H.R., Zhang, C, Panning, B., Shokat, K.M., Lavail, M.M. and Walter, P. (2007). IRE1 signaling affects cell fate during the unfolded protein response. *Science* **318**(5852):944-9.

Lin, Y., Henderson, P., Pettersson, S., Satsangi, J., Hupp, T. and Stevens, C. (2011). Tuberous sclerosis-2 (TSC2) regulates the stability of death-associated protein kinase-1 (DAPK) through a lysosome-dependent degradation pathway. *FEBS J.* **278**(2):354-70.

Liu, Y., Shoji-Kawata, S., Sumpter, R.M. Jr, Wei, Y., Ginet, V., Zhang, L., Posner, B., Tran, K.A., Green, D.R., Xavier, R.J., Shaw, S.Y., Clarke, P.G., Puyal, J. and Levine, B. (2013). Autosis is a Na+,K+-ATPase-regulated form of cell death triggered by autophagy-inducing peptides, starvation, and hypoxia-ischemia. *Proc Natl Acad Sci U S A* **110**(51):20364-71.

Liu, Y., Tang, G., Li, Y., Wang, Y., Chen, X., Gu, X., Zhang, Z., Wang, Y. and Yang, G.Y (2014). Metformin attenuates blood-brain barrier disruption in mice following middle cerebral artery occlusion. *J Neuroinflammation* **11**:177.

Liu Z, Zhao W, Xu T, Pei D, Peng Y. (2010). Alterations of NMDA receptor subunits NR1, NR2A and NR2B mRNA expression and their relationship to apoptosis following transient forebrain ischemia. *Brain Res.* **1361**:133-9.

Lockshin, R.A. and Zakeri, Z. (2004). Apoptosis, autophagy, and more. *Int J Biochem Cell Biol.* **36**(12):2405-19.

Longa, E.Z., Weinstein, P.R., Carlson, S. and Cummins, R. (1989). Reversible middle cerebral artery occlusion without craniectomy in rats. *Stroke* **20**(1):84-91.

Lou, D., Griffith, N. and Noonan, D.J. (2001). The tuberous sclerosis 2 gene product can localize to nuclei in a phosphorylation-dependent manner. *Mol Cell Biol Res Commun* **4**:374-80

Lugnier, C., Majores, M., Fassunke, J., Pernhorst, K., Niehusmann, P., Simon, M., Nellist, M., Schoch, S. and Becker, A. (2009). Hamartin variants that are frequent in focal dysplasias and cortical tubers have reduced tuberin binding and aberrant subcellular distribution in vitro. *J Neuropathol Exp Neurol* **68**:1136-46.

Ma, X., Liu, H., Foyil, S.R., Godar, R.J., Weinheimer, C.J., Hill, J.A. and Diwan, A. (2012). Impaired autophagosome clearance contributes to cardiomyocyte death in ischemia/reperfusion injury. *Circulation* **125**(25): 3170-81.

MacManus, J.P., Buchan, A.M., Hill, I.E., Rasquinha, I. and Preston, E. (1993). Global ischemia can cause DNA fragmentation indicative of apoptosis in rat brain. *Neuroscience letters* **164**(1-2): 89-92.

MacManus, J.P., Hill, I.E., Preston, E., Rasquinha, I., Walker, T. and Buchan, A.M. (1995). Differences in DNA fragmentation following transient cerebral or decapitation ischemia in rats. *J Cereb Blood Flow Metab*. **15**(5): 728-37.

MacManus, J.P. and Linnik, M.D. (1997). Gene expression induced by cerebral ischemia: an apoptotic perspective. *J Cereb Blood Flow Metab*. **17**(8): 815-32.

Macrae, I.M. (2011). Preclinical stroke research—advantages and disadvantages of the most common rodent models of focal ischaemia. *Br J Pharmacol.* **164**(4):1062-1078.

Maheshwar, M.M., Cheadle, J.P., Jones, A.C., Myring, J., Fryer, A.E., Harris, P.C. and Sampson, J.R. (1997). The GAP-related domain of tuberin, the product of the TSC2 gene, is a target for missense mutations in tuberous sclerosis. *Hum Mol Genet.* **6**(11):1991-6.

Mak, B.C., Kenerson, H.L, Aicher, L.D, Barnes, E.A. and Yeung, R.S. (2005). Aberrant beta-catenin signaling in tuberous sclerosis. *Am J Pathol.* **167**(1):107-16.

Maren S. (2011). Seeking a spotless mind: extinction, deconsolidation, and erasure of fear memory. *Neuron.* **70**(5):830-45.

Martin, D., Li, Y., Yang, J., Wang, G., Margariti, A., Jiang, Z., Yu, H., Zampetaki, A., Hu, Y., Xu, Q., Zeng, L. (2014). Unspliced X-box-binding protein 1 (XBP1) protects endothelial cells from oxidative stress through interaction with histone deacetylase 3. *J Biol Chem.* **289**(44):30625-34.

Matsui, Y., Takagi, H, Qu, X., Abdellatif, M., Sakoda, H., Asano, T., Levine, B. and Sadoshima, J. (2007). Distinct roles of autophagy in the heart during ischemia and reperfusion: roles of AMP-activated protein kinase and Beclin 1 in mediating autophagy. *Circ Res.* **100**(6):914-22.

Matsumoto, S., Bandyopadhyay, A., Kwiatkowski, D. J., Maitra, U. and Matsumoto, T. (2002). Role of the Tsc1-Tsc2 complex in signaling and transport across the cell membrane in the fission yeast *Schizosaccharomyces pombe. Genetics* **161**:1053–1063.

Mattson, M.P., Guthrie, P.B. and Kater, S.B. (1989). Intrinsic factors in the selective vulnerability of hippocampal pyramidal neurons. *Prog Clin Biol Res.* **317**:333-51.

McCay, C.M., Crowel, M.F. and Maynard, L.A. (1935). The effect of retarded growth upon the length of the life span and upon the ultimate body size. *J Nutr.* **10**:63–79.

McCullough, K.D., Martindale, J.L., Klotz, L.O., Aw, T.Y. and Holbrook, N.J. (2001). Gadd153 sensitizes cells to endoplasmic reticulum stress by down-regulating Bcl2 and perturbing the cellular redox state. *Mol Cell Biol.* **21**(4):1249-59.

McMahon J, Huang X, Yang J, Komatsu M, Yue Z, Qian J, Zhu, X. and Huang, Y. (2012). Impaired autophagy in neurons after disinhibition of mammalian target of rapamycin and its contribution to epileptogenesis. The Journal of neuroscience : the official journal of the Society for Neuroscience. 2012; *J Neurosci.* **32**(45): 15704-14.

Meijer A.J. and Codogno, P. (2006). Signalling and autophagy regulation in health, aging and disease. *Mol Aspects Med* **27**: 411–25.

Meikle, L., Talos, D.M., Onda, H., Pollizzi, K., Rotenberg, A., Sahin, M., Jensen, F.E., Kwiatkowski, D.J. (2007). A mouse model of tuberous sclerosis: neuronal loss of Tsc1 causes dysplastic and ectopic neurons, reduced myelination, seizure activity, and limited survival. *J Neurosci.* **27**(21):5546-58.

Mendes, C.S., Levet, C., Chatelain, G., Dourlen, P., Fouillet, A., Dichtel-Danjoy, M.L., Gambis, A., Ryoo, H.D., Steller, H. and Mollereau, B (2009). ER stress protects from retinal degeneration. *EMBO J.* **28**(9):1296-307.

Menon, S., Dibble, C.C., Talbott, G., Hoxhaj, G., Valvezan, A.J., Takahashi, H., Cantley, L.C. and Manning, B.D. (2014). Spatial control of the TSC complex integrates insulin and nutrient regulation of mTORC1 at the lysosome. *Cell* **156**(4):771-85.

Mileson, B.E. and Schwartz, R.D. (1991). The use of locomotor activity as a behavioral screen for neuronal damage following transient forebrain ischemia in gerbils. *Neurosci Lett.* **128**(1):71-6.

Miloloza, A., Kubista, M., Rosner, M. and Hengstschläger, M. (2002). Evidence for separable functions of tuberous sclerosis gene products in mammalian cell cycle regulation. *J Neuropathol Exp Neurol.* **61**(2):154-63.

Miloloza, A., Rosner, M., Nellist, M., Halley, D., Bernaschek, G. and Hengstschläger, M. (2000) The TSC1 gene product, hamartin, negatively regulates cell proliferation. *Hum Mol Genet.* **9**(12):1721-7.

Morikawa, E., Ginsberg, M.D, Dietrich, W.D., Duncan, R.C., Kraydieh, S., Globus, M.Y.and Busto, R. (1992). The significance of brain temperature in focal cerebral ischemia: histopathological consequences of middle cerebral artery occlusion in the rat. *J Cereb Blood Flow Metab.* **12**(3):380-9.

Moyer, M.W. (2013). The myth of antioxidants. *Sci Am.* **308(**2): 62-7.

Murry, C.E., Jennings, R.B. and Reimer, K.A. (1986). Preconditioning with ischemia: a delay of lethal cell injury in ischemic myocardium. *Circulation* **74**(5):1124-36.

Nakagawa, T., Zhu, H., Morishima, N., Li, E., Xu, J., Yankner, B.A. and Yuan, J. (2000). Caspase-12 mediates endoplasmic-reticulum-specific apoptosis and cytotoxicity by amyloid-beta. *Nature* **403**(6765):98-103.

Nakka, V.P., Gusain, A. and Raghubir, R. (2010). Endoplasmic reticulum stress plays critical role in brain damage after cerebral ischemia/ reperfusion in rats. *Neurotox Res* **17**:189–202

Nakka, V.P., Prakash-Babu, P. and Vemuganti, R. (2016). Crosstalk Between Endoplasmic Reticulum Stress, Oxidative Stress, and Autophagy: Potential Therapeutic Targets for Acute CNS Injuries. *Mol Neurobiol.* **53**(1):532-44.

Nellist, M., van Slegtenhorst, M.A., Goedbloed, M., van den Ouweland, A.M., Halley, D.J. and van der Sluijs. P. (1999). Characterization of the cytosolic tuberin-hamartin complex. Tuberin is a cytosolic chaperone for hamartin. *J Biol Chem* **274**:35647-52

Neuhaus, A.A., Rabie, T., Sutherland, B.A., Papadakis, M., Hadley, G., Cai, R. and Buchan, A.M. (2014). Importance of preclinical research in the development of neuroprotective strategies for ischemic stroke. *JAMA Neurol*. **71**(5):634-9.

Neuman, N.A. and Henske, E.P. (2011). Non-canonical functions of the tuberous sclerosis complex-Rheb signalling axis. *EMBO Mol Med.* **3**(4):189-200.

Nguyen, H.N., Wang, C. and Perry, D.C. (2002). Depletion of intracellular calcium stores is toxic to SH-SY5Y neuronal cells. *Brain Res.* **924(**2):159-66.

NICE interventional procedure guidance [IPG548] https://www.nice.org.uk/guidance/ipg548 Accessed 14/03/2016

Nikić, I., Merkler, D., Sorbara, C., Brinkoetter, M., Kreutzfeldt, M., Bareyre, F.M., Brück, W., Bishop D., Misgeld, T. and Kerschensteiner M. (2011). A reversible form of axon damage in experimental autoimmune encephalomyelitis and multiple sclerosis. *Nat Med.* **17**(4):495-9.

NINDS. Tissue plasminogen activator for acute ischemic stroke. The National Institute of Neurological Disorders and Stroke rt-PA Stroke Study Group. (1995). *N Engl J Med.* **333**(24):1581-7.

O'Callaghan, F.J., Shiell, A.W., Osborne, J.P. and Martyn, C.N. (1998). Prevalence of tuberous sclerosis estimated by capture-recapture analysis. *Lancet* **351**(9114):1490.

O'Collins, V.E., Macleod, M.R., Donnan, G.A., Horky, L.L., van der Worp, B.H. and Howells, D.W. (2006). 1,026 experimental treatments in acute stroke. *Ann Neurol.* **59**(3):467-77.

O'Keefe, J. and Dostrovsky, J. (1971). The hippocampus as a spatial map. Preliminary evidence from unit activity in the freely-moving rat. *Brain Res.* **34**(1):171-5.

Ogata, M., Hino, S., Saito, A., Morikawa, K., Kondo, S., Kanemoto, S., Murakami, T., Taniguchi, M., Tanii, I., Yoshinaga, K., Shiosaka, S., Hammarback, J.A., Urano, F. and Imaizumi, K. (2006). Autophagy is activated for cell survival after endoplasmic reticulum stress. *Mol Cell Biol.* **26**(24):9220-31.

Oida Y, Izuta H, Oyagi A, Shimazawa M, Kudo T, Imaizumi K. and Hara, H. (2008). Induction of BiP, an ER-resident protein, prevents the neuronal death induced by transient forebrain ischemia in gerbil. *Brain Res.* **1208**: 217-24.

Ordy. J.M., Wengenack, T.M., Bialobok, P., Coleman, P.D., Rodier, P., Baggs, R.B., Dunlap, W.P. and Kates, B. (1993). Selective vulnerability and early progression of hippocampal CA1 pyramidal cell degeneration and GFAP-positive astrocyte reactivity in the rat four-vessel occlusion model of transient global ischemia. *Exp Neurol.* **119**(1):128-39.

Orlova, K.A. and Crino, P.B. (2010). The tuberous sclerosis complex. *Ann N Y Acad Sci.* **1184**:87-105.

Ouyang, Y.B., Voloboueva, L.A., Xu, L.J. and Giffard, R.G. (2007). Selective dysfunction of hippocampal CA1 astrocytes contributes to delayed neuronal damage after transient forebrain ischemia. *J Neurosci.* **27**(16): 4253-60.

Oyadomari, S. and Mori, M. (2004). Roles of CHOP/GADD153 in endoplasmic reticulum stress. *Cell Death Differ.* **11**(4):381-9.

Papadakis, M., Hadley, G., Xilouri, M., Hoyte, L.C., Nagel, S., McMenamin, M.M., Tsaknakis, G., Watt, S.M., Drakesmith, C.W., Chen, R., Wood, M.J., Zhao, Z., Kessler, B., Vekrellis, K. and Buchan, A.M. (2013). Tsc1 (hamartin) confers neuroprotection against ischemia by inducing autophagy. *Nat Med.* **19**(3):351-7.

Pass, S.L. and Pass, M. (2013). Optimization of potent and selective dual mTORC1 and mTORC2 inhibitors: the discovery of AZD8055 and AZD2014. *Bioorg Med Chem Lett.* **23**(5):1212-6.

Pattingre, S., Tassa, A., Qu, X., Garuti, R., Liang, X.H., Mizushima, N., Packer, M., Schneider, M.D. and Levine B. (2005). Bcl-2 antiapoptotic proteins inhibit Beclin 1-dependent autophagy. *Cell* **122**:927–939.

Pauly, M., Daussin, F., Burelle, Y., Li, T., Godin, R., Fauconnier, J., Koechlin-Ramonatxo, C., Hugon, G., Lacampagne, A., Coisy-Quivy, M., Liang, F., Hussain, S., Matecki, S. and Petrof, B.J. (2012). AMPK activation stimulates autophagy and ameliorates muscular dystrophy in the mdx mouse diaphragm. *Am J Pathol.* **181**(2):583-92.

Pérez-Rodríguez, D., Anuncibay-Soto, B., Llorente, I.L., Pérez-García, C.C. and Fernández-López, A. (2015). Hippocampus and cerebral cortex present a different autophagic response after oxygen and glucose deprivation in an ex vivo rat brain slice model. *Neuropathol Appl Neurobiol.* **41**(4):e68-79.

Petrovski, G., Das, S., Juhasz, B., Kertesz, A., Tosaki, A. and Das, D.K. (2011). Cardioprotection by endoplasmic reticulum stress-induced autophagy. *Antioxid Redox Signal.* **14**(11):2191-200.

Phan, T.G., Wright, P.M., Markus, R., Howells, D.W., Davis, S.M. and Donnan, G.A. (2002). Salvaging the ischaemic penumbra: more than just reperfusion? *Clin Exp Pharmacol Physiol.* **29**(1-2):1-10.

Pignataro, G., Scorziello, A., Di Renzo, G. and Annunziato L. (2009). Post-ischemic brain damage: effect of ischemic preconditioning and postconditioning and identification of potential candidates for stroke therapy. *FEBS J.* **276**(1):46-57.

Pike, K.G., Malagu, K., Hummersone, M.G., Menear, K.A., Duggan, H.M., Gomez, S., Martin, N.M., Ruston, L., Pass, S.L. and Pass, M. (2013). Optimization of potent and selective dual mTORC1 and mTORC2 inhibitors: the discovery of AZD8055 and AZD2014. *Bioorg Med Chem Lett.* **23**(5):1212-6.

Plank, T.L., Yeung, R.S. and Henske, E.P. (1998) Hamartin, the product of the tuberous sclerosis 1 (TSC1) gene, interacts with tuberin and appears to be localized to cytoplasmic vesicles. *Cancer Res* **58**:4766-70

Pluta, R.M., Rak, R., Wink, D.A., Woodward, J.J., Khaldi, A., Oldfield, E.H. and Watson, J.C (2001). Effects of nitric oxide on reactive oxygen species production and infarction size after brain reperfusion injury. *Neurosurgery* **48**(4):884-92; discussion 892-3.

Poignet, H., Beaughard, M., Lecoin, G., Massingham, R. (1989). Functional, behavioral, and histological changes induced by transient global cerebral ischemia in rats: effects of cinnarizine and flunarizine. *J Cereb Blood Flow Metab.* **9**(5):646-54.

Potter, C.J., Huang, H. and Xu, T. (2001) Drosophila Tsc1 functions with Tsc2 to antagonize insulin signaling in regulating cell growth, cell proliferation, and organ size. *Cell* **105**:357-68

Pulsinelli, W.A. and Brierley, J.B. (1979). A new model of bilateral hemispheric ischemia in the unanesthetized rat. *Stroke* **10**(3):267-72.

Pulsinelli, W.A., Brierley, J.B. and Plum, F. (1982 a). Temporal profile of neuronal damage in a model of transient forebrain ischemia. *Ann Neurol.* **11**(5):491-8

Pulsinelli, W.A. and Buchan, A.M. (1988) The four-vessel occlusion rat model: method for complete occlusion of vertebral arteries and control of collateral circulation. *Stroke*. **19**(7):913-4

Pulsinelli, W.A. and Duffy, T.E. (1983). Regional energy balance in rat brain after transient forebrain ischemia. *J Neurochem*. **40**(5):1500-3.

Pulsinelli, W.A., Levy, D.E. and Duffy, T.E. (1982 b). Regional cerebral blood flow and glucose metabolism following transient forebrain ischemia. *Ann Neurol*. **11**(5):499-502.

Puyal, J and Clarke, P.G. (2009).Targeting autophagy to prevent neonatal stroke damage. *Autophagy* **5**(7):1060-1.

Qin, A.P., Liu, C.F., Qin, Y.Y., Hong, L.Z., Yang, L., Liu, J., Qin, Z.H. and Zhang, H.L. (2010 a). Autophagy was activated in injured astrocytes and mildly decreased cell survival following glucose and oxygen deprivation and focal cerebral ischemia. *Autophagy* **6**:738–753.

Qin, J., Wang, Z., Hoogeveen-Westerveld, M., Shen, G., Gong, W., Nellist, M. and Xu, W. (2016). Structural Basis of the Interaction between Tuberous Sclerosis Complex 1 (TSC1) and Tre2-Bub2-Cdc16 Domain Family Member 7 (TBC1D7). *J Biol Chem.* Feb 18. pii: jbc.M115.701870. [Epub ahead of print]

Qin, L., Wang, Z., Tao, L., Wang, Y. (2010 b). ER stress negatively regulates AKT/TSC/mTOR pathway to enhance autophagy. *Autophagy* **6**(2): 239-47.

Ramos, A.B., Vasconcelos-Dos-Santos, A., Lopes de Souza, S.A., Rosado-de-Castro, P.H., Barbosa da Fonseca, L.M., Gutfilen, B., Cintra, W.M. and Mendez-Otero, R. (2013). Bone-marrow mononuclear cells reduce neurodegeneration in hippocampal CA1 layer after transient global ischemia in rats. *Brain Res.* **1522**:1-11.

Ravikumar B, Vacher C, Berger Z, Davies JE, Luo S, Oroz LG, Scaravilli, F., Easton, D.F., Duden, R., O'Kane, C.J. and Rubinsztein, D.C.(2004). Inhibition of mTOR induces autophagy and reduces toxicity of polyglutamine expansions in fly and mouse models of Huntington disease. *Nature genetics* **36**(6): 585-95.

Rebsamen, M., Pochini, L., Stasyk, T., de Araújo, M.E., Galluccio, M., Kandasamy, R.K., Snijder, B., Fauster, A.,

Rudashevskaya, E.L., Bruckner, M., Scorzoni, S., Filipek, P.A., Huber, K.V., Bigenzahn, J.W., Heinz, L.X., Kraft, C., Bennett, K.L., Indiveri, C., Huber, L.A. and Superti-Furga, G. (2015). SLC38A9 is a component of the lysosomal amino acid sensing machinery that controls mTORC1. *Nature* **519**(7544):477-81.

Rena, G., Pearson, E.R. and Sakamoto, K. (2013). Molecular mechanism of action of metformin: old or new insights? *Diabetologia.* **56**(9):1898-906.

Ringler, S.L., Aye, J., Byrne, E., Anderson, M., Turner, C.P. (2008). Effects of disrupting calcium homeostasis on neuronal maturation: early inhibition and later recovery. *Cell Mol Neurobiol.* **28**(3):389-409.

Roberts, G.G., Di Loreto, M.J., Marshall, M., Wang, J. and DeGracia, D.J. (2007). Hippocampal cellular stress responses after global brain ischemia and reperfusion. *Antioxid Redox Signal.* **9**(12):2265-75.

Rosner, M., Freilinger, A. and Hengstschläger, M. (2004). Proteins interacting with the tuberous sclerosis gene products. *Amino Acids* **27**(2):119-28.

Rosner, M., Hanneder, M., Siegel, N., Valli, A., Fuchs, C. and Hengstschläger, M. (2008a). The mTOR pathway and its role in human genetic diseases. *Mutat Res.* **659**(3):284-92.

Rosner, M., Hanneder, M., Siegel, N., Valli, A. and Hengstschläger, M. (2008b) The tuberous sclerosis gene products hamartin and tuberin are multifunctional proteins with a wide spectrum of interacting partners. *Mutat Res.* **658**(3):234-46.

Rosner, M. and Hengstschläger, M (2008). Cytoplasmic and nuclear distribution of the protein complexes mTORC1 and mTORC2: rapamycin triggers dephosphorylation and delocalization of the mTORC2 components rictor and sin1. *Hum Mol Genet.* **17**(19):2934-48.

Rouschop, K.M., van den Beucken, T., Dubois, L., Niessen, H., Bussink, J., Savelkouls, K., Keulers, T., Mujcic, H., Landuyt, W., Voncken, J.W., Lambin P, van der Kogel, A.J., Koritzinsky, M. and Wouters, B.G. (2010). The unfolded protein response protects human tumor cells during hypoxia through regulation of the autophagy genes MAP1LC3B and ATG5. *J Clin Invest.* **120**(1):127-41.

Roussel, B.D., Kruppa, A.J., Miranda, E., Crowther, D.C., Lomas, D.A. and Marciniak, S.J. (2013). Endoplasmic reticulum dysfunction in neurological disease. *Lancet Neurol.* **12**(1): 105-18.

Ruan, Y.W., Han, X.J., Shi, Z.S., Lei, Z.G., Xu, Z.C. (2012). Remodeling of synapses in the CA1 area of the hippocampus after transient global ischemia. *Neuroscience* **218**:268-77.

Rusten, T.E. and Stenmark, H. (2010).p62, an autophagy hero or culprit? *Nat Cell Biol.* **12**(3):207-9.

Sabatini, D.M., Erdjument-Bromage, H., Lui, M., Tempst, P. and Snyder, S.H. (1994). RAFT1: a mammalian protein that binds to FKBP12 in a rapamycin-dependent fashion and is homologous to yeast TORs. *Cell* **78**:35-43

Safdie, F.M., Dorff, T., Quinn, D., Fontana, L., Wei, M., Lee, C., Cohen, P., and Longo, V.D. (2009). Fasting and cancer treatment in humans: A case series report. Aging **1**:988–1007.

Sakaki, K. and Kaufman, R.J. (2008). Regulation of ER stress-induced macroautophagy by protein kinase C. *Autophagy* **4**(6):841-3.

Samara, C., Syntichaki, P. *and* Tavernarakis, N. *(2008).* Autophagy is required for necrotic cell death in *Caenorhabditis elegans. Cell Death Differ* **15***:*105–112.

Sancak, Y., Peterson, T.R., Shaul, Y.D., Lindquist, R.A., Thoreen, C.C., Bar-Peled, L. and Sabatini, D.M. (2008). The Rag GTPases bind raptor and mediate amino acid signaling to mTORC1.*Science* **320**(5882):1496-501.

Sanderson, T.H., Deogracias, M.P., Nangia, K.K., Wang, J., Krause, G.S. and Kumar, R. (2010). PKR-like endoplasmic reticulum kinase (PERK) activation following brain ischemia is independent of unfolded nascent proteins. *Neuroscience* **169**(3):1307-14.

Sanderson, T.H., Gallaway, M. and Kumar, R. (2015). Unfolding the Unfolded Protein Response: Unique Insights into Brain Ischemia. *Int J Mol Sci.* **16**(4):7133-7142.

Santiago Lima, A.J., Hoogeveen-Westerveld, M, Nakashima A, Maat-Kievit A, van den Ouweland A, Halley D, Kikkawa U, Nellist M. (2014). Identification of regions critical for the integrity of the TSC1-TSC2-TBC1D7 complex. *PLoS One.* **9**(4):e93940.

Sarbassov, D.D., Guertin, D.A., Ali, S.M., Sabatini, D.M. (2005). Phosphorylation and regulation of Akt/PKB by the rictor-mTOR complex. *Science* **307**:1098–1101.

Sardiello, M., Palmieri, M., di Ronza, A., Medina, D.L., Valenza, M., Gennarino, V.A., Di Malta, C., Donaudy, F., Embrione, V., Polishchuk, R.S., Banfi, S., Parenti, G., Cattaneo, E. and Ballabio, A. (2009). A gene network regulating lysosomal biogenesis and function. *Science* **325**(5939):473-7.

Sarkar, S., Krishna, G., Imarisio, S., Saiki, S., O'Kane, C.J. and Rubinsztein, D.C. (2008). A rational mechanism for combination treatment of Huntington's disease using lithium and rapamycin. *Hum Mol Genet.* **17**(2):170-8.

Saver JL. (2006). Time is brain--quantified. *Stroke*.**37**(1):263-6.

Saver, J.L., Goyal, M., Bonafe, A., Diener, H.C., Levy, E.I., Pereira, V.M., Albers, G.W., Cognard, C., Cohen, D.J., Hacke, W., Jansen, O., Jovin, T.G., Mattle, H.P., Nogueira, R.G., Siddiqui, A.H., Yavagal, D.R., Baxter, B.W., Devlin, T.G., Lopes, D.K., Reddy, V.K., de Rochemont, R.D., Singer, O.C. and Jahan, R.; SWIFT PRIME

Investigators. (2015). Stent-Retriever Thrombectomy after Intravenous t-PA vs. t-PA Alone in Stroke. *N Engl J Med.* **372**(24):2285-95.

Schapansky, J., Nardozzi, J.D., Felizia, F., LaVoie, M.J. (2014). Membrane recruitment of endogenous LRRK2 precedes its potent regulation of autophagy. *Hum Mol Genet*. **23**(16):4201-14.

Serena, J, Leira, R., Castillo, J., Pumar, J.M., Castellanos, M. and Dávalos, A. (2001). Neurological deterioration in acute lacunar infarctions: the role of excitatory and inhibitory neurotransmitters. *Stroke* **32**:1154-1161

Sheardown, M.J., Nielsen, D., Hanse, A.J., Jacobsen, P. and Honore, T. (1990). 2,3-dihydroxy-6-nitro-7-sulfamoyl-benzo (F) quinoxaline: A neuroprotectant for cerebral ischemia. *Science* **247**: 571–574.

Sheng, R., Liu, X.Q., Zhang, L.S., Gao, B., Han, R., Wu, Y.Q., Zhang, X.Y., and Qin, Z.H. (2012). Autophagy regulates endoplasmic reticulum stress in ischemic preconditioning. *Autophagy* **8**(3): 310-25.

Sheng, R., Zhang, L.S., Han, R., Liu, X.Q., Gao, B. and Qin, Z.H. (2010) Autophagy activation is associated with neuroprotection in a rat model of focal cerebral ischemic preconditioning. *Autophagy* **6**(4):482–494.

Shi, R., Weng, J., Zhao, L., Li, X.M., Gao, T.M. and Kong, J. (2012). Excessive autophagy contributes to neuron death in cerebral ischemia. *CNS Neurosci Ther.* **18**(3):250-60.

Shinojima, N., Yokoyama, T., Kondo, Y. and Kondo, S. (2007). Roles of the Akt/mTOR/p70S6K and ERK1/2 signaling pathways in curcumin-induced autophagy. *Autophagy* **3**:635–637.

Siegel, R., Ma, J., Zou, Z. and Jemal, A. (2014), Cancer statistics, 2014. *CA: A Cancer Journal for Clinicians* **64**: 9–29.

Siroky, B.J., Czyzyk-Krzeska, M.F. and Bissler, J.J. (2009). Renal involvement in tuberous sclerosis complex and von Hippel-Lindau disease: shared disease mechanisms? *Nat Clin Pract Nephrol* **5**:143-56

Soares, B.P., Tong, E., Hom, J., Cheng, S.C., Bredno, J., Boussel, L., Smith, W.S. and Wintermark, M. (2010). Reperfusion is a more accurate predictor of follow-up infarct volume than recanalization: a proof of conceptusing CT in acute ischemic stroke patients. *Stroke* **41**(1):e34-40.

Sokka, A.L., Putkonen, N., Mudo, G., Pryazhnikov, E., Reijonen, S., Khiroug, L., Belluardo, N., Lindholm, D., Korhonen, L. (2007). Endoplasmic reticulum stress inhibition protects against excitotoxic neuronal injury in the rat brain. *J Neurosci.* **27**(4):901-8.

Song YM, Lee YH, Kim JW, Ham DS, Kang ES, Cha BS, Lee HC, Lee BW. (2015). Metformin alleviates hepatosteatosis by restoring SIRT1-mediated autophagy induction via an AMP-activated protein kinase-independent pathway. *Autophagy* **11**(1):46-59.

Speakman, J.R. and Mitchell, S.E. (2011). Caloric restriction. *Mol. Aspects Med.* **32**:159–221.

Spencer, S.J., Mouihate, A. and Pittman, Q.J. (2007). Peripheral inflammation exacerbates damage after global ischemia independently of temperature and acute brain inflammation. *Stroke* **38(**5):1570-7.

Spielmeyer W (1927). Die pathogenese des epileptischen Krampfes. *Z Dtsch Ges Neurol Psychiatr.* **109**: 501-520

Spielmeyer W (1930). The anatomic substratum of the convulsive state. *Arch Neurol Psychiatry* **23**: 869-875.

State of the Nation: stroke statistics: https://www.stroke.org.uk/resources/state-nation-stroke-statistics. Accessed 14/03/16

Stevens, C., Lin, Y., Harrison, B., Burch, L., Ridgway, R.A., Sansom, O. and Hupp, T. (2009). Peptide combinatorial libraries identify TSC2 as a death-associated protein kinase (DAPK) death domain-binding protein and reveal a stimulatory role for DAPK in mTORC1 signaling. *J Biol Chem.* **284**(1):334-44.

Stipp, D. (2012). A new path to longevity. Sci Am **306**(1): 32-9.

Stroke Therapy Academic Industry Roundtable (STAIR). (1999). Recommendations for standards regarding preclinical neuroprotective and restorative drug development. *Stroke* **30**(12):2752-8.

Su, J., Zhang, T., Wang, K., Zhu, T. and Li, X. (2014). Autophagy Activation Contributes to the Neuroprotection of Remote Ischemic Perconditioning Against Focal Cerebral Ischemia in Rats. *Neurochem Res.* **39**(11):2068-77.

Sun, S.Y. (2013). mTOR kinase inhibitors as potential cancer therapeutic drugs. *Cancer Lett.* **340**:1–8.

Sun, W., Zhu, Y.J., Wang, Z., Zhong, Q., Gao, F., Lou, J., Gong, W., Xu, W. (2013). Crystal structure of the yeast TSC1 core domain and implications for tuberous sclerosis pathological mutations. *Nat Commun*. **4**:2135.

Sutherland, B.A., Minnerup, J., Balami, J.S., Arba, F., Buchan, A.M. and Kleinschnitz, C. (2012). Neuroprotection for ischaemic stroke: translation from the bench to the bedside. *Int J Stroke*. **7**(5):407-18.

Sutherland, B.A., Neuhaus, A.A., Couch, Y., Balami, J.S., DeLuca, G.C., Hadley. G., Harris, S.L., Grey, A.N. and Buchan AM. (2016). The transient intraluminal filament middle cerebral artery occlusion model as a model of endovascular thrombectomy in stroke. *J Cereb Blood Flow Metab.* **36**(2):363-9.

Sutherland, B.A., Papadakis, M., Chen, R.L. and Buchan, A.M. (2011). Cerebral blood flow alteration in neuroprotection following cerebral ischaemia. *J Physiol.* **589**(Pt 17):4105-14.

Symon, L., Lassen, N.A., Astrup, J. and Branston, N.M. (1977). Thresholds of ischaemia in brain cortex. *Adv Exp Med Biol*. **94**:775-82.

Szydlowska, K. and Tymianski M. (2010). Calcium, ischemia and excitotoxicity *Cell Calcium*. **47**(2):122-9.

Takagi, H., Matsui, Y., Hirotani, S., Sakoda, H., Asano, T. and Sadoshima, J. (2007). AMPK mediates autophagy during myocardial ischemia in vivo. *Autophagy* **3**(4):405-7.

Takahashi, T., Morita, K., Akagi, R., Sassa, S. (2004). Heme oxygenase-1: a novel therapeutic target in oxidative tissue injuries. *Curr Med Chem.* **11**(12):1545-61.

Talos, D.M., Kwiatkowski, D,J., Cordero, K., Black, P.M. and Jensen, F.E. (2008). Cell-specific alterations of glutamate receptor expression in tuberous sclerosis complex cortical tubers. *Ann Neurol.* **63**(4):454-65.

Tan, J.M., Wong, E.S., Dawson, V.L., Dawson, T.M. and Lim, K.L. (2007). Lysine 63-linked polyubiquitin potentially partners with p62 to promote the clearance of protein inclusions by autophagy. *Autophagy* **4**:251–253.

Tanaka, Y., Takata, T., Satomi, T., Sakurai, T. and Yokono, K. (2008). The double-edged effect of insulin on the neuronal cell death associated with hypoglycemia on the hippocampal slice culture. *The Kobe journal of medical sciences* **54**(2): E97-107.

Tapon, N., Ito, N., Dickson, B.J., Treisman, J.E. and Hariharan, I.K. (2001) The *Drosophila* tuberous sclerosis complex gene homologs restrict cell growth and cell proliferation. *Cell* **105**:345-55

Tavazoie, S.F., Alvarez, V.A., Ridenour, D.A., Kwiatkowski, D.J. and Sabatini, B.L. (2005) Regulation of neuronal morphology and function by the tumor suppressors Tsc1 and Tsc2. *Nat Neurosci* **8**:1727-34

Thien, A., Prentzell, M.T., Holzwarth, B., Kläsener, K., Kuper, I., Boehlke, C., Sonntag, A.G., Ruf, S., Maerz, L., Nitschke, R., Grellscheid, S.N., Reth, M., Walz, G., Baumeister, R., Neumann-Haefelin, E., Thedieck, K.

(2015). TSC1 activates TGF-β-Smad2/3 signaling in growth arrest and epithelial-to-mesenchymal transition. *Dev Cell*.32(5):617-30.

Thompson, H.J., Marklund, N., LeBold, D.G., Morales, D.M., Keck, C.A., Vinson, M., Royo, N.C., Grundy, R., McIntosh, T.K. (2006). Tissue sparing and functional recovery following experimental traumatic brain injury is provided by treatment with an anti-myelin-associated glycoprotein antibody. Eur J Neurosci. **24**(11):3063-72.

Traystman, R.J. (2003). Animal models of focal and global cerebral ischemia. *ILAR J.* **44**(2):85-95.

Tremblay F. and Marette A. (2001). Amino acid and insulin signaling via the mTOR/p70 S6 kinase pathway. A negative feedback mechanism leading to insulin resistance in skeletal muscle cells. *J Biol Chem.* **276**(41):38052-60.

Tsvetkov, A.S., Miller, J., Arrasate, M., Wong, J.S., Pleiss, M.A. and Finkbeiner, S. (2010). A small-molecule scaffold induces autophagy in primary neurons and protects against toxicity in a Huntington disease model. *Proc Natl Acad Sci U S A.* **107**(39):16982-7.

Tsujimoto, Y. and Shimizu, S. (2005). Another way to die: autophagic programmed cell death. *Cell Death Differ.* **12** Suppl 2:1528-34.

Tsvetkov, A.S., Miller, J., Arrasate, M., Wong, J.S., Pleiss, M.A. and Finkbeiner, S. (2010). A small-molecule scaffold induces autophagy in primary neurons and protects against toxicity in a Huntington disease model. *Proc Natl Acad Sci U S A.* **107**(39):16982-7.

Uchimura (1928). Über die Gefässversorgung des Ammons-hornes. *Z Gesamte Neurol Psychistr* **112**: 1-19

Uchino, H., Lundgren, J., Smith, M.L. and Siesjö, B.K. (1994). Preischemic hyperglycemia leads to delayed postischemic hyperthermia. *Stroke* **25**(9):1825-9.

Uchiyama, Y., Koike, M. and Shibata, M. (2008). Autophagic neuron death in neonatal brain ischemia/hypoxia. *Autophagy* **4**:404–408.

van de Beek D, Kremers W, Daly RC, Edwards BS, Clavell AL, McGregor CG, Wijdicks EF. (2008). Effect of neurologic complications on outcome after heart transplant. Arch Neurol. **65**(2):226-31.

van de Beek. D., Kremers, W.K., Kushwaha, S.S., McGregor, C.G. and Wijdicks, E.F. (2009). No major neurologic complications with sirolimus use in heart transplant recipients. *Mayo Clin Proc*. **84**(4): 330-2.

van der Worp, H.B., Macleod, M.R., Bath, P.M., Demotes, J., Durand-Zaleski, I., Gebhardt, B., Gluud, C., Kollmar, R., Krieger, D.W., Lees, K.R., Molina, C., Montaner, J., Roine, R.O., Petersson, J., Staykov, D., Szabo, I., Wardlaw, J.M. and Schwab, S,; EuroHYP-1 investigators. (2014). EuroHYP-1: European multicenter, randomized, phase III clinical trial of therapeutic hypothermia plus best medical treatment vs. best medical treatment alone for acute ischemic stroke. *Int J Stroke* **9**(5):642-5.

van der Worp, H.B., Sena, E.S., Donnan, G.A., Howells, D.W. and Macleod, M.R. (2007). Hypothermia in animal models of acute ischaemic stroke: a systematic review and meta-analysis. *Brain* **130**(Pt 12):3063-74.

van der Worp, H.B. and van Gijn, J. (2007). Clinical practice. Acute ischemic stroke. *N Engl J Med.* **357**(6):572-9.

van Slegtenhorst, M., de Hoogt, R., Hermans, C., Nellist, M., Janssen, B., Verhoef, S., Lindhout, D., van den Ouweland, A., Halley, D., Young, J., Burley, M., Jeremiah, S., Woodward, K., Nahmias, J., Fox, M., Ekong, R., Osborne, J., Wolfe, J., Povey, S., Snell, R.G., Cheadle. J.P., Jones. A.C., Tachataki, M., Ravine, D., Sampson, J.R., Reeve, M.P., Richardson, P., Wilmer, F., Munro, C., Hawkins, T.L., Sepp, T., Ali, J.B., Ward, S., Green, A.J.,

Yates, J.R., Kwiatkowska, J., Henske, E.P., Short, M.P., Haines, J.H., Jozwiak, S. and Kwiatkowski, D.J. (1997). Identification of the tuberous sclerosis gene TSC1 on chromosome 9q34. *Science* **277**:805-8

van Slegtenhorst, M., Nellist, M., Nagelkerken, B., Cheadle, J., Snell, R., van den Ouweland, A., Reuser, A., Sampson, J., Halley, D. and van der Sluijs, P. (1998). Interaction between hamartin and tuberin, the TSC1 and TSC2 gene products. *Hum Mol Genet* **7**:1053-7.

Varendi, K., Airavaara, M., Anttila, J., Vose, S., Planken, A., Saarma, M., Mitchell, J.R. and Andressoo, J.O. (2014). Short-term preoperative dietary restriction is neuroprotective in a rat focal stroke model. PLoS One **9**(4): e93911.

Vellai, T., Takacs-Vellai, K., Zhang, Y., Kovacs, A.L., Orosz, L. and Müller, F.(2003).Genetics: influence of TOR kinase on lifespan in C. elegans. *Nature* **426**(6967):620

Villamil-Ortiz, J.G. and Cardona-Gomez, G.P. (2015). Comparative analysis of autophagy and tauopathy related markers in cerebral ischemia and Alzheimer's disease animal models. *Front Aging Neurosci.* **19**;7:84.

Vogiatzi, T., Xilouri, M., Vekrellis, K. and Stefanis, L. (2008). Wild type alpha-synuclein is degraded by chaperone-mediated autophagy and macroautophagy in neuronal cells. *J. Biol. Chem.* **283**:23542–23556.

Wan, X., Harkavy, B., Shen, N., Grohar, P. and Helman, L.J. (2007). Rapamycin induces feedback activation of Akt signaling through an IGF-1R-dependent mechanism. *Oncogene* **26**(13):1932-40.

Wang, J.Y., Xia, Q.A., Chu, K.T., Pan, J., Sun, L.N., Zeng, B., Zhu, Y.J., Wang, Q., Wang, K. and Luo, B.Y. (2011a). Severe global cerebral ischemia-induced programmed necrosis of hippocampal CA1 neurons in rat is prevented by 3-methyladenine: a widely used inhibitor of autophagy. *J Neuropathol Exp Neurol* **70**:314–322

Wang, L.T., Chen, B.L., Wu, C.T., Huang, K.H., Chiang, C.K. and Hwa Liu, S (2013). Protective role of AMP-activated protein kinase-evoked autophagy on an in vitro model of ischemia/reperfusion-induced renal tubular cell injury. *PLoS One* **8**(11):e79814.

Wang, P., Guan, Y.F., Du, H., Zhai, Q.W., Su, D.F. and Miao, C.Y. (2012). Induction of autophagy contributes to the neuroprotection of nicotinamidephosphoribosyltransferase in cerebral ischemia. *Autophagy* **8**(1):77-87.

Wang, S., Tsun, Z.Y., Wolfson, R.L., Shen, K., Wyant, G.A., Plovanich, M.E., Yuan, E.D., Jones, T,D,, Chantranupong, L., Comb, W., Wang, T., Bar-Peled, L., Zoncu, R., Straub, C., Kim, C., Park, J., Sabatini, B.L. and Sabatini, D.M. (2015). Metabolism. Lysosomal amino acid transporter SLC38A9 signals arginine sufficiency to mTORC1. *Science* **347**(6218):188-94.

Wang, X.S., Armstrong, M.E., Cairns, B.J., Key, T.J., and Travis, R.C. (2011b). Shift work and chronic disease: the epidemiological evidence. *Occup. Med. (Lond.)* **61**:78–89.

Wang, YC., Zhang, S., Du, T.Y., Wang, B. and Sun, X.Q. (2010). Hyperbaric oxygen preconditioning reduces ischemia-reperfusion injury by stimulating autophagy in neurocyte. *Brain Res.* **1323**:149-51.

Wardlaw, J.M., Smith, C. and Dichgans, M. (2013). Mechanisms of sporadic cerebral small vessel disease: insights from neuroimaging. *Lancet Neurol* **12**:483-497

Weis, S.N., Toniazzo, A.P., Ander, B.P., Zhan, X., Careaga, M., Ashwood, P., Wyse, A.T., Netto, C.A. and Sharp, F.R. (2014). Autophagy in the brain of neonates following hypoxia-ischemia shows sex- and region-specific effects. Neuroscience **256**:201-9.

Wen, Y.D., Sheng, R., Zhang, L.S., Han, R., Zhang, X., Zhang, X.D., Han, F., Fukunaga, K. and Qin, Z.H. (2008). Neuronal injury in rat model of permanent focal cerebral ischemia is associated with activation of autophagic and lysosomal pathways. *Autophagy* **4**:762–769.

Wienecke, R., Maize, J.C., Jr., Shoarinejad, F., Vass, W.C., Reed, J., Bonifacino, J.S., Resau, J.H., de Gunzburg, J., Yeung, R.S. and DeClue, J.E. (1996) Co-localization of the TSC2 product tuberin with its target Rap1 in the Golgi apparatus. *Oncogene* **13**:913-23

Wilde, G.J., Pringle, A.K., Wright, P. and Iannotti, F. (1997). Differential vulnerability of the CA1 and CA3 subfields of the hippocampus to superoxide and hydroxyl radicals in vitro. Journal of neurochemistry. **69**(2): 883-6.

Willette, A.A., Coe, C.L., Birdsill, A.C., Bendlin, B.B., Colman, R.J., Alexander, A.L., Allison, D.B., Weindruch, R.H., Johnson, S.C. (2013). Interleukin-8 and interleukin-10, brain volume and microstructure, and the influence of calorie restriction in old rhesus macaques. *Age (Dordr.)* **35**:2215–2227

Wolpe, J. and Rowan, V.C. (1988). Panic disorder: a product of classical conditioning. *Behav Res Ther.***26**:441–450.

Wong, E. and Cuervo, A.M. (2010). Autophagy gone awry in neurodegenerative diseases. *Nat Neurosci.* **13**(7):805-11.

Wong, M. (2010). Mammalian Target of Rapamycin (mTOR) Inhibition as a Potential Antiepileptogenic Therapy: From Tuberous Sclerosis to Common Acquired Epilepsies *Epilepsia* **51**(1): 27–36.

Xie, Z., Lau, K., Eby, B., Lozano, P., He, C., Pennington, B., Li, H., Rathi, S., Dong, Y., Tian, R., Kem, D. and Zou, M.H. (2011). Improvement of cardiac functions by chronic metformin treatment is associated with enhanced cardiac autophagy in diabetic OVE26 mice. *Diabetes* **60**(6):1770-8.

Xing, S., Zhang, Y., Li, J., Zhang, J., Li, Y., Dang, C., Li, C., Fan, Y., Yu, J., Pei, Z. and Zeng, J. (2012). Beclin 1 knockdown inhibits autophagic activation and prevents the secondary neurodegenerative damage in the ipsilateral thalamus following focal cerebral infarction. *Autophagy* **8**(1):63-76.

Xue, L.Z., Fletcher, G.C., Tolkovsky, A.M. *(1999).* Autophagy is activated by apoptotic signalling in sympathetic neurons: an alternative mechanism of death execution. *Mol Cell Neurosci* **14**:180–198.

Yamamoto, A., Cremona, M.L., Rothman, J.E. (2006). Autophagy-mediated clearance of huntingtin aggregates triggered by the insulin-signaling pathway. *J Cell Biol.* **172**(5):719-31.

Yamamoto, K., Hayakawa, T., Mogami, H., Akai, F. and Yanagihara, T. (1990). Ultrastructural investigation of the CA1 region of the hippocampus after transient cerebral ischemia in gerbils. *Acta neuropathologica* **80**(5): 487-92.

Yamamoto, Y., Jones, K.A., Mak, B.C., Muehlenbachs, A. and Yeung, R.S. (2002). Multicompartmental distribution of the tuberous sclerosis gene products, hamartin and tuberin. *Arch Biochem Biophys* **404**:210-7

Yamori, Y., Horie, R., Sato, M. and Fukase, M. (1976). Hypertension as an important factor for cerebrovascular atherogenesis in rats. Stroke **7**(2):120-5.

Yang, D.S., Stavrides, P., Mohan, P.S., Kaushik, S., Kumar, A., Ohno, M., Schmidt, S.D., Wesson, D., Bandyopadhyay, U, Jiang, Y., Pawlik, M., Peterhoff, C.M., Yang, A.J., Wilson, D.A., St George-Hyslop, P., Westaway, D., Mathews, P.M., Levy, E., Cuervo, A.M. and Nixon, R.A. (2011). Reversal of autophagy dysfunction in the TgCRND8 mouse model of Alzheimer's disease ameliorates amyloid pathologies and memory deficits. *Brain* **134**(Pt 1): 258-77.

Yang, G.Y. and Betz, A.L. (1994). Reperfusion-induced injury to the blood-brain barrier after middle cerebral artery occlusion in rats. *Stroke* **25**(8):1658-64; discussion 1664-5.

Yang, T., Li, D., Liu, F., Qi, L., Yan, G., Wang, M. (2015). Regulation on Beclin-1 expression by mTOR in CoCl2-induced HT22 cell ischemia-reperfusion injury. *Brain Res.* **1614**:60-6.

Yasui, S., Tsuzaki, K., Ninomiya, H., Floricel, F., Asano, Y., Maki, H., Takamura, A., Nanba, E., Higaki, K. and Ohno, K. (2007). The TSC1 gene product hamartin interacts with NADE. *Mol Cell Neurosci.* **35**(1):100-8.

Yemisci, M., Gursoy-Ozdemir, Y., Vural, A., Can, A., Topalkara, K. and Dalkara, T. (2009). Pericyte contraction induced by oxidative-nitrative stress impairs capillary reflow despite successful opening of an occluded cerebral artery. *Nat Med.* **15**(9):1031-7.

Yorimitsu, T. and Klionsky, D.J. (2005). Autophagy: molecular machinery for self-eating. *Cell Death Differ.* **2**:1542-52.

Yorimitsu, T., Nair, U., Yang, Z. and Klionsky, D.J. (2006). Endoplasmic reticulum stress triggers autophagy. *J Biol Chem.* **281**(40):30299-304.

Yoshitomi, H., Xu, Q., Gao, M. and Yamori, Y. (2011). Phosphorylated endothelial NOS Ser1177 via the PI3K/Akt pathway is depressed in the brain of stroke-prone spontaneously hypertensive rat. *J Stroke Cerebrovasc Dis*. **20**(5):406-12.

Yu, L., Alva, A., Su, H., Dutt, P., Freundt, E., Welsh, S., Baehrecke, E.H. and Lenardo, M.J. (2004). Regulation of an ATG7-beclin 1 program of autophagic cell death by caspase-8. *Science* **304**(5676):1500-2.

Yu, W.H., Cuervo, A.M., Kumar, A., Peterhoff, C.M., Schmidt, S.D., Lee, J.H., Mohan, P.S., Mercken, M., Farmery, M.R., Tjernberg, L.O., Jiang, Y., Duff, K., Uchiyama, Y., Näslund, J., Mathews, P.M., Cataldo, A.M. and Nixon, R.A. (2005). Macroautophagy—a novel Beta-amyloid peptide-generating pathway activated in Alzheimer's disease. *J Cell Biol.* **171**(1):87-98.

Zhang, J., Chiu, J., Zhang, H., Qi, T., Tang, Q., Ma, K., Lu, H. and Li, G. (2013a). Autophagic cell death induced by resveratrol depends on the Ca(2+)/AMPK/mTOR pathway in A549 cells. *Biochem Pharmacol.* **86**(2):317–328.

Zhang, J., Kim, J., Alexander, A., Cai, S., Tripathi, D.N., Dere, R., Tee, A.R., Tait-Mulder, J., Di Nardo, A., Han, J.M., Kwiatkowski, E., Dunlop, E.A., Dodd, K.M., Folkerth, R.D., Faust, P.L., Kastan, M.B., Sahin, M. and Walker, C.L. (2013b). A tuberous sclerosis complex signalling node at the peroxisome regulates mTORC1 and autophagy in response to ROS. *Nat Cell Biol.* **15**(10):1186-96.

Zhang, L., Niu, W., He, Z., Zhang, Q., Wu, Y., Jiang, C., Tang, C., Hu, Y. and Jia, J. (2014a). Autophagy suppression by exercise pretreatment and p38 inhibition is neuroprotective in cerebral ischemia. *Brain Res.* **1587**:127-32.

Zhang, X., Yuan, Y., Jiang, L., Zhang, J., Gao, J., Shen, Z., Zheng, Y., Deng, T., Yan, H., Li, W., Hou, W.W., Lu, J., Shen, Y., Dai, H., Hu, W.W., Zhang, Z. and Chen, Z. (2014b). Endoplasmic reticulum stress induced by tunicamycin and thapsigargin protects against transient ischemic brain injury: Involvement of PARK2-dependent mitophagy. Autophagy **10**(10):1801-13.

Zhang, X.D., Wang, Y., Wang. Y., Zhang, X., Han, R., Wu, J.C., Liang, Z.Q., Gu, Z.L., Han, F., Fukunaga, K. and Qin, Z.H. (2009). p53 mediates mitochondria dysfunction-triggered autophagy activation and cell death in rat striatum. *Autophagy* **5**:339–350.

Zheng, Y.Q., Liu, J.X., Li, X.Z., Xu, L. and Xu, Y.G. (2009). RNA interference-mediated downregulation of Beclin1 attenuates cerebral ischemic injury in rats. *Acta Pharmacol Sin.* **30**(7):919-27.

Zheng, B., Mao, J.H., Qian, L., Zhu, H., Gu, D.H., Pan, X.D., Yi, F., Ji, D.M. (2015). Pre-clinical evaluation of AZD-2014, a novel mTORC1/2 dual inhibitor, against renal cell carcinoma. *Cancer Lett.* **357**(2):468-75.

Zhou, X., Ikenoue, T., Chen, X., Li, L., Inoki, K. and Guan, K.L. (2009). Rheb controls misfolded protein metabolism by inhibiting aggresome formation and autophagy. *Proc Natl Acad Sci U S A.* **106**(22):8923-8.

Zoncu, R., Bar-Peled, L., Efeyan, A., Wang, S., Sancak, Y. and Sabatini, D.M. (2011). mTORC1 senses lysosomal amino acids through an inside-out mechanism that requires the vacuolar H(+)-ATPase. *Science* **334**(6056):678-83.

Appendix: Surgeries for primary data in the thesis

Rat	Weight/g	Sham/Ischaemia	Time point	Notes
1	180	For H&E	7 days	Temp 36.4°C. Had to remove ligature and then use it again. Had cerebellar ischemia. No corneal reflex, no running response, response to pain.
2	268	Sham	6 hours	Telemetry probe insertion
3	232	Sham	6 hours	Telemetry probe insertion
4	180	Ischaemia	3hours	Telemetry probe insertion 8 minutes. No running response. No corneal response. No response to pain.
5	172	Ischaemia	3 hours	Telemetry probe insertion 10 minutes. No corneal response. Response to pain.
6	159	Ischaemia	3 hours	Telemetry probe insertion Initially <1 minute. Not ischaemic so reanaesthetized. Corneal response. No response to pain. No running response. Unsure about Ca1/CA3 dissection.
7	213	Sham	3 hours	Telemetry probe insertion.
8	199	Sham	3 hours	Telemetry probe insertion
9	195	Sham	3 hours	Telemetry probe insertion Frothing at mouth, airway obstructed by sawdust. No seizure activity. Recovered quickly.
10	211	Ischaemia	3 hours	Telemetry probe insertion Pupils fully dilated. Slight response to pain one side. After 8.5 minutes, moved all 4 limbs.
11	197	Ischaemia	3 hours	Telemetry probe insertion Running response. Pupils fully dilated. No response to pain. Ischaemic posture. Slight response to pain at 9 mins 30.

12	185	Sham	3 hours	Telemetry probe insertion
13	206	Sham	3 hours	Telemetry probe insertion
14	194			Telemetry probe insertion. Died as last stitch applied following vertebral occlusion did have some erratic breathing.
15	197	Ischaemia	3 hours	Telemetry probe insertion Temp 36.1 slight running response, no righting response, no reponse to pain, pupil dilation approx. 80%. Approx 10 mins. ?temperature probe malfunctioning temp 35.2-34??
16	195	Ischaemia	3 hours	Telemetry probe insertion Running response. No response to pain cornea fully dilated hyperventilation. Temp 37.3. 10 mins ischemia. Signs of depolarisation.
17	210	Sham	3 hours	Telemetry probe insertion
18	184	Sham	3 hours	Telemetry probe insertion
19	175	Sham	6 hours	Telemetry probe insertion.
20	183	Sham Pre 4VO (no vertebral cauterisation) 3 hours		Telemetry probe insertion. 4VO Temp >37°C. Vertebrals not adequately visualised – some difficulty in ear bars.
21	181	Sham Pre 4VO (no vertebral cauterisation) 3 hours		Telemetry probe insertion. Pre 4VO Temp >37°C. Vertebrals visualised.
22	150	Sham Pre 4VO (no vertebral cauterisation) 3 hours		Telemetry probe insertion. Pre 4VO Temp >37°C. Erratic breathing ? stopped when in ear bars. Vertebrals not adequately visualised. Difficult neck dissection.
23	186	Sham Pre 4VO (no vertebral cauterisation)		Telemetry probe insertion. Pre 4VO Temp >37°C. Vertebrals visualised.

		3 hours		
24	167	Sham Pre 4VO (no vertebral cauterisation) 3 hours		Telemetry probe insertion. Pre 4VO Temp >37°C. Difficult neck dissection. Erratic breathing in ear bars. Recovered well. Vertebrals adequately visualised.
25	174	Sham Pre 4VO (no vertebral cauterisation) 3 hours		Telemetry probe insertion. Pre 4VO Temp >37°C. Difficult and high neck dissection.
26	232	12hr sham		Telemetry probe insertion. Pre 4VO. Good neck dissection, good visualisation of vertebrals. Recovered quickly.
27	229	12hr sham		Telemetry probe insertion. Pre 4VO. 36.2°C. Good recovery. Some blood loss vertebrals and carotids.
28	173	Naïve		
29	189	Naïve		
30	175	Naïve		
31	179	Naïve		
32	181	Naïve		
33	180	Naïve		
34	214	12hr sham		Telemetry probe insertion. Pre 4VO. 36.7°C. Some blood loss from vertebrals breathing fine. 4VO 36.1°C.
35	210	12hr sham		Telemetry probe insertion. Pre 4VO. Good neck dissection. Vertebrals well visualised. Good recovery. 4VO 36.1°C
36	194	12hr sham		Telemetry probe insertion. Pre 4VO. Good neck dissection. Vertebrals well visualised. Good recovery. 4VO 36.1°C

37	152	12hr sham		Telemetry probe insertion. Pre 4VO. Temp 36.6°C. 4VO. Stopped breathing momentarily will manipulating neck. Wet mash given.
38	201	12hr ischaemia		Telemetry probe insertion. 36.9°C. Some bleeding. Vetebral cauterisation otherwise uncomplicated. No running response, response to pain, woke after 2 mins. Running response, then woke up. Reanaesthetised. No response to pain. Pupil dilated. Temp 33.3°C but ?problem with temperature probe. 10 mins. 35.4°C recorded on telemetry.
39	201	12hr ischaemia		Telemetry probe insertion. 37.2°C. Recovered quickly. No complications vetebrals well visualised. Some bleeding. 4VO. No response to pain. 80% pupil dilation. Corneal reflex. 10mins (did have response to pain then).
40	175	12hr ischaemia		Telemetry probe insertion. New temp probe. Pre 4VO – 36.6-37.2°C. Some bleeding at vetebrals. Breathing good throughout. Improved positioning of spinal needle. No corneal reflex, no response to pain, turning on 1 side 35.4°C. Good posture. Fully dilated pupil. Laboured breathing. 35.9°C at 7 mins. 9 mins 30 No corneal reflex. No response to pain
41	188	12hr ischaemia		Telemetry probe insertion. 4VO Difficult insertion of spinal needle ?trauma. Vertebrals visualised. Quick recovery. 37.2°C 4VO. Ischaemic posture. Pupil dilated no response to pain. Increased respiratory rate. No corneal reflex. 34.9°C 5 min 35.1°C 9 min 35.7 °C, 36.2°C on telemetry.
42	171	12hr ischaemia		Telemetry probe insertion. Relatively uncomplicated. Vertebrals well visulaised. 36.6°C 4VO running response. Had to reposition carotid clips as stopped breathing. Temp 35.9-36.0°C. No response to pain. No corneal reflex. Fast breathing. Dissection of CA1 and CA3 not as good as

				previous as dropped small dissection scissors – will replace for next dissection.
43	179	12hr ischaemia		Telemetry probe insertion. Pre 4VO 34.5-37.1 °C covered with drape as had used EtOH to clean urine from rat. Good carotid dissection, good spinal needle insertion, blood loss at vertebrals, quick recovery. 4VO 36.1°C No response to pain, slight corneal reflex at 9 mins righting reflex reaction to pain, running response. 10 mins.
44	183	12hr ischaemia		Telemetry probe insertion. Some swelling front of neck. Needed to replace spinal needle as too high initially. Vertebrals cauterised but difficult due to erratic breathing in ear bars. 4VO 36.1°C. No response to pain, dilated pupil, no corneal reflex, increased breathing. 10 mins.
45	255		Pericyte experiments. Laser doppler	Pre 4VO: Temp 36.6°C. Some erratic breathing when attempting spinal needle step. One vertebral visualised well, other not. Lost a lot of blood. 4VO: 36.9°C 10 minutes of global ischaemia under anaesthesia. CBF: Data Q crashed, no full recording Pre: 360 to 330 (first side) 330 to 60 bilateral Turned over at 80, 1st tightening had no effect 2nd no change (75 to 84) 3rd 80 to 64 4th momentary drop to 59, returned to 66 at 5 mins 82. Reperfusion 482. 10 minutes ischaemia under anaesthesia (27/05/14: 36.5°C, resutured head wound, otherwise healthy.
46	267		Pericyte experiments. Laser doppler	Some bleeding post procedure from head wound (slight).

				Sham temp 36.5°C and 36.3°C.
47	205		Pericyte experiments. Laser Doppler	Pre 4VO. 37.0°C Neck dissection with spinal needle fine. Some erratic breathing in ear bars but otherwise fine. Moderate blood loss at vertebrals. 4VO 35.8°C 80 baseline, 10 at BCCAO
48	227		Pericyte experiments. Laser Doppler	Pre 4VO 36.5°C Very good visualisation right vertebral. Minimal blood loss. Diarrhoea. Thick tissue neck dissection. Breathing fine with spinal needle. 2 seconds of erratic breathing at end of whole procedure. Sham 36.4°C LDF 270 baseline, 220 when manipulated.
49	226		Pericyte experiments. Laser Doppler	Pre 4VO A lot of blood when dissecting right carotid but recovered 36.9°C. Some erratic breathing after spinal needle. Difficult neck dissection. Messy tracheal visualisation. Lost more blood at vertebrals. Sham 36.1°C Baseline 201
50	226		Pericyte experiments. Laser Doppler	Pre 4VO 36.8°C Difficult neck dissection. Some bleeding at right carotid. Trachea visualised. Some bleeding with vertebrals. 4VO 37.1°C Baseline 200 BCCAO 116 Reperf 60 ?probe came off.